

Master's Thesis

---

# Robust long-term growth rate of expected utility and optimal leverage for LETFs

---

Department of Mathematics  
Ludwig-Maximilians-Universität München

**Leonard Averdunk**

Munich, January 5<sup>th</sup>, 2026



Submitted in partial fulfillment of the requirements for the degree of M. Sc.  
Supervised by Prof. Dr. Biagini

# Contents

<b>1</b>	<b>Introduction</b>	<b>3</b>
1.1	Overview . . . . .	3
1.2	Related literature . . . . .	4
1.2.1	Early portfolio optimization . . . . .	4
1.2.2	Robustness . . . . .	4
1.2.3	Long-run growth . . . . .	6
1.2.4	LETFs . . . . .	6
1.2.5	New possibilities with LETFs . . . . .	7
1.2.6	LETF long run . . . . .	8
1.2.7	Research gap . . . . .	8
<b>2</b>	<b>LETF price dynamics</b>	<b>9</b>
<b>3</b>	<b>Mathematical tools</b>	<b>13</b>
3.1	Hansen-Scheinkman decomposition . . . . .	13
3.2	Recurrence and ergodicity . . . . .	14
3.3	Comparison principle . . . . .	16
<b>4</b>	<b>Uncertainty in the reference process</b>	<b>17</b>
4.1	GBM model . . . . .	18
4.2	CIR model . . . . .	21
4.3	3/2 model . . . . .	27
<b>5</b>	<b>Uncertainty in the stochastic volatility reference process</b>	<b>33</b>
5.1	Heston model . . . . .	35
5.2	3/2 volatility model . . . . .	41
<b>6</b>	<b>Uncertainty in the reference process and interest rate process</b>	<b>45</b>
6.1	Vasicek interest rate . . . . .	46
6.2	Inverse GARCH interest rate . . . . .	51
<b>7</b>	<b>Jump diffusion processes</b>	<b>57</b>
7.1	Merton jump diffusion model . . . . .	57
7.2	Bates model . . . . .	62

## Contents

---

<b>8 Comparative analysis of robust and average optimal leverage</b>	<b>69</b>
8.1 Analysis of the reference process model . . . . .	71
8.2 Analysis of the stochastic volatility reference model . . . . .	76
8.3 Analysis of the reference and interest rate model . . . . .	83
8.4 Analysis of the jump diffusion process model . . . . .	88
<b>9 Empirical validation</b>	<b>97</b>
9.1 S&P 500 modeled by a geometric Brownian motion . . . . .	98
9.2 Stress testing different leverage strategies . . . . .	109
<b>10 Conclusion</b>	<b>121</b>
10.1 Summary of objectives and main findings . . . . .	121
10.2 Economic interpretation . . . . .	121
10.3 Comparison across models . . . . .	122
10.4 Practical implications . . . . .	123
10.5 Limitations and future research . . . . .	124
<b>A Code repository</b>	<b>127</b>



# Abstract

In this thesis we analyze the robust long-term growth rate of the expected utility and expected return of a leverage exchange-traded fund. We investigate uncertainty both in the reference index and for the short interest rate, and thereby allow for uncertainty inside our stochastic modeling of an asset. The uncertainty is assumed to lie within a compact interval and the robust long-term growth rate is derived by analyzing the worst-case parameters within these uncertainty sets. Our analysis relies on the comparison principle and the Hansen–Scheinkman decomposition. We state explicit long-term growth rates under numerous models for the reference index and the short rate. We begin with uncertainty only in the reference process itself and examine the geometric Brownian motion, Cox–Ingersoll–Ross and 3/2 model. We then extend the framework and add more uncertainty by incorporating stochastic volatility on the reference process and analyze Heston and 3/2 stochastic volatility models. Further, we study the effects of stochastic interest rates and consider Vasicek and inverse GARCH short rate models. Finally, we consider the reference index to be a jump diffusion process, which adds additional uncertainty and modeling flexibility of an asset. Under this setup, we investigate the Merton jump diffusion and Bates model. This thesis builds upon and extends the work of Leung et al. [1], both by expanding the class of models considered and by providing additional models for the existing classes. After establishing the theoretical results, we complement the analysis with an empirical validation by comparing the performance of portfolios based on our derived optimal leverage strategies with historical ETF data. Our objective is to assess whether the long-run optimal policies derived from the robust modeling framework translate into tangible advantages relative to standard investment approaches.



# Chapter 1

## Introduction

### 1.1 Overview

Over the past few years the number of Exchange-Traded Fund (ETF) investors has increased significantly. In particular, ETFs are the fastest-growing investment product in Europe since 2022, according to BlackRock [2]. Among standard ETFs, leveraged ETFs (LETFs) have become increasingly more popular. It is expected that the number of investors in this segment will continue to increase in the coming years. An ETF is a financial product that is typically designed to track the performance of an underlying index, such as the S&P 500. ETFs are traded on public exchanges like individual stocks and offer investors a low-cost, liquid and diversified exposure to broad market segments or specific sectors, which make them highly attractive to the broad public. A LETF, by contrast, is a type of ETF that aims to amplify the daily returns of its reference index by a constant factor  $\beta$ . Common leverage ratios are  $\{-3, -2, -1, 2, 3\}$ . For instance, a 2x LETF seeks to replicate twice the daily performance of the index. While this leverage increases the potential for gains, it also magnifies volatility and losses. Crucially, because the leverage is reset daily, LETFs do not simply scale long-term returns by  $\beta$ , making their behavior over longer horizons more complex and path-dependent. LETFs effectively increase exposure ahead of a losing session and decrease exposure ahead of a winning session. This is called volatility drag or volatility tax, cf. Maxey [3]. This makes it challenging to analyze the long-term growth of leveraged investments, especially when the parameters of the underlying reference asset are uncertain.

In this thesis we explore and extend the work of Leung et al. [1], who studied the robust long-term growth rate of expected utility and expected return from holding an LETF under uncertain parameters of a reference asset and short interest rate. Building on that foundation, we extend the analysis to a broader class of models, namely jump-diffusion processes.

As mathematical tools for the derivation of the robust long-term growth rate we use the comparison principle and the Hansen-Scheinkman decomposition. We determine an optimal leverage ratio that maximizes the robust long-term growth rate for the various models. The models analyzed include the geometric Brownian-motion (GBM), Cox-Ingersoll-Ross (CIR), 3/2 models for the reference index. For stochastic volatility in the reference index we consider the Heston and 3/2 volatility models. Additionally, we consider stochastic in-

terest rate models such as the Vasicek and inverse Generalized AutoRegressive Conditional Heteroscedasticity (GARCH) short rate model. Finally, we incorporate jump–diffusion models for the reference index, which allow for discontinuities in the price of an underlying index of an ETF and introduce additional layers of uncertainty and modeling flexibility beyond the standard diffusion framework. Within this class, we study both the Merton jump diffusion model and the Bates model. These extensions allow us to investigate how optimal leverage decisions adjust in the presence of sudden price jumps, thereby providing a more comprehensive and realistic assessment of robust long-run portfolio behavior. Next, we extend our analysis by comparing the optimal leverage derived under worst-case parameter uncertainty with the corresponding leverage obtained under more optimistic market conditions. This comparison allows us to quantify how strongly uncertainty affects portfolio decisions and to assess whether the robust strategy is overly conservative relative to a more optimistic specification. By contrasting the worst-case and mid-case outcomes, we obtain a clearer picture of the economic cost of robustness and the practical implications of ambiguity in long-run portfolio selection. Beyond the theoretical contributions, we complement our analysis with an empirical validation designed to assess the practical relevance of the derived optimal strategies in real world investment settings. In particular, we compare the performance of portfolios constructed using the robust optimal leverage ratios with the historical returns of one of the most widely traded exchange-traded funds, the S&P 500. This serves to evaluate whether the long-run growth advantages predicted by our model materialize when applied to actual market data.

## 1.2 Related literature

### 1.2.1 Early portfolio optimization

Continuous time portfolio selection theory builds on early work by Samuelson [4], who solved continuous time consumption investment problems for investors with Constant Relative Risk Aversion (CRRA) preferences. Building on this, Merton [5] extended the framework using stochastic calculus and continuous time control methods, deriving the optimal investment consumption policy under known dynamics for asset returns. Their models laid the foundation for subsequent portfolio selection theory in finance.

However, a fundamental limitation of these classical models is the assumption that investors know the true data generating process, e.g. the exact drift and volatility of returns. In reality, model misspecification and parameter uncertainty can significantly impair portfolio performance. Later research addressed these issues by incorporating stochastic interest rates, alternative utility functions and incomplete markets (see Duffie and Zame [6]; Cvitanić and Karatzas [7]; Brennan [8]; Cox and Huang [9]).

### 1.2.2 Robustness

As previously mentioned, assuming that investors know the exact model parameters is unrealistic. Therefore, methods are required to account for this uncertainty. Two major research directions have emerged in this context. On the one hand, asset dynamics have been generalized beyond the classical Black–Scholes framework. These models capture

empirical features such as volatility clustering and asymmetric return distributions that constant volatility models fail to represent. Similarly, for interest rates and other macro financial factors, mean reverting processes such as the Cox–Ingersoll–Ross (CIR) model and its more complex variants (e.g., the 3/2 model) have been proposed to better fit term structure dynamics. The proliferation of stochastic volatility (SV) and jump diffusion models, such as Merton’s jump diffusion model for asset returns, has enhanced empirical realism but also increased the complexity of portfolio optimization by introducing additional sources of uncertainty (e.g., volatility, jump frequency, and jump size). On the other hand, these insights have motivated the development of robust control methods in economics and finance. Robust control formalizes ambiguity aversion by allowing decision makers to guard against misspecification of a reference model. Incorporating robustness into these richer stochastic frameworks is challenging but essential when model uncertainty is suspected.

Early work on uncertain volatility introduced a worst-case pricing approach that treated volatility as an unknown variable constrained to a specified range, leading to the Black–Scholes–Barenblatt nonlinear partial differential equation (PDE), c.f. Avellaneda et al. [10]. In a portfolio context, robust control in stochastic volatility environments has been analyzed also using second order backward stochastic differential equations (2BSDEs) or by solving for worst-case volatility scenarios. For example, Matoussi et al. [11] study robust optimization under uncertain volatility and show that the value function can be represented as the initial value of a particular 2BSDE, proving the existence of an optimal strategy.

The robust treatment of these enriched dynamics is technically demanding yet rapidly evolving. Important contributions include Liu and Pan [12] and Hernández-Hernández and Schied [13] for robust optimization under stochastic volatility and jumps, as well as long-run and spectral approaches with ambiguity by Scheinkman and Hansen [14], Hansen and Sargent [15], Hansen and Sargent [16], Anderson et al. [17], and Hansen and Sargent [18]. Foundational studies further include Fleming and Sheu [19].

Maenhout [20] integrated robust control directly into the continuous time portfolio choice problem, embedding ambiguity aversion within the investor’s utility maximization framework. He demonstrated that a robust investor’s policy may resemble that of a more risk-averse agent, as model misspecification concerns induce more conservative portfolio weights. In follow up work, Maenhout [21] introduced a methodology for computing detection error probabilities to calibrate the degree of ambiguity aversion, thereby quantifying how robust portfolio rules deviate from the Merton benchmark.

Subsequent research examined robust utility maximization in incomplete markets with uncertain parameters using advanced techniques such as backward stochastic differential equations (Matoussi et al. [11]) or explicit Hamilton–Jacobi–Bellman–Isaacs (HJBI) solutions when both drift and volatility are uncertain (Tevzadze et al. [22]). Robust portfolio choice has even been extended to models with jumps (Neufeld and Nutz [23]), where uncertainty is specified by a set of possible Lévy triplets, representing alternative instantaneous drift, volatility, and jump characteristics. They proved the existence of an optimal investment strategy and derived semi-closed form solutions.

The general finding across these studies is that when volatility or jump intensity is ambiguous, investors behave as though volatility were higher or more persistent, or as though

jump risks were more frequent or severe, than suggested by the nominal model. Consequently, ambiguity aversion leads to reduced exposure to risky assets and more defensive portfolio positions. Overall, the intersection of stochastic volatility modeling and robust control represents a frontier in portfolio theory, combining realistic market dynamics with prudence under model misspecification to produce more resilient investment strategies in the presence of model uncertainty.

### 1.2.3 Long-run growth

A further major branch of the literature focuses on long-term investment performance under model uncertainty. This is particularly relevant for problems such as retirement savings or endowment management, where the investment horizon is long and uncertainty accumulates over time.

The concept of maximizing long-term growth originates with Breiman [24] and Kelly [25], who proposed the Kelly criterion (log-utility maximization) as a rule that maximizes the almost sure exponential growth rate of wealth. In continuous time, Merton's log-utility solution yields the growth-optimal portfolio given known parameters.

More recent research revisits this classical problem through the lens of robustness: How does ambiguity aversion alter the portfolio that maximizes long-run growth? The robust utility maximization framework typically leads to a Hamilton–Jacobi–Bellman–Isaacs (HJBI) equation that characterizes the worst-case-adjusted value function. Solving this in the infinite-horizon limit can yield a lower guaranteed growth rate that the investor secures against adversarial model perturbations.

In diffusion settings with uncertain drift and volatility, the worst-case dynamics often correspond to a lower drift or higher volatility than the nominal estimate, thereby reducing the achievable growth rate and that robust investors behave as though the economy operates under less favorable drift or higher jump intensity conditions, and their optimal policies can be interpreted as those maximizing a conservative, guaranteed growth rate, c.f. Larsen and Branger [26]. Even so, the robust-optimal strategy is chosen to maximize this conservative growth rate. With power or logarithmic utility, semi-analytic solutions have been derived. For instance, Neufeld and Nutz [23] study a Lévy-process model with ambiguity, obtaining explicit worst-case portfolios and highlighting substantial deviations from non-robust outcomes.

These findings underscore that worst-case dynamics can significantly affect long-term wealth accumulation. Investors who neglect model uncertainty may adopt excessively exposed or risk-seeking portfolios, while robust investors deliberately trade off some upside potential to avoid catastrophic losses under adverse model realizations.

### 1.2.4 LETFs

Leveraged exchange-traded funds (LETFs) offer a modern and practical setting in which many of the preceding theoretical themes converge. Since their introduction in 2006, LETFs have attracted substantial academic interest due to their inherently path-dependent long-term behavior.

Early studies demonstrated that the interaction between daily leverage and volatility

produces a drag on long-term returns. Specifically, a leveraged fund's cumulative return over time typically falls short of  $\beta$  times the underlying index's return due to volatility and compounding effects. This phenomenon, often referred to as volatility decay, arises because leveraged ETFs must rebalance daily to maintain a fixed leverage ratio. After a loss, the ETF has less capital to recover, and after a gain, the fund scales up and becomes exposed to larger subsequent fluctuations. As a result, higher volatility leads to a systematic reduction in long-run growth. Analyses by Cheng and Madhavan [27] and Avellaneda and Zhang [28] formalized these effects by modeling LETF dynamics in continuous-time diffusion frameworks, showing that the long-run return depends not only on the leverage ratio but also on the realized variance of the underlying index. Their results established that LETF performance is inherently path-dependent sensitive to volatility clustering and rebalancing frequency and that deviations from the target multiple are an unavoidable consequence.

Jarrow [29] further highlighted that LETFs can diverge significantly from their intended  $\beta$ -multiple over long horizons. Empirical evidence by Leung and Guo [30] on commodity-based LETFs confirmed pronounced volatility decay in tracking performance. These studies revealed that selecting an optimal leverage factor for long-term investment is nontrivial. Higher leverage amplifies expected return but also increases volatility drag, implying that more leverage is not necessarily better, see Trainor and Baryla [31]. Beyond return erosion, Leung et al. [32] and Lee and Wang [33] investigated the relationship between ETF and LETF implied volatility surfaces, illustrating how leverage impacts derivative pricing. Similarly, Figueroa-López et al. [34], Leung and Sircar [35], and Trainor and Gregory [36] analyzed options written on LETFs, emphasizing the nonlinear interaction between leverage, stochastic volatility, and pricing kernels.

### 1.2.5 New possibilities with LETFs

Traditionally, portfolio optimization involves selecting a vector of asset weights to balance expected return and risk, c.f. Markowitz [37] and Merton [5]. An alternative perspective now is to treat diversification as given through a broad ETF and to optimize a single decision variable, the leverage ratio  $\beta$  of a daily rebalanced LETF. This reformulation reduces a high-dimensional allocation problem to a one-dimensional control problem while preserving the stochastic environment of the benchmark, including drift, volatility, and jump components.

Within this framework, theory characterizes nominal and robust long-run utility growth as functions of  $\beta$ , trading off amplified drift with volatility drag and producing explicit optimal leverage ratios  $\beta^*$  under both baseline and worst-case scenarios, c.f. Avellaneda and Zhang [28], Leung and Park [38] and Park and Yeo [39].

For robustness applications to LETF derivatives, Cox and Kinsley [40] investigate robust hedging of options on LETFs deriving model independent price bounds. Although their focus is on option pricing, the implications for portfolio choice are consistent in a way that ambiguity in LETF volatility or jump behavior necessitates more cautious investment and leverage strategies.

### 1.2.6 LETF long run

Building upon this foundation, recent studies have examined long-term growth rates and optimal leverage decisions for LETF investors. Leung and Park [38] provided one explicit analysis of the long-term growth rate of expected utility for an LETF investment under various stochastic models of the reference index. By deriving closed-form growth exponents for dynamics such as geometric Brownian motion and mean-reverting processes, they identified the leverage ratio that maximizes long-run growth for a risk averse investor. Their results show that an intermediate level of leverage can be optimal, whereas excessive leverage overshoots due to volatility drag and insufficient leverage underutilizes growth opportunities.

More recent research incorporates model uncertainty into this framework. Robust control methods have been applied to determine worst-case growth rates and optimal leverage under parameter ambiguity. These approaches define uncertainty sets for the index dynamics and interest rate, then compute the robust long-term growth rate by optimizing over worst-case parameters. The resulting optimal leverage is typically more conservative than the non-robust optimum.

The long-run robust perspective often employs spectral and ergodic techniques, where principal eigenvalues of modified generators yield asymptotic certainty equivalents and worst-case dynamics, c.f. Hansen and Scheinkman [41] and Donsker and Varadhan [42]. In finance, risk-sensitive and robust growth criteria connect to portfolio problems under incomplete information and stochastic environments, c.f. Bielecki and Pliska [43], Hansen and Sargent [18] and Kraft et al. [44]). For utility based long-run analyses of a single LETF martingale extraction and eigenfunction methods deliver closed-form growth rates of expected utility and the corresponding optimal leverage  $\beta^*$  as functions of preferences and model parameters, see Leung and Park [38]. Additional contributions include Brown [45], who derive long-run bounds for leveraged ETF log-returns.

### 1.2.7 Research gap

Despite considerable progress in both robust portfolio theory and LETF-specific research, an important gap remains. Prior studies on robust investment typically rely on simplified settings, assuming constant volatility or the absence of jumps, while the LETF literature on long-term performance usually adopts fixed, non-ambiguous models.

This thesis aims to bridge that gap by combining the robust optimization framework with sophisticated asset dynamics, including stochastic volatility, stochastic interest rates, and jump processes. Specifically, we analyze LETF long-run growth rates under parameter uncertainty, derive worst-case parameters and long-run utility growth using eigenfunction and eigenvalue methods, and characterize both nominal and robust optimal leverage ratios  $\beta^*$  for a single LETF.

By addressing model misspecification alongside realistic market features, this work provides a comprehensive understanding of how an ambiguity-averse investor should choose leverage for long-horizon growth.

# Chapter 2

## LETF price dynamics

This chapter lays the foundation for our subsequent analysis. Similar formulations of ETF and LETF price processes and their dynamics can be found, for example, in Avellaneda and Zhang [28] and Leung and Park [38]. We formulate the dynamics of the underlying reference index of LETFs and infer the dynamics of the resulting LETF from which we express the expected utility from holding the LETF up to time  $T$  in different forms. In the following we assume a filtered probability space  $(\Omega, \mathcal{F}, \mathbb{F}, \mathbb{P})$ , where the filtration  $\mathbb{F} := (\mathcal{F}_t)_{t \geq 0}$  is generated by a  $d$ -dimensional standard Brownian motion  $B$ . Let a reference index  $X$  be a diffusion process given by an equation

$$\frac{dX_t}{X_t} = \mu_t dt + \sigma_t dB_t, \quad t \geq 0, \tag{2.1}$$

where both the drift  $\mu = (\mu_t)_{t \geq 0}$  and the diffusion process  $\sigma = (\sigma_t^1, \dots, \sigma_t^d)_{t \geq 0}$  are  $\mathbb{F}$ -adapted. A leveraged exchange-traded fund (LETF) is a portfolio constructed in such a way that it maintains a constant proportional exposure  $\beta$ , which we call a leverage ratio, to the reference  $X$ . In various countries, this ratio can vary due to regulation policies, c.f. Pagano et al. [46], U.S. Securities and Exchange Commission [47]. We set the allowable leverage ratios to be ranging from a  $\underline{\beta} < 0$  to a  $\bar{\beta} > 1$ . We denote the process  $L = (L_t)_{t \geq 0}$  as the LETF price process. We assume that at time  $t$  an investor chooses to invest a proportion  $\beta L_t$  in  $X$  and  $(1 - \beta)L_t$  in a bank account with short rate  $r_t$ . Note that the investment in  $X$  is  $|\beta|L_t$  if  $\beta < 0$ . Now we can write the dynamics of  $L_t$  as

$$\begin{aligned} dL_t &= \beta L_t \left( \frac{dX_t}{X_t} \right) + (1 - \beta)L_t r_t dt \\ &= \beta L_t (\mu_t dt + \sigma_t dB_t) - (\beta - 1)L_t r_t dt \\ &= L_t ((\beta \mu_t - (\beta - 1)r_t) dt + \beta \sigma_t dB_t) \end{aligned}$$

resulting in

$$\frac{dL_t}{L_t} = (\beta \mu_t - (\beta - 1)r_t) dt + \beta \sigma_t dB_t.$$

We assume w.l.o.g  $L_0 = X_0 = 1$ . Since the LETF price  $L_t$  is a log-normal process we can express the expected utility from holding the LETF up to time  $T \geq 0$ .

First we express  $X_T$ . For this define  $Z_t := \log X_t$ , then by Itô's formula:

$$\begin{aligned} dZ_t &= \frac{1}{X_t} dX_t - \frac{1}{2X_t^2} d\langle X, X \rangle_t \\ &= \mu_t dt + \sigma_t dB_t - \frac{1}{2X_t^2} |\sigma_t|^2 X_t^2 dt \\ &= \mu_t - \frac{1}{2} |\sigma_t|^2 dt + \sigma_t dB_t. \end{aligned}$$

Hence we get for  $X_T$ :

$$X_T = X_0 \exp \left\{ \int_0^T \mu_s - \frac{|\sigma_s|^2}{2} ds + \int_0^T \sigma_s dB_s \right\}.$$

Similarly we now compute  $L_t$  by defining  $Y_t := \log L_t$  and using Itô's formula:

$$\begin{aligned} dY_t &= \frac{1}{L_t} dL_t - \frac{1}{2L_t^2} d\langle L, L \rangle_t \\ &= (\beta \mu_t - (\beta - 1)r_t) dt + \beta \sigma_t dB_t - \frac{1}{2L_t^2} L_t^2 \beta^2 |\sigma_t|^2 dt \\ &= (\beta \mu_t - (\beta - 1)r_t - \frac{1}{2}\beta |\sigma_t|^2) dt + \beta \sigma_t dB_t. \end{aligned}$$

Therefore  $L_T = e^{Y_T} = L_0 \exp \left\{ \int_0^T \beta \mu_s - (\beta - 1)r_s - \frac{1}{2}\beta^2 |\sigma_s|^2 ds + \int_0^T \beta \sigma_s dB_s \right\}$  and since  $L_0 = X_0 = 1$  this simplifies to:

$$L_T = \exp \left\{ \int_0^T \beta \mu_s - (\beta - 1)r_s - \frac{1}{2}\beta^2 |\sigma_s|^2 ds + \int_0^T \beta \sigma_s dB_s \right\}.$$

By our previous computation of  $X_T$  we can also see that:

$$\begin{aligned} L_T &= \exp \left\{ \int_0^T \beta \mu_s - \beta \frac{|\sigma_s|^2}{2} ds + \int_0^T \beta \sigma_s dB_s \right\} \\ &\quad \exp \left\{ \int_0^T -(\beta - 1)r_s - \frac{1}{2}\beta^2 |\sigma_s|^2 + \frac{1}{2}\beta |\sigma_s|^2 ds \right\} \\ &= X_T \exp \left\{ \int_0^T -(\beta - 1)r_s - \frac{1}{2}\beta(\beta - 1) |\sigma_s|^2 ds \right\}. \end{aligned}$$

So now the expected utility from holding the LETF up to time T is given by

$$\begin{aligned} \mathbb{E}^{\mathbb{P}} [L_T^p] &= \mathbb{E}^{\mathbb{P}} \left[ X_T^{p\beta} e^{\int_0^T (p(1-\beta)r_s + \frac{1}{2}p\beta(1-\beta)|\sigma_s|^2) ds} \right] \\ &= \mathbb{E}^{\mathbb{P}} \left[ e^{\int_0^T (p\beta\mu_s + p(1-\beta)r_s - \frac{1}{2}p\beta^2|\sigma_s|^2) ds + p\beta \int_0^T \sigma_s dB_s} \right]. \end{aligned} \tag{2.2}$$

We introduce a new measure  $\hat{\mathbb{P}}_t$  on  $\mathcal{F}_t$  by

$$\frac{d\hat{\mathbb{P}}_t}{d\mathbb{P}} = \mathcal{E} \left( p\beta \int_0^{\cdot} \sigma_s dB_s \right)_t, \quad t \geq 0,$$

---

where we assume that the Doléans-Dade exponential  $\mathcal{E}(p\beta \int_0^\cdot \sigma_s dB_s)$  is a true martingale. Note that this assumption implicitly has implications on the process  $(\sigma_t)_{t \geq 0}$ . We point out that

$$\langle B_\cdot, p\beta \int_0^\cdot \sigma_u dB_u \rangle_s = \langle \int_0^\cdot dB_u, p\beta \int_0^\cdot \sigma_u dB_u \rangle_s = p\beta \int_0^s 1 \sigma_u du = p\beta \int_0^s \sigma_u du.$$

So the process  $\hat{B}$  defined as

$$\hat{B}_s := -p\beta \int_0^s \sigma_u du + B_s = B_s - \langle B_\cdot, p\beta \int_0^\cdot \sigma_u dB_u \rangle_s, \quad 0 \leq s \leq t \quad (2.3)$$

is a standard Brownian motion under  $\hat{\mathbb{P}}_t$  by Girsanov's theorem. We see also that  $(\hat{\mathbb{P}}_s)_{s \geq 0}$  is consistent in the sense that  $\hat{\mathbb{P}}_T|_{\mathcal{F}_t} = \hat{\mathbb{P}}_t$  for all  $T \geq t \geq 0$ . Hence, we might drop the index  $t$  in  $\hat{\mathbb{P}}_t$  without causing confusion. Correspondingly, the process (2.3) can be viewed as a standard Brownian motion under the measure  $\hat{\mathbb{P}}$  on any finite time horizon. Adopting the universal notation for  $\hat{\mathbb{P}}$  and  $\hat{B}$ , and substituting (2.3) into (2.1) and (2.2), we obtain for  $0 \leq t \leq T$ ,  $T > 0$

$$\begin{aligned} \frac{dX_t}{X_t} &= \mu_t dt + \sigma_t dB_t = \sigma_t \left( d\hat{B}_t + p\beta \sigma_t dt \right) \\ &= (\mu_t + p\beta |\sigma_t|^2) dt + \sigma_t d\hat{B}_t \end{aligned}$$

and

$$\mathbb{E}^{\mathbb{P}} [L_T^p] = \mathbb{E}^{\hat{\mathbb{P}}} \left[ \frac{d\mathbb{P}}{d\hat{\mathbb{P}}} L_T^p \right] = \mathbb{E}^{\hat{\mathbb{P}}} \left[ e^{\int_0^T (p\beta \mu_s + p(1-\beta)r_s - \frac{1}{2}p(1-p)\beta^2|\sigma_s|^2) ds} \right]. \quad (2.4)$$



# Chapter 3

## Mathematical tools

To analyze the long-run utility of leveraged portfolios under model uncertainty, we require mathematical tools. In this chapter we introduce the main concepts and tools used for our study. First, we present the Hansen–Scheinkman decomposition, which allows us to express path-dependent expectations into tractable eigenvalue problems. We discuss recurrence and ergodicity, which guarantee a meaningful long-term behavior of the desired expectation. Finally, we introduce the comparison principle for stochastic differential equations, which is a powerful tool for deriving worst-case scenarios in the presence of uncertainty. These tools form the backbone of our theoretical derivations in all subsequent chapters. In this chapter, we consider a filtered probability space  $(\Omega, \mathcal{F}, \mathbb{F}, \mathbb{P})$ , where the filtration  $\mathbb{F} := (\mathcal{F}_t)_{t \geq 0}$  is the natural filtration of a  $d$ -dimensional Brownian motion  $B$ .

### 3.1 Hansen-Scheinkman decomposition

Let  $X$  be an  $d$ -dimensional time-homogeneous Markov diffusion process satisfying the SDE

$$dX_t = b(X_t) dt + \sigma(X_t) dB_t$$

with an deterministic initial value  $X_0$ . We also assume that  $X$  stays in a domain  $D \subset \mathbb{R}^d$  for all  $t \geq 0$ . Here,  $X$  might represent multiple components of the model, not just the reference index, but also stochastic volatility or stochastic interest rate.

We often will have a representation of the expected utility (2.4) in the form

$$\mathbb{E}^\mathbb{P} \left[ e^{-\int_0^T \mathcal{V}(X_s) ds} h(X_T) \right]. \quad (3.1)$$

We see that in (3.1) the exponent relies on information on the whole path of  $(X_t)_{0 \leq t \leq T}$ . To derive this expectation it would be better if we manage to transform (3.1) into a form depending only on the marginal distribution of  $X_T$  at time  $T$ . For this we will use a method that is introduced and strongly motivated by Deuschel and Stroock [48] and Scheinkman and Hansen [14].

Consider the operator

$$\mathcal{L} := \frac{1}{2} \sum_{i,j=1}^d (\sigma \sigma^\top)_{ij}(x) \frac{\partial^2}{\partial x_i \partial x_j} + \sum_{i=1}^d b_i(x) \frac{\partial}{\partial x_i} - \mathcal{V}(x) \quad (3.2)$$

defined on  $D$  where  $\top$  denotes the transpose. We aim to find an eigenpair with  $\lambda \in \mathbb{R}$  and a twice continuously differentiable and positive function  $\phi(\lambda, \phi)$  such that

$$\mathcal{L}\phi = -\lambda\phi. \quad (3.3)$$

If such a pair exists, then

$$M_t := e^{\lambda t - \int_0^t \mathcal{V}(X_s) ds} \frac{\phi(X_t)}{\phi(X_0)}, \quad t \geq 0 \quad (3.4)$$

is a local martingale, cf. Scheinkman and Hansen [14]. If  $M$  is even a true martingale, then we can define for fixed  $T > 0$  a new measure  $\mathbb{Q}$  on  $\mathcal{F}_T$  by

$$\mathbb{Q}(A) := \int_A M_T d\mathbb{P}, \quad A \in \mathcal{F}_T.$$

With the change of measure to  $\mathbb{Q}$ , the expectation in (3.1) can now be reformulated in the intended way:

$$\begin{aligned} \mathbb{E}^{\mathbb{P}} \left[ e^{-\int_0^T \mathcal{V}(X_s) ds} h(X_T) \right] &= e^{-\lambda T} \phi(X_0) \mathbb{E}^{\mathbb{P}} \left[ M_T \frac{h(X_T)}{\phi(X_T)} \right] \\ &= e^{-\lambda T} \phi(X_0) \mathbb{E}^{\mathbb{Q}} \left[ \frac{h(X_T)}{\phi(X_T)} \right]. \end{aligned} \quad (3.5)$$

Now, for a standard  $\mathbb{Q}$ -Brownian motion

$$W_t := B_t - \int_0^t \left( \sigma^\top \frac{\nabla \phi}{\phi} \right)(X_s) ds, \quad 0 \leq t \leq T, \quad (3.6)$$

the dynamics of  $X$  are modified as

$$dX_t = \left( b + \sigma \sigma^\top \frac{\nabla \phi}{\phi} \right)(X_t) dt + \sigma(X_t) dW_t, \quad 0 \leq t \leq T. \quad (3.7)$$

Having this method established, still two natural questions arise. First, since we need such an eigenpair satisfying (3.3) to exist, we should ask if this always exist? And the second question should be: when does (3.4) become a true martingale? By [49, Theorem 4.3.2 and 4.3.3 (iii)] we know that if  $\mathcal{V} \geq 0$  and  $\mathcal{V} \not\equiv 0$  such an eigenpair exists. To answer the second question, one can apply Pinsky [49, Theorem 4.8.5 (ii)], which implies that the process in (3.4) is a true martingale as long as a solution to the SDE in (3.7) does not explode.

## 3.2 Recurrence and ergodicity

We are interested in finding the long run growth rate of the expected utility. To this end we analyze the longterm behavior of the expectation term in (3.5). We will see that this expectation converges if the underlying process  $X$  is positive recurrent. In this section, we will introduce and discuss the concepts of recurrence and ergodicity, which as mentioned

are key to characterizing the expectation.

We adopt the definitions of recurrence as formalized in Pinsky [49]. For this, we suppose a domain  $D \subset \mathbb{R}^d$ , a  $d \times 1$  vector-valued continuously differentiable function,  $b$ , in  $D$  with locally Hölder continuous first-order derivatives and exponent  $\alpha$  and a  $d \times d$  matrix-valued function,  $\sigma$ , in  $D$  such that  $\sigma\sigma^\top$  is twice-continuously differentiable whose second-order partial derivatives are locally Hölder continuous with exponent  $\alpha$  and is positive definite for all  $x \in D$ . Now, we consider the  $D$ -valued diffusion process

$$dX_t^x = b(X_t^x) dt + \sigma(X_t^x) dB_t, \quad X_0^x = x \in D, \quad (3.8)$$

which we call *recurrent* if for all  $x, y \in D$  and  $r > 0$ ,  $\mathbb{P}\{\tau_{\bar{B}_r(y)} < \infty\} = 1$ , where  $\bar{B}_r(y) = \{z \in D : |y - z| \leq r\}$  and  $\tau_{\bar{B}_r(y)} = \inf\{t \geq 0 : X_t^x \in \bar{B}_r(y)\}$ .

In the special case where the process is one-dimensional, this condition simplifies to the condition that for all  $x, y \in D$ ,  $\mathbb{P}\{X_t^x = y \text{ for some } t \in [0, \infty)\} = 1$ . We define the corresponding generator of  $X^x$  as

$$\mathcal{L}_0 := \frac{1}{2} \sum_{i,j=1}^d (\sigma\sigma^\top)_{ij}(x) \frac{\partial^2}{\partial x_i \partial x_j} + \sum_{i=1}^d b_i(x) \frac{\partial}{\partial x_i},$$

and the formal adjoint of  $\mathcal{L}_0$  as

$$\tilde{\mathcal{L}}_0 := \frac{1}{2} \sum_{i,j=1}^d \frac{\partial^2}{\partial x_i \partial x_j} \left( (\sigma\sigma^\top)_{ij}(x) \cdot \right) - \sum_{i=1}^d \frac{\partial}{\partial x_i} (b_i(x) \cdot).$$

Pinsky [49, Theorem 4.3.3.(v) and 4.3.4] showed that for a recurrent diffusion process there exists a unique - up to positive multiples - positive function  $\tilde{\phi}$  such that  $\tilde{\mathcal{L}}_0 \tilde{\phi} = 0$  with its second derivative  $\tilde{\phi}''$  being locally Hölder continuous in the domain  $D$ . If  $\tilde{\phi}$  is integrable over  $D$  the diffusion process is called positive recurrent. Further, it is also shown in Pinsky [49, Theorem 4.8.6] that for a positive recurrent process  $X$  with  $p(t, x, dy)$  as the transition measure,  $\tilde{\phi}$  is an invariant density for  $p(t, x, dy)$ , meaning,  $\int_D p(t, x, dy) \tilde{\phi}(y) dy = \tilde{\phi}(x)$  for all  $t \geq 0$ . Now, without loss of generality we can assume that  $\int_D \tilde{\phi}(x) dx = 1$  and therefore  $\tilde{\phi}$  becomes the invariant probability density. Otherwise one just needs to normalize. This invariant density enables us to describe the long-term behavior of expected values, so that for a function  $h$  such that  $\int_D |h(x)| \tilde{\phi}(x) dx < \infty$  we have  $\mathbb{E}^{\mathbb{P}}[|h(X_t^x)|] < \infty$  for all  $x \in D$  and  $t \geq 0$ , as well as  $\lim_{t \rightarrow \infty} \mathbb{E}^{\mathbb{P}}[h(X_t^x)] = \int_D h(x) \tilde{\phi}(x) dx$  (e.g., Robertson and Xing [50, Remark 4.2]). In one-dimensional cases, where  $d = 1$  and  $D = (\alpha, \beta)$ ,  $-\infty \leq \alpha < \beta \leq \infty$ , there are practical criteria verifying both recurrence and positive recurrence. Additionally, for recurrent processes the invariant density can be derived explicitly. These conditions, formulas as well as the following proposition are detailed in Pinsky [49].

**Proposition 3.1** *Leung et al. [1, Proposition 1]*

*The diffusion process (3.8) taking values in  $(\alpha, \beta)$ ,  $-\infty \leq \alpha < \beta \leq \infty$  is recurrent if and only if*

$$\int_{\alpha}^c e^{-\int_c^x \frac{2b}{\sigma^2}(y) dy} dx = \int_c^{\beta} e^{-\int_c^x \frac{2b}{\sigma^2}(y) dy} dx = \infty$$

for  $c \in (\alpha, \beta)$ . In this case, the invariant density  $\tilde{\phi}$  is given by

$$\tilde{\phi}(x) = \frac{1}{\sigma^2(x)} e^{\int_c^x \frac{2b}{\sigma^2}(y) dy}.$$

Thus, a recurrent process is positive recurrent if and only if

$$\int_{\alpha}^{\beta} \frac{1}{\sigma^2(x)} e^{\int_c^x \frac{2b}{\sigma^2}(y) dy} dx < \infty.$$

### 3.3 Comparison principle

We are interested in the worst-cases scenario of investing in an LETF. This can be described by investigating the expected utility from holding an LETF and finding the minimum possible value of it. We identify this minimum for given uncertainty sets of parameters, by taking the infimum for the expected utility over the whole parameter set. A natural next step is to identify the specific parameters that lead to this minimum. These derivations can be done with the *comparison principle* for SDEs, that will be described in the next proposition, which can also be found in Karatzas and Shreve [51, Proposition 5.2.18].

**Proposition 3.2** *Leung et al. [1, Proposition 2]*

Let  $d = 1$ . Suppose that we have two continuous and adapted processes  $X^j, j = 1, 2$ , such that

$$dX_t^{(j)} = b_j(t, X_t^{(j)}) dt + \sigma(t, X_t^{(j)}) dB_t, \quad 0 \leq t < \infty$$

hold a.s. for  $j = 1, 2$ . We assume that

$$(i) \quad X_0^{(1)} \leq X_0^{(2)} \text{ a.s.,}$$

(ii) the coefficients  $b_j$  are continuous and real-valued functions on  $[0, \infty) \times \mathbb{R}$ , satisfying the relation

$$b_1(t, x) \leq b_2(t, x)$$

and condition

$$|b_j(t, x) - b_j(t, y)| \leq K|x - y|$$

for either  $j = 1$  or  $j = 2$ , for every  $0 \leq t < \infty$  and  $x, y \in \mathbb{R}$ .

(iii) the coefficient  $\sigma$  is a continuous, real-valued function on  $[0, \infty) \times \mathbb{R}$  satisfying the condition

$$|\sigma(t, x) - \sigma(t, y)| \leq h(|x - y|) \tag{3.9}$$

for every  $0 \leq t < \infty$  and  $x, y \in \mathbb{R}$ , where  $h : [0, \infty) \rightarrow [0, \infty)$  is a strictly increasing function with  $h(0) = 0$  and

$$\int_{(0, \epsilon)} h^{-2}(u) du = \infty, \quad \text{for all } \epsilon > 0.$$

Then

$$\mathbb{P} \left\{ X_t^{(1)} \leq X_t^{(2)} \text{ for all } t \in [0, \infty) \right\} = 1.$$

# Chapter 4

## Uncertainty in the reference process

We begin our analysis of model uncertainty by first considering uncertainty solely in the reference process. In this chapter, we assume a constant interest rate  $r$  and a deterministic initial value of the reference process  $X_0 = 1$ . We set  $\alpha = (\alpha_1, \dots, \alpha_n) \in \mathbb{R}^n$  to be the set of model parameters, meaning the drift and diffusion terms of  $X$  depend on  $\alpha$ . To point out the dependence of  $\mu$  and  $\sigma$  (and thus  $X$ ) on  $\alpha$  we can write the dynamics of  $X$  as

$$\frac{dX_t^\alpha}{X_t^\alpha} = \mu(X_t^\alpha; \alpha) dt + \sigma(X_t^\alpha; \alpha) dB_t, \quad X_0 = 1.$$

As we have seen in the derivation of formula (2.2), we can now also write the expected utility in (2.2) with drift  $\mu(X_t^\alpha; \alpha)$  and diffusion  $\sigma(X_t^\alpha; \alpha)$  as

$$\mathbb{E}^{\mathbb{P}} [(L_t^\alpha)^p] = e^{-pr(\beta-1)t} \mathbb{E}^{\mathbb{P}} \left[ (X_t^\alpha)^{p\beta} e^{-\frac{1}{2}p\beta(\beta-1)\int_0^t \sigma(X_s^\alpha; \alpha)^2 ds} \right], \quad t \geq 0.$$

Suppose the vector  $\alpha$  is subject to uncertainty, but known to lie within a compact subset of  $\mathbb{R}^d$ . In this case, we can define lower and upper bounds  $\underline{\alpha} := (\underline{\alpha}_1, \dots, \underline{\alpha}_n) \in \mathbb{R}^n$  and  $\bar{\alpha} = (\bar{\alpha}_1, \dots, \bar{\alpha}_n) \in \mathbb{R}^n$  such that  $\underline{\alpha}_i \leq \bar{\alpha}_i$  for each component  $i = 1, 2, \dots, n$  and

$$\alpha \in [\underline{\alpha}, \bar{\alpha}] := \prod_{i=1}^n [\underline{\alpha}_i, \bar{\alpha}_i].$$

We want to analyze the growth rate of the worst-case expected utility

$$\frac{1}{T} \log \inf_{\alpha \in [\underline{\alpha}, \bar{\alpha}]} \mathbb{E}^{\mathbb{P}} [(L_T^\alpha)^p] \tag{4.1}$$

as  $T$  approaches infinity and determine the value of this limit assuming it converges. We denote the dependence on  $\alpha$  of the process  $X$  in the expectation by  $\mathbb{E}^{\mathbb{P}^\alpha} [\cdot]$ . This eases notation, since we can write  $X_t = X_t^\alpha$ . For instance now:

$$\mathbb{E}^{\mathbb{P}^\alpha} \left[ X_T^{p\beta} e^{-\frac{1}{2}p\beta(\beta-1)\int_0^T \sigma^2(X_s) ds} \right] = \mathbb{E}^{\mathbb{P}} \left[ (X_T^\alpha)^{p\beta} e^{-\frac{1}{2}p\beta(\beta-1)\int_0^T \sigma^2(X_s^\alpha; \alpha) ds} \right].$$

We set the worst-case expectation as

$$v_T := \inf_{\alpha \in [\underline{\alpha}, \bar{\alpha}]} \mathbb{E}^{\mathbb{P}^\alpha} [L_T^p] = e^{-pr(\beta-1)T} \inf_{\alpha \in [\underline{\alpha}, \bar{\alpha}]} V(T; \alpha), \tag{4.2}$$

where

$$V(T; \alpha) := \mathbb{E}^{\mathbb{P}^\alpha} \left[ X_T^{p\beta} e^{-\frac{1}{2}p\beta(\beta-1)\int_0^T \sigma^2(X_s)ds} \right]. \quad (4.3)$$

Therefore we can rewrite formula (4.1) in the following way

$$\begin{aligned} (4.1) &= \lim_{T \rightarrow \infty} \frac{1}{T} \inf_{\alpha \in [\underline{\alpha}, \bar{\alpha}]} \mathbb{E}^{\mathbb{P}} [(L_T^\alpha)^p] = \lim_{T \rightarrow \infty} \frac{1}{T} \log v_T \\ &= \lim_{T \rightarrow \infty} \frac{1}{T} \log \left( e^{-pr(\beta-1)T} \inf_{\alpha \in [\underline{\alpha}, \bar{\alpha}]} V(T; \alpha) \right) = -pr(\beta-1) + \lim_{T \rightarrow \infty} \frac{1}{T} \log \inf_{\alpha \in [\underline{\alpha}, \bar{\alpha}]} V(T; \alpha). \end{aligned}$$

Using Proposition 3.2 we can find a  $\alpha^* \in [\underline{\alpha}, \bar{\alpha}]$  and a positive constant  $C > 0$  such that

$$Ce^{-pr(\beta-1)T} V(T; \alpha^*) \leq v_T,$$

which can be used to analyze the worst-case expected utility, as this leads to the inequalities

$$\begin{aligned} -pr(\beta-1) + \limsup_{T \rightarrow \infty} \frac{1}{T} \log V(T; \alpha^*) &\geq \limsup_{T \rightarrow \infty} \frac{1}{T} \log v_T \\ &\geq \liminf_{T \rightarrow \infty} \frac{1}{T} \log v_T \\ &\geq -pr(\beta-1) + \liminf_{T \rightarrow \infty} \frac{1}{T} \log V(T; \alpha^*). \end{aligned}$$

Hence, we only need to establish an equality of the upper and lower limits

$$\limsup_{T \rightarrow \infty} \frac{1}{T} \log V(T; \alpha^*) = \liminf_{T \rightarrow \infty} \frac{1}{T} \log V(T; \alpha^*)$$

so that the limit itself exists and can be computed as

$$\lim_{T \rightarrow \infty} \frac{1}{T} \log V(T; \alpha^*).$$

Note that the leverage ratio  $\beta$  may influence the set of parameters in the worst-case.

## 4.1 GBM model

To demonstrate the theory in an example we will start with analyzing the GBM model. Hence, the underlying process,  $X$ , will be modeled as a geometric Brownian motion

$$dX_t = \mu X_t dt + \sigma X_t dB_t, t \geq 0$$

where drift and diffusion uncertainty are expressed as  $(\mu, \sigma) \in [\underline{\mu}, \bar{\mu}] \times [\underline{\sigma}, \bar{\sigma}]$  and  $\underline{\mu}, \underline{\sigma} > 0$ . For any pair  $(\mu, \sigma)$ , we can explicitly give the expected utility by

$$\begin{aligned} \mathbb{E}^{\mathbb{P}^{\mu, \sigma}} [L_T^p] &\stackrel{(2.2)}{=} \mathbb{E}^{\mathbb{P}} \left[ e^{(p\beta\mu - p(\beta-1)r - \frac{1}{2}p\beta^2\sigma^2)T + p\beta\sigma B_T} \right] \\ &= \mathbb{E}^{\mathbb{P}} \left[ e^{p(\beta\mu - (\beta-1)r)T - \frac{1}{2}p\beta^2\sigma^2T + p\beta\sigma B_T} \right] \\ &= e^{p(\beta\mu - (\beta-1)r)T - \frac{1}{2}p\beta^2\sigma^2T} \mathbb{E}^{\mathbb{P}} \left[ e^{p\beta\sigma B_T} \right], \text{ where } B_T \sim \mathcal{N}(0, T) \text{ and } \mathbb{E}[e^{cB_T}] = e^{\frac{Tc^2}{2}} \\ &= e^{p(\beta\mu - (\beta-1)r)T - \frac{1}{2}p\beta^2\sigma^2T} e^{\frac{1}{2}p^2\beta^2\sigma^2T} \\ &= e^{p(\beta\mu - (\beta-1)r)T - \frac{1}{2}p(1-p)\beta^2\sigma^2T}. \end{aligned}$$

Now, by inserting the highest respectively the lowest value of  $\mu$  we can see that:

$$\inf_{(\mu,\sigma) \in [\underline{\mu},\bar{\mu}] \times [\underline{\sigma},\bar{\sigma}]} \mathbb{E}^{\mathbb{P}^{\mu,\sigma}} [L_T^p] \geq e^{p(\beta\mu^*(\beta) - (\beta-1)r)T - \frac{1}{2}p(1-p)\bar{\sigma}^2\beta^2T} \quad (4.4)$$

where

$$\mu^*(\beta) = \begin{cases} \frac{\mu}{\bar{\mu}}, & \beta \geq 0 \\ \frac{\bar{\mu}}{\mu}, & \beta < 0 \end{cases}.$$

Using also the definition of the infimum we also have

$$\inf_{(\mu,\sigma) \in [\underline{\mu},\bar{\mu}] \times [\underline{\sigma},\bar{\sigma}]} \mathbb{E}^{\mathbb{P}^{\mu,\sigma}} [L_T^p] \leq \mathbb{E}^{\mathbb{P}^{\mu^*(\beta),\bar{\sigma}}} [L_T^p] = e^{p(\beta\mu^*(\beta) - (\beta-1)r)T - \frac{1}{2}p(1-p)\bar{\sigma}^2\beta^2T}.$$

Hence, together with (4.4), we can readily derive the equality

$$\lim_{T \rightarrow \infty} \frac{1}{T} \log \inf_{(\mu,\sigma) \in [\underline{\mu},\bar{\mu}] \times [\underline{\sigma},\bar{\sigma}]} \mathbb{E}^{\mathbb{P}^{\mu,\sigma}} [L_T^p] = pr + p(\mu^*(\beta) - r)\beta - \frac{1}{2}p(1-p)\bar{\sigma}^2\beta^2. \quad (4.5)$$

We now turn to the task of identifying the optimal leverage ratio, denoted  $\beta^*$ , which maximizes the long-term growth rate of the worst-case scenario described in equation (4.5). To this end, consider the function  $\Lambda(\beta)$  defined as

$$\Lambda(\beta) := pr + p(\mu^*(\beta) - r)\beta - \frac{1}{2}p(1-p)\bar{\sigma}^2\beta^2.$$

We are now trying to maximize this function. The value of the optimal leverage ratio  $\beta^*$  depends on the relationship between the interest rate  $r$  and the bounds of the drift parameter uncertainty interval  $[\underline{\mu}, \bar{\mu}]$ . We analyze three different cases based on this relationship and determine the optimal  $\beta^*$  for each case, since this distinction is necessary. Since  $\Lambda$  is a quadratic function in  $\beta$ , the optimal leverage ratio in each scenario can be derived explicitly. First, we differentiate  $\Lambda$  with respect to  $\beta$ :  $\Lambda'(\beta) = p(\mu^*(\beta) - r) - p(1-p)\bar{\sigma}^2\beta$ . Then we distinguish based on the relationship between  $[\underline{\mu}, \bar{\mu}]$  and  $r$ :

**Case 1**  $\bar{\mu} < r$ : We see that  $\Lambda'(\beta) = 0$  for  $\beta = \frac{\mu^*-r}{(1-p)\bar{\sigma}^2}$ . Since

$$\Lambda(0) = pr < pr + \frac{1}{2}p\frac{(\bar{\mu}-r)^2}{(1-p)\bar{\sigma}^2} = \Lambda\left(\frac{\bar{\mu}-r}{(1-p)\bar{\sigma}^2}\right),$$

we infer  $\beta^* = \frac{\bar{\mu}-r}{(1-p)\bar{\sigma}^2}$  for  $\beta < 0$  and  $\beta^* = 0$  for  $\beta \geq 0$ .

**Case 2**  $\underline{\mu} \leq r \leq \bar{\mu}$ : Clearly, the optimal leverage ratio here is  $\beta^* = 0$ .

**Case 3**  $r < \underline{\mu}$ : For non-negative  $\beta$ ,  $\beta^* = \frac{\mu-r}{(1-p)\bar{\sigma}^2}$ . Since  $\Lambda$  does not attain a maximum on  $[-5, 0)$ , but  $\sup_{\beta \in [-5, 0)} \Lambda(\beta) = \Lambda(0) = pr$ ,  $\beta^* = 0$ .

The outcomes align with economic intuition. A risk-averse investor who prepares for the worst-case will not invest in a leveraged ETF unless the entire range of potential reference asset returns consistently exceeds or falls below the interest rate. In other words, a positive leverage (long) is optimal only when even the worst-case drift parameter  $\underline{\mu}$  is greater than

$r$ , while a negative leverage (short) is chosen only if even the best-case drift parameter  $\bar{\mu}$  falls short of  $r$ .

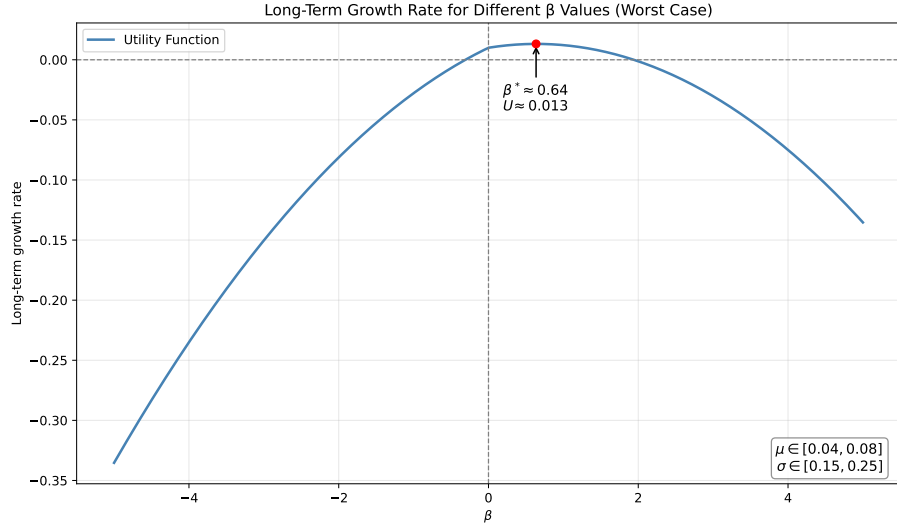


Figure 4.1: Long-term growth rate of the worst-case expected utility as a function of the leverage ratio  $\beta$  under the GBM model.

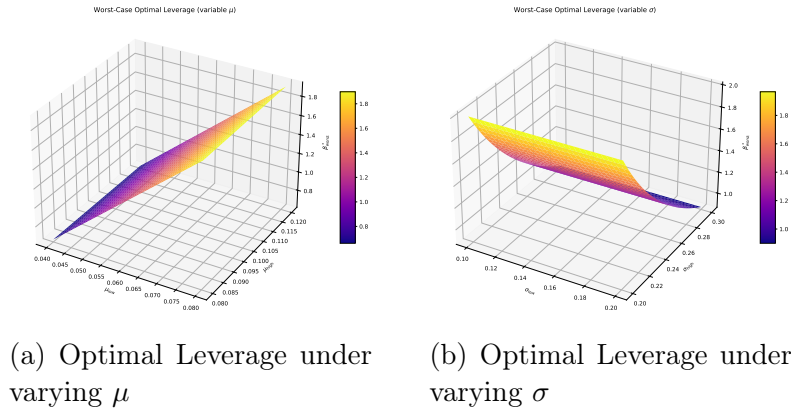


Figure 4.2: Impact of different intervals on the optimal leverage ratio.

**Remark 4.1** *Leung et al. [1, Remark 1]*

The results remains valid even when  $\mu$  and  $\sigma$  are extended to bounded progressively measurable processes. Indeed, the SDE

$$dX_t = \mu_t X_t dt + \sigma_t X_t dB_t, t \geq 0$$

has a unique strong solution, and a representation of the expected utility corresponding to (2.4) is written in the form

$$\begin{aligned} \mathbb{E}^{\mathbb{P}} [L_T^p] &= e^{-p(\beta-1)r} \mathbb{E}^{\hat{\mathbb{P}}} \left[ e^{\int_0^T (p\beta\mu_s - \frac{1}{2}p(1-p)\beta^2\sigma_s^2) ds} \right] \\ &\geq e^{p(\beta\mu^*(\beta) - (\beta-1)r)T - \frac{1}{2}p(1-p)\bar{\sigma}^2\beta^2 T}. \end{aligned}$$

Therefore, (4.5) holds for generalized  $\mu$  and  $\sigma$ .

## 4.2 CIR model

In this next example we will consider the Cox-Ingersoll-Ross model introduced in Cox et al. [52] as a short interest rate model. Hence we assume for the underlying  $X$  that it has the following dynamics:

$$dX_t = (b - aX_t) dt + \sigma \sqrt{X_t} dB_t, \quad (4.6)$$

with parameters  $a, \sigma > 0$  and  $2b \geq \sigma^2$ . The second condition,  $2b \geq \sigma^2$ , is the so called Feller condition and it ensures us that the process  $X$  is recurrent and a positive domain,  $D = (0, \infty)$ . In the CIR model, we assume uncertainty in  $b, a, \sigma$ . Therefore  $\underline{\alpha} = (\underline{b}, \underline{a}, \underline{\sigma})$ ,  $\bar{\alpha} = (\bar{b}, \bar{a}, \bar{\sigma})$  and  $[\underline{\alpha}, \bar{\alpha}] = [\underline{b}, \bar{b}] \times [\underline{a}, \bar{a}] \times [\underline{\sigma}, \bar{\sigma}]$  for  $\underline{a}, \underline{\sigma} > 0$  and  $\underline{b} \geq \bar{\sigma}^2$ . Next, the worst-case expected utility  $v_T$  is now derived with formulas (4.2) and (4.3) and noting that  $\frac{dX_t}{X_t} = \frac{(b-aX_t)}{X_t} dt + \sigma X_t^{-1/2} dB_t$

$$\begin{aligned} v_T &\stackrel{(4.2)}{=} \inf_{\alpha \in [\underline{\alpha}, \bar{\alpha}]} \mathbb{E}^{\mathbb{P}^\alpha}[L_T^p] = e^{-pr(\beta-1)T} \inf_{\alpha \in [\underline{\alpha}, \bar{\alpha}]} V(T; \alpha) \\ &\stackrel{(4.3)}{=} e^{-pr(\beta-1)T} \inf_{\alpha \in [\underline{\alpha}, \bar{\alpha}]} \mathbb{E}^{\mathbb{P}^\alpha} \left[ X_T^{p\beta} e^{-\frac{1}{2}p\beta(\beta-1) \int_0^T \sigma^2 X_s^{-1} ds} \right]. \end{aligned}$$

Consider the SDE

$$dY_t = \left( \frac{b}{\sigma^2} - aY_t \right) dt + \sqrt{Y_t} dB_t, \quad Y_0 = \frac{1}{\sigma^2}.$$

Then,  $Y := X/\sigma^2$  is the unique solution to this SDE, since

$$\begin{aligned} dY_t &= \frac{1}{\sigma^2} (b - aX_t) dt + \frac{1}{\sigma} \sqrt{X_t} dB_t = \left( \frac{b}{\sigma^2} - a \frac{X_t}{\sigma^2} \right) dt + \sqrt{\frac{1}{\sigma^2} X_t} dB_t \\ &= \left( \frac{b}{\sigma^2} - aY_t \right) dt + \sqrt{Y_t} dB_t, \\ Y_0 &= \frac{X_0}{\sigma^2} = \frac{1}{\sigma^2}. \end{aligned}$$

Furthermore,  $V$  satisfies

$$\begin{aligned} V(T; \alpha) &= \mathbb{E}^{\mathbb{P}^\alpha} \left[ X_T^{p\beta} e^{-\frac{1}{2}p\beta(\beta-1) \int_0^T \sigma^2 X_s^{-1} ds} \right] = \mathbb{E}^{\mathbb{P}^\alpha} \left[ \sigma^{2p\beta} Y_T^{p\beta} e^{-\frac{1}{2}p\beta(\beta-1) \int_0^T \sigma^2 \sigma^{-2} Y_s^{-1} ds} \right] \\ &= \sigma^{2p\beta} \mathbb{E}^{\mathbb{P}^\alpha} \left[ Y_T^{p\beta} e^{-\frac{1}{2}p\beta(\beta-1) \int_0^T Y_s^{-1} ds} \right]. \end{aligned} \quad (4.7)$$

Next, we consider the eigenpair problem for the infinitesimal generator of  $Y$ . For the operator  $\mathcal{L}$  as in (3.2) the eigenpair problem  $\mathcal{L}\phi = -\lambda\phi$  is expressed as

$$-\lambda\phi(y) = \frac{1}{2}y\phi''(y) + \left( \frac{b}{\sigma^2} - ay \right) \phi'(y) - \frac{1}{2}p\beta(\beta-1)y^{-1}\phi(y).$$

We show that a pair

$$(\lambda(b, a, \sigma), \phi(y)) = (a\eta(b, \sigma), y^{\eta(b, \sigma)})$$

where

$$\eta(b, \sigma) = -\left(\frac{b}{\sigma^2} - \frac{1}{2}\right) + \sqrt{\left(\frac{b}{\sigma^2} - \frac{1}{2}\right)^2 + p\beta(\beta - 1)} \quad (4.8)$$

is a solution to the eigenpair problem. To show that  $(\lambda(b, a, \sigma), \phi(y)) = (a\eta(b, \sigma), y^{\eta(b, \sigma)})$  is indeed a solution we follow a standard approach of solving eigenpair problems by assuming  $\phi$  to have form  $\phi(y) = y^\eta$  for some exponent  $\eta$ . First we compute derivatives  $\phi'(y) = \eta y^{\eta-1}$  and  $\phi''(y) = \eta(\eta-1)y^{\eta-2}$  and substitute this into the generator equation:

$$\begin{aligned} -\lambda y^\eta &= \frac{1}{2}y\eta(\eta-1)y^{\eta-2} + \left(\frac{b}{\sigma^2} - ay\right)\eta y^{\eta-1} - \frac{1}{2}p\beta(\beta-1)y^{-1}y^\eta \\ &= \frac{1}{2}\eta(\eta-1)y^{\eta-1} + \left(\frac{b}{\sigma^2} - ay\right)\eta y^{\eta-1} - \frac{1}{2}p\beta(\beta-1)y^{\eta-1} \\ &= y^{\eta-1} \left( \frac{1}{2}\eta(\eta-1) + \frac{b}{\sigma^2}\eta - \frac{1}{2}p\beta(\beta-1) \right) - a\eta y^\eta. \end{aligned} \quad (4.9)$$

For this equality to hold all coefficients in front of  $y^{\eta-1}$  have to be zero:

$$0 = \frac{1}{2}\eta(\eta-1) + \frac{b}{\sigma^2}\eta - \frac{1}{2}p\beta(\beta-1).$$

Rearranging the equation we arrive at

$$0 = \eta^2 + \left(\frac{2b}{\sigma^2} - 1\right)\eta - p\beta(\beta-1),$$

where the right hand sight now is just a quadratic function of  $\eta$ . Hence we get a solution as:

$$\begin{aligned} \eta(b, \sigma) &= \frac{1}{2} \left( \sqrt{\left(\frac{2b}{\sigma^2} - 1\right)^2 - 4(\beta p - \beta^2 p)} - \frac{2b}{\sigma^2} + 1 \right) \\ &= \sqrt{\left(\frac{b}{\sigma^2} - \frac{1}{2}\right)^2 - \beta p + \beta^2 p} - \frac{b}{\sigma^2} + \frac{1}{2} \\ &= -\left(\frac{b}{\sigma^2} - \frac{1}{2}\right) + \sqrt{\left(\frac{b}{\sigma^2} - \frac{1}{2}\right)^2 + p\beta(\beta-1)}. \end{aligned}$$

Therefore  $\phi(y) = y^{\eta(b, \sigma)}$  provides a solution to the eigenpair problem with  $\lambda(b, a, \sigma) = a\eta(b, \sigma)$  which we get by setting the coefficients of  $y^{\eta-1}$  in (4.9) to zero. Note that since we assumed  $b \geq \bar{\sigma}^2$ ,  $\eta$  is real.

Define the stochastic process  $(M_t)_{0 \leq t \leq T}$

$$M_t = \left(\frac{Y_t}{y}\right)^{\eta(b, \sigma)} e^{\lambda(b, a, \sigma)t - \frac{1}{2}p\beta(\beta-1) \int_0^t Y_s^{-1} ds}, \quad 0 \leq t \leq T.$$

We showed in Section 3.1 that  $e^{\lambda t - \int_0^t \mathcal{V}(X_s) ds} \frac{\phi(X_t)}{\phi(X_0)}$ , with  $\mathcal{V}(X_s)$  stemming from the expected utility (3.1) is a local martingale. Indeed  $M_t$  is of the form (3.4), since we have:

$$\mathbb{E}^{\mathbb{P}^\alpha} \left[ \sigma^{2p\beta} Y_T^{p\beta} e^{-\frac{1}{2}p\beta(\beta-1) \int_0^T Y_s^{-1} ds} \right] \text{ and } \mathcal{V}(Y_s) = \frac{1}{2}p\beta(\beta-1)Y_s^{-1}.$$

Hence

$$\begin{aligned} e^{\lambda t - \int_0^t \mathcal{V}(X_s) ds} \frac{\phi(X_t)}{\phi(X_0)} &= e^{\lambda(b,a,\sigma)t - \int_0^t \frac{1}{2} p\beta(\beta-1) Y_s^{-1} ds} \frac{Y_t^{\eta(b,a)}}{Y_0^{\eta(b,a)}} \\ &= \left( \frac{Y_t}{y} \right)^{\eta(b,a)} e^{\lambda(b,a,\sigma)t - \frac{1}{2} p\beta(\beta-1) \int_0^T Y_s^{-1} ds}, \text{ where } y = Y_0 = \frac{1}{\sigma^2}. \end{aligned}$$

Since  $\mathcal{V} \geq 0$  and  $\mathcal{V} \not\equiv 0$ ,  $M_t$  is even a true martingale and we can define a probability measure  $\mathbb{Q}^{b,a,\sigma}$  on  $\mathcal{F}_T$  via

$$\frac{d\mathbb{Q}^{b,a,\sigma}}{d\mathbb{P}} \Big|_{\mathcal{F}_T} = M_T.$$

Under  $\mathbb{Q}^{b,a,\sigma}$  the process  $Y$  satisfies

$$\begin{aligned} dY_t &= \left( \frac{b}{\sigma^2} - aY_t \right) dt + \sqrt{Y_t} dB_t = \left( \frac{b}{\sigma^2} - aY_t \right) dt + \sqrt{Y_t} \left( dB_t^{\mathbb{Q}^{b,a,\sigma}} + \eta(b,\sigma) \frac{1}{\sqrt{Y_t}} dt \right) \\ &= \left( \frac{b}{\sigma^2} + \eta(b,\sigma) - aY_t \right) dt + \sqrt{Y_t} dB_t^{\mathbb{Q}^{b,a,\sigma}}, \quad 0 \leq t \leq T, \end{aligned}$$

for a  $\mathbb{Q}^{b,a,\sigma}$ -Brownian motion

$$B_t^{\mathbb{Q}^{b,a,\sigma}} : \stackrel{(3.6)}{=} -\eta(b,\sigma) \int_0^t \frac{1}{\sqrt{Y_s}} ds + B_t, \quad 0 \leq t \leq T.$$

Now, we can rewrite (4.7) as follows:

$$\begin{aligned} V(T; b, a, \sigma) &\stackrel{(4.7)}{=} \sigma^{2p\beta} \mathbb{E}^{\mathbb{P}^\alpha} \left[ Y_T^{p\beta} e^{-\frac{1}{2} p\beta(\beta-1) \int_0^T Y_s^{-1} ds} \right] \\ &= \sigma^{2p\beta} \mathbb{E}^{\mathbb{Q}^{b,a,\sigma}} \left[ \frac{d\mathbb{P}}{d\mathbb{Q}^{b,a,\sigma}} Y_T^{p\beta} e^{-\frac{1}{2} p\beta(\beta-1) \int_0^T Y_s^{-1} ds} \right] \\ &= \sigma^{2p\beta} \mathbb{E}^{\mathbb{Q}^{b,a,\sigma}} \left[ \left( \frac{Y_T}{y} \right)^{-\eta(b,\sigma)} e^{-\lambda(b,a,\sigma)T + \frac{1}{2} p\beta(\beta-1) \int_0^T Y_s^{-1} ds} Y_T^{p\beta} e^{-\frac{1}{2} p\beta(\beta-1) \int_0^T Y_s^{-1} ds} \right] \\ &= e^{-\lambda(b,a,\sigma)T} \sigma^{2p\beta} \mathbb{E}^{\mathbb{Q}^{b,a,\sigma}} \left[ Y_T^{p\beta - \eta(b,\sigma)} y^{\eta(b,\sigma)} \right] \\ &= e^{-\lambda(b,a,\sigma)T} \sigma^{2(p\beta - \eta(b,\sigma))} \mathbb{E}^{\mathbb{Q}^{b,a,\sigma}} \left[ Y_T^{p\beta - \eta(b,\sigma)} \right]. \end{aligned} \tag{4.10}$$

The process  $Y$  is recurrent, since it satisfies the Feller condition. Hence, reasoning with Proposition 3.1, the invariant probability density of the process  $Y$  under  $\mathbb{Q}^{b,a,\sigma}$  is given as

$$\psi(y) = \frac{(2a)^{\frac{2b}{\sigma^2} + 2\eta(b,\sigma)}}{\Gamma(\frac{2b}{\sigma^2} + 2\eta(b,\sigma))} y^{\frac{2b}{\sigma^2} + 2\eta(b,\sigma) - 1} e^{-2ay}.$$

Also,

$$\int_0^\infty y^{p\beta - \eta(b,\sigma)} \psi(y) dy < \infty \tag{4.11}$$

and the expectation  $\mathbb{E}^{\mathbb{Q}^{b,a,\sigma}} \left[ Y_T^{p\beta-\eta(b,\sigma)} \right]$  converges to (4.11) as  $T \rightarrow \infty$ .

Now we differentiate between different values of  $\beta$ :

**Case 1**  $\beta \geq 1$ :

We verify our conditions for Proposition 3.2. Let  $(b, a, \sigma) \in [\underline{b}, \bar{b}] \times [\underline{a}, \bar{a}] \times [\underline{\sigma}, \bar{\sigma}]$  and  $y \in (0, \infty)$ . First we see that  $Y_0^{b,a\sigma} = \frac{1}{\sigma^2} \geq \frac{1}{\bar{\sigma}^2} = Y_0^{b,\bar{a},\bar{\sigma}}$ . Next, we also see that  $\frac{b}{\sigma^2} - ay \geq \frac{b}{\bar{\sigma}^2} - \bar{a}y$  and  $\frac{b}{\sigma^2} - ax - \frac{b}{\sigma^2} + ay = a(-x + y) \leq a|x - y|$ . Hence the drift term is a Lipschitz continuous in  $y$ . Lastly, the diffusion term satisfies the condition (3.9) with  $h(y) = \sqrt{y}$ :

$$|\sigma(t, x) - \sigma(t, y)| = |\sqrt{x} - \sqrt{y}| \leq \sqrt{|x - y|}.$$

Thus, we can apply Proposition 3.2 to get the inequality

$$\begin{aligned} V(T; b, a, \sigma) &= \sigma^{2p\beta} \mathbb{E}^{\mathbb{P}^{p,a,\sigma}} \left[ Y_T^{p\beta} e^{-\frac{1}{2}p\beta(\beta-1) \int_0^T Y_s^{-1} ds} \right] \\ &\geq \underline{\sigma}^{2p\beta} \mathbb{E}^{\mathbb{P}^{b,\bar{a},\bar{\sigma}}} \left[ Y_T^{p\beta} e^{-\frac{1}{2}p\beta(\beta-1) \int_0^T Y_s^{-1} ds} \right] \end{aligned}$$

and therefore

$$\begin{aligned} v_T &= e^{-pr(\beta-1)T} \inf_{\alpha \in [\underline{\alpha}, \bar{\alpha}]} \underbrace{V(T, \alpha)}_{\mathbb{E}^{\mathbb{P}^{b,\bar{a},\bar{\sigma}}} \left[ Y_T^{p\beta} e^{-\frac{1}{2}p\beta(\beta-1) \int_0^T Y_s^{-1} ds} \right]} \\ &\geq \underbrace{\underline{\sigma}^{2p\beta}}_{\geq (\frac{\underline{\sigma}}{\bar{\sigma}})^{2p\beta}, \text{ since } \underline{\sigma} \geq 0} \mathbb{E}^{\mathbb{P}^{b,\bar{a},\bar{\sigma}}} \left[ Y_T^{p\beta} e^{-\frac{1}{2}p\beta(\beta-1) \int_0^T Y_s^{-1} ds} \right] \\ &\geq e^{-pr(\beta-1)T} (\underline{\sigma}/\bar{\sigma})^{2p\beta} \mathbb{E}^{\mathbb{P}^{b,\bar{a},\bar{\sigma}}} \left[ Y_T^{p\beta} e^{-\frac{1}{2}p\beta(\beta-1) \int_0^T Y_s^{-1} ds} \right] \\ &= e^{-pr(\beta-1)T} (\underline{\sigma}/\bar{\sigma})^{2p\beta} V(T; \underline{b}, \bar{a}, \bar{\sigma}). \end{aligned}$$

We apply the Hansen-Scheinkman decomposition to  $V(T; \underline{b}, \bar{a}, \bar{\sigma})$ , so that

$$V(T; \underline{b}, \bar{a}, \bar{\sigma}) = e^{-\lambda(\underline{b}, \bar{a}, \bar{\sigma})T} \bar{\sigma}^{2(p\beta-\eta(\underline{b}, \bar{\sigma}))} \mathbb{E}^{\mathbb{Q}^{\underline{b}, \bar{a}, \bar{\sigma}}} \left[ Y_T^{p\beta-\eta(\underline{b}, \bar{\sigma})} \right], \quad (4.12)$$

where the dynamics of  $Y$  are now

$$dY_t = (\underline{b}/\bar{\sigma}^2 + \eta(\underline{b}, \bar{\sigma}) - \bar{a}Y_t) dt + \sqrt{Y_t} dB_t^{\mathbb{Q}^{\underline{b}, \bar{a}, \bar{\sigma}}}, \quad 0 \leq t \leq T, \quad Y_0 = 1/\bar{\sigma}^2, \quad \mathbb{Q}^{\underline{b}, \bar{a}, \bar{\sigma}}\text{-a.s.}$$

For  $2\underline{b}/\bar{\sigma}^2 + \eta(\underline{b}, \bar{\sigma}) + p\beta > 0$ , convergence of the gamma function in terms of (4.11) with changed  $b$  and  $\sigma$  is assured and the expectation on the right-hand side of (4.12) converges to some positive constant. Hence,

$$\begin{aligned} &\liminf_{T \rightarrow \infty} \frac{1}{T} \log v_T \\ &\geq \liminf_{T \rightarrow \infty} \frac{1}{T} \log \left( e^{-pr(\beta-1)T} \left( \frac{\underline{\sigma}}{\bar{\sigma}} \right)^{2p\beta} e^{-\overbrace{\lambda(\underline{b}, \bar{a}, \bar{\sigma})T}^{=a\eta(\underline{b}, \bar{\sigma})} \bar{\sigma}^{2(p\beta-\eta(\underline{b}, \bar{\sigma}))}} \mathbb{E}^{\mathbb{Q}^{\underline{b}, \bar{a}, \bar{\sigma}}} \left[ Y_T^{p\beta-\eta(\underline{b}, \bar{\sigma})} \right] \right) \\ &= \liminf_{T \rightarrow \infty} \frac{1}{T} \log \left( e^{-pr(\beta-1)T} e^{-a\eta(\underline{b}, \bar{\sigma})T} \underline{\sigma}^{2p\beta} \bar{\sigma}^{-2\eta(\underline{b}, \bar{\sigma})} \mathbb{E}^{\mathbb{Q}^{\underline{b}, \bar{a}, \bar{\sigma}}} \left[ Y_T^{p\beta-\eta(\underline{b}, \bar{\sigma})} \right] \right) \quad (4.13) \\ &= -pr(\beta-1) - \bar{a}\eta(\underline{b}, \bar{\sigma}) + \lim_{T \rightarrow \infty} \frac{1}{T} \left( \log \underbrace{\underline{\sigma}^{2p\beta} \bar{\sigma}^{-2\eta(\underline{b}, \bar{\sigma})}}_{<\infty} + \log \underbrace{\mathbb{E}^{\mathbb{Q}^{\underline{b}, \bar{a}, \bar{\sigma}}} \left[ Y_T^{p\beta-\eta(\underline{b}, \bar{\sigma})} \right]}_{\text{converges to 4.11 for } T \rightarrow \infty} \right) \\ &= -pr(\beta-1) - \bar{a}\eta(\underline{b}, \bar{\sigma}). \end{aligned}$$

On the other hand the definition of  $v_T$  implies the following inequality:

$$v_T = e^{-pr(\beta-1)T} \inf_{\alpha \in [\underline{\alpha}, \bar{\alpha}]} V(T; b, a, \sigma) \leq e^{-pr(\beta-1)T} V(T; \underline{b}, \bar{a}, \bar{\sigma}).$$

This implies

$$\log v_T \leq -(pr(\beta-1) + \bar{a}\eta(\underline{b}, \bar{\sigma}))T + 2(p\beta - \eta(\underline{b}, \bar{\sigma})) \log \bar{\sigma} + \log \mathbb{E}^{\mathbb{Q}^{\underline{b}, \bar{a}, \bar{\sigma}}} \left[ Y_T^{p\beta - \eta(\underline{b}, \bar{\sigma})} \right].$$

This leads now to

$$\limsup_{T \rightarrow \infty} \frac{1}{T} \log v_T \leq -pr(\beta-1) - \bar{a}\eta(\underline{b}, \bar{\sigma}), \quad (4.14)$$

since  $\mathbb{E}^{\mathbb{Q}^{\underline{b}, \bar{a}, \bar{\sigma}}} \left[ Y_T^{p\beta - \eta(\underline{b}, \bar{\sigma})} \right]$  is finite for  $2\underline{b}/\bar{\sigma}^2 + \eta(\underline{b}, \bar{\sigma}) + p\beta > 0$  as mentioned above. Thus both inequalities, (4.13) and (4.14), together we get

$$\lim_{T \rightarrow \infty} \frac{1}{T} \log v_T = -pr(\beta-1) - \bar{a}\eta(\underline{b}, \bar{\sigma}).$$

**Case 2**  $0 \leq \beta < 1$ :

Similarly to Case 1, we apply Proposition 3.2 to (4.10), so that

$$V(T; b, a, \sigma) \geq e^{-\underline{a}\eta(\bar{b}, \underline{\sigma})T} \sigma^{2(p\beta - \eta(\bar{b}, \underline{\sigma}))} \mathbb{E}^{\mathbb{Q}^{\bar{b}, \bar{a}, \bar{\sigma}}} \left[ Y_T^{p\beta - \eta(\bar{b}, \underline{\sigma})} \right].$$

By representation (4.8) we can readily see that in this case  $\eta < 0$ . Next, we have on the one hand

$$v_T \leq e^{-pr(\beta-1)T} V(T; \bar{b}, \underline{a}, \underline{\sigma})$$

and on the other hand

$$\begin{aligned} v_t &= e^{-pr(\beta-1)T} \inf_{\alpha \in [\underline{\alpha}, \bar{\alpha}]} \underbrace{V(T, \alpha)}_{\geq e^{-\underline{a}\eta(\bar{b}, \underline{\sigma})T} \sigma^{2(p\beta - \eta(\bar{b}, \underline{\sigma}))} \mathbb{E}^{\mathbb{Q}^{\bar{b}, \bar{a}, \bar{\sigma}}} \left[ Y_T^{p\beta - \eta(\bar{b}, \underline{\sigma})} \right] } \\ &\geq e^{-(pr(\beta-1) + \underline{a}\eta(\bar{b}, \underline{\sigma}))T} \sigma^{2(p\beta - \eta(\bar{b}, \underline{\sigma}))} \mathbb{E}^{\mathbb{Q}^{\bar{b}, \bar{a}, \bar{\sigma}}} \left[ Y_T^{p\beta - \eta(\bar{b}, \underline{\sigma})} \right]. \end{aligned}$$

Combining both inequalities we end up with the following result:

$$\lim_{T \rightarrow \infty} \frac{1}{T} \log v_T = -pr(\beta-1) - \underline{a}\eta(\bar{b}, \underline{\sigma}).$$

**Case 3**  $\beta < 0$ :

Let  $(b, \sigma) \in [\underline{b}, \bar{b}] \times [\underline{\sigma}, \bar{\sigma}]$ . Then,

$$\begin{aligned} p\beta - \eta(b, \sigma) &= p\beta + \left( \frac{b}{\sigma^2} - \frac{1}{2} \right) - \sqrt{\left( \frac{b}{\sigma^2} - \frac{1}{2} \right)^2 + \underbrace{p\beta(\beta-1)}_{>0}} \\ &< p\beta + \left( \frac{b}{\sigma^2} - \frac{1}{2} \right) - \sqrt{\left( \frac{b}{\sigma^2} - \frac{1}{2} \right)^2} \\ &= p\beta < 0. \end{aligned}$$

Similar to what we have seen now twice before, Proposition 3.2 leads in this case to the inequality

$$e^{-(pr(\beta-1)+\bar{a}\eta(\underline{b},\bar{\sigma}))T}\sigma^{2(p\beta-\eta(\underline{b},\bar{\sigma}))}\mathbb{E}^{\mathbb{Q}^{\bar{b},\underline{a},\sigma}}\left[Y_T^{p\beta-\eta(\underline{b},\bar{\sigma})}\right]\leq v_T\leq e^{-pr(\beta-1)T}V(T;\underline{b},\bar{a},\bar{\sigma}).$$

This then results with similar argumentation as before in

$$\lim_{T\rightarrow\infty}\frac{1}{T}\log v_T=-pr(\beta-1)-\bar{a}\eta(\underline{b},\bar{\sigma}).$$

We now summarize these results in the following Proposition.

**Proposition 4.2** *Leung et al. [1, Proposition 3]*

Let  $0 < \underline{a} \leq \bar{a}$ ,  $0 < \underline{\sigma} \leq \bar{\sigma}$ ,  $\bar{\sigma}^2 \leq \underline{b} \leq \bar{b}$  and  $X^\alpha$  be the CIR process (4.6) with set of parameters  $\alpha = (b, a, \sigma)$  ranging over  $[\underline{\alpha}, \bar{\alpha}] = [\underline{b}, \bar{b}] \times [\underline{a}, \bar{a}] \times [\underline{\sigma}, \bar{\sigma}]$ . Then, the long-term growth rate of the worst-case expected utility of the LETF  $L^\alpha = (L_t^\alpha)_{t \geq 0}$ , with the reference process  $X$ , is given by

$$\lim_{T\rightarrow\infty}\frac{1}{T}\log_{\alpha\in[\underline{\alpha},\bar{\alpha}]}\mathbb{E}^{\mathbb{P}^\alpha}[L_T^p]=-pr(\beta-1)-a^*(\beta)\eta(b^*(\beta),\sigma^*(\beta),\beta),$$

provided  $2\underline{b}/\bar{\sigma}^2 + \eta + p\beta > 0$ , where  $\eta(b, \sigma, \beta) = -\left(\frac{\underline{b}}{\sigma^2} - \frac{1}{2}\right) + \sqrt{\left(\frac{\underline{b}}{\sigma^2} - \frac{1}{2}\right)^2 + p\beta(\beta-1)}$ ,

$$b^*(\beta)=\begin{cases}\underline{b}, & \beta\geq 1, \beta<0\\\bar{b}, & 0\leq\beta<1\end{cases}, a^*(\beta)=\begin{cases}\bar{a}, & \beta\geq 1, \beta<0\\\underline{a}, & 0\leq\beta<1\end{cases}, \sigma^*(\beta)=\begin{cases}\bar{\sigma}, & \beta\geq 1, \beta<0\\\underline{\sigma}, & 0\leq\beta<1\end{cases}.$$

To find the optimal leverage ratio  $\beta^* \in [\underline{\beta}, \bar{\beta}]$ , which maximizes the robust long term growth rate we will need to differentiate between different cases. Proposition 4.2 indicates how the  $\beta$  depends on the parameters. We define a function  $\Lambda$  as the robust long term growth rate depending on  $\beta$ , i.e.

$$\Lambda(\beta):=-pr(\beta-1)-a^*(\beta)\eta(b^*(\beta),\sigma^*(\beta),\beta).$$

**Case 1**  $\beta \geq 1$  :

We differentiate the function  $\Lambda$  and see that

$$\Lambda'(\beta)=-pr-\frac{\bar{a}p(2\beta-1)}{2\sqrt{\left(\underline{b}/\bar{\sigma}^2-\frac{1}{2}\right)^2+p\beta(\beta-1)}}$$

is definitely negative. Hence  $\Lambda$  achieves its maximum value on the lowest possible value on  $[1, 5]$ , hence at  $\beta = 1$ . However, since not investing in a LETF is also always an option, we rule out  $\beta = 1$  to be optimal, since

$$\Lambda(1)=0 < pr = \Lambda(0).$$

**Case 2**  $0 \leq \beta < 1$  :

In case of  $r^p \geq \bar{a}^2$ , or under the condition that both  $r^2p < \bar{a}^2$  and  $2\underline{b}/\bar{\sigma}^2 - 1 \geq \bar{a}/r$ , one can obtain that  $\Lambda'(\beta) < 0$  on  $[0, 1]$ . Therefore,  $\beta^* = 0$ . Otherwise,  $\beta^* =$

$$\frac{1}{2} \left( 1 - \sqrt{\frac{(2b/\bar{\sigma}^2 - 1)^2 - p}{(\bar{a}/r)^2 - p}} \right).$$

**Case 3**  $\beta < 0$  :

In case of  $r^p \geq \underline{a}^2$ , or under the condition that both  $r^2 p < \underline{a}^2$  and  $2\bar{b}/\underline{\sigma}^2 - 1 \leq \underline{a}/r$ , one can obtain that  $\Lambda'(\beta) < 0$  on  $[-5, 0)$ . Therefore,  $\beta^* = -5$ . Otherwise,  $\beta^* = \frac{1}{2} \left( 1 - \sqrt{\frac{(2\bar{b}/\underline{\sigma}^2 - 1)^2 - p}{(\underline{a}/r)^2 - p}} \right)$ .

Hence we see that the overall optimal value of  $\beta^*$  is depending on the relationship between the parameters  $a, b, \sigma, r, p$ . Therefore  $\beta^*$  may change with the uncertainty set. The table below illustrates our results.

Table 4.1: Optimal leverage ratio candidates based on the parameter relationships for the CIR reference process.

Parameter relationship	Condition 1	Condition 2	Candidates for $\beta^*$
$p \geq \frac{\bar{a}^2}{r^2}$			$0, \underline{\beta}$
$\frac{\underline{a}^2}{r^2} \leq p < \frac{\bar{a}^2}{r^2}$	$\frac{2b}{\bar{\sigma}^2} - 1 \geq \frac{\bar{a}}{r}$	$\frac{2b}{\bar{\sigma}^2} - 1 < \frac{\bar{a}}{r}$	$\frac{1}{2} \left( 1 - \sqrt{\frac{(\frac{2b}{\bar{\sigma}^2} - 1)^2 - p}{(\frac{\bar{a}}{r})^2 - p}} \right), \underline{\beta}$
$p < \frac{\underline{a}^2}{r^2}$	$\frac{2b}{\bar{\sigma}^2} - 1 \geq \frac{\bar{a}}{r}$		$0, \frac{1}{2} \left( 1 - \sqrt{\frac{(\frac{2b}{\bar{\sigma}^2} - 1)^2 - p}{(\frac{\bar{a}}{r})^2 - p}} \right)$
	$\frac{2b}{\bar{\sigma}^2} - 1 < \frac{\bar{a}}{r}$	$\frac{2\bar{b}}{\underline{\sigma}^2} - 1 > \frac{\underline{a}}{r}$	$\frac{1}{2} \left( 1 - \sqrt{\frac{(\frac{2b}{\bar{\sigma}^2} - 1)^2 - p}{(\frac{\bar{a}}{r})^2 - p}} \right), \frac{1}{2} \left( 1 - \sqrt{\frac{(\frac{2\bar{b}}{\underline{\sigma}^2} - 1)^2 - p}{(\frac{\underline{a}}{r})^2 - p}} \right)$
		$\frac{2\bar{b}}{\underline{\sigma}^2} - 1 \leq \frac{\underline{a}}{r}$	$\frac{1}{2} \left( 1 - \sqrt{\frac{(\frac{2b}{\bar{\sigma}^2} - 1)^2 - p}{(\frac{\bar{a}}{r})^2 - p}} \right), \underline{\beta}$

### 4.3 3/2 model

For our next example we will investigate the 3/2 model, which is a non-affine model and has dynamics

$$dX_t = (b - aX_t) X_t dt + \sigma X_t^{3/2} dB_t \quad (4.15)$$

with  $b, \sigma > 0$ , and  $a \geq -\sigma^2/2$ . The CIR process, the solution to (4.15) is always positive, i.e.  $D = (0, \infty)$ . The 3/2 model arised as an alternative to the CIR model for stochastic volatility (Carr and Sun [53], Drimus [54]) and short interest rates (Ahn and Gao [55]). Here, we set the model parameters to be  $\underline{\alpha} = (\underline{b}, \underline{a}, \underline{\sigma})$ ,  $\bar{\alpha} = (\bar{b}, \bar{a}, \bar{\sigma})$  and  $[\underline{\alpha}, \bar{\alpha}] = [\underline{b}, \bar{b}] \times [\underline{a}, \bar{a}] \times [\underline{\sigma}, \bar{\sigma}]$ , where  $\underline{b}, \bar{a}, \underline{\sigma}, \bar{\sigma} > 0$ . The worst-case expected utility  $v_T$  in this model is expressed as

$$\begin{aligned} v_T &= e^{-pr(\beta-1)T} \inf_{\alpha \in [\underline{\alpha}, \bar{\alpha}]} V(T; \alpha) \\ &= e^{-pr(\beta-1)T} \inf_{\alpha \in [\underline{\alpha}, \bar{\alpha}]} \mathbb{E}^{\mathbb{P}^\alpha} \left[ X^{p\beta} e^{-\frac{1}{2}p\beta(\beta-1) \int_0^T \sigma^2 X_s ds} \right]. \end{aligned}$$

Define  $Y := \sigma^2 X$ . Then we readily see that this can be seen as another  $3/2$  process with dynamics

$$dY_t = \left( b - \frac{a}{\sigma^2} Y_t \right) Y_t dt + Y_t^{3/2} dB_t, \quad Y_0 = \sigma^2.$$

Hence, with our definition of  $Y$  at hand we can rewrite  $V$  in terms of this new process:

$$\begin{aligned} V(T; \alpha) &= \mathbb{E}^{\mathbb{P}^\alpha} \left[ X_T^{p\beta} e^{-\frac{1}{2}p\beta(\beta-1) \int_0^T \overbrace{\sigma^2(X_s)}^{\sigma X_s^{1/2}} X_s ds} \right] \\ &= \mathbb{E}^{\mathbb{P}^\alpha} \left[ \left( \frac{Y_T}{\sigma^2} \right)^{p\beta} e^{-\frac{1}{2}p\beta(\beta-1) \int_0^T \sigma^2 X_s^{1/2} X_s ds} \right] \\ &= \sigma^{-2p\beta} \mathbb{E}^{\mathbb{P}^\alpha} \left[ Y_T^{p\beta} e^{-\frac{1}{2}p\beta(\beta-1) \int_0^T Y_s ds} \right]. \end{aligned} \tag{4.16}$$

We seek a solution to the eigenpair problem  $\mathcal{L}\phi = -\lambda\phi$  for the infinitesimal generator of  $Y$ :

$$-\lambda\phi = \frac{1}{2}\sigma^2(y)\phi''(y) + \mu(y)\phi'(y) - \frac{1}{2}p\beta(\beta-1)y\phi(y).$$

One can show that one solution is given by

$$(\lambda(b, a, \sigma), \phi(y)) = (b\eta(a, \sigma), y^{-\eta(a, \sigma)}),$$

where

$$\eta(a, \sigma) = -\left(\frac{a}{\sigma^2} + \frac{1}{2}\right) + \sqrt{\left(\frac{a}{\sigma^2} + \frac{1}{2}\right)^2 + p\beta(\beta-1)}.$$

Since we assumed  $a/\sigma^2 > 0$ ,  $\eta$  is real.

In the following we will show again how we can use the Hansen-Scheinkman decomposition on  $V(T; b, a, \sigma)$ . We showed in Section 3.1 that

$$M_t = e^{\lambda t - \int_0^t \mathcal{V}(X_s) ds} \frac{\phi(X_t)}{\phi(X_0)} = \left( \frac{Y_t}{y} \right)^{-\eta(a, \sigma)} e^{\lambda(b, a, \sigma)t - \frac{1}{2}p\beta(\beta-1) \int_0^t Y_s ds}, \quad 0 \leq t \leq T$$

with  $\mathcal{V}(X_s)$  stemming from the expected utility (3.1) and  $y = \sigma^2$  is a local martingale. Since  $\mathcal{V} \geq 0$  and  $\mathcal{V} \not\equiv 0$ ,  $M_t$  is even a true martingale and we can define a probability measure  $\mathbb{Q}^{b, a, \sigma}$  on  $\mathcal{F}_T$  via

$$\frac{d\mathbb{Q}^{b, a, \sigma}}{d\mathbb{P}} \Big|_{\mathcal{F}_T} = M_T = \left( \frac{Y_T}{y} \right)^{-\eta(a, \sigma)} e^{\lambda(b, a, \sigma)T - \frac{1}{2}p\beta(\beta-1) \int_0^T Y_s ds}. \tag{4.17}$$

Under  $\mathbb{Q}^{b, a, \sigma}$  the process  $Y$  now satisfies

$$\begin{aligned} dY_t &= \left( b - \frac{a}{\sigma^2} Y_t \right) Y_t dt + Y_t^{3/2} dB_t \\ &= \left( b - \frac{a}{\sigma^2} Y_t \right) Y_t + Y_t^{3/2} \left( dB_t^{\mathbb{Q}^{b, a, \sigma}} - \eta(a, \sigma) \sqrt{Y_t} dt \right) \\ &= \left( b - \left( \frac{a}{\sigma^2} + \eta(a, \sigma) \right) Y_t \right) Y_t dt + Y_t^{3/2} dB_t^{\mathbb{Q}^{b, a, \sigma}} dt, \quad 0 \leq t \leq T, \end{aligned}$$

for a  $\mathbb{Q}^{b,a,\sigma}$ -Brownian motion

$$B_t^{\mathbb{Q}^{b,a,\sigma}} := \eta(a, \sigma) \int_0^t \sqrt{Y_s} ds + B_t, \quad 0 \leq t \leq T.$$

Now we can also rewrite  $V$  in (4.16):

$$\begin{aligned} V(T; b, a, \sigma) &= \sigma^{-2p\beta} \mathbb{E}^{\mathbb{P}^\alpha} \left[ Y_T^{p\beta} e^{-\frac{1}{2}p\beta(\beta-1) \int_0^T Y_s ds} \right] \\ &= \sigma^{-2p\beta} \mathbb{E}^{\mathbb{Q}^{b,a,\sigma}} \left[ \frac{d\mathbb{P}}{d\mathbb{Q}^{b,a,\sigma}} Y_T^{p\beta} e^{-\frac{1}{2}p\beta(\beta-1) \int_0^T Y_s ds} \right] \\ &= \sigma^{-2p\beta} \mathbb{E}^{\mathbb{Q}^{b,a,\sigma}} \left[ \left( \frac{Y_T}{y} \right)^{\eta(a,\sigma)} e^{-\lambda(b,a,\sigma)T + \frac{1}{2}p\beta(\beta-1) \int_0^T Y_s ds} Y_T^{p\beta} e^{-\frac{1}{2}p\beta(\beta-1) \int_0^T Y_s ds} \right] \\ &= \sigma^{-2p\beta} \mathbb{E}^{\mathbb{Q}^{b,a,\sigma}} \left[ \sigma^{-2\eta(a,\sigma)} Y_T^{\eta(a,\sigma)} e^{-\lambda(b,a,\sigma)T} \right] \\ &= e^{-\lambda(b,a,\sigma)T} \sigma^{-2(p\beta+\eta(a,\sigma))} \mathbb{E}^{\mathbb{Q}^{b,a,\sigma}} \left[ Y_T^{\eta(a,\sigma)} \right]. \end{aligned} \tag{4.18}$$

Using Proposition 3.1, we derive that the invariant probability density of the process  $Y$  under  $\mathbb{Q}^{b,a,\sigma}$  is

$$\psi(y) = \frac{(2b)^{\frac{2a}{\sigma^2} + 2\eta(b,\sigma)}}{\Gamma(\frac{2a}{\sigma^2} + 2\eta(b,\sigma) + 2)} y^{-\frac{2a}{\sigma^2} - 2\eta(b,\sigma) - 3} e^{-\frac{2b}{y}}.$$

Thus, we can show that

$$\int_0^\infty y^{p\beta+\eta(a,\sigma)} \psi(y) dy < \infty. \tag{4.19}$$

As a result, the expectation on the right-hand side of (4.18) converges to the expression in (4.19). Moreover, Proposition 3.2 can also be applied to the process  $Y$ , assuming  $Y^{-1}$  also has CIR dynamics.

### Case 1 $\beta \geq 1$ :

Similar to before in the CIR model we can apply Proposition 3.2 to (4.18), to derive the inequality

$$V(T; b, a, \sigma) \geq e^{-\bar{b}\eta(\underline{a}, \bar{\sigma})T} \bar{\sigma}^{-2(p\beta+\eta(\underline{a}, \bar{\sigma}))} \mathbb{E}^{\mathbb{Q}^{\underline{b}, \bar{a}, \underline{\sigma}}} \left[ Y_T^{p\beta+\eta(\underline{a}, \bar{\sigma})} \right],$$

Multiplying by  $e^{-pr(\beta-1)T}$  and using the definition of  $v_T$  we derive

$$e^{-pr(\beta-1)+\bar{b}\eta(\underline{a}, \bar{\sigma})T} \bar{\sigma}^{-2(p\beta+\eta(\underline{a}, \bar{\sigma}))} \mathbb{E}^{\mathbb{Q}^{\underline{b}, \bar{a}, \underline{\sigma}}} \left[ Y_T^{p\beta+\eta(\underline{a}, \bar{\sigma})} \right] \leq v_T \leq e^{-pr(\beta-1)T} V(T; \bar{b}, \underline{a}, \bar{\sigma}).$$

Hence by using the Hansen-Scheinkman decomposition of  $V(T; \bar{b}, \underline{a}, \bar{\sigma})$  and since the expectation,  $\mathbb{E}^{\mathbb{Q}^{\underline{b}, \bar{a}, \underline{\sigma}}} \left[ Y_T^{p\beta+\eta(\underline{a}, \bar{\sigma})} \right]$ , is finite in the limit  $T \rightarrow \infty$  we get:

$$\lim_{T \rightarrow \infty} \frac{1}{T} \log v_T = -pr(\beta-1) - \bar{b}\eta(\underline{a}, \bar{\sigma}).$$

### Case 2 $0 \leq \beta < 1$ :

We note that  $\eta < 0$  for  $0 < \beta < 1$  and  $p\beta + \eta(a, \sigma) < 0$  for all  $(a, \sigma) \in [\underline{a}, \bar{a}] \times [\underline{\sigma}, \bar{\sigma}]$ . Hence we obtain,

$$\lim_{T \rightarrow \infty} \frac{1}{T} \log v_T = -pr(\beta-1) - \underline{b}\eta(\bar{a}, \underline{\sigma}),$$

where we see that this is exactly the reverse outcome of what we derive in Case 1.

**Case 3**  $\beta < 0$  :

Let  $\alpha = (b, a, \sigma) \in [\underline{a}, \bar{a}]$ , then similarly to Case 1 in the CIR model we derive

$$\begin{aligned} V(T; b, a, \sigma) &= \sigma^{-2p\beta} \mathbb{E}^{\mathbb{P}^{b,a,\sigma}} \left[ Y_T^{p\beta} e^{-\frac{1}{2}p\beta(\beta-1) \int_0^T Y_s ds} \right] \\ &\geq \underline{\sigma}^{-2p\beta} \mathbb{E}^{\mathbb{P}^{\bar{b},\underline{a},\bar{\sigma}}} \left[ Y_T^{p\beta} e^{-\frac{1}{2}p\beta(\beta-1) \int_0^T Y_s ds} \right] \\ &= (\underline{\sigma}/\bar{\sigma})^{-2p\beta} V(T; \bar{b}, \underline{a}, \bar{\sigma}) \end{aligned}$$

and hence

$$v_T \geq e^{-pr(\beta-1)T} (\underline{\sigma}/\bar{\sigma})^{-2p\beta} V(T; \bar{b}, \underline{a}, \bar{\sigma}).$$

Similarly to what we have seen some times now, applying the Hansen-Scheinkman decomposition to  $V(T; \bar{b}, \underline{a}, \bar{\sigma})$  we have

$$V(T; \bar{b}, \underline{a}, \bar{\sigma}) = e^{-\lambda(\bar{b}, \underline{a}, \bar{\sigma})T} \bar{\sigma}^{-2(p\beta + \eta(\underline{a}, \bar{\sigma}))} \mathbb{E}^{\mathbb{Q}^{\bar{b}, \underline{a}, \bar{\sigma}}} \left[ Y_T^{p\beta + \eta(\underline{a}, \bar{\sigma})} \right], \quad (4.20)$$

where the process  $Y$  now has dynamics

$$dY_t = \left( \bar{b} - \left( \frac{\underline{a}}{\bar{\sigma}^2} + \eta(\underline{a}, \bar{\sigma}) \right) Y_t \right) Y_t dt + Y_t^{3/2} dB_t^{\mathbb{Q}}, \quad Y_0 = \bar{\sigma}^2, \quad \mathbb{Q}^{\bar{b}, \underline{a}, \bar{\sigma}}\text{-a.s.}$$

If  $2(\underline{a}/\bar{\sigma}^2 + 1) + \eta(\underline{a}, \bar{\sigma}) - p\beta > 0$ , the convergence of the gamma function in terms of (4.19) with changed  $a$  and  $\sigma$  is assured and the expectation on the right-hand side of (4.20) converges to some constant and we derive that  $\frac{1}{T} \log V(T; \bar{b}, \underline{a}, \bar{\sigma})$  converges to  $-\lambda(\bar{b}, \underline{a}, \bar{\sigma}) = -\bar{b}\eta(\underline{a}, \bar{\sigma})$  as  $T \rightarrow \infty$ . Hence,

$$\begin{aligned} \liminf_{T \rightarrow \infty} \frac{1}{T} \log v_T &\geq -pr(\beta-1) - \bar{b}\eta(\underline{a}, \bar{\sigma}) \\ &\quad + \liminf_{T \rightarrow \infty} \frac{1}{T} \left( \log \frac{\underline{\sigma}^{-2p\beta}}{\bar{\sigma}^{-2\eta(\underline{a}, \bar{\sigma})}} + \log \mathbb{E}^{\mathbb{Q}^{\bar{b}, \underline{a}, \bar{\sigma}}} \left[ Y_T^{p\beta + \eta(\underline{a}, \bar{\sigma})} \right] \right) \\ &= -pr(\beta-1) - \bar{b}\eta(\underline{a}, \bar{\sigma}). \end{aligned}$$

Conversely, we can derive from the definition of  $v_T$ , that for  $\bar{b}, \underline{a}$ , and  $\bar{\sigma}$  the inequality

$$e^{-pr(\beta-1)T} V(T; \bar{b}, \underline{a}, \bar{\sigma}) \geq v_T$$

holds, which implies by taking the log of the Hansen-Scheinkman decomposition of  $V$

$$-(pr(\beta-1) + \bar{b}\eta(\underline{a}, \bar{\sigma}))T - 2(p\beta + \eta(\underline{a}, \bar{\sigma})) \log \bar{\sigma} + \log \mathbb{E}^{\mathbb{Q}^{\bar{b}, \underline{a}, \bar{\sigma}}} \left[ Y_T^{p\beta + \eta(\underline{a}, \bar{\sigma})} \right] \geq \log v_T.$$

Since the expectation  $\mathbb{E}^{\mathbb{Q}^{b,a,\sigma}} \left[ Y_T^{p\beta + \eta(a,\sigma)} \right]$  is finite in the limit  $T \rightarrow \infty$  we derive

$$-pr(\beta-1) - \bar{b}\eta(\underline{a}, \bar{\sigma}) \geq \limsup_{T \rightarrow \infty} \frac{1}{T} \log v_T.$$

Together, assuming  $2(\underline{a}/\bar{\sigma}^2 + 1) + \eta(\underline{a}, \bar{\sigma}) - p\beta > 0$ , these two preceding inequalities yield

$$\lim_{T \rightarrow \infty} \frac{1}{T} \log v_T = -pr(\beta-1) - \bar{b}\eta(\underline{a}, \bar{\sigma}).$$

We now summarize these results in the following Proposition.

**Proposition 4.3** *Leung et al. [1, Proposition 4]*

Let  $0 < \underline{b} \leq \bar{b}, 0 < \underline{\sigma} \leq \bar{\sigma}, 0 < \underline{a} \leq \bar{a}$  and  $X^\alpha$  be the 3/2 process (4.15) with set of parameters  $\alpha = (b, a, \sigma)$  ranging over  $[\underline{\alpha}, \bar{\alpha}] = [\underline{b}, \bar{b}] \times [\underline{a}, \bar{a}] \times [\underline{\sigma}, \bar{\sigma}]$ . Then the long-term growth rate of the worst-case expected utility of the LETF  $L^\alpha = (L_t^\alpha)_{t \geq 0}$ , with the reference process  $X^\alpha$  is given by

$$\lim_{T \rightarrow \infty} \frac{1}{T} \log \inf_{\alpha \in [\underline{\alpha}, \bar{\alpha}]} \mathbb{E}^{\mathbb{P}^\alpha} [L_T^p] = -pr(\beta - 1) - b^*(\beta)\eta(a^*(\beta), \sigma^*(\beta), \beta),$$

provided  $2(\underline{a}/\bar{\sigma}^2 + 1) + \eta(\underline{a}, \bar{\sigma}) - p\beta > 0$ , where

$$\eta(a, \sigma, \beta) = -\left(\frac{a}{\sigma^2} + \frac{1}{2}\right) + \sqrt{\left(\frac{a}{\sigma^2} + \frac{1}{2}\right)^2 + p\beta(\beta - 1)},$$

$$b^*(\beta) = \begin{cases} \bar{b}, & \beta \geq 1, \beta < 0 \\ \underline{b}, & 0 \leq \beta < 1 \end{cases}, a^*(\beta) = \begin{cases} \underline{a}, & \beta \geq 1, \beta < 0 \\ \bar{a}, & 0 \leq \beta < 1 \end{cases}, \sigma^*(\beta) = \begin{cases} \bar{\sigma}, & \beta \geq 1, \beta < 0 \\ \underline{\sigma}, & 0 \leq \beta < 1 \end{cases}.$$

Proposition 4.3 is alike 4.2 and we summarize the optimal leverage ratio candidates according to the parameter relationship in the following table as before.

Table 4.2: Optimal leverage ratio candidates based on the parameter relationships for the 3/2 reference process.

Parameter relationship	Condition 1	Condition 2	Candidates for $\beta^*$
$p \geq \frac{\bar{b}^2}{r^2}$			$0, \underline{\beta}$
$\frac{\underline{b}^2}{r^2} \leq p < \frac{\bar{b}^2}{r^2}$	$\frac{2\underline{a}}{\bar{\sigma}^2} + 1 > \frac{\bar{b}}{r}$		$0, \frac{1}{2} \left( 1 - \sqrt{\frac{\left(\frac{2\underline{a}}{\bar{\sigma}^2} + 1\right)^2 - p}{\left(\frac{\bar{b}}{r}\right)^2 - p}} \right)$
	$\frac{2\underline{a}}{\bar{\sigma}^2} + 1 \leq \frac{\bar{b}}{r}$		$0, \underline{\beta}$
$p < \frac{\underline{b}^2}{r^2}$	$\frac{2\underline{a}}{\bar{\sigma}^2} + 1 > \frac{\bar{b}}{r}$		$0, \frac{1}{2} \left( 1 - \sqrt{\frac{\left(\frac{2\underline{a}}{\bar{\sigma}^2} + 1\right)^2 - p}{\left(\frac{\bar{b}}{r}\right)^2 - p}} \right)$
	$\frac{2\underline{a}}{\bar{\sigma}^2} + 1 \leq \frac{\bar{b}}{r}$	$\frac{2\bar{a}}{\underline{\sigma}^2} + 1 \geq \frac{\bar{b}}{r}$	$0, \underline{\beta}$
		$\frac{2\bar{a}}{\underline{\sigma}^2} + 1 < \frac{\bar{b}}{r}$	$\frac{1}{2} \left( 1 - \sqrt{\frac{\left(\frac{2\bar{a}}{\underline{\sigma}^2} + 1\right)^2 - p}{\left(\frac{\bar{b}}{r}\right)^2 - p}} \right), \underline{\beta}$



# Chapter 5

## Uncertainty in the stochastic volatility reference process

Building on the previous chapter, we now assume that the volatility of the reference index is itself a stochastic process, driven by its own dynamics and subject to uncertainty. Stochastic volatility models are more aligned with empirical observations of financial markets, where volatility clusters and evolves over time. In this chapter we will remain the previous assumption of a constant interest rate  $r_t \equiv r$  and an deterministic initial value of the reference process  $X_0 = 1$ . Here we model the underlying process  $X$  as

$$\begin{aligned} dX_t &= \mu X_t dt + \sqrt{\nu_t} X_t dW_t \\ d\nu_t &= b(\nu_t) dt + \sigma(\nu_t) dB_t \quad \nu_0 > 0. \end{aligned}$$

We assume that the uncertainties in this chapter will lie in  $\mu$ , the instantaneous correlation coefficient between the Brownian motions  $W$  and  $B$ ,  $\rho$ , and the set of parameters  $\tilde{\alpha}$  of  $\nu$ . So we have  $\alpha = (\mu, \rho, \tilde{\alpha})$  and  $[\alpha, \bar{\alpha}] = [\underline{\mu}, \bar{\mu}] \times [\underline{\rho}, \bar{\rho}] \times [\underline{\tilde{\alpha}}, \bar{\tilde{\alpha}}]$  where  $-1 \leq \underline{\rho} \leq \bar{\rho} \leq 1$ . Now to emphasize the dependency of  $X$  and  $\nu$  on  $\alpha$ , we can rewrite their dynamics as

$$\begin{aligned} dX_t^\alpha &= \mu X_t^\alpha dt + \sqrt{\nu_t^\alpha} X_t^\alpha dW_t^\rho \\ d\nu_t^\alpha &= b(\nu_t^\alpha; \alpha) dt + \sigma(\nu_t^\alpha; \alpha) dB_t^\rho \end{aligned}$$

with  $\langle W^\rho, B^\rho \rangle_t = \rho t$ . Next we will investigate  $L_T^\alpha$ . Using standard computations and Itô's Lemma, we derive:

$$(L_t^\alpha)^p = e^{p(r+\beta(\mu-r))t - \frac{1}{2}p\beta^2 \int_0^t \nu_s^\alpha ds + p\beta \int_0^t \sqrt{\nu_s^\alpha} dW_s^\rho}.$$

Now we can use that

$$\mathcal{E}\left(p\beta \int_0^\cdot \sqrt{\nu_s^\alpha} dW_s^\rho\right)_t = e^{p\beta \int_0^T \sqrt{\nu_s^\alpha} dW_s^\rho} e^{-\frac{1}{2}p^2\beta^2 \int_0^t \nu_s^\alpha ds}$$

to follow

$$(L_t^\alpha)^p = e^{p(r+\beta(\mu-r))t - \frac{1}{2}p(1-p)\beta^2 \int_0^t \nu_s^\alpha ds} \mathcal{E}\left(p\beta \int_0^\cdot \sqrt{\nu_s^\alpha} dW_s^\rho\right)_t, \quad t \geq 0.$$

We fix a time horizon  $T > 0$  and assume that the above Doléans-Dade exponential is a true martingale on  $0 \leq t \leq T$ . This allows us to introduce a probability measure  $\hat{\mathbb{P}}^\alpha$  on  $\mathcal{F}_T$  via

$$\frac{d\hat{\mathbb{P}}^\alpha}{d\mathbb{P}} \Big|_{\mathcal{F}_T} = \mathcal{E} \left( p\beta \int_0^{\cdot} \sqrt{\nu_s^\alpha} dW_s^\rho \right)_T. \quad (5.1)$$

Hence we can rewrite the expected utility for an investor who holds the LETF for the measure  $\hat{\mathbb{P}}^\alpha$  as

$$\mathbb{E}^{\mathbb{P}^\alpha} [L_T^p] = \mathbb{E}^{\hat{\mathbb{P}}^\alpha} \left[ e^{p(r+\beta(\mu-r))T - \frac{1}{2}p(1-p)\beta^2 \int_0^T \nu_s^\alpha ds} \right], \quad T \geq 0. \quad (5.2)$$

Then by Girsanov's theorem the  $\hat{\mathbb{P}}^\alpha$ -dynamics of  $\nu^\alpha$  are altered as

$$\begin{aligned} d\nu_t^\alpha &= b(\nu_t^\alpha; \alpha) dt + \sigma(\nu_t^\alpha; \alpha) \widehat{dB_t^\rho} \\ &= \left( b(\nu_t^\alpha; \alpha) + p\beta\rho\sqrt{\nu_t^\alpha} \sigma(\nu_t^\alpha; \alpha) \right) dt + \sigma(\nu_t^\alpha; \alpha) d\hat{B}_t^\alpha, \quad 0 \leq t \leq T, \end{aligned}$$

for a  $\hat{\mathbb{P}}^\alpha$ -Brownian motion

$$\hat{B}_t^\alpha := -p\beta\rho \int_0^t \sqrt{\nu_s^\alpha} ds + B_t^\rho, \quad 0 \leq t \leq T,$$

since  $p\beta\rho \int_0^t \sqrt{\nu_s^\alpha} ds = \langle p\beta \int_0^{\cdot} \nu_s^\alpha dW_s^\rho, B_\cdot^\rho \rangle_t$ . From (5.2) we get the following inequality

$$\mathbb{E}^{\mathbb{P}^\alpha} [L_T^p] \geq e^{p(r+\beta(\mu^*-r))T} \mathbb{E}^{\hat{\mathbb{P}}^\alpha} \left[ e^{-\frac{1}{2}p(1-p)\beta^2 \int_0^T \nu_s^\alpha ds} \right], \quad T \geq 0, \quad (5.3)$$

for every  $\alpha \in [\underline{\alpha}, \bar{\alpha}]$ , where

$$\mu^* = \begin{cases} \frac{\mu}{\bar{\mu}}, & \beta \geq 0 \\ \frac{\bar{\mu}}{\mu}, & \beta < 0 \end{cases}.$$

We define

$$V(T; \alpha) := \mathbb{E}^{\hat{\mathbb{P}}^\alpha} \left[ e^{-\frac{1}{2}p(1-p)\beta^2 \int_0^T \nu_s^\alpha ds} \right]$$

and

$$v_T := \inf_{\alpha \in [\underline{\alpha}, \bar{\alpha}]} \mathbb{E}^{\mathbb{P}^\alpha} [L_T^p]$$

similar to previous chapter. We note that  $V(T; \alpha)$  is independent of  $\mu$ , so we can directly infer from inequality (5.3) and the fact that  $v_T \leq \mathbb{E}^{\hat{\mathbb{P}}^\alpha} \left[ e^{p(r+\beta(\mu^*-r))T - \frac{1}{2}p(1-p)\beta^2 \int_0^T \nu_s^\alpha ds} \right]$  by (5.2):

$$v_T = e^{p(r+\beta(\mu^*-r))T} \inf_{\alpha \in [\underline{\alpha}, \bar{\alpha}]} V(T; \alpha). \quad (5.4)$$

Now we can apply again Proposition 3.2 to  $v^\alpha$  and the Hansen-Scheinkman decomposition to  $V(T; \alpha)$ .

## 5.1 Heston model

The first model we will discuss is the Heston stochastic volatility model, which was introduced by Heston [56]. It extends in a sense the more simple Black-Scholes model, which assumes constant volatility over time. Hence, here we assume that the reference follows the Heston model

$$\begin{aligned} dX_t &= \mu X_t dt + \sqrt{\nu_t} X_t dW_t \\ d\nu_t &= (b - a\nu_t) dt + \sigma\sqrt{\nu_t} dB_t, \end{aligned} \tag{5.5}$$

where  $W_t$  and  $B_t$  are two correlated Brownian motions with correlation parameter  $\rho \in [\underline{\rho}, \bar{\rho}]$  and  $\langle W, B \rangle_t = \rho t$ . Our model parameters here are  $\alpha = (\mu, \rho, b, a, \sigma)$  and  $[\underline{\alpha}, \bar{\alpha}] = [\underline{\mu}, \bar{\mu}] \times [\underline{\rho}, \bar{\rho}] \times [\underline{b}, \bar{b}] \times [\underline{\sigma}, \bar{\sigma}]$ , with  $\underline{\mu}, \underline{a}, \underline{\sigma} > 0$  and  $\underline{b} > \bar{\sigma}^2/2$ . We assume  $\underline{a} - p|\beta|\bar{\sigma} > 0$  so that  $a - p\beta\rho\sigma > 0$  for every  $(a, \rho, \sigma) \in [\underline{a}, \bar{a}] \times [-1, 1] \times [\underline{\sigma}, \bar{\sigma}]$ , and the SDE

$$d\nu_t = (b - (a - p\beta\rho\sigma)\nu_t) dt + \sigma\sqrt{\nu_t} dB_t, \quad \nu_0 > 0,$$

has a unique strong solution and we can define a probability measure  $\hat{\mathbb{P}}^\alpha$  on  $\mathcal{F}_T$  for each  $T \geq 0$  by (5.1). Furthermore, inequality (5.3) holds and  $\nu$  has dynamics

$$d\nu_t = (b - (a - p\beta\rho\sigma)\nu_t) dt + \sigma\sqrt{\nu_t} d\hat{B}_t^\alpha$$

under probability measure  $\hat{\mathbb{P}}^\alpha$  and a  $\hat{\mathbb{P}}^\alpha$ -Brownian motion

$$\hat{B}_t^\alpha = -p\beta\rho \int_0^t \sqrt{\nu_s} ds + B_t.$$

We want to apply Proposition 3.2 on  $\nu$ , so we check the three conditions:

(i)

$$\nu_0^{\mu, \rho, b, a, \sigma} \leq \nu_0^{\mu^*, \rho^*, \bar{b}, \underline{a}, \sigma} \text{ with } \rho^* = \begin{cases} \bar{\rho}, & \beta \geq 0 \\ \underline{\rho}, & \beta < 0 \end{cases}.$$

(ii)

$$\begin{aligned} b - (a - p\beta\rho\sigma)x &\leq \bar{b} - (\underline{a} - p\beta\rho^*\sigma)x \\ &\quad \text{and} \\ (b - (a - p\beta\rho\sigma)x) - (b - (a - p\beta\rho\sigma)y) &\leq (-a + p\beta\rho\sigma)|x - y| \end{aligned}$$

(iii) The volatility term fulfills the continuity assumption and for  $h(z) = \sigma\sqrt{z}$ , where  $\int_0^\epsilon h^{-2}(z)dz = \infty$  for all  $\epsilon > 0$  and satisfying:

$$|\sigma\sqrt{x} - \sigma\sqrt{y}| \leq h(|x - y|).$$

Therefore by Proposition 3.2  $\nu_t^{\mu, \rho, b, a, \sigma} \leq \nu_t^{\mu^*, \rho^*, \bar{b}, \underline{a}, \sigma}$  for almost every  $t \in [0, \infty)$  and hence because of our representation of  $L_t^p$ :

$$\mathbb{E}^{\mathbb{P}^\alpha}[L_T^p] \geq e^{p(r+\beta(\mu^*-r))T} \mathbb{E}^{\hat{\mathbb{P}}^{\mu^*, \rho^*, \bar{b}, \underline{a}, \sigma}}[e^{-\frac{1}{2}p(1-p)\beta^2 \int_0^T \nu_s ds}], \quad T \geq 0$$

for every  $\alpha = (\mu, \rho, b, a, \sigma)$ . Until now, we have not specified  $\sigma$ . Set

$$\alpha^*(\sigma) := (\mu^*, \rho^*, \bar{b}, \underline{a}, \sigma).$$

With

$$\mathcal{L}\phi(\nu) = \frac{1}{2}\sigma^2\nu\phi''(\nu) + (\bar{b} - (\underline{a} - p\beta\rho^*\sigma)\nu)\phi'(\nu) - \frac{1}{2}p(1-p)\beta^2\nu\phi(\nu) = -\lambda\phi(\nu)$$

the eigenpair problem for the infinitesimal generator of  $\nu$  under the measure  $\hat{\mathbb{P}}^{\alpha^*(\sigma)}$  is expressed as

$$-\lambda\phi(\nu) = \frac{1}{2}\sigma^2\nu\phi''(\nu) + (\bar{b} - (\underline{a} - p\beta\rho^*\sigma)\nu)\phi'(\nu) - \frac{1}{2}p(1-p)\beta^2\nu\phi(\nu).$$

One can prove that one solution pair is given by

$$(\lambda(\sigma), \phi_\sigma(\nu)) = (\bar{b}\eta(\sigma), e^{-\eta(\sigma)\nu})$$

with

$$\eta(\sigma) = \frac{1}{\sigma^2} \left( \sqrt{(a - p\beta\rho^*\sigma)^2 + p(1-p)\beta^2\sigma^2} - (a - p\beta\rho^*\sigma) \right).$$

Similar to what we have seen in Chapter 4 we can use the theory of Chapter 3 to define a probability measure  $\hat{\mathbb{Q}}^{\alpha^*(\sigma)}$  on  $\mathcal{F}_T$  by

$$\frac{d\hat{\mathbb{Q}}^{\alpha^*(\sigma)}}{d\hat{\mathbb{P}}^{\alpha^*(\sigma)}} \Bigg|_{\mathcal{F}_T} = e^{\lambda(\sigma)T - \frac{1}{2}p\beta(\beta-1)\int_0^T \nu_s ds - \eta(\sigma)\nu_T + \eta(\sigma)\nu_0} \quad (5.6)$$

for which the process  $\nu$  now has dynamics

$$d\nu_t = \left( \bar{b} - \sqrt{(\underline{a} - p\beta\rho^*\sigma)^2 + p(1-p)\beta^2\sigma^2} \nu_t \right) dt + \sigma\sqrt{\nu_t} dB_t^{\hat{Q}^*(\sigma)}, \quad 0 \leq t \leq T,$$

for a  $\hat{\mathbb{Q}}^{\alpha^*(\sigma)}$ -Brownian motion  $B^{\hat{Q}^*(\sigma)}$

$$B_t^{\hat{Q}^*(\sigma)} := \eta(\sigma) \int_0^t \sigma\sqrt{\nu_s} ds + \hat{B}_t^{\alpha^*(\sigma)}, \quad 0 \leq t \leq T.$$

Since

$$V(T; \alpha^*(\sigma)) = e^{-p(r+\beta(\mu^*-r))T} \mathbb{E}^{\hat{\mathbb{P}}^{\alpha^*}} [L_T^p]$$

and  $\mathbb{E}^{\hat{\mathbb{P}}^{\alpha^*}} [L_T^p]$  in turn by the Hansen-Scheinkman decomposition

$$\mathbb{E}^{\hat{\mathbb{P}}^{\alpha^*}} [L_T^p] = e^{-\lambda(\sigma)T - \eta(\sigma)\nu_0} \mathbb{E}^{\hat{\mathbb{Q}}^{\alpha^*(\sigma)}} \left[ \frac{e^{p(r+\beta(\mu^*-r))T}}{e^{-\eta(\sigma)\nu_T}} \right]$$

we together have

$$V(T; \alpha^*(\sigma)) = e^{-\lambda(\sigma)T - \eta(\sigma)\nu_0} \mathbb{E}^{\hat{\mathbb{Q}}^{\alpha^*(\sigma)}} [e^{\eta(\sigma)\nu_T}].$$

Note that  $\nu_T \geq 0$  and  $\eta(\sigma) \geq 0$  for any  $T \geq 0$  and fixed  $\sigma_0 \in [\underline{\sigma}, \bar{\sigma}]$ . Hence  $e^{\eta(\sigma)\nu_T} \geq 0$  and therefore

$$1 \leq \inf_{\sigma \in [\underline{\sigma}, \bar{\sigma}], T \geq 0} E^{\hat{Q}^{\alpha^*(\sigma)}} [e^{\eta(\sigma)\nu_T}] \leq E^{\hat{Q}^{\alpha^*(\sigma_0)}} [e^{\eta(\sigma_0)\nu_T}].$$

We know from Section 4.2 that under  $\hat{Q}^{\alpha^*(\sigma_0)}$  that

$$\lim_{T \rightarrow \infty} \mathbb{E}^{\hat{Q}^{\alpha^*(\sigma_0)}} [e^{\eta(\sigma_0)\nu_T}] = \int_0^\infty e^{\eta(\sigma_0)y} \psi(y) dy < \infty,$$

where  $\psi$  is invariant density of  $\nu_T$  under  $\hat{Q}^{\alpha^*(\sigma_0)}$ , meaning that the upper bound converges. Therefore,

$$\lim_{T \rightarrow \infty} \frac{1}{T} \log \inf_{\sigma \in [\underline{\sigma}, \bar{\sigma}]} E^{\hat{Q}^{\alpha^*(\sigma)}} [e^{\eta(\sigma)\nu_T}] = 0$$

and

$$\liminf_{T \rightarrow \infty} \frac{1}{T} \log \inf_{\sigma \in [\underline{\sigma}, \bar{\sigma}]} V(T; \alpha^*(\sigma)) \geq \inf_{\sigma \in [\underline{\sigma}, \bar{\sigma}]} -\lambda(\sigma) = -\bar{b} \sup_{\sigma \in [\underline{\sigma}, \bar{\sigma}]} \eta(\sigma). \quad (5.7)$$

Next, to get also the inverse inequality we note that the function  $\sigma \mapsto \eta(\sigma)$  is continuous and hence the supremum of  $\eta(\sigma)$  is in fact a maximum and we can choose  $\sigma^* \in [\underline{\sigma}, \bar{\sigma}]$  that achieves this supremum. With this  $\sigma^*$  we derive

$$\lim_{T \rightarrow \infty} \frac{1}{T} \log V(T; \alpha^*(\sigma^*)) = -\bar{b}\eta(\sigma^*). \quad (5.8)$$

Combining (5.7) and (5.8) we achieve the equality

$$\lim_{T \rightarrow \infty} \frac{1}{T} \log \inf_{\sigma \in [\underline{\sigma}, \bar{\sigma}]} V(T; \alpha^*(\sigma)) = -\bar{b}\eta(\sigma^*).$$

Lastly, together with representation (5.4) we get the convergence

$$\begin{aligned} \lim_{T \rightarrow \infty} \frac{1}{T} \log v_T &\stackrel{(5.4)}{=} \lim_{T \rightarrow \infty} \frac{1}{T} \log \left( e^{p(r+\beta(\mu^*-r))T} \inf_{\alpha \in [\underline{\alpha}, \bar{\alpha}]} V(T; \alpha) \right) \\ &= p(r + \beta(\mu^* - r)) + \lim_{T \rightarrow \infty} \frac{1}{T} \log \inf_{\alpha \in [\underline{\alpha}, \bar{\alpha}]} V(T; \alpha) \\ &= p(r + \beta(\mu^* - r)) - \bar{b} \max_{\sigma \in [\underline{\sigma}, \bar{\sigma}]} \eta(\sigma), \end{aligned}$$

where the infimum over all parameters could be reduced to the infimum only over  $\sigma$  since all parameters except  $\sigma$  were fixed.

**Proposition 5.1** *Leung et al. [1, Proposition 5]*

Let  $0 < \underline{\mu} \leq \bar{\mu}, 0 < \underline{a} \leq \bar{a}, 0 < \underline{\sigma} \leq \bar{\sigma}, \bar{\sigma}^2/2 < \underline{b} \leq \bar{b}$  and  $X^\alpha$  be the Heston model (5.5) with set of parameters  $\alpha = (\mu, \rho, b, a, \sigma)$  ranging over  $[\underline{\mu}, \bar{\mu}] \times [\underline{\rho}, \bar{\rho}] \times [\underline{b}, \bar{b}] \times [\underline{a}, \bar{a}] \times [\underline{\sigma}, \bar{\sigma}]$ . Then, the long-term growth rate of the worst-case expected utility of the LETF  $L^\alpha = (L_t^\alpha)_{t \geq 0}$  with the reference process  $X^\alpha$  is given by

$$\lim_{T \rightarrow \infty} \frac{1}{T} \log \inf_{\alpha \in [\underline{\alpha}, \bar{\alpha}]} \mathbb{E}^{\mathbb{P}^\alpha} [L_T^p] = p(r + \beta(\mu^*(\beta) - r)) - \bar{b}\eta(\sigma^*(\beta), \beta),$$

where

$$\eta(\sigma, \beta) = \frac{1}{\sigma^2} \left( \sqrt{(\underline{a} - p\beta\rho^*(\beta)\sigma)^2 + p(1-p)\beta^2\sigma^2} - (\underline{a} - p\beta\rho^*(\beta)\sigma) \right),$$

$$\mu^*(\beta) = \begin{cases} \underline{\mu}, & \beta \geq 0 \\ \bar{\mu}, & \beta < 0 \end{cases}, \quad \rho^*(\beta) = \begin{cases} \bar{\rho} & \beta \geq 0 \\ \underline{\rho} & \beta < 0 \end{cases},$$

and  $\sigma^*(\beta)$  maximizes  $\eta$  on  $[\underline{\sigma}, \bar{\sigma}]$  for each  $\beta \in [\underline{\beta}, \bar{\beta}]$ , provided  $\underline{a} - p\beta\rho^*(\beta)\bar{\sigma} > 0$ . The long-run limit is achieved for  $(\mu^*(\beta), \rho^*(\beta), \bar{b}, \underline{a}, \sigma^*(\beta))$ .

While the existence of a worst-case parameter set within the uncertainty range is certainly assured, determining the corresponding optimal leverage ratio  $\beta^*$  analytically is highly challenging. This difficulty arises because the procedure involves identifying the worst-case volatility  $\sigma^*(\beta)$ , evaluating the function  $\eta(\sigma^*(\beta), \beta)$  for each leverage value  $\beta$ , and comparing the limits for all  $\beta$  in the interval  $[\underline{\beta}, \bar{\beta}]$ . Such computations are generally infeasible or at least nearly impossible to perform manually. As a result, one might take a numerical approach. We compute the long-term growth rate and identify the optimal leverage  $\beta^*$  across a range of parameter values. We define

$$\Lambda(\beta) := p(r + \beta(\mu^*(\beta) - r)) - \bar{b}\eta(\sigma^*(\beta), \beta)$$

and aim to find a suitable mesh size for any given error bound. With the inequalities

$$\begin{aligned} \left| \frac{\eta(\sigma^*(\beta + h), \beta + h) - \eta(\sigma^*(\beta), \beta)}{h} \right| &= \left| \frac{\sup_{\sigma} \eta(\sigma, \beta + h) - \sup_{\sigma} \eta(\sigma, \beta)}{h} \right| \\ &\leq \sup_{\sigma} \left| \frac{\eta(\sigma, \beta + h) - \eta(\sigma, \beta)}{h} \right| \\ &\leq \sup_{\sigma} \sup_{\beta} |\eta_{\beta}(\sigma, \beta)|, \end{aligned}$$

where  $\eta_{\beta}$  denotes the partial derivative of  $\eta$  with respect to  $\beta$ , we derive

$$\begin{aligned} |\Lambda(\beta + h) - \Lambda(\beta)| &= |ph(\mu^*(\beta) - r) - \bar{b}(\eta(\sigma^*(\beta + h), \beta + h) - \eta(\sigma^*(\beta), \beta))| \\ &\leq (p(\bar{\mu} - r) + \bar{b} \sup_{\sigma, \beta} |\eta_{\beta}(\sigma, \beta)|)h. \end{aligned}$$

For the equality note that for sufficiently small  $h$   $\mu^*(\beta + h) = \mu^*(\beta)$ . Now for any  $\epsilon > 0$  we see that

$$|\Lambda(\beta + h) - \Lambda(\beta)| \leq \epsilon$$

is ensured for any  $h \leq \epsilon/M$ , where  $M := p(\bar{\mu} - r) + \bar{b} \sup_{\sigma, \beta} |\eta_{\beta}(\sigma, \beta)|$ . One can show, that in the Heston model

$$\begin{aligned} &\sup_{\sigma, \beta} |\eta_{\beta}(\sigma, 5)| \\ &= \sup_{\sigma} \frac{p}{\sigma} \max \left\{ \frac{\underline{\alpha}\underline{\rho} - \sigma\underline{\beta}(1 - p(1 - \underline{\rho}^2))}{\sqrt{(\underline{a} - p\underline{\beta}\underline{\rho}\sigma)^2 + p(1-p)\underline{\beta}^2\sigma^2}} - \underline{\rho}, \frac{-\underline{a}\bar{\rho} + \sigma\bar{\beta}(1 - p(1 - \bar{\rho}^2))}{\sqrt{(\underline{a} - p\bar{\beta}\bar{\rho}\sigma)^2 + p(1-p)\bar{\beta}^2\sigma^2}} + \bar{\rho} \right\}. \end{aligned}$$

For  $\beta \in [-5, 5]$ ,  $p = 0.5$ ,  $r = 0.015$ ,  $[\underline{\mu}, \bar{\mu}] = [0.05, 0.08]$ ,  $[\underline{\rho}, \bar{\rho}] = [-0.93, -0.75]$ ,  $[\underline{b}, \bar{b}] = [0.1, 0.2]$ ,  $[\underline{a}, \bar{a}] = [3, 10]$ ,  $[\underline{\sigma}, \bar{\sigma}] = [0.82, 0.93]$ . Figure 5.1 shows that the optimal leverage ratio is approximately 1.25 and the corresponding long-term growth rate is approximately 0.0179. Moreover we can see in Figure 5.2 that for  $\sigma$  and  $\rho$ , the optimal leverage ratio increases in  $\sigma$  and decreases in  $\bar{\rho}$ . Therefore, within the Heston framework, the optimal leverage ratio increases as the lower bound of the volatility-of-volatility parameter increases and as the upper bound of the correlation parameter decreases.

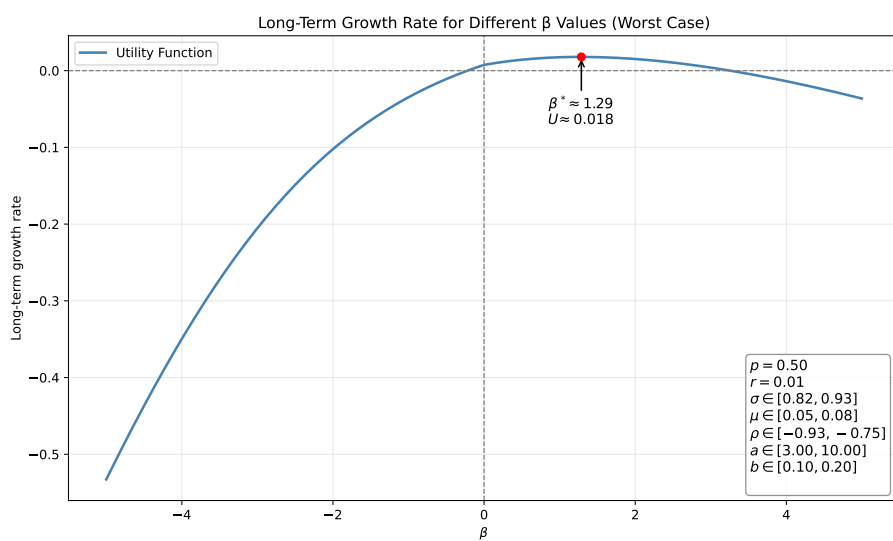


Figure 5.1: Long-term growth rate of the worst-case expected utility as a function of the leverage ratio  $\beta$  under the Heston model.

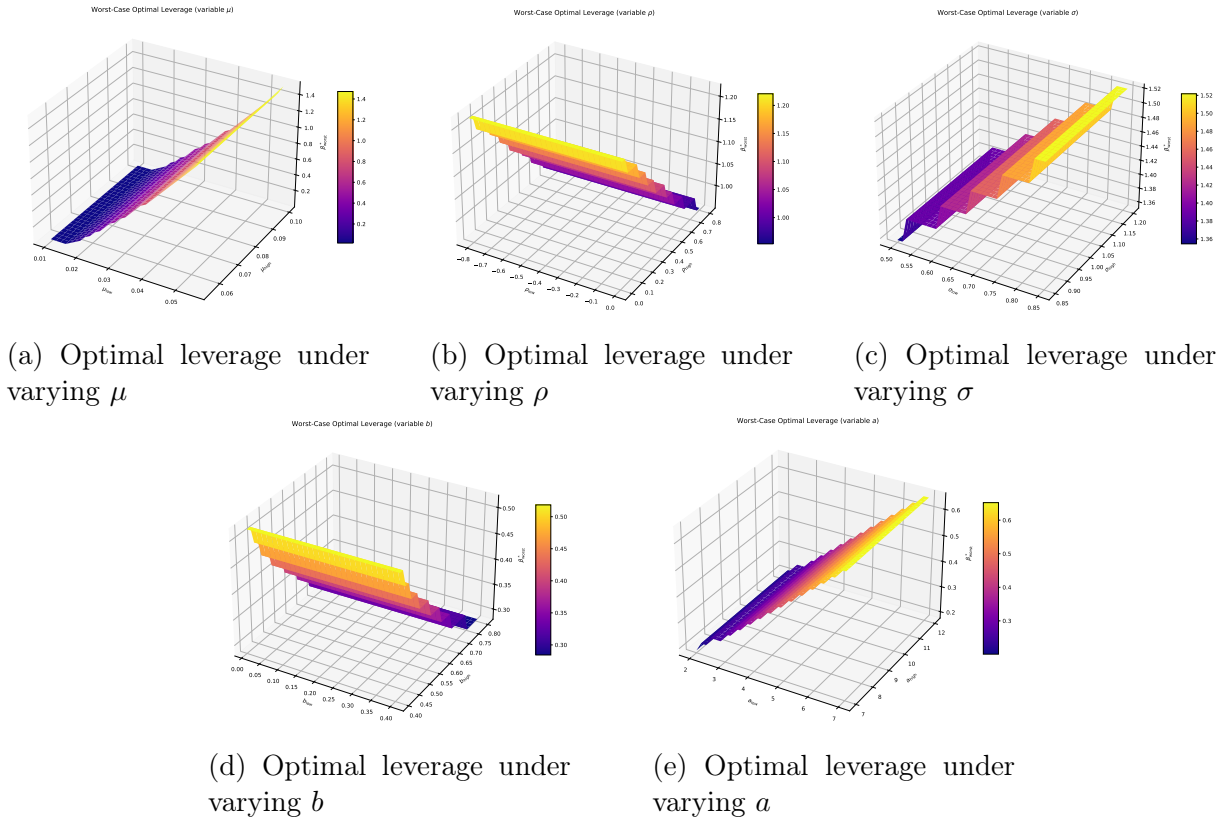


Figure 5.2: Impact of different intervals on the optimal leverage ratio.

**Remark 5.2** These results can even be extended to a progressively measurable process  $\mu$  which is taking values in  $[\underline{\mu}, \bar{\mu}]$  and  $b$  and  $a$  are the Markovian controls (i.e. there exist functions  $b_0 : [0, \infty) \times (0, \infty) \rightarrow [\underline{b}, \bar{b}]$ ,  $a_0 : [0, \infty) \times (0, \infty) \rightarrow [\underline{a}, \bar{a}]$  such that  $b(t, \omega) = b_0(t, X_t(\omega))$ ,  $a(t, \omega) = a_0(t, X_t(\omega))$ ) since at least the existence and uniqueness of the SDE

$$\begin{aligned} dX_t &= \mu_t X_t dt + \sqrt{\nu_t} X_t dW_t^{\rho(t)} \\ d\nu_t &= (b_0(t, \nu_t) - a_0(t, \nu_t) \nu_t) dt + \sigma \sqrt{\nu_t} dB_t^{\rho(t)}, \end{aligned}$$

in the weak sense are guaranteed Stroock and Varadhan [57, Chapter 10], and hence Proposition 3.2 remains valid.

**Corollary 5.3** Leung et al. [1, Corollary 1]

Let the reference process  $X$  follow

$$\begin{aligned} dX_t &= \mu_t X_t dt + \sqrt{\nu_t} X_t dW_t^{\rho(t)}, \\ d\nu_t &= (b_0(t, \nu_t) - a_0(t, \nu_t) \nu_t) dt + \sigma \sqrt{\nu_t} dB_t^{\rho(t)}, \end{aligned} \tag{5.9}$$

where  $\mu : \Omega \times [0, \infty) \rightarrow [\underline{\mu}, \bar{\mu}]$  is progressively measurable and  $b_0, a_0$ , and  $\rho$  range over  $[\underline{b}, \bar{b}]$ ,  $[\underline{a}, \bar{a}]$ , and  $[\rho, \bar{\rho}]$ , respectively. Then, Proposition 5.1 holds for the LETF with the reference process (5.9).

**Remark 5.4** Leung et al. [1, Remark 2] Furthermore,  $b$  and  $a$  can be merely progressively measurable processes whenever the existence and uniqueness of the SDE

$$\begin{aligned} dX_t &= \mu_t X_t dt + \sqrt{\nu_t} X_t dW_t^{\rho(t)} \\ d\nu_t &= (b_t - a_t \nu_t) dt + \sigma \sqrt{\nu_t} dB_t^{\rho(t)} \end{aligned}$$

are guaranteed.

## 5.2 3/2 volatility model

In our next example we will investigate the 3/2 volatility model. Several studies researched the 3/2 volatility model and came to the conclusion that it outperforms the Heston model in a sense that it better captures the volatility smiles Drimus [54] and evolution of the volatility index Goard and Mazur [58].

The reference process  $X$  has the same dynamics as in the Heston model but the volatility process has 3/2 dynamics, so

$$\begin{aligned} dX_t &= \mu X_t dt + \sqrt{\nu_t} X_t dW_t \\ d\nu_t &= (b - a \nu_t) \nu_t dt + \sigma \nu_t^{3/2} dB_t, \end{aligned} \tag{5.10}$$

where  $W_t$  and  $B_t$  are two standard Brownian motions with correlation parameter  $\rho \in [\underline{\rho}, \bar{\rho}]$ . We assume uncertainties in  $\mu, \rho, b, a, \sigma$ , so the model parameters are  $\alpha = (\mu, \rho, b, a, \sigma) \in [\underline{\alpha}, \bar{\alpha}] = [\underline{\mu}, \bar{\mu}] \times [\underline{\rho}, \bar{\rho}] \times [\underline{b}, \bar{b}] \times [\underline{a}, \bar{a}] \times [\underline{\sigma}, \bar{\sigma}]$ , where  $\underline{\mu}, \underline{b}, \underline{\sigma} > 0$ , and  $\underline{a} > -\underline{\sigma}^2/2$ . We additionally assume  $\underline{a} - p|\beta| \bar{\sigma} > -\underline{\sigma}^2/2$  so that  $a - p\beta\rho\sigma > -\underline{\sigma}^2/2$  for every  $(a, \rho, \sigma) \in [\underline{a}, \bar{a}] \times [\underline{\rho}, \bar{\rho}] \times [\underline{\sigma}, \bar{\sigma}]$  and the SDE

$$d\nu_t = (b - (a - p\beta\rho\sigma)\nu_t) \nu_t dt + \sigma \nu_t^{3/2} dB_t, \quad \nu_0 > 0,$$

is ensured to have a unique strong solution. We define for each  $T \geq 0$  a probability measure  $\hat{\mathbb{P}}^\alpha$  on  $\mathcal{F}_T$  by (5.1) and  $\nu$  then has dynamics

$$d\nu_t = (b - (a - p\beta\rho\sigma)\nu_t) \nu_t dt + \sigma \nu_t^{3/2} d\hat{B}_t^\alpha$$

under  $\hat{\mathbb{P}}^\alpha$ , with a  $\hat{\mathbb{P}}^\alpha$ -Brownian motion

$$\hat{B}_t^\alpha = -p\beta\rho \int_0^t \sqrt{\nu_s} ds + B_t.$$

Similar to Section 5.1 we apply Proposition 3.2 to  $\nu$ , to derive

$$\mathbb{E}^{\mathbb{P}^\alpha} [L_T^p] \geq e^{p(r+\beta(\mu^*-r))T} \mathbb{E}^{\hat{\mathbb{P}}^{\mu^*, \rho^*, \bar{b}, \underline{a}, \sigma}} \left[ e^{-\frac{1}{2}p(1-p)\beta^2 \int_0^T \nu_s ds} \right], \quad T \geq 0,$$

for every  $\alpha = (\mu, \rho, b, a, \sigma)$ , where

$$\rho^* = \begin{cases} \bar{\rho} & \beta \geq 0 \\ \underline{\rho} & \beta < 0 \end{cases}.$$

We set

$$\alpha^*(\sigma) := (\mu^*, \rho^*, \bar{b}, \underline{a}, \sigma).$$

Next, we again solve the eigenpair problem for the infinitesimal generator of  $\nu$  under the measure  $\hat{\mathbb{P}}^{\alpha^*(\sigma)}$ , which can be expressed as

$$-\lambda\phi(\nu) \stackrel{(3.2)}{=} \frac{1}{2}\sigma^2\nu^3\phi''(\nu) + (\bar{b} - (\underline{a} - p\beta\rho^*\sigma)\nu)\nu\phi'(\nu) - \frac{1}{2}p(1-p)\beta^2\nu\phi(\nu).$$

One can show that one solution pair is given by

$$(\lambda(\sigma), \phi_\sigma(\nu)) = (\bar{b}\eta(\sigma), \nu^{-\eta(\sigma)})$$

with

$$\eta(\sigma) = \frac{1}{\sigma^2} \left( \sqrt{\left( \underline{a} - p\beta\rho^*\sigma + \frac{\sigma^2}{2} \right)^2 + p(1-p)\beta^2\sigma^2} - \left( \underline{a} - p\beta\rho^*\sigma + \frac{\sigma^2}{2} \right) \right).$$

As we have seen before, a local martingale

$$M_t := e^{\lambda(\sigma)t - \frac{1}{2}p\beta(\beta-1)\int_0^t \nu_s ds} e^{-\eta(\sigma)\nu_T + \eta(\sigma)\nu_0}, \quad 0 \leq t \leq T$$

can also be shown to be a true martingale. We define the probability measure  $\hat{\mathbb{Q}}^{\alpha^*(\sigma)}$  by

$$\left. \frac{d\hat{\mathbb{Q}}^{\alpha^*(\sigma)}}{d\hat{\mathbb{P}}^{\alpha^*(\sigma)}} \right|_{\mathcal{F}_T} = M_T$$

on  $\mathcal{F}_T$  and a  $\hat{\mathbb{Q}}^{\alpha^*(\sigma)}$ -Brownian motion

$$B_t^{\hat{\mathbb{Q}}^{\alpha^*(\sigma)}} := \eta(\sigma) \int_0^t \sigma\sqrt{\nu_s} ds + \hat{B}_t^{\alpha^*(\sigma)}, \quad 0 \leq t \leq T.$$

Under  $\hat{\mathbb{Q}}^{\alpha^*(\sigma)}$  the process  $\nu$  now satisfies, using the solution to  $\eta(\sigma)$

$$d\nu_t = \left( \bar{b} - \left( \sqrt{\left( \underline{a} - p\beta\rho^*\sigma + \frac{\sigma^2}{2} \right)^2 + p(1-p)\beta^2\sigma^2} - \frac{\sigma^2}{2} \right) \nu_t \right) \nu_t dt + \sigma\nu_t^{3/2} dB_t^{\alpha^*(\sigma)},$$

$0 \leq t \leq T$ . With  $\hat{\mathbb{Q}}^{\alpha^*(\sigma)}$  at hand and Chapter 3 with formula (3.5) we have

$$V(T; \alpha^*(\sigma)) = e^{-\lambda(\sigma)T} \nu_0^{-\eta(\sigma)} \mathbb{E}^{\hat{\mathbb{Q}}^{\alpha^*(\sigma)}} \left[ \nu_T^{\eta(\sigma)} \right]. \quad (5.11)$$

Fix any  $\sigma_0 \in [\underline{\sigma}, \bar{\sigma}]$  and  $T \geq 0$ , and note several things. First, for any  $\sigma \in [\underline{\sigma}, \bar{\sigma}]$  and  $T \geq 0$ , the expectation  $\mathbb{E}^{\hat{\mathbb{Q}}^{\alpha^*(\sigma)}} \left[ \nu_T^{\eta(\sigma)} \right]$  is positive. We even have that  $\liminf_{T \rightarrow \infty} \mathbb{E}^{\hat{\mathbb{Q}}^{\alpha^*(\sigma)}} \left[ \nu_T^{\eta(\sigma)} \right] > 0$ , since the function  $T \mapsto \mathbb{E}^{\hat{\mathbb{Q}}^{\alpha^*(\sigma)}} \left[ \nu_T^{\eta(\sigma)} \right]$  is continuous on  $[0, \infty)$  by Park and Yeo [39, Lemma D.2], and converges to some positive constant as  $T \rightarrow \infty$ . Next, also  $\mathbb{E}^{\hat{\mathbb{Q}}^{\alpha^*(\sigma_0)}} \left[ e^{\eta(\sigma_0)\nu_T} \right]$  converges to some positive constant as  $T \rightarrow \infty$ , c.f. Sect. 4.3. Hence

$$0 < \inf_{\sigma \in [\underline{\sigma}, \bar{\sigma}], T \geq 0} \mathbb{E}^{\hat{\mathbb{Q}}^{\alpha^*(\sigma)}} \left[ \nu_T^{\eta(\sigma)} \right] \leq \mathbb{E}^{\hat{\mathbb{Q}}^{\alpha^*(\sigma_0)}} \left[ \nu_T^{\eta(\sigma_0)} \right],$$

because the function  $\sigma \mapsto \inf_{T \geq 0} \mathbb{E}^{\hat{Q}^{\alpha^*(\sigma)}} [\nu_T^{\eta(\sigma)}]$  is continuous on  $[\underline{\sigma}, \bar{\sigma}]$ . Therefore we also have

$$\lim_{T \rightarrow \infty} \frac{1}{T} \log \inf_{\sigma \in [\underline{\sigma}, \bar{\sigma}]} \mathbb{E}^{\hat{Q}^{\alpha^*(\sigma)}} [\nu_T^{\eta(\sigma)}] = 0,$$

which leads with our above mentioned representation of  $V(T; \alpha^*(\sigma))$  to the inequality

$$\liminf_{T \rightarrow \infty} \frac{1}{T} \log \inf_{\sigma \in [\underline{\sigma}, \bar{\sigma}]} V(T; \alpha^*(\sigma)) \geq \inf_{\sigma \in [\underline{\sigma}, \bar{\sigma}]} -\lambda(\sigma) = -\bar{b} \sup_{\sigma \in [\underline{\sigma}, \bar{\sigma}]} \eta(\sigma). \quad (5.12)$$

Conversely, the supremum of  $\eta(\sigma)$  is achieved for some  $\sigma^* \in [\underline{\sigma}, \bar{\sigma}]$ , since the function  $\sigma \mapsto \eta(\sigma)$  is continuous. Hence

$$\begin{aligned} \lim_{T \rightarrow \infty} \frac{1}{T} \log V(T; \alpha^*(\sigma^*)) &\stackrel{(5.11)}{=} \lim_{T \rightarrow \infty} \frac{1}{T} \log \left( e^{-\lambda(\sigma^*)T} \nu_0^{-\eta(\sigma^*)} \mathbb{E}^{\hat{Q}^{\alpha^*(\sigma^*)}} [\nu_T^{\eta(\sigma^*)}] \right) \\ &= -\lambda(\sigma^*) - \lim_{T \rightarrow \infty} \frac{1}{T} \eta(\sigma^*) \log(\nu_0) + \lim_{T \rightarrow \infty} \frac{1}{T} \log \mathbb{E}^{\hat{Q}^{\alpha^*(\sigma^*)}} [\nu_T^{\eta(\sigma^*)}] \\ &= -\bar{b}\eta(\sigma^*). \end{aligned} \quad (5.13)$$

Incorporating (5.12) and (5.13) we derive

$$\lim_{T \rightarrow \infty} \frac{1}{T} \log \inf_{\sigma \in [\underline{\sigma}, \bar{\sigma}]} V(T; \alpha^*(\sigma)) = -\bar{b}\eta(\sigma^*).$$

Altogether we now have derived the convergence

$$\lim_{T \rightarrow \infty} \frac{1}{T} \log v_T = p(r + \beta(\mu^* - r)) - \bar{b} \max_{\sigma \in [\underline{\sigma}, \bar{\sigma}]} \eta(\sigma)$$

from (5.4).

**Proposition 5.5** *Leung et al. [1, Proposition 6]*

Let  $0 < \underline{\mu} \leq \bar{\mu}$ ,  $0 < \underline{b} \leq \bar{b}$ ,  $0 < \underline{\sigma} \leq \bar{\sigma}$ ,  $-\underline{\sigma}^2/2 < \underline{a} \leq \bar{a}$  and  $X^\alpha$  be the 3/2 volatility model (5.10) with set of parameters  $\alpha = (\mu, \rho, b, a, \sigma)$  ranging over  $[\underline{\alpha}, \bar{\alpha}] = [\underline{\mu}, \bar{\mu}] \times [\underline{\rho}, \bar{\rho}] \times [\underline{b}, \bar{b}] \times [\underline{a}, \bar{a}] \times [\underline{\sigma}, \bar{\sigma}]$ . Then, the long-term growth rate of the worst-case expected utility of the LETF  $L^\alpha = (L_t^\alpha)_{t \geq 0}$ , with the reference process  $X^\alpha$  is given by

$$\lim_{T \rightarrow \infty} \frac{1}{T} \log \inf_{\alpha \in [\underline{\alpha}, \bar{\alpha}]} \mathbb{E}^{\mathbb{P}^\alpha} [L_T^p] = p(r + \beta(\mu^*(\beta) - r)) - \bar{b}\eta(\sigma^*(\beta), \beta),$$

where

$$\begin{aligned} \eta(\sigma, \beta) &= \frac{\sqrt{(\underline{a} - p\beta\rho^*(\beta)\sigma + \frac{\sigma^2}{2})^2 + p(1-p)\beta^2\sigma^2} - \left(\underline{a} - p\beta\rho^*(\beta)\sigma + \frac{\sigma^2}{2}\right)}{\sigma^2}, \\ \mu^*(\beta) &= \begin{cases} \underline{\mu}, & \beta \geq 0 \\ \bar{\mu}, & \beta < 0 \end{cases}, \quad \rho^*(\beta) = \begin{cases} \bar{\rho}, & \beta \geq 0 \\ \underline{\rho}, & \beta < 0 \end{cases}, \end{aligned}$$

and  $\sigma^*(\beta)$  maximizes  $\eta$  on  $[\underline{\sigma}, \bar{\sigma}]$  for each  $\beta \in [\underline{\beta}, \bar{\beta}]$ , provided  $\underline{a} - p\beta\rho^*(\beta)\bar{\sigma} + \underline{\sigma}^2/2 > 0$ . The long-run limit is achieved for  $\alpha = (\mu^*(\beta), \rho^*(\beta), \bar{b}, \underline{a}, \sigma^*(\beta))$ .

We obtain similar results as in the Heston model, which again arise the problem of computing the optimal leverage ratio  $\beta^*$  by hand. As a way out we may solve this numerically as mentioned in the last section to find the optimal leverage ratio and according robust long-term growth rate. Again, similar as before we can generalize this case as follows in the next corollary.

**Corollary 5.6** *Leung et al. [1, Corollary 2]*

*Let the reference process  $X$  follow*

$$\begin{aligned} dX_t &= \mu_t X_t dt + \sqrt{\nu_t} X_t dW_t^{\rho(t)} \\ d\nu_t &= (b_0(t, \nu_t) - a_0(t, \nu_t) \nu_t) \nu_t dt + \sigma \nu_t^{3/2} dB_t^{\rho(t)} \end{aligned}$$

*where  $\mu$  is a progressively measurable process taking values in  $[\underline{\mu}, \bar{\mu}]$ , and  $b_0, a_0$  and  $\rho$  are functions mapping to  $[\underline{b}, \bar{b}], [\underline{a}, \bar{a}]$ , and  $[\underline{\rho}, \bar{\rho}]$ , respectively. Then, Proposition 5.5 holds for the LETF with the reference  $X$ .*

# Chapter 6

## Uncertainty in the reference process and interest rate process

In this chapter, we explore another layer of realism by allowing the short interest rate to evolve stochastically. Until now, we have only considered uncertainty in the reference process, whereas we now extended the framework to include a stochastic short rate. The risk-free rate is a critical component in the valuation of LETFs. This also adds uncertainty and can significantly impact the leverage ratio and the long-run performance of a leveraged strategy. Explicitly, we will assume models of the following form

$$\begin{aligned} dX_t &= \mu X_t dt + \varsigma X_t dW_t, \\ dr_t &= b(r_t) dt + \sigma(r_t) dB_t, \quad r_0 > 0, \end{aligned}$$

where  $W_t$  and  $B_t$  are two Brownian motions with  $\langle W, B \rangle_t = \rho t$ ,  $-1 \leq \underline{\rho} \leq \rho \leq \bar{\rho} \leq 1$ , and  $r_0$  is deterministic. We allow for uncertainties in  $\mu, \varsigma, \rho$ , and the set of parameters  $\tilde{\alpha}$  of  $r$ . Thus,  $\alpha = (\mu, \varsigma, \rho, \tilde{\alpha})$  and  $[\underline{\alpha}, \bar{\alpha}] = [\underline{\mu}, \bar{\mu}] \times [\underline{\varsigma}, \bar{\varsigma}] \times [\underline{\rho}, \bar{\rho}] \times [\underline{\tilde{\alpha}}, \bar{\tilde{\alpha}}]$  with  $\underline{\mu}, \underline{\varsigma} > 0$ . We again introduce the notation as in Chapter 5 that we include the parameters  $\alpha$  in the notation:

$$\begin{aligned} dX_t^\alpha &= \mu X_t^\alpha dt + \varsigma X_t^\alpha dW_t^\rho \\ dr_t^\alpha &= b(r_t^\alpha; \alpha) dt + \sigma(r_t^\alpha; \alpha) dB_t^\rho. \end{aligned}$$

We can express  $L_T^p$  at time  $T \geq 0$  as

$$\begin{aligned} L_T^p &= e^{p(\beta\mu - \frac{1}{2}\beta^2\varsigma^2)T - p(\beta-1)\int_0^T r_s^\alpha ds + p\beta\varsigma W_T^\rho} \\ &= e^{p\beta\mu T - \frac{1}{2}p(1-p)\beta^2\varsigma^2 T - p(\beta-1)\int_0^T r_s^\alpha ds} \mathcal{E}(p\beta\varsigma W_T^\rho)_T. \end{aligned}$$

We define a probability measure  $\hat{\mathbb{P}}^\alpha$  on  $\mathcal{F}_T$  for each  $T \geq 0$  by

$$\left. \frac{d\hat{\mathbb{P}}^\alpha}{d\mathbb{P}} \right|_{\mathcal{F}_T} = \mathcal{E}(p\beta\varsigma W_T^\rho)_T, \quad (6.1)$$

and the expected utility of an investor is given as

$$\mathbb{E}^{\mathbb{P}^\alpha}[L_T^p] = \mathbb{E}^{\hat{\mathbb{P}}^\alpha} \left[ e^{p\beta\mu T - \frac{1}{2}p(1-p)\beta^2\varsigma^2 T - p(\beta-1)\int_0^T r_s^\alpha ds} \right], \quad T \geq 0. \quad (6.2)$$

Under the new measure  $\hat{\mathbb{P}}^\alpha$  the dynamics of  $X^\alpha$  and  $r^\alpha$  are given by

$$\begin{aligned} dX_t^\alpha &= (\mu + p\beta\varsigma^2) X_t^\alpha dt + \varsigma X_t^\alpha d\hat{W}_t \\ dr_t^\alpha &= (b(r_t^\alpha; \alpha) + p\beta\varsigma\rho\sigma(r_t^\alpha; \alpha)) dt + \sigma(r_t^\alpha; \alpha) d\hat{B}_t^\alpha, \quad 0 \leq t \leq T \end{aligned}$$

for two standard  $\hat{\mathbb{P}}^\alpha$ -Brownian motions  $\hat{W}_t^\alpha$  and  $\hat{B}_t^\alpha$ , which are given through Girsanov's theorem by

$$\begin{aligned} \hat{W}_t^\alpha &= -p\beta\varsigma t + W_t, \quad 0 \leq t \leq T, \\ \hat{B}_t^\alpha &= -p\beta\varsigma\rho t + B_t, \quad 0 \leq t \leq T. \end{aligned} \tag{6.3}$$

For any  $\alpha \in [\underline{\alpha}, \bar{\alpha}]$ , we get from (6.2) the inequality

$$\mathbb{E}^{\mathbb{P}^\alpha}[L_T^p] \geq e^{p\beta\mu^*T} \mathbb{E}^{\hat{\mathbb{P}}^\alpha}\left[e^{-\frac{1}{2}p(1-p)\beta^2\varsigma^2T - p(\beta-1)\int_0^T r_s^\alpha ds}\right], \quad T \geq 0,$$

where

$$\mu^* = \begin{cases} \frac{\mu}{\bar{\mu}}, & \beta \geq 0 \\ \frac{\mu}{\bar{\mu}}, & \beta < 0 \end{cases}. \tag{6.4}$$

In this chapter, we set  $V$  and  $v$  as

$$\begin{aligned} V(T; \alpha) &= \mathbb{E}^{\hat{\mathbb{P}}^\alpha}\left[e^{-\frac{1}{2}p(1-p)\beta^2\varsigma^2T - p(\beta-1)\int_0^T r_s^\alpha ds}\right], \\ v_T &= \inf_{\alpha \in [\underline{\alpha}, \bar{\alpha}]} \mathbb{E}^{\mathbb{P}}[(L_T^\alpha)^p] = e^{p\beta\mu^*T} \inf_{\alpha \in [\underline{\alpha}, \bar{\alpha}]} V(T; \alpha) \end{aligned} \tag{6.5}$$

and we use Proposition 3.2 on  $r^\alpha$  and the Hansen-Scheinkman decomposition on  $V(T; \alpha)$  in the essential steps in the following derivations.

## 6.1 Vasicek interest rate

In the first example we will investigate the Vasicek interest rate model, which was introduced and named after Vasicek [59]. The model assumes a geometric Brownian motion for the reference and models the short interest rate using an Ornstein–Uhlenbeck process, i.e.

$$\begin{aligned} dX_t &= \mu X_t dt + \varsigma X_t dW_t, \\ dr_t &= (b - ar_t) dt + \sigma dB_t, \end{aligned} \tag{6.6}$$

where  $W$  and  $B$  are two Brownian motions with  $\langle W, B \rangle_t = \rho t$  and correlation parameter  $-1 \leq \underline{\rho} \leq \rho \leq \bar{\rho} \leq 1$ . Note that the Ornstein–Uhlenbeck process admits all real numbers and hence the domain of  $r$  is  $D = \mathbb{R}$ . We allow for uncertainties in  $\mu, \varsigma, \rho, b, a, \sigma$  and the model parameters are  $\alpha = (\mu, \varsigma, \rho, b, a, \sigma) \in [\underline{\alpha}, \bar{\alpha}] = [\underline{\mu}, \bar{\mu}] \times [\underline{\varsigma}, \bar{\varsigma}] \times [\underline{\rho}, \bar{\rho}] \times [\underline{b}, \bar{b}] \times [\underline{a}, \bar{a}] \times [\underline{\sigma}, \bar{\sigma}]$  with  $\underline{\mu}, \underline{\varsigma}, \underline{b}, \underline{a}, \underline{\sigma} > 0$ . For the probability measure  $\hat{\mathbb{P}}^\alpha$  introduced in (6.1), the SDE (6.6) has the dynamics

$$\begin{aligned} dX_t &= (\mu + p\beta\varsigma^2) X_t dt + \varsigma X_t d\hat{W}_t, \\ dr_t &= (b + p\beta\varsigma\rho\sigma - ar_t) dt + \sigma d\hat{B}_t^\alpha, \quad 0 \leq t \leq T. \end{aligned}$$

Interestingly, making a distinction to the cases before, the interest rate might also be negative, which means Proposition 3.2 cannot identify the parameter  $a$  when finding parameters achieving the worst-case scenario. Additionally, also for the parameters  $\varsigma, a$ , and  $\sigma$  we will see that it becomes more difficult to determine, since they depend not only on the sign of  $\beta$  but also on the signs of  $\underline{\rho}$  and  $\bar{\rho}$ .

With

$$\mathcal{L}\phi \stackrel{(3.2)}{=} \frac{1}{2}\sigma^2\phi''(r) + (b + p\beta\varsigma\rho\sigma - ar)\phi'(r) - p(\beta - 1)r\phi(r)$$

the eigenpair problem for the infinitesimal generator of  $r$  under the probability measure  $\hat{\mathbb{P}}^\alpha$  is expressed as

$$-\lambda\phi(r) = \frac{1}{2}\sigma^2\phi''(r) + (b + p\beta\varsigma\rho\sigma - ar)\phi'(r) - p(\beta - 1)r\phi(r).$$

One solution pair can be shown to be

$$(\lambda(\alpha), \phi(r)) := \left( -\frac{1}{2} \left( p(\beta - 1) \frac{\sigma}{a} \right)^2 + p^2\beta(\beta - 1)\varsigma\rho\frac{\sigma}{a} + \frac{bp(\beta - 1)}{a}, e^{-\frac{p(\beta-1)r}{a}} \right).$$

We define a new probability measure  $\hat{\mathbb{Q}}^\alpha$  on  $\mathcal{F}_T$  for each  $T > 0$  by

$$\frac{d\hat{\mathbb{Q}}^\alpha}{d\hat{\mathbb{P}}^\alpha} \Big|_{\mathcal{F}_T} = e^{\lambda(\alpha)T - p(\beta-1) \int_0^T r_s ds - \frac{p(\beta-1)}{a} r_T + \frac{p(\beta-1)}{a} r_0},$$

which makes sense by Chapter 3. Then, the process  $r$  satisfies

$$dr_t = \left( b + p\beta\varsigma\rho\sigma - \frac{p(\beta - 1)\sigma^2}{a} - ar_t \right) dt + \sigma dB_t^{\hat{\mathbb{Q}}^\alpha}, \quad 0 \leq t \leq T,$$

where  $B_t^{\hat{\mathbb{Q}}^\alpha}$  is a  $\hat{\mathbb{Q}}$ -Brownian motion

$$B_t^{\hat{\mathbb{Q}}^\alpha} = \frac{p(\beta - 1)\sigma}{a}t + \hat{B}_t^\alpha, \quad 0 \leq t \leq T.$$

Hence,

$$\begin{aligned} V(T; \alpha) &\stackrel{(6.5)}{=} \mathbb{E}^{\hat{\mathbb{P}}^\alpha} \left[ e^{-\frac{1}{2}p(1-p)\beta^2\varsigma^2T - p(\beta-1) \int_0^T r_s^\alpha ds} \right] \\ &= e^{-\frac{1}{2}p(1-p)\beta^2\varsigma^2T - \lambda(\alpha)T + \frac{p(1-\beta)}{a}r_0} \mathbb{E}^{\hat{\mathbb{Q}}^\alpha} \left[ e^{\frac{p(\beta-1)}{a}r_T} \right]. \end{aligned}$$

We observe that the term  $\mathbb{E}^{\hat{\mathbb{Q}}^\alpha} \left[ e^{\frac{p(\beta-1)}{a}r_T} \right]$  corresponds to evaluating the moment generating function of  $r_T$  at the point  $p(\beta - 1)/a$ . Since it is well-known that the distribution of  $r_T$  is given by

$$r_T \sim \mathcal{N} \left( e^{-aT} + \frac{1}{a} \left( b + p\beta\varsigma\rho\sigma - \frac{p(\beta - 1)\sigma^2}{a} \right) (1 - e^{-aT}), \frac{\sigma^2}{2a} (1 - e^{-2aT}) \right),$$

with both the mean and variance being bounded and converging to positive constants as  $T \rightarrow \infty$ , independently of the choice of  $\alpha$ , we can directly deduce the following convergence:

$$\lim_{T \rightarrow \infty} \frac{1}{T} \log \inf_{\alpha \in [\underline{\alpha}, \bar{\alpha}]} V(T; \alpha) = \inf_{\alpha \in [\underline{\alpha}, \bar{\alpha}]} -\frac{1}{2}p(1-p)\beta^2\varsigma^2 - \lambda(\alpha).$$

We are now left with determining  $\alpha^* \in [\underline{\alpha}, \bar{\alpha}]$  achieving the infimum. As already mentioned before, the value of  $\alpha^*$  depends on the signs of  $\rho$  and  $\bar{\rho}$ . We denote  $\alpha^* = (\mu^*, \varsigma^*, \rho^*, b^*, a^*, \sigma^*)$  and remind us that  $\mu^*$  is already given in (6.4).

We want to find the infimum of

$$-\frac{1}{2}p(1-p)\beta^2\varsigma^2 + \frac{1}{2}\left(p(\beta-1)\frac{\sigma}{a}\right)^2 - p^2\beta(\beta-1)\varsigma\rho\frac{\sigma}{a} - \frac{bp(\beta-1)}{a}$$

with respect to all parameters  $(\varsigma, \rho, b, a, \sigma)$ . We consider the following case distinction:

**Case 1**  $\beta \in [1, \bar{\beta}]$  and  $\bar{\rho} > 0$ :

So in this case:

$$\underbrace{-\frac{1}{2}p(1-p)\beta^2\varsigma^2}_{\leq 0} + \underbrace{\frac{1}{2}\left(p(\beta-1)\frac{\sigma}{a}\right)^2}_{\geq 0} \underbrace{-p^2\beta(\beta-1)\varsigma\rho\frac{\sigma}{a}}_{\text{can be negative for } \bar{\rho}} \underbrace{-\frac{bp(\beta-1)}{a}}_{\leq 0}.$$

So to get the infimum we can directly choose  $b^* = \bar{b}, \varsigma^* = \bar{\varsigma}, \rho^* = \bar{\rho}$ , and are only left with

$$(a^*, \sigma^*) \in \arg \max_{(a, \sigma) \in [\underline{a}, \bar{a}] \times [\underline{\sigma}, \bar{\sigma}]} \lambda(\bar{\varsigma}, \bar{\rho}, \bar{b}, a, \sigma).$$

**Case 2**  $\beta \in [1, \bar{\beta}]$  and  $\bar{\rho} < 0$ :

In this case:

$$\underbrace{-\frac{1}{2}p(1-p)\beta^2\varsigma^2}_{\leq 0} + \underbrace{\frac{1}{2}\left(p(\beta-1)\frac{\sigma}{a}\right)^2}_{\geq 0} \underbrace{-p^2\beta(\beta-1)\varsigma\rho\frac{\sigma}{a}}_{\geq 0} \underbrace{-\frac{bp(\beta-1)}{a}}_{\leq 0}.$$

So to get the infimum we can directly choose  $b^* = \bar{b}, \rho^* = \bar{\rho}, \sigma^* = \underline{\sigma}$ , and

$$(\varsigma^*, a^*) \in \arg \max_{(\varsigma, a) \in [\underline{\varsigma}, \bar{\varsigma}] \times [\underline{a}, \bar{a}]} \left\{ \frac{1}{2}p(1-p)\beta^2\varsigma^2 + \lambda(\varsigma, \bar{\rho}, \bar{b}, a, \underline{\sigma}) \right\}.$$

Similarly, we proceed with the other cases:

**Case 3**  $\beta \in [0, 1)$  and  $\rho < 0$ :

We directly deduce  $b^* = \underline{b}, \varsigma^* = \bar{\varsigma}, \rho^* = \underline{\rho}$ , and are left only with

$$(a^*, \sigma^*) \in \arg \max_{(a, \sigma) \in [\underline{a}, \bar{a}] \times [\underline{\sigma}, \bar{\sigma}]} \lambda(\bar{\varsigma}, \underline{\rho}, \underline{b}, a, \sigma).$$

**Case 4**  $\beta \in [0, 1)$  and  $\rho > 0$ :

We directly deduce  $b^* = \underline{b}, \rho^* = \underline{\rho}, a^* = \bar{a}, \sigma^* = \underline{\sigma}$ , and are only left with

$$\varsigma^* = \arg \max_{\varsigma \in [\underline{\varsigma}, \bar{\varsigma}]} \left\{ \frac{1}{2}p(1-p)\beta^2\varsigma^2 + p^2\beta(\beta-1)\underline{\rho}\sigma\underline{\varsigma}/\bar{a} \right\}.$$

**Case 5**  $\beta \in [\underline{\beta}, 0)$  and  $\bar{\rho} > 0$ :

We directly deduce  $b^* = \underline{b}, \varsigma^* = \bar{\varsigma}, \rho^* = \bar{\rho}$ , and are only left with

$$(a^*, \sigma^*) \in \arg \max_{(a, \sigma) \in [\underline{a}, \bar{a}] \times [\underline{\sigma}, \bar{\sigma}]} \lambda(\bar{\varsigma}, \bar{\rho}, \underline{b}, a, \sigma).$$

**Case 6**  $\beta \in [\underline{\beta}, 0)$  and  $\bar{\rho} < 0$ :

We directly deduce  $b^* = \underline{b}$ ,  $\rho^* = \bar{\rho}$ ,  $a^* = \bar{a}$ ,  $\sigma^* = \underline{\sigma}$ , and are only left with

$$\varsigma^* = \arg \max_{\varsigma \in [\underline{\varsigma}, \bar{\varsigma}]} \left\{ \frac{1}{2} p(1-p)\beta^2 \varsigma^2 + p^2 \beta(\beta-1) \bar{\rho} \underline{\sigma} \varsigma / \bar{a} \right\}.$$

**Proposition 6.1** *Leung et al. [1, Proposition 7]*

Let  $0 < \underline{\mu} \leq \bar{\mu}$ ,  $0 < \underline{\varsigma} \leq \bar{\varsigma}$ ,  $0 < \underline{b} \leq \bar{b}$ ,  $0 < \underline{a} \leq \bar{a}$ ,  $0 < \underline{\sigma} \leq \bar{\sigma}$ , and  $(X^\alpha, r^\alpha)$  be the process 6.6 with set of parameters  $\alpha = (\mu, \varsigma, \rho, b, a, \sigma)$  ranging over  $[\underline{\mu}, \bar{\mu}] \times [\underline{\varsigma}, \bar{\varsigma}] \times [\underline{\rho}, \bar{\rho}] \times [\underline{b}, \bar{b}] \times [\underline{a}, \bar{a}] \times [\underline{\sigma}, \bar{\sigma}]$ . Then, the long-term growth rate of the worst-case expected utility of the LETF  $L^\alpha = (L_t^\alpha)_{t \geq 0}$  with reference process and interest rate  $X^\alpha$  and  $r^\alpha$ , respectively, is given by

$$\lim_{T \rightarrow \infty} \frac{1}{T} \log \inf_{\alpha \in [\underline{\alpha}, \bar{\alpha}]} \mathbb{E}^{\mathbb{P}^\alpha} [L_T^p] = p\beta\mu^*(\beta) - \frac{1}{2} p(1-p)\beta^2 \varsigma^*(\beta, \underline{\rho}, \bar{\rho})^2 - \lambda(\alpha^*(\beta, \underline{\rho}, \bar{\rho})),$$

where

$$\begin{aligned} \alpha^*(\beta, \underline{\rho}, \bar{\rho}) &= (\mu^*(\beta), \varsigma^*(\beta, \underline{\rho}, \bar{\rho}), \rho^*(\beta), b^*(\beta), a^*(\beta, \underline{\rho}, \bar{\rho}), \sigma^*(\beta, \underline{\rho}, \bar{\rho})) \\ \lambda(\alpha, \beta) &= -\frac{1}{2} \left( p(\beta-1) \frac{\sigma}{a} \right)^2 + p^2 \beta(\beta-1) \varsigma \rho \frac{\sigma}{a} + \frac{p(\beta-1)b}{a}, \\ \mu^*(\beta) &= \begin{cases} \underline{\mu}, & \beta \geq 0 \\ \bar{\mu}, & \beta < 0 \end{cases}, \quad \rho^*(\beta) = \begin{cases} \bar{\rho}, & \beta \in [\underline{\beta}, 0) \cup [1, \bar{\beta}] \\ \underline{\rho}, & \beta \in [0, 1) \end{cases}, \quad b^*(\beta) = \begin{cases} \bar{b}, & \beta \geq 1 \\ \underline{b}, & \beta < 1 \end{cases}, \end{aligned}$$

and  $(\varsigma^*(\beta, \underline{\rho}, \bar{\rho}), a^*(\beta, \underline{\rho}, \bar{\rho}), \sigma^*(\beta, \underline{\rho}, \bar{\rho}))$  is defined in the case-by-case manner as

$$\begin{cases} (\bar{\varsigma}, \arg \max_{(a,\sigma) \in [\underline{a}, \bar{a}] \times [\underline{\sigma}, \bar{\sigma}]} \lambda(\bar{\varsigma}, \bar{\rho}, \bar{b}, a, \sigma)) & \beta \in [1, \bar{\beta}], \bar{\rho} > 0 \\ (\arg \max_{(\varsigma,a) \in [\underline{\varsigma}, \bar{\varsigma}] \times [\underline{a}, \bar{a}]} \{ \frac{1}{2} p(1-p)\beta^2 \varsigma^2 + \lambda(\varsigma, \bar{\rho}, \bar{b}, a, \underline{\sigma}) \}, \underline{\sigma}) & \beta \in [1, \bar{\beta}], \bar{\rho} < 0 \\ (\bar{\varsigma}, \arg \max_{(a,\sigma) \in [\underline{a}, \bar{a}] \times [\underline{\sigma}, \bar{\sigma}]} \lambda(\bar{\varsigma}, \underline{\rho}, \underline{b}, a, \sigma)) & \beta \in [0, 1], \underline{\rho} < 0 \\ (\arg \max_{\varsigma \in [\underline{\varsigma}, \bar{\varsigma}]} \{ \frac{1}{2} p(1-p)\beta^2 \varsigma^2 + p^2 \beta(\beta-1) \bar{\rho} \underline{\sigma} \varsigma / \bar{a} \}, \underline{\sigma}) & \beta \in [0, 1], \underline{\rho} > 0 \\ (\bar{\varsigma}, \arg \max_{(a,\sigma) \in [\underline{a}, \bar{a}] \times [\underline{\sigma}, \bar{\sigma}]} \lambda(\bar{\varsigma}, \bar{\rho}, \underline{b}, a, \sigma)) & \beta \in [\underline{\beta}, 0], \bar{\rho} > 0 \\ (\arg \max_{\varsigma \in [\underline{\varsigma}, \bar{\varsigma}]} \{ \frac{1}{2} p(1-p)\beta^2 \varsigma^2 + p^2 \beta(\beta-1) \bar{\rho} \underline{\sigma} \varsigma / \bar{a} \}, \underline{\sigma}) & \beta \in [\underline{\beta}, 0], \bar{\rho} < 0 \end{cases}.$$

Similar to Chapter 5 calculating the explicit optimal leverage ratio and the corresponding worst-case long-term growth rate is very difficult in this model. Therefore we solve this through numerical computations. We define

$$\Lambda(\beta) := p\beta\mu^*(\beta) - \frac{1}{2} p(1-p)\beta^2 \varsigma^*(\beta, \underline{\rho}, \bar{\rho})^2 - \lambda(\alpha^*(\beta, \underline{\rho}, \bar{\rho})).$$

By setting  $f := \Lambda(\beta) + \lambda(\alpha^*(\beta, \underline{\rho}, \bar{\rho}))$  and using the  $\Delta$ -inequality we get

$$\begin{aligned} |\Lambda(\beta+h) - \Lambda(\beta)| &\leq |f(\beta+h) - f(\beta)| + |\lambda(\alpha^*(\beta+h, \underline{\rho}, \bar{\rho})) - \lambda(\alpha^*(\beta, \underline{\rho}, \bar{\rho}))| \\ &\leq \sup_{\beta \in [\underline{\beta}, \bar{\beta}] \atop \leq p\bar{\mu} + (1-p)\bar{\varsigma}^2 \max\{|\beta|, \bar{\beta}\}} \underbrace{|f'(\beta)|}_{} h + \sup_{a, \sigma, \beta} |\lambda_\beta(a, \sigma, \beta)| h \\ &\leq \left( p\bar{\mu} + p(1-p)\bar{\varsigma}^2 \max\{|\underline{\beta}|, \bar{\beta}\} + \sup_{a, \sigma, \beta} |\lambda_\beta(a, \sigma, \beta)| \right) h. \end{aligned}$$

With this inequality we can set a mesh size for a given error bound similar as in the section on the Heston model 5.1. For  $\beta \in [-5, 5]$ ,  $p = 0.5$ ,  $[\underline{\mu}, \bar{\mu}] = [0.06, 0.1]$ ,  $[\underline{\varsigma}, \bar{\varsigma}] = [0.08, 0.25]$ ,  $[\underline{\rho}, \bar{\rho}] = [-0.9, -0.5]$ ,  $[\underline{b}, \bar{b}] = [0.06, 0.1]$ ,  $[\underline{a}, \bar{a}] = [6, 9]$ ,  $[\underline{\sigma}, \bar{\sigma}] = [0.2, 0.5]$  the approximate optimal leverage ratio is 1.68 and the approximate robust long-term growth rate is 0.025. The worst-case long-term growth rate of the expected utility as a function of  $\beta$  is visualized in Figure 6.1.

One can see that the optimal leverage ratios corresponding to various ranges of  $\sigma$  and  $\rho$  in the Vasicek model exhibit greater dynamism compared to those in the Heston model, as shown in Fig. 6.2.

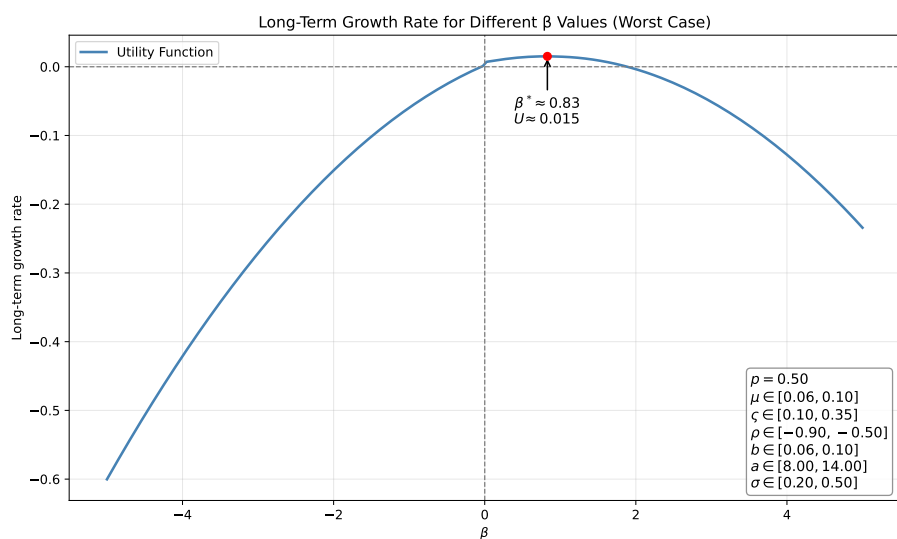


Figure 6.1: Long-term growth rate of the worst-case expected utility as a function of the leverage ratio  $\beta$  under the Vasicek model.

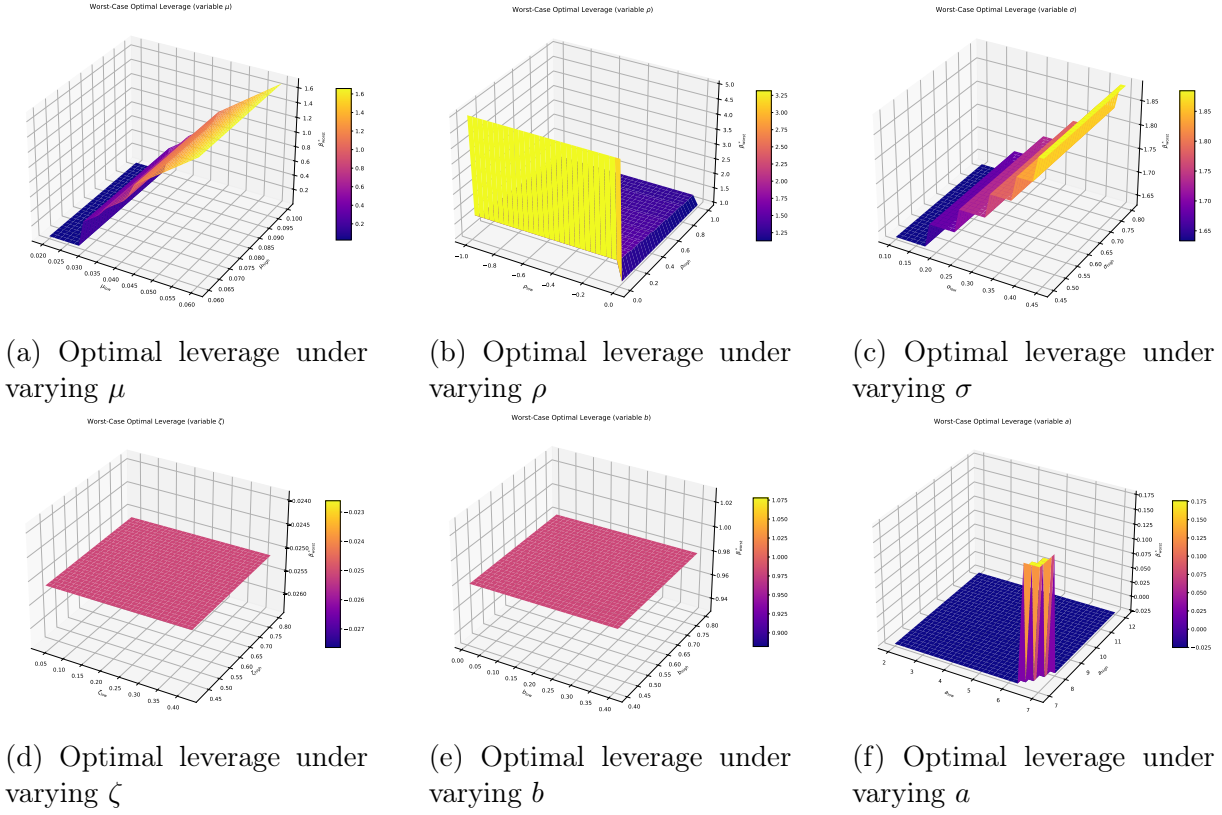


Figure 6.2: Impact of different intervals on the optimal leverage ratio.

**Corollary 6.2** *Leung et al. [1, Corollary 3]*

Let the reference process  $X$  and the interest rate  $r$  follow

$$dX_t = \mu_t X_t dt + \varsigma_t X_t dW_t^{\rho(t)}, \\ dr_t = (b_0(t, r_t) - ar_t) dt + \sigma dB_t^{\rho(t)},$$

where  $\mu$  and  $\varsigma$  are progressively measurable processes mapping to  $[\underline{\mu}, \bar{\mu}]$  and  $[\underline{\varsigma}, \bar{\varsigma}]$ , respectively, and  $b_0$  and  $\rho$  range over  $[\underline{b}, \bar{b}]$  and  $[\underline{\rho}, \bar{\rho}]$ , respectively. Then, Proposition 6.1 holds for the LETF with the reference  $X$  and the interest rate  $r$ .

## 6.2 Inverse GARCH interest rate

Next, we assume that the short interest rate  $r$  follows an inverse GARCH process. Hence the reference process  $X$  and short interest rate  $r$  satisfy the SDEs

$$dX_t = \mu X_t dt + \varsigma X_t dW_t, \\ dr_t = (b - ar_t) r_t dt + \sigma r_t dB_t, \quad (6.7)$$

where  $a, \sigma > 0$ ,  $2b \geq \sigma^2$ ,  $W$  and  $B$  are two Brownian motions with  $\langle W, B \rangle_t = \rho t$  and  $-1 \leq \underline{\rho} \leq \rho \leq \bar{\rho} \leq 1$ . As we have seen before, the condition  $2b \geq \sigma^2$  ensures again a positive

domain, i.e.  $D = (0, \infty)$ . We allow for uncertainties in  $\mu, \varsigma, \rho, b, a, \sigma$ , and our model parameter set is  $\alpha = (\mu, \varsigma, \rho, b, a, \sigma) \in [\underline{\alpha}, \bar{\alpha}] = [\underline{\mu}, \bar{\mu}] \times [\underline{\varsigma}, \bar{\varsigma}] \times [\underline{\rho}, \bar{\rho}] \times [\underline{b}, \bar{b}] \times [\underline{a}, \bar{a}] \times [\underline{\sigma}, \bar{\sigma}]$  with  $\underline{\mu}, \underline{\varsigma}, \underline{a}, \underline{\sigma} > 0$ , and  $\bar{b} - p|\beta|\bar{\varsigma}\bar{\sigma} \geq \bar{\sigma}^2/2$ . For the probability measure  $\hat{\mathbb{P}}^\alpha$  defined by (6.1) and the Brownian motions defined by (6.3), the process (6.7) has the dynamics

$$\begin{aligned} dX_t &= (\mu + p\beta\varsigma^2) X_t dt + \varsigma X_t d\hat{W}_t, \\ dr_t &= (b + p\beta\varsigma\rho\sigma - ar_t) r_t dt + \sigma r_t d\hat{B}_t^\alpha, \quad 0 \leq t \leq T. \end{aligned}$$

We apply Proposition 3.2 to show that

$$\mathbb{E}^{\mathbb{P}^\alpha} [L_T^p] \geq e^{p\beta\mu^*T - \frac{1}{2}p(1-p)\beta^2\varsigma^2T} \mathbb{E}^{\hat{\mathbb{P}}^{\mu^*, \varsigma, \rho, b^*, a^*, \sigma}} \left[ e^{-p(\beta-1)\int_0^T r_s ds} \right], \quad (6.8)$$

where

$$b^* = \begin{cases} \bar{b}, & \beta \geq 1 \\ \underline{b}, & \beta < 1 \end{cases}, \quad \text{and} \quad a^* = \begin{cases} \underline{a}, & \beta \geq 1 \\ \bar{a}, & \beta < 1 \end{cases}. \quad (6.9)$$

Set  $\alpha^*(\varsigma, \rho, \sigma) = (\mu^*, \varsigma, \rho, b^*, a^*, \sigma)$ .

The eigenpair problem for the infinitesimal generator of  $r$  under the probability measure  $\hat{\mathbb{P}}^\alpha$  is expressed as

$$-\lambda\phi(r) = \frac{1}{2}\sigma^2r^2\phi''(r) + (b^* + p\beta\varsigma\rho\sigma - a^*r)\phi'(r) - p(\beta-1)r\phi(r),$$

and one can show that

$$\begin{aligned} &(\lambda(\alpha^*), \phi(r)) : \\ &= \left( -\frac{p(\beta-1)}{2a^*} \left( \frac{p(\beta-1)}{a^*} + 1 \right) \sigma^2 + \frac{p^2\beta(\beta-1)\varsigma\rho}{a^*}\sigma + \frac{p(\beta-1)b^*}{a^*}, r^{-\frac{p(\beta-1)}{a^*}} \right) \end{aligned}$$

is one solution pair. Reasoned on (3.4), we define a probability measure  $\hat{\mathbb{Q}}^{\alpha^*(\varsigma, \rho, \sigma)}$  on  $\mathcal{F}_T$  for each  $T \geq 0$  by

$$\frac{d\hat{\mathbb{Q}}^{\alpha^*(\varsigma, \rho, \sigma)}}{d\hat{\mathbb{P}}^{\alpha^*(\varsigma, \rho, \sigma)}} \Big|_{\mathcal{F}_T} = \left( \frac{r_T}{r_0} \right)^{-\frac{p(\beta-1)}{a^*}} e^{\lambda(\alpha^*(\varsigma, \rho, \sigma))T - p(\beta-1)\int_0^T r_s ds} \quad (6.10)$$

and hence we can derive by the Hansen-Scheinkman decomposition, (3.5) and (6.8) that

$$V(T; \alpha^*(\varsigma, \rho, \sigma)) = e^{-\frac{1}{2}p(1-p)\beta^2\varsigma^2T - \lambda(\alpha^*(\varsigma, \rho, \sigma))T} r_0^{-\frac{p(\beta-1)}{a^*}} \mathbb{E}^{\hat{\mathbb{Q}}^{\alpha^*(\sigma)}} \left[ r_T^{\frac{p(\beta-1)}{a^*}} \right]. \quad (6.11)$$

The short rate process  $r$  satisfies under  $\hat{\mathbb{Q}}^{\alpha^*(\varsigma, \rho, \sigma)}$

$$dr_t = \left( b^* + p\beta\bar{\varsigma}\sigma\rho - \frac{p(\beta-1)\sigma^2}{a^*} - a^*r_t \right) r_t dt + \sigma r_t dB_t^{\hat{\mathbb{Q}}^{\alpha^*(\sigma)}}, \quad 0 \leq t \leq T,$$

with a  $\hat{\mathbb{Q}}^{\alpha^*(\varsigma, \rho, \sigma)}$ -Brownian motion

$$B_t^{\hat{\mathbb{Q}}^{\alpha^*(\varsigma, \rho, \sigma)}} \stackrel{(3.6)}{=} \frac{p(\beta-1)\sigma}{a^*} t + \hat{B}_t, \quad 0 \leq t \leq T.$$

Next, we aim to establish that

$$\inf_{\varsigma, \rho, \sigma, T} \mathbb{E}^{\hat{\mathbb{Q}}^{\alpha^*(\sigma)}} \left[ r_T^{\frac{p(\beta-1)}{a^*}} \right] > 0.$$

To begin, we point out that the process  $r^{-1} = (r_t^{-1})_{t \geq 0}$  is a GARCH process represented by a linear SDE. As shown in Klebaner [60], the process  $r^{-1}$  admits the explicit form

$$r_t^{-1} = r_0^{-1} e^{-\left(b^* + p\beta\varsigma\rho\sigma - \frac{p(\beta-1)\sigma^2}{a^*} - \frac{\sigma^2}{2}\right)t - \sigma B_t} \\ + a^* \int_0^t e^{-\left(b^* + p\beta\varsigma\rho\sigma - \frac{p(\beta-1)\sigma^2}{a^*} - \frac{\sigma^2}{2}\right)(t-s) - \sigma(B_t - B_s)} ds, \quad 0 \leq t \leq T.$$

Now we can differentiate between two cases to show the desired inequality.

**Case 1**  $\beta \geq 1$ :

Note that  $\frac{p(1-\beta)}{a^*} \leq 0$ . By the Jensen's inequality,

$$\mathbb{E}^{\hat{\mathbb{Q}}^{\alpha^*(\sigma)}} \left[ r_T^{-\frac{p(1-\beta)}{a^*}} \right] \geq \mathbb{E}^{\hat{\mathbb{Q}}^{\alpha^*(\sigma)}} \left[ r_T^{-1} \right]^{\frac{p(1-\beta)}{a^*}} \\ = \left( \underbrace{r_0^{-1} e^{-\left(b^* + p\beta\varsigma\rho\sigma - \frac{p(\beta-1)\sigma^2}{a^*} - \sigma^2\right)T}}_{>0} + \underbrace{\frac{a^* \left(1 - e^{-\left(b^* + p\beta\varsigma\rho\sigma - \frac{p(\beta-1)\sigma^2}{a^*} - \sigma^2\right)T}\right)}{b^* + p\beta\varsigma\rho\sigma - \frac{p(\beta-1)\sigma^2}{a^*} - \sigma^2}} \right)^{\frac{p(1-\beta)}{a^*}}.$$

Now

$$a^* \frac{1 - e^{-xT}}{x} = a^* \frac{e^{-Tx}(e^{Tx} - 1)}{x} > 0.$$

**Case 2**  $\beta < 1$ :

In contrast we now have  $\frac{p(1-\beta)}{a^*} > 0$ . Since the second term of  $r_t^{-1}$  is non-negative, we get the trivial inequality

$$\mathbb{E}^{\hat{\mathbb{Q}}^{\alpha^*(\sigma)}} \left[ r_T^{-\frac{p(1-\beta)}{a^*}} \right] \geq \mathbb{E}^{\hat{\mathbb{Q}}^{\alpha^*(\sigma)}} \left[ r_0^{-\frac{p(1-\beta)}{a^*}} e^{-\frac{p(1-\beta)}{a^*} \left( \left(b^* + p\beta\varsigma\rho\sigma - \frac{p(\beta-1)\sigma^2}{a^*} - \frac{\sigma^2}{2}\right)T + \sigma B_T \right)} \right] \\ = r_0^{-\frac{p(1-\beta)}{a^*}} e^{-\frac{p(1-\beta)}{a^*} \left( b^* + p\beta\varsigma\rho\sigma - \frac{p(\beta-1)\sigma^2}{2a^*} - \sigma^2 \right)T}.$$

Thus, we derived in both cases that  $\mathbb{E}^{\hat{\mathbb{Q}}^{\alpha^*(\sigma)}} \left[ r_T^{\frac{p(\beta-1)}{a^*}} \right] > 0$ . If, additionally  $b^* + p\beta\varsigma\rho\sigma - p(\beta-1)\sigma^2/a^* - \sigma^2 > 0$  holds we can derive by the argument shown in Chapter 4 that

$\mathbb{E}^{\hat{Q}^{\alpha^*(\sigma)}} \left[ r_T^{p(\beta-1)/a^*} \right]$  converges as  $T \rightarrow \infty$ . Hence,

$$\begin{aligned} & \lim_{T \rightarrow \infty} \frac{1}{T} \log \inf_{\alpha \in [\underline{\alpha}, \bar{\alpha}]} V(T; \alpha) \\ & \stackrel{(6.11)}{=} \lim_{T \rightarrow \infty} \frac{1}{T} \log \inf_{\alpha \in [\underline{\alpha}, \bar{\alpha}]} e^{-\frac{1}{2}p(1-p)\beta^2\zeta^2T - \lambda(\alpha^*(\zeta, \rho, \sigma))T} r_0^{-\frac{p(\beta-1)}{a^*}} \mathbb{E}^{\hat{Q}^{\alpha^*(\sigma)}} \left[ r_T^{\frac{p(\beta-1)}{a^*}} \right] \\ & = \inf_{\alpha \in [\underline{\alpha}, \bar{\alpha}]} -\frac{1}{2}p(1-p)\beta^2\zeta^2 - \lambda(\alpha^*(\zeta, \rho, \sigma)) + \lim_{T \rightarrow \infty} \left( -\frac{1}{T} \frac{p(\beta-1)}{a^*} \log(r_0) \right. \\ & \quad \left. + \frac{1}{T} \log(\mathbb{E}^{\hat{Q}^{\alpha^*(\sigma)}} \left[ r_T^{\frac{p(\beta-1)}{a^*}} \right]) \right) \\ & = \inf_{(\zeta, \rho, \sigma) \in [\underline{\zeta}, \bar{\zeta}] \times [\underline{\rho}, \bar{\rho}] \times [\underline{\sigma}, \bar{\sigma}]} \left\{ -\frac{1}{2}p(1-p)\beta^2\zeta^2 - \lambda(\alpha^*(\zeta, \rho, \sigma)) \right\}, \end{aligned}$$

assuming  $\inf_{(\zeta, \rho, \sigma) \in [\underline{\zeta}, \bar{\zeta}] \times [\underline{\rho}, \bar{\rho}] \times [\underline{\sigma}, \bar{\sigma}]} \left\{ b^* + p\beta\zeta\rho\sigma - \frac{p(\beta-1)\sigma^2}{a^*} - \sigma^2 \right\} > 0$ .

We denote  $\alpha^* = (\mu^*, \zeta^*, \rho^*, b^*, a^*, \sigma^*)$  as the parameter that achieves the infimum and reminds us that  $\mu^*$ ,  $b^*$  and  $a^*$  are already determined in (6.4) and (6.9). We want to find the infimum of

$$-\frac{1}{2}p(1-p)\beta^2(\zeta^*)^2 + \frac{p(\beta-1)}{2a^*} \left( \frac{p(\beta-1)}{a^*} + 1 \right) (\sigma^*)^2 - \frac{p^2\beta(\beta-1)\zeta^*\rho^*}{a^*}\sigma^* - \frac{p(\beta-1)b^*}{a^*}$$

**Case 1**  $\beta \in [1, \bar{\beta}]$  and  $\bar{\rho} > 0$  :

If we have the same equal signs for multiple occurrences of a parameter, we can determine the parameter for the infimum. In this first case:

$$\underbrace{-\frac{1}{2}p(1-p)\beta^2(\zeta^*)^2}_{\leq 0} + \underbrace{\frac{p(\beta-1)}{2a^*} \left( \frac{p(\beta-1)}{a^*} + 1 \right) (\sigma^*)^2}_{\geq 0} - \underbrace{\frac{p^2\beta(\beta-1)\zeta^*\rho^*}{a^*}\sigma^*}_{\leq 0} - \underbrace{\frac{p(\beta-1)b^*}{a^*}}_{\leq 0}.$$

Hence we can determine  $b^* = \bar{b}$ ,  $a^* = \underline{a}$ ,  $\zeta^* = \bar{\zeta}$ ,  $\rho^* = \bar{\rho}$ , and are left only with

$$\sigma^* \in \arg \min_{\sigma \in [\underline{\sigma}, \bar{\sigma}]} \left\{ \frac{p(\beta-1)}{2\underline{a}} \left( \frac{p(\beta-1)}{\underline{a}} + 1 \right) \sigma^2 - \frac{p^2\beta(\beta-1)\bar{\zeta}\bar{\rho}}{\underline{a}}\sigma \right\}.$$

We continue with this same scheme and find for the following cases:

**Case 2**  $\beta \in [1, \bar{\beta}]$  and  $\bar{\rho} < 0$  :

$b^* = \bar{b}$ ,  $a^* = \underline{a}$ ,  $\rho^* = \bar{\rho}$ ,  $\sigma^* = \underline{\sigma}$ , and

$$\zeta^* \in \arg \min_{\zeta \in [\underline{\zeta}, \bar{\zeta}]} \left\{ -\frac{1}{2}p(1-p)\beta^2\zeta^2 - \frac{p^2\beta(\beta-1)\bar{\rho}\underline{\sigma}}{\underline{a}}\zeta \right\}.$$

**Case 3**  $\beta \in [0, 1)$  and  $\rho < 0$  :

$b^* = \underline{b}$ ,  $a^* = \bar{a}$ ,  $\zeta^* = \bar{\zeta}$ ,  $\rho^* = \underline{\rho}$ , and

$$\sigma^* \in \arg \min_{\sigma \in [\underline{\sigma}, \bar{\sigma}]} \left\{ \frac{p(\beta - 1)}{2\bar{a}} \left( \frac{p(\beta - 1)}{\bar{a}} + 1 \right) \sigma^2 - \frac{p^2 \beta (\beta - 1) \bar{\varsigma} \bar{\rho}}{\bar{a}} \sigma \right\}.$$

**Case 4**  $\beta \in [0, 1)$  and  $\underline{\rho} > 0$  :

$b^* = \underline{b}$ ,  $a^* = \bar{a}$ ,  $\rho^* = \underline{\rho}$ , and

$$(\varsigma^*, \sigma^*) = \arg \min_{(\varsigma, \sigma) \in [\underline{\varsigma}, \bar{\varsigma}] \times [\underline{\sigma}, \bar{\sigma}]} \left\{ -\frac{1}{2} p(1-p) \beta^2 \varsigma^2 + \frac{p(\beta - 1)}{2\bar{a}} \left( \frac{p(\beta - 1)}{\bar{a}} + 1 \right) \sigma^2 - \frac{p^2 \beta (\beta - 1) \bar{\varsigma} \bar{\rho}}{\bar{a}} \varsigma \sigma \right\}.$$

**Case 5**  $\beta \in [\underline{\beta}, 0)$  and  $\bar{\rho} > 0$  :

$b^* = \underline{b}$ ,  $a^* = \bar{a}$ ,  $\varsigma^* = \bar{\varsigma}$ ,  $\rho^* = \bar{\rho}$ , and

$$\sigma^* \in \arg \min_{\sigma \in [\underline{\sigma}, \bar{\sigma}]} \left\{ \frac{p(\beta - 1)}{2\bar{a}} \left( \frac{p(\beta - 1)}{\bar{a}} + 1 \right) \sigma^2 - \frac{p^2 \beta (\beta - 1) \bar{\varsigma} \bar{\rho}}{\bar{a}} \sigma \right\}.$$

**Case 6**  $\beta \in [\underline{\beta}, 0)$  and  $\bar{\rho} < 0$  :

$b^* = \underline{b}$ ,  $a^* = \bar{a}$ ,  $\rho^* = \bar{\rho}$ , and

$$(\varsigma^*, \sigma^*) = \arg \min_{(\varsigma, \sigma) \in [\underline{\varsigma}, \bar{\varsigma}] \times [\underline{\sigma}, \bar{\sigma}]} \left\{ -\frac{1}{2} p(1-p) \beta^2 \varsigma^2 + \frac{p(\beta - 1)}{2\bar{a}} \left( \frac{p(\beta - 1)}{\bar{a}} + 1 \right) \sigma^2 - \frac{p^2 \beta (\beta - 1) \bar{\rho}}{\bar{a}} \varsigma \sigma \right\}.$$

**Proposition 6.3** *Leung et al. [1, Proposition 8]*

Let  $0 < \underline{\mu} \leq \bar{\mu}$ ,  $0 < \underline{\varsigma} \leq \bar{\varsigma}$ ,  $0 < \underline{a} \leq \bar{a}$ ,  $0 < \underline{\sigma} \leq \bar{\sigma}$ ,  $\bar{\sigma}^2/2 + p|\beta| \bar{\varsigma} \bar{\sigma} < \underline{b} \leq \bar{b}$ , and  $(X^\alpha, r^\alpha)$  be the process (6.7) with set of parameters  $\alpha = (\mu, \varsigma, \rho, b, a, \sigma)$  ranging over  $[\underline{\alpha}, \bar{\alpha}] = [\underline{\mu}, \bar{\mu}] \times [\underline{\varsigma}, \bar{\varsigma}] \times [\underline{\rho}, \bar{\rho}] \times [\underline{b}, \bar{b}] \times [\underline{a}, \bar{a}] \times [\underline{\sigma}, \bar{\sigma}]$ . Then, the long-term growth rate of the worst-case expected utility of the LETF  $L^\alpha = (L_t^\alpha)_{t \geq 0}$  with reference process and interest rate  $X^\alpha$  and  $r^\alpha$  respectively, is given by

$$\begin{aligned} \lim_{T \rightarrow \infty} \frac{1}{T} \log \inf_{\alpha \in [\underline{\alpha}, \bar{\alpha}]} \mathbb{E}^{\mathbb{P}^\alpha} [L_T^p] &= p\beta \mu^*(\beta) - \frac{1}{2} p(1-p) \beta^2 \varsigma^*(\beta, \underline{\rho}, \bar{\rho})^2 - \frac{p(\beta - 1) b^*(\beta)}{a^*(\beta)} \\ &\quad + \frac{p(\beta - 1)}{2a^*(\beta)} \left( \frac{p(\beta - 1)}{a^*(\beta)} + 1 \right) \sigma^*(\beta, \underline{\rho}, \bar{\rho})^2 - \frac{p^2 \beta (\beta - 1)}{a^*(\beta)} (\varsigma^* \sigma^*)(\beta, \underline{\rho}, \bar{\rho}), \end{aligned}$$

where

$$\mu^*(\beta) = \begin{cases} \underline{\mu}, & \beta \geq 0 \\ \bar{\mu}, & \beta < 0 \end{cases}, \quad \rho^*(\beta) = \begin{cases} \bar{\rho}, & \beta \in [\underline{\beta}, 0) \cup [1, \bar{\beta}] \\ \underline{\rho}, & \beta \in [0, 1) \end{cases}, \quad (b^*(\beta), a^*(\beta)) = \begin{cases} (\bar{b}, \underline{a}), & \beta \geq 1 \\ (\underline{b}, \bar{a}), & \beta < 1 \end{cases},$$

and  $(\varsigma^*(\beta, \underline{\rho}, \bar{\rho}), \sigma^*(\beta, \underline{\rho}, \bar{\rho}))$  is defined in the case-by-case manner as

$$\begin{cases} \left( \bar{\varsigma}, \arg \min_{\sigma \in [\underline{\sigma}, \bar{\sigma}]} \left\{ \frac{p(\beta-1)}{2\underline{a}} \left( \frac{p(\beta-1)}{\underline{a}} + 1 \right) \sigma^2 - \frac{p^2 \beta (\beta-1) \bar{\varsigma} \bar{\rho}}{\underline{a}} \sigma \right\} \right), & \beta \in [1, \bar{\beta}], \bar{\rho} > 0 \\ \left( \arg \min_{\varsigma \in [\underline{\varsigma}, \bar{\varsigma}]} \left\{ -\frac{1}{2} p(1-p) \beta^2 \varsigma^2 - \frac{p^2 \beta (\beta-1) \bar{\rho} \underline{\sigma}}{\underline{a}} \varsigma, \underline{\sigma} \right\} \right), & \beta \in [1, \bar{\beta}], \bar{\rho} < 0 \\ \left( \bar{\varsigma}, \arg \min_{\sigma \in [\underline{\sigma}, \bar{\sigma}]} \left\{ \frac{p(\beta-1)}{2\bar{a}} \left( \frac{p(\beta-1)}{\bar{a}} + 1 \right) \sigma^2 - \frac{p^2 \beta (\beta-1) \bar{\varsigma} \rho}{\bar{a}} \sigma \right\} \right), & \beta \in [0, 1), \underline{\rho} < 0 \\ \arg \max_{(\varsigma, \sigma) \in [\underline{\varsigma}, \bar{\varsigma}] \times [\underline{\sigma}, \bar{\sigma}]} \left\{ \frac{1}{2} (1-p) \beta^2 \varsigma^2 - \frac{\beta-1}{2\bar{a}} \left( \frac{p(\beta-1)}{\bar{a}} + 1 \right) \sigma^2 + \frac{p\beta(\beta-1)\rho}{\bar{a}} \varsigma \sigma \right\}, & \beta \in [0, 1), \underline{\rho} > 0 \\ \left( \bar{\varsigma}, \arg \min_{\sigma \in [\underline{\sigma}, \bar{\sigma}]} \left\{ \frac{p(\beta-1)}{2\bar{a}} \left( \frac{p(\beta-1)}{\bar{a}} + 1 \right) \sigma^2 - \frac{p^2 \beta (\beta-1) \bar{\varsigma} \bar{\rho}}{\bar{a}} \sigma \right\} \right), & \beta \in [\underline{\beta}, 0), \bar{\rho} > 0 \\ \arg \max_{(\varsigma, \sigma) \in [\underline{\varsigma}, \bar{\varsigma}] \times [\underline{\sigma}, \bar{\sigma}]} \left\{ \frac{1}{2} (1-p) \beta^2 \varsigma^2 - \frac{\beta-1}{2\bar{a}} \left( \frac{p(\beta-1)}{\bar{a}} + 1 \right) \sigma^2 + \frac{p\beta(\beta-1)\bar{\rho}}{\bar{a}} \varsigma \sigma \right\}, & \beta \in [\underline{\beta}, 0), \bar{\rho} < 0 \end{cases}$$

provided that

$$\inf_{(\varsigma, \rho, \sigma) \in [\underline{\varsigma}, \bar{\varsigma}] \times [\underline{\rho}, \bar{\rho}] \times [\underline{\sigma}, \bar{\sigma}]} \left\{ b^*(\beta) + p\beta \varsigma \rho \sigma - \frac{p(\beta-1)\sigma^2}{a^*(\beta)} - \sigma^2 \right\} > 0$$

for all  $\beta \in [\underline{\beta}, \bar{\beta}]$ .

The issue of determining the optimal leverage ratio can, as previously discussed, also be addressed through numerical methods.

**Corollary 6.4** Leung et al. [1, Corollary 4]

Let the reference process  $X$  and interest rate  $r$  follow

$$\begin{aligned} dX_t &= \mu_t X_t dt + \varsigma_t X_t dW_t^{\rho(t)} \\ dr_t &= (b_0(t, r_t) - a_0(t, r_t) r_t) dt + \sigma dB_t^{\rho(t)} \end{aligned}$$

where  $\mu$  and  $\varsigma$  are progressively measurable processes mapping to  $[\underline{\mu}, \bar{\mu}]$  and  $[\underline{\varsigma}, \bar{\varsigma}]$ , respectively, and  $b_0, a_0$ , and  $\rho$  take values in  $[\underline{b}, \bar{b}]$ ,  $[\underline{a}, \bar{a}]$ , and  $[\underline{\rho}, \bar{\rho}]$ , respectively. Then, Proposition 6.3 holds for the LETF with the reference  $X$  and interest rate  $r$ .

# Chapter 7

## Jump diffusion processes

In previous chapters, we have assumed that the dynamics of the reference index  $X$  evolve continuously, driven by Brownian motion and possibly influenced by stochastic volatility or stochastic interest rates. However, real financial markets frequently experience sudden price movements due to news, macroeconomic events, or systemic shocks. These features cannot be captured by continuous diffusions alone. To model such discontinuities, we now extend our framework to jump-diffusion processes for the reference index. In doing so, we move beyond the purely continuous setting and allow for possibly rare but significant discontinuities in the index.

We revisit also models we have studied before, augmented by jumps, including settings with constant and stochastic volatility. While we retain the general structure of wealth dynamics and uncertainty modeling, the presence of jumps alters the expected utility calculations. We will show how these jump terms enter naturally into the analysis and derive the long-run growth rates in the presence of such risks.

**Proposition 7.1** *Itô's Lemma for 1-Dimensional Jump-Diffusions:*

Let  $X_t$  be a jump process and  $f(x)$  a function for which  $f'(x), f''(x)$  are defined and continuous. Then:

$$f(X_t) = f(X_0) + \int_0^t f'(X_s)dX_s^c + \frac{1}{2} \int_0^t f''(X_s)dX_s^c dX_s^c + \sum_{0 < s \leq t} [f(X_s) - f(X_{s-})]$$

where  $X_t^c$  denotes the continuous, i.e. non-jump, component of  $X_t$  and the summation is over the jump times of the process, c.f. Haugh [61].

### 7.1 Merton jump diffusion model

We consider the Merton jump diffusion model, where the reference index  $X$  is assumed to follow the following SDE

$$\frac{dX_t}{X_t} = \mu dt + \sigma dB_t + (k - 1)dN_t,$$

where  $N_t$  is a Poisson process with intensity  $\xi$ ,  $k$  is log-normally distributed with parameters  $\mu_k, \sigma_k^2$  and  $B_t$  a Brownian motion. Hence our uncertainty parameters are  $\alpha =$

$(\mu, \sigma, \mu_k, \sigma_k, \xi) \in [\underline{\mu}, \bar{\mu}] \times [\underline{\sigma}, \bar{\sigma}] \times [\underline{\mu}_k, \bar{\mu}_k] \times [\underline{\sigma}_k, \bar{\sigma}_k] \times [\underline{\xi}, \bar{\xi}]$  with  $\underline{\mu}, \underline{\sigma}, \underline{\xi} > 0$ .  
 First let us compute  $\mathbb{E}^{\mathbb{P}}[(L_t^{\alpha})^p]$ :

$$\begin{aligned} dL_{t^-}^{\alpha} &= L_t^{\alpha} \beta \frac{dX_t}{X_{t^-}} + L_{t^-}^{\alpha} (1 - \beta) r dt \\ &= L_t^{\alpha} \beta (\mu dt + \sigma dB_t + (k - 1) dN_t) + L_{t^-}^{\alpha} (1 - \beta) r dt \\ &= L_t^{\alpha} (\beta \mu + (1 - \beta)r) dt + L_t^{\alpha} \beta \sigma dB_t + L_t^{\alpha} \beta (k - 1) dN_t \end{aligned}$$

and by Itô's formula for jump processes

$$d \log(L_t^{\alpha}) = \left( \beta \mu + (1 - \beta)r - \frac{1}{2} \beta^2 \sigma^2 \right) dt + \beta \sigma dB_t + (\log(L_t^{\alpha}) - \log(L_{t^-}^{\alpha})) dN_t.$$

At jump time  $u$ , we have

$$L_u^{\alpha} - L_{u^-}^{\alpha} = L_{u^-}^{\alpha} \beta (k - 1) \iff L_u^{\alpha} = L_{u^-}^{\alpha} (1 + \beta(k - 1))$$

and therefore

$$\log(L_u^{\alpha}) - \log(L_{u^-}^{\alpha}) = \log\left(\frac{L_u^{\alpha}}{L_{u^-}^{\alpha}}\right) = \log(1 + \beta(k - 1)).$$

Hence

$$\log(L_t^{\alpha}) = \left( \beta \mu + (1 - \beta)r - \frac{1}{2} \beta^2 \sigma^2 \right) t + \beta \sigma B_t + \sum_{j=1}^{N_t} \log(1 + \beta(k_j - 1)).$$

Since we can rewrite  $\sum_{j=1}^{N_t} \log(1 + \beta(k_j - 1)) = \log\left(\prod_{j=1}^{N_t} (1 + \beta(k_j - 1))\right)$  we infer

$$L_t^{\alpha} = e^{(\beta \mu + (1 - \beta)r)t - \frac{1}{2} \beta^2 \int_0^t \nu_t dt + \beta \int_0^t \sqrt{\nu_t} dB_t^{(1)}} \prod_{j=1}^{N_t} (1 + \beta(k_j - 1)).$$

Hence

$$\begin{aligned} \mathbb{E}^{\mathbb{P}}[L_T^p] &= \mathbb{E}^{\mathbb{P}} \left[ e^{p(\beta \mu + (1 - \beta)r - \frac{1}{2} p \beta^2 \sigma^2)T + p \beta \sigma B_T} \left( \prod_{j=1}^{N_T} (1 + \beta(k_j - 1)) \right)^p \right] \\ &= e^{p(\beta \mu + (1 - \beta)r - \frac{1}{2} p \beta^2 \sigma^2)T} \mathbb{E}^{\mathbb{P}} \left[ e^{p \beta \sigma B_T} \right] \mathbb{E}^{\mathbb{P}} \left[ \left( \prod_{j=1}^{N_T} (1 + \beta(k_j - 1)) \right)^p \right] \\ &= e^{p(\beta \mu + (1 - \beta)r - \frac{1}{2} p \beta^2 \sigma^2)T} e^{\frac{p^2 \beta^2 \sigma^2}{2} T} \mathbb{E}^{\mathbb{P}} \left[ \left( \prod_{j=1}^{N_T} (1 + \beta(k_j - 1)) \right)^p \right] \\ &= e^{T(pr + p(\mu - r)\beta - \frac{1}{2} p(1-p)\sigma^2\beta^2)} \mathbb{E}^{\mathbb{P}} \left[ \left( \prod_{j=1}^{N_T} (1 + \beta(k_j - 1)) \right)^p \right]. \end{aligned}$$

From

$$\begin{aligned}
 \mathbb{E}^{\mathbb{P}} \left[ \left( \prod_{j=1}^{N_T} (1 + \beta(k_j - 1)) \right)^p \right] &= \sum_{n=0}^{\infty} \mathbb{E}^{\mathbb{P}} [(1 + \beta(k - 1))^{np}] \mathbb{E}^{\mathbb{P}} [N_T = n] \\
 &= \sum_{n=0}^{\infty} \mathbb{E}^{\mathbb{P}} [1 + \beta(k - 1)]^{np} \frac{(\xi T)^n}{n!} e^{-\xi T} \\
 &= e^{-\xi T} \sum_{n=0}^{\infty} (1 + \beta(\mu_k - 1))^{np} \frac{(\xi T)^n}{n!} \\
 &= e^{-\xi T} \sum_{n=0}^{\infty} \frac{(\xi T (1 + \beta(\mu_k - 1))^p)^n}{n!} \\
 &= e^{T\xi(-1+(1+\beta(\mu_k-1))^p)}
 \end{aligned}$$

we can infer

$$\mathbb{E}^{\mathbb{P}}[L_T^p] = e^{T(pr+p(\mu-r)\beta-\frac{1}{2}p(1-p)\sigma^2\beta^2)} e^{T\xi(-1+(1+\beta(\mu_k-1))^p)}.$$

Now

$$\mathbb{E}^{\mathbb{P}}[L_T^p] \geq e^{T(pr+p(\mu^*-r)\beta-\frac{1}{2}p(1-p)\bar{\sigma}^2\beta^2)} e^{T\xi^*(-1+(1+\beta(\mu_k^*-1))^p)}$$

for

$$\mu^* = \begin{cases} \underline{\mu}, & \beta \geq 0 \\ \bar{\mu}, & \beta < 0 \end{cases}, \quad \mu_k^* = \begin{cases} \underline{\mu}_k, & \beta \geq 0 \\ \bar{\mu}_k, & \beta < 0 \end{cases}, \quad \xi^* = \begin{cases} \underline{\xi}, & -1 + (1 + \beta(\mu_k^* - 1))^p \geq 0 \\ \bar{\xi}, & -1 + (1 + \beta(\mu_k^* - 1))^p < 0 \end{cases}.$$

Putting all together we now see that

$$\begin{aligned}
 \lim_{T \rightarrow \infty} \frac{1}{T} \log \inf_{\alpha \in [\underline{\alpha}, \bar{\alpha}]} \mathbb{E}^{\mathbb{P}}[L_T^p] &= pr + p(\mu^*(\beta) - r)\beta - \frac{1}{2}p(1-p)\bar{\sigma}^2\beta^2 + \xi^*(-1 + (1 + \beta(\mu_k^* - 1))^p). \tag{7.1}
 \end{aligned}$$

We now turn to the task of identifying the optimal leverage ratio, denoted  $\beta^*$ , which maximizes the long-term growth rate of the worst-case scenario described in equation (7.1). To this end, consider the function  $\Lambda(\beta)$  defined as

$$\Lambda(\beta) := pr + p(\mu^*(\beta) - r)\beta - \frac{1}{2}p(1-p)\bar{\sigma}^2\beta^2 + \xi^*(-1 + (1 + \beta(\mu_k^* - 1))^p).$$

The expression for the long-term growth rate  $\Lambda(\beta)$  involves several interacting nonlinear components, most notably the jump term and the parameter switches induced by the worst-case selection. These features make the optimization cumbersome and unattractive to handle by hand. Numerical maximization therefore offers an easy and reliable way to obtain the optimal leverage without introducing unnecessary technical detours or lengthy case distinctions. We set the uncertainty set as  $[\mu, \bar{\mu}] \times [\underline{\sigma}, \bar{\sigma}] \times [\underline{\mu}_k, \bar{\mu}_k] \times [\underline{\sigma}_k, \bar{\sigma}_k] \times [\underline{\xi}, \bar{\xi}] = [0.04, 0.08] \times [0.15, 0.25] \times [0.80, 0.98] \times [0.5, 0.8] \times [2.0, 9.0]$ ,  $r = 0.02$ ,  $p = 0.5$  and continue with numerical computations:

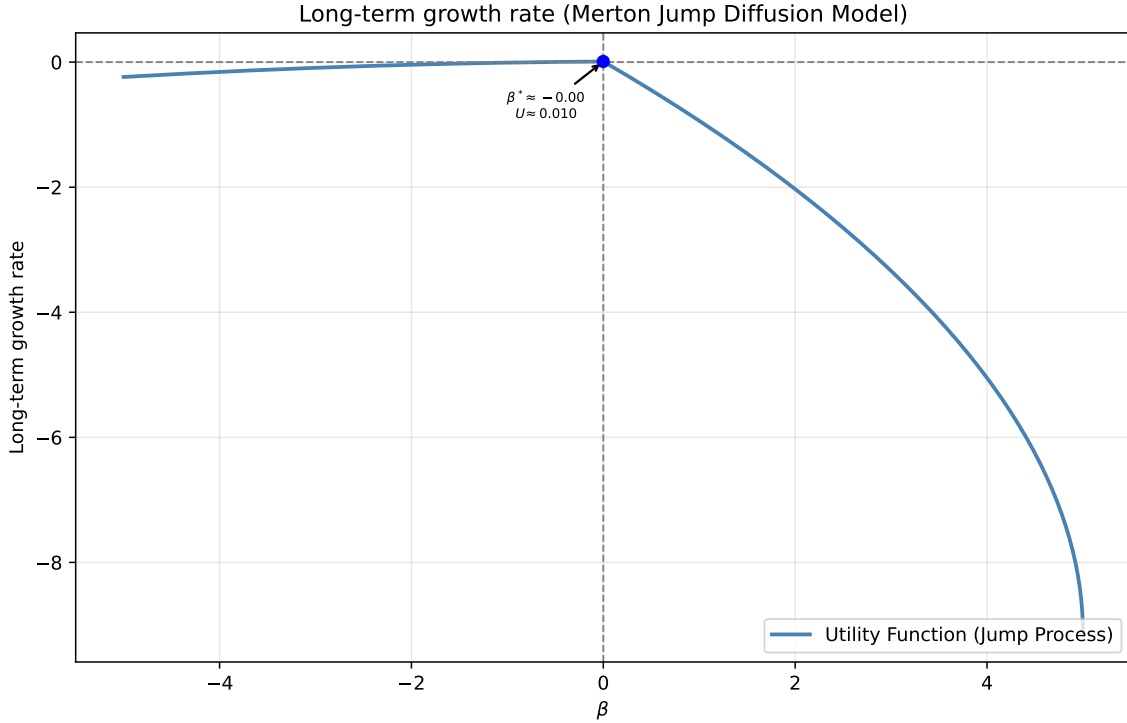


Figure 7.1: Long-term growth rate of the worst-case expected utility as a function of the leverage ratio  $\beta$  under the Merton Jump Diffusion model.

Figure 7.1 illustrates the long-term growth rate  $\Lambda(\beta)$  of the worst-case expected utility in the Merton Jump Diffusion model as a function of the leverage ratio  $\beta$ . The curve shows how the presence of jumps affects the optimal leverage ratio for the LETF. The maximum of the function identifies the optimal leverage ratio  $\beta^* = 0$ , at which the asymptotic growth rate is maximized under worst-case model uncertainty. In practical terms, this means that no investment should be allocated to the risky asset, the LETF. Instead, one should rely solely on the positive risk-free rate  $r$  to generate long-term growth. The sharp decline for positive values of  $\beta$  highlights the significant impact of more extreme parameters for the jump, such as intensity or jumps size on leveraged positions, leading to substantially reduced long-term growth.

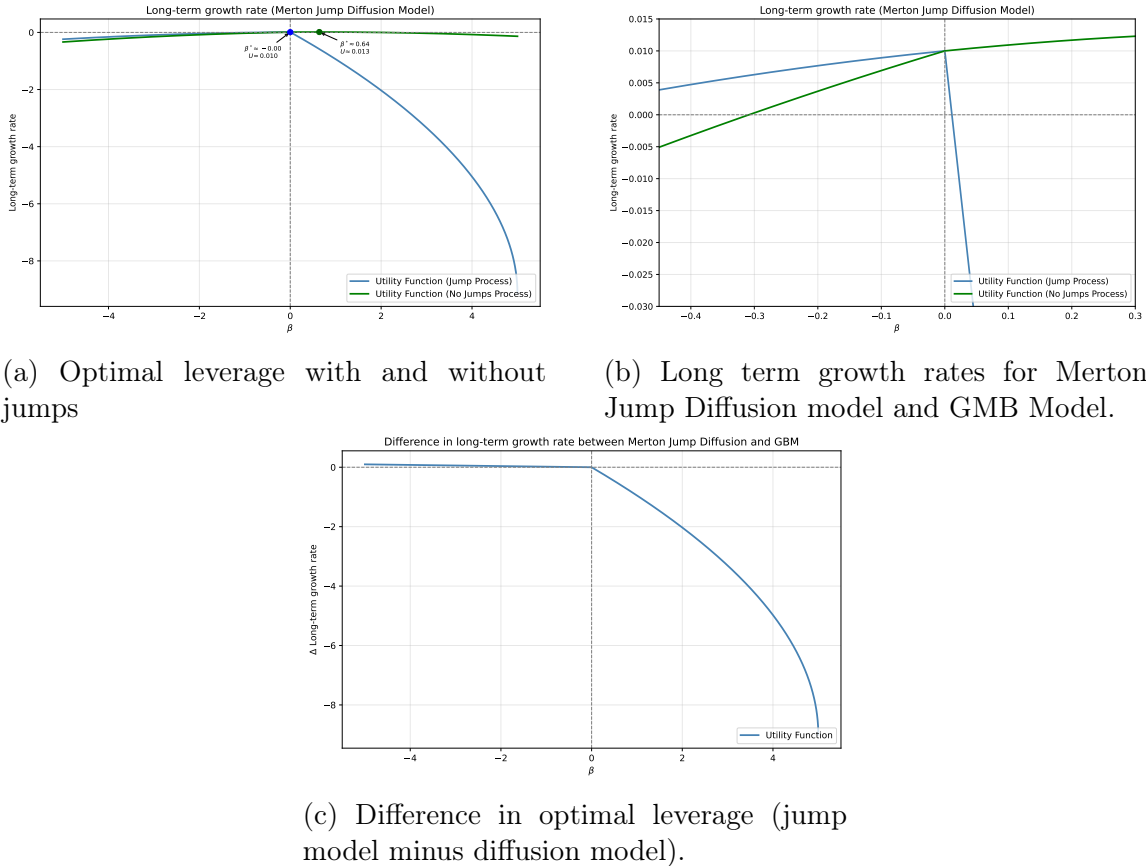


Figure 7.2: Optimal leverage with and without jumps, and resulting difference.

Figures 7.2 compares optimal leverage decisions under the Merton Jump Diffusion model with those under the pure diffusion (GBM) model. Panels (a) and (b) show the long-term growth rates for both models, illustrating that the presence of jumps shifts the maximum downward and leads to a more conservative optimal leverage. Panel (b) displays the individual growth rate curves for values  $\beta$  around 0, highlighting how the change from negative to positive leverages dramatically change the long-term growth rate. Panel (c) plots the pointwise difference between the two growth functions, demonstrating that jumps show a very small positive effect for negative  $\beta$  but a negative effect for all  $\beta$  slightly larger than zero. The comparison shows that jump risk substantially suppresses long-term growth rate and leverage. Even small adverse jumps selected by the worst case model can significantly reduce the slope of  $\Lambda$ , pushing the optimal  $\beta^*$  towards zero.

In the following, we will examine how changes in the model parameters influence the optimal leverage ratio  $\beta^*$ , and by that, how these changes affect the investor's long-term growth rate. Since  $\beta^*$  reflects the balance between expected return and risk under model uncertainty, varying the underlying parameters, such as the drift, volatility, jump intensity, or jump size, directly alters this trade-off. By systematically studying how  $\beta^*$  reacts to these parameter variations, we gain a clearer understanding of the sensitivity of the optimal investment strategy to different sources of uncertainty, as well as the robustness of long-run performance across different market environments.

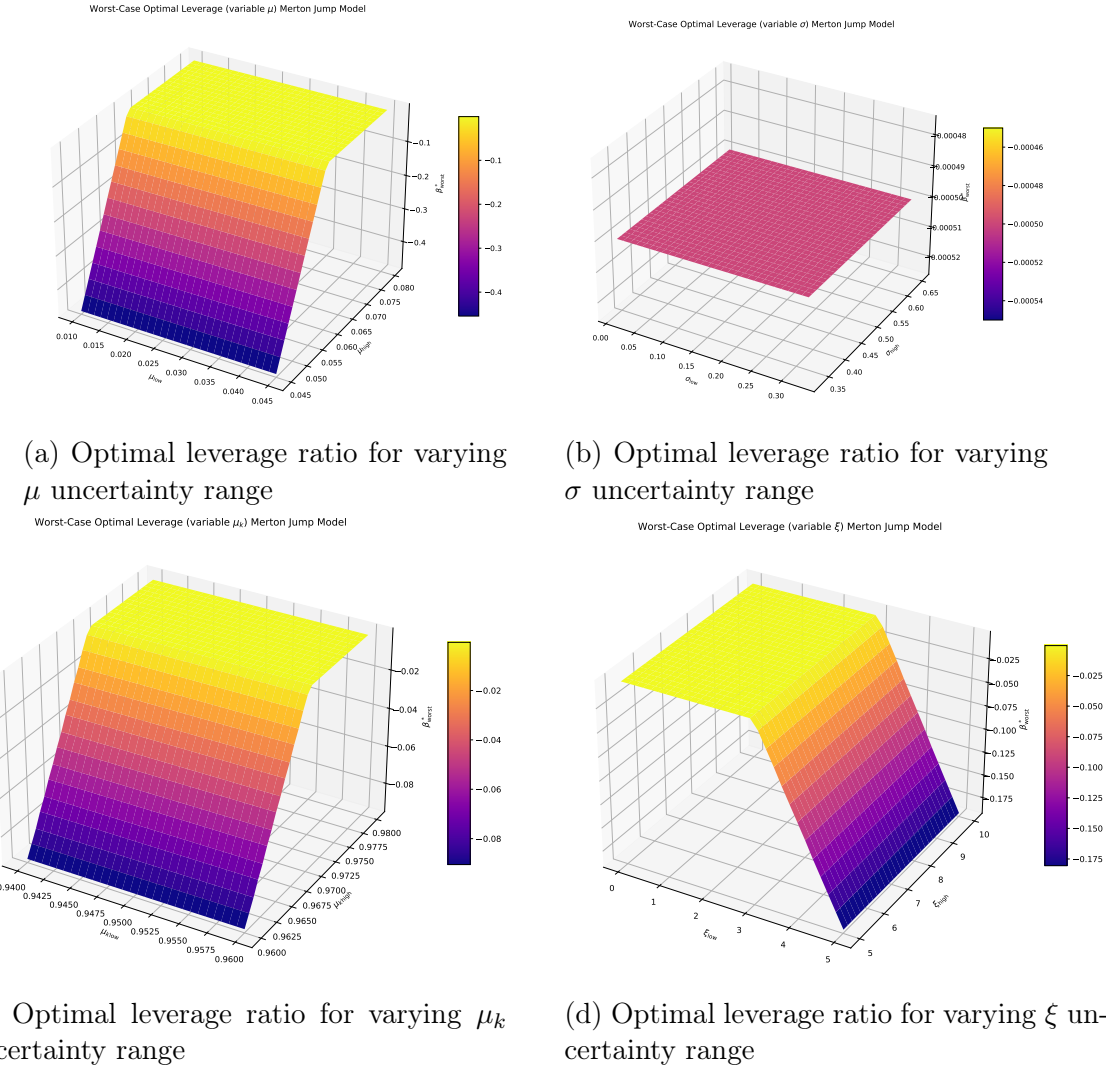


Figure 7.3: Optimal Leverage ratio for varying parameter uncertainty range.

Figure 7.3 illustrates the dependence of the worst-case optimal leverage ratio on the size of the parameter uncertainty sets in the Merton jump–diffusion model. Each panel shows how variations in a single source of uncertainty affect the optimal leverage while holding the remaining parameters’ intervals fixed. The figure highlights the sensitivity of the robust leverage choice to different forms of model uncertainty.

## 7.2 Bates model

We consider the Bates model, where the reference index  $X$  is assumed to follow the following SDE

$$\begin{aligned} \frac{dX_t}{X_t} &= \mu dt + \sqrt{\nu_t} dB_t^{(1)} + (k-1)dN_t, \\ d\nu_t &= (b - a\nu_t)dt + \sigma\sqrt{\nu}dB_t^{(2)}, \end{aligned}$$

where  $N_t$  is a Poisson process with intensity  $\xi$  and  $k$  is log-normally distributed with parameters  $\mu_k, \sigma_k^2$ , c.f. Haugh [61], where  $B_t^{(1)}$  and  $B_t^{(2)}$  are two Brownian motions with correlation parameter  $\rho \in [\underline{\rho}, \bar{\rho}]$  and  $\langle B_t^{(1)}, B_t^{(2)} \rangle_t = \rho t$ . Hence our parameters are  $\alpha = (\mu, \mu_k, \sigma_k, \xi, \rho, b, a, \sigma) \in [\underline{\mu}, \bar{\mu}] \times [\underline{\mu}_k, \bar{\mu}_k] \times [\underline{\sigma}_k, \bar{\sigma}_k] \times [\underline{\xi}, \bar{\xi}] \times [\underline{\rho}, \bar{\rho}] \times [\underline{b}, \bar{b}] \times [\underline{a}, \bar{a}] \times [\underline{\sigma}, \bar{\sigma}]$  with  $\underline{\mu}, \underline{a}, \underline{\sigma} > 0$  and  $\underline{b} > \bar{\sigma}^2/2$ . We also assume  $\underline{a} - p|\beta|\bar{\sigma} > 0$ ,  $\mu_k \in (0.8, 1.2)$ ,  $\underline{\mu} \geq \frac{\beta-1}{\beta}$  for  $\beta \geq 0$  and  $\bar{\mu} \leq \frac{\beta-1}{\beta}$  for  $\beta < 0$ .

First let us compute  $\mathbb{E}^{\mathbb{P}}[(L_t^\alpha)^p]$ :

$$\begin{aligned} dL_{t-}^\alpha &= L_t^\alpha \beta \frac{dX_t}{X_{t-}} + L_{t-}^\alpha (1 - \beta) r dt \\ &= L_t^\alpha \beta \left( \mu dt + \sqrt{\nu_t} dB_t^{(1)} + (k - 1) dN_t \right) + L_{t-}^\alpha (1 - \beta) r dt \\ &= L_t^\alpha (\beta\mu + (1 - \beta)r) dt + L_t^\alpha \beta \sqrt{\nu_t} dB_t^{(1)} + L_t^\alpha \beta (k - 1) dN_t \end{aligned}$$

and by Itô's formula for jump processes

$$d \log(L_t^\alpha) = \left( \beta\mu + (1 - \beta)r - \frac{1}{2}\beta^2 \nu_t \right) dt + \beta \sqrt{\nu_t} dB_t^{(1)} + (\log(L_t^\alpha) - \log(L_{t-}^\alpha)) dN_t.$$

At jump time  $u$ , we have

$$L_u^\alpha - L_{u-}^\alpha = L_{u-}^\alpha \beta(k - 1) \iff L_u^\alpha = L_{u-}^\alpha (1 + \beta(k - 1))$$

and therefore

$$\log(L_u^\alpha) - \log(L_{u-}^\alpha) = \log \left( \frac{L_u^\alpha}{L_{u-}^\alpha} \right) = \log(1 + \beta(k - 1)).$$

Hence

$$\log(L_t^\alpha) = (\beta\mu + (1 - \beta)r)t - \frac{1}{2}\beta^2 \int_0^t \nu_s ds + \beta \int_0^t \sqrt{\nu_s} dB_s^{(1)} + \sum_{j=1}^{N_t} \log(1 + \beta(k_j - 1)).$$

Since we can rewrite  $\sum_{j=1}^{N_t} \log(1 + \beta(k_j - 1)) = \log \left( \prod_{j=1}^{N_t} (1 + \beta(k_j - 1)) \right)$  we infer

$$L_t^\alpha = e^{(\beta\mu + (1 - \beta)r)t - \frac{1}{2}\beta^2 \int_0^t \nu_s ds + \beta \int_0^t \sqrt{\nu_s} dB_s^{(1)}} \prod_{j=1}^{N_t} (1 + \beta(k_j - 1)).$$

Hence

$$\begin{aligned} \mathbb{E}^{\mathbb{P}}[L_T^p] &= \mathbb{E}^{\mathbb{P}} \left[ e^{p(\beta\mu + (1 - \beta)r)T - \frac{1}{2}p\beta^2 \int_0^T \nu_s ds + p\beta \int_0^T \sqrt{\nu_s} dB_s^{(1)}} \left( \prod_{j=1}^{N_T} (1 + \beta(k_j - 1)) \right)^p \right] \\ &= \mathbb{E}^{\mathbb{P}} \left[ e^{p(\beta\mu + (1 - \beta)r)T} \left( \prod_{j=1}^{N_T} (1 + \beta(k_j - 1)) \right)^p \mathcal{E} \left( p\beta \int_0^{\cdot} \sqrt{\nu_s} dB_s^{(1)} \right)_T e^{-\frac{1}{2}p(1-p)\beta^2 \int_0^T \nu_s ds} \right]. \end{aligned}$$

We can define a new probability measure  $\hat{\mathbb{P}}$  on  $\mathcal{F}_T$  via

$$\frac{d\hat{\mathbb{P}}^\alpha}{d\mathbb{P}} \Big|_{\mathcal{F}_T} = \mathcal{E} \left( p\beta \int_0^{\cdot} \sqrt{\nu_s^\alpha} dB_s^{(1)} \right)_T.$$

Therefore we can derive the expected utility of holding an LETF up to time  $T$  as

$$\begin{aligned} & \mathbb{E}^\mathbb{P}[L_T^p] \\ &= \mathbb{E}^\mathbb{P} \left[ e^{p(\beta\mu+(1-\beta)r)T} \left( \prod_{j=1}^{N_T} (1 + \beta(k_j - 1)) \right)^p \mathcal{E} \left( p\beta \int_0^{\cdot} \sqrt{\nu_s} dB_s^{(1)} \right)_T e^{-\frac{1}{2}p(1-p)\beta^2 \int_0^T \nu_s ds} \right] \\ &= e^{p(\beta\mu+(1-\beta)r)T} \mathbb{E}^\mathbb{P} \left[ \left( \prod_{j=1}^{N_T} (1 + \beta(k_j - 1)) \right)^p \right] \mathbb{E}^{\hat{\mathbb{P}}} \left[ e^{-\frac{1}{2}p(1-p)\beta^2 \int_0^T \nu_s ds} \right]. \end{aligned}$$

From

$$\begin{aligned} \mathbb{E}^\mathbb{P} \left[ \left( \prod_{j=1}^{N_T} (1 + \beta(k_j - 1)) \right)^p \right] &= \sum_{n=0}^{\infty} \mathbb{E}^\mathbb{P} [(1 + \beta(k - 1))^{np}] \mathbb{E}^\mathbb{P}[N_T = n] \\ &= \sum_{n=0}^{\infty} \mathbb{E}^\mathbb{P} [1 + \beta(k - 1)]^{np} \frac{(\xi T)^n}{n!} e^{-\xi T} \\ &= e^{-\xi T} \sum_{n=0}^{\infty} (1 + \beta(\mu_k - 1))^{np} \frac{(\xi T)^n}{n!} \\ &= e^{-\xi T} \sum_{n=0}^{\infty} \frac{(\xi T (1 + \beta(\mu_k - 1))^p)^n}{n!} \\ &= e^{T\xi(-1+(1+\beta(\mu_k-1))^p)} \end{aligned}$$

we can infer

$$\begin{aligned} \mathbb{E}^\mathbb{P}[L_T^p] &= e^{p(\beta\mu+(1-\beta)r)T} e^{T\xi(-1+(1+\beta(\mu_k-1))^p)} \mathbb{E}^{\hat{\mathbb{P}}} \left[ e^{-\frac{1}{2}p(1-p)\beta^2 \int_0^T \nu_s ds} \right] \\ &= e^{T(p(\beta\mu+(1-\beta)r)+\xi(-1+(1+\beta(\mu_k-1))^p))} \mathbb{E}^{\hat{\mathbb{P}}} \left[ e^{-\frac{1}{2}p(1-p)\beta^2 \int_0^T \nu_s ds} \right]. \end{aligned}$$

We can now see that if we define

$$\mu^* = \begin{cases} \frac{\mu}{\bar{\mu}} & \text{if } \beta \geq 0 \\ \underline{\mu} & \text{if } \beta < 0 \end{cases}, \quad \mu_k^* = \begin{cases} \frac{\mu_k}{\bar{\mu}_k} & \text{if } \beta \geq 0 \\ \underline{\mu}_k & \text{if } \beta < 0 \end{cases}, \quad \rho^* = \begin{cases} \bar{\rho}, & \beta \geq 0 \\ \underline{\rho}, & \beta < 0 \end{cases},$$

and by the calculations derived in Section 5.1 we can derive

$$\mathbb{E}^\mathbb{P}[L_T^p] \geq e^{T(p(\beta\mu^*+(1-\beta)r)+\xi(-1+(1+\beta(\mu_k^*-1))^p))} \mathbb{E}^{\hat{\mathbb{P}}^{\rho^*, \bar{b}, \underline{a}, \sigma}} \left[ e^{-\frac{1}{2}p(1-p)\beta^2 \int_0^T \nu_s ds} \right].$$

We define

$$V(T, \alpha) := \mathbb{E}^{\hat{\mathbb{P}}} \left[ e^{-\frac{1}{2}p(1-p)\beta^2 \int_0^T \nu_s ds} \right]$$

and

$$v_T := \inf_{\alpha \in [\underline{\alpha}, \bar{\alpha}]} \mathbb{E}^\mathbb{P}[L_T^p].$$

We can infer that

$$v_T = e^{T(p(\beta\mu + (1-\beta)r) + \xi(-1 + (1+\beta(\mu_k^*-1))^p))} \inf_{\alpha \in [\underline{\alpha}, \bar{\alpha}]} V(T, \alpha).$$

Since

$$V(T, \alpha^*(\sigma)) = e^{-T(p(\beta\mu^* + (1-\beta)r) + \xi(-1 + (1+\beta(\mu_k^*-1))^p))} \mathbb{E}^{\hat{\mathbb{P}}} [L_T^p]$$

and by the Hansen-Scheinkman decomposition together with Section 5.1 we have

$$\mathbb{E}^{\hat{\mathbb{P}}^\alpha} [L_T^p] = e^{-\lambda(\sigma)T - \eta(\sigma)\nu_0} \mathbb{E}^{\hat{\mathbb{Q}}^{\alpha^*(\sigma)}} \left[ \frac{e^{T(p(\beta\mu^* + (1-\beta)r) + \xi(-1 + (1+\beta(\mu_k^*-1))^p))}}{e^{-\eta(\sigma)\nu_T}} \right]$$

for

$$(\lambda(\sigma), \phi_\sigma(\nu)) = (\bar{b}\eta(\sigma), e^{-\eta(\sigma)\nu}),$$

with

$$\eta(\sigma) = \frac{1}{\sigma^2} \left( \sqrt{(\underline{a} - p\beta\rho^*\sigma)^2 + p(1-p)\beta^2\sigma^2} - (\underline{a} - p\beta\rho^*\sigma) \right).$$

Therefore

$$V(T, \alpha^*(\sigma)) = e^{-\lambda(\sigma)T - \eta(\sigma)\nu_0} \mathbb{E}^{\hat{\mathbb{Q}}^{\alpha^*(\sigma)}} [e^{\eta(\sigma)\nu_T}]$$

for a probability measure

$$\left. \frac{d\hat{\mathbb{Q}}^{\alpha^*(\sigma)}}{d\hat{\mathbb{P}}^{\alpha^*(\sigma)}} \right|_{\mathcal{F}_T} = e^{\lambda(\sigma)T - \frac{1}{2}p\beta(\beta-1) \int_0^T \nu_s ds - \eta(\sigma)\nu_T + \eta(\sigma)\nu_0}.$$

Next, we also showed in Section 5.1 that

$$\lim_{T \rightarrow \infty} \frac{1}{T} \log \inf_{\sigma \in [\underline{\sigma}, \bar{\sigma}]} V(T; \alpha^*(\sigma)) = -\bar{b}\eta(\sigma^*).$$

Hence altogether we get

$$\begin{aligned} \lim_{T \rightarrow \infty} \frac{1}{T} \log v_T &= \lim_{T \rightarrow \infty} \frac{1}{T} \log \left( e^{T(p(\beta\mu^* + (1-\beta)r) + \xi(-1 + (1+\beta(\mu_k^*-1))^p))} \inf_{\alpha \in [\underline{\alpha}, \bar{\alpha}]} V(T, \alpha) \right) \\ &= \min_{\sigma \in [\underline{\sigma}, \bar{\sigma}]} (p(\beta\mu^* + (1-\beta)r) + \xi(-1 + (1+\beta(\mu_k^*-1))^p) - \bar{b}\eta(\sigma)) \\ &= p(\beta\mu^* + (1-\beta)r) + \xi(-1 + (1+\beta(\mu_k^*-1))^p) - \bar{b} \max_{\sigma \in [\underline{\sigma}, \bar{\sigma}]} \eta(\sigma). \end{aligned}$$

While the existence of a worst-case parameter set within the uncertainty range is certainly assured, determining the corresponding optimal leverage ratio  $\beta^*$  analytically is highly challenging. This difficulty arises because the procedure involves identifying the worst-case volatility  $\sigma^*(\beta)$ , evaluating the function  $\eta(\sigma^*(\beta), \beta)$  for each leverage value  $\beta$ , and comparing the limits for all  $\beta$  in the interval  $[\underline{\beta}, \bar{\beta}]$ . Such computations are generally infeasible or at least nearly impossible to perform manually. As a result, one might take a numerical approach similar to Section 5.1.

For  $\beta \in [-5, 5], p = 0.5, r = 0.015, [\underline{\mu}, \bar{\mu}] = [0.05, 0.08], [\underline{\mu}_k, \bar{\mu}_k] = [0.82, 0.98], [\underline{\xi}, \bar{\xi}] = [0.05, 0.25], [\underline{\rho}, \bar{\rho}] = [-0.93, -0.75], [\underline{b}, \bar{b}] = [0.1, 0.2], [\underline{a}, \bar{a}] = [3, 10], [\underline{\sigma}, \bar{\sigma}] = [0.82, 0.93]$  we

can compute that the optimal leverage ratio is approximately 0.02 and the corresponding long-term growth rate is approximately 0.007 (Fig. 7.4).

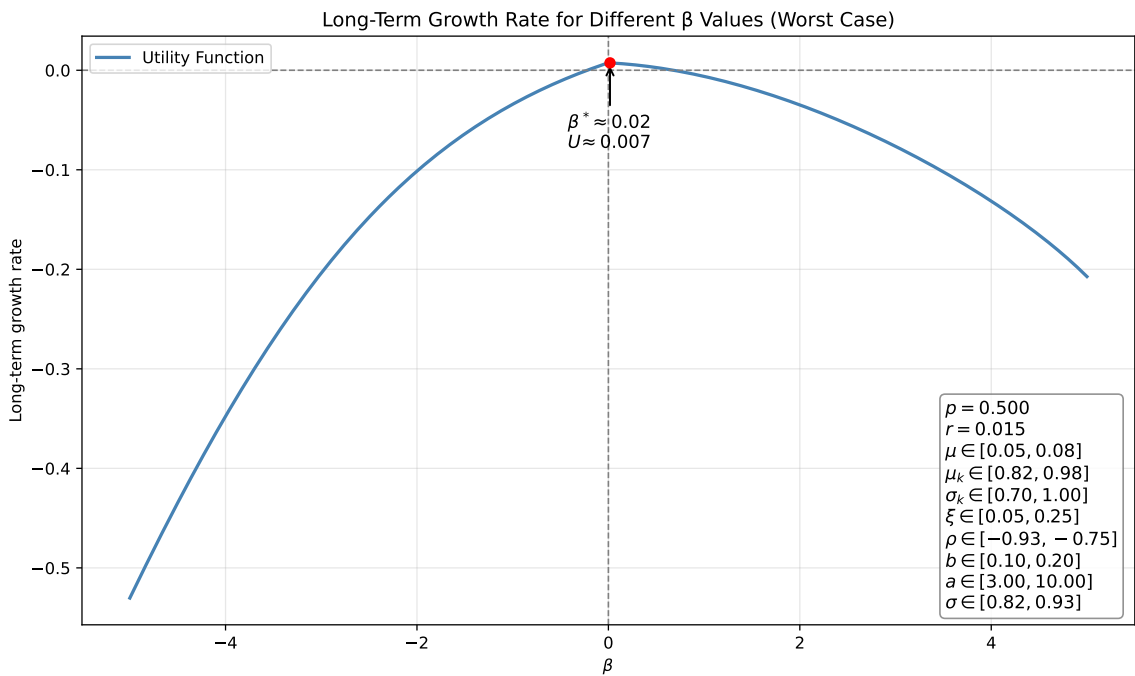


Figure 7.4: Long-term growth rate of the worst-case expected utility as a function of the leverage ratio  $\beta$  under the Bates model.

In the following, we will examine how changes in the model parameters influence the optimal leverage ratio  $\beta^*$ . Since  $\beta^*$  reflects the balance between expected return and risk under model uncertainty, varying the underlying parameters, such as the drift, volatility, jump intensity, or jump size, directly alters this trade-off. By systematically studying how  $\beta^*$  reacts to these parameter variations, we gain a clearer understanding of the sensitivity of the optimal investment strategy to different sources of uncertainty, as well as the robustness of long-run performance across different market environments.

## 7.2. Bates model

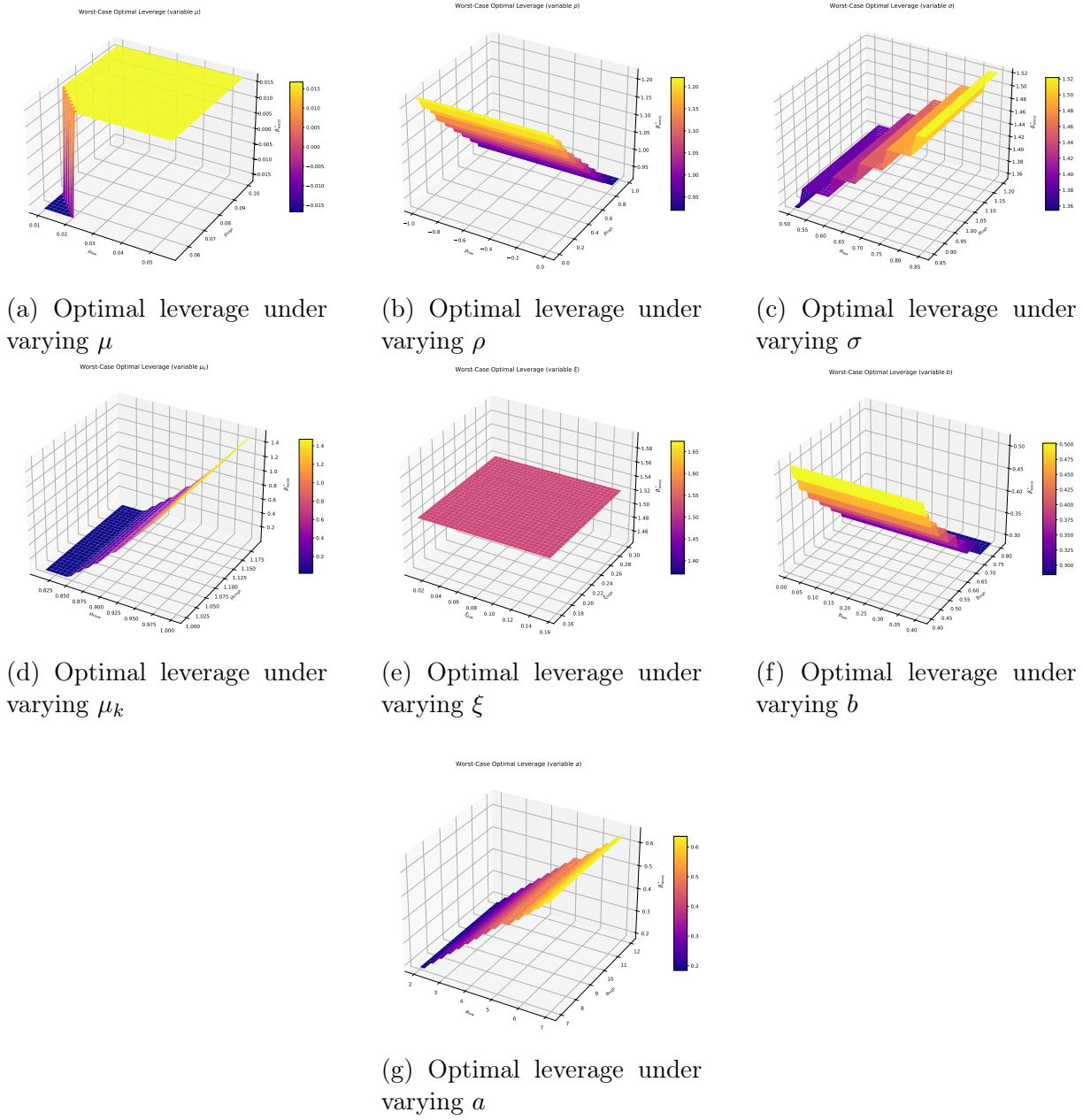


Figure 7.5: Impact of different intervals on the optimal leverage ratio.



# Chapter 8

## Comparative analysis of robust and average optimal leverage

In the preceding chapters, we analyzed the long-term behavior of LETFs under model uncertainty, with particular focus on robust long-term growth rate utility maximization. The robust investor, uncertain about the true dynamics, selects a strategy that performs optimally under the worst plausible realization of model parameters. This yields an optimal leverage ratio that guards against adverse deviations. In practical terms, a robust investor deliberately forgoes some upside potential to hedge against worst-case scenarios. The mid-case analysis quantifies this trade-off. It highlights how much long-term growth or utility is potentially lost by guarding against extreme model misspecifications. This is both economically relevant (since worst-cases may be rare in practice) and mathematically illuminating, as it helps identify the sensitivity of the optimal leverage to different degrees of model misspecification. Indeed, the notion of a “price of robustness” has been studied, c.f. Bertsimas and Sim [62], in order to analyze the impact on conservatism. From a theoretical standpoint, there exist frameworks that explicitly incorporate average-case model uncertainty or interpolate between nominal and worst-case formulations or optimism and pessimism in decision making under uncertainty. Classical decision theory offers the Hurwicz criterion, which is a weighted blend of pessimistic and optimistic outcomes, c.f. Hurwicz [63] and modern ambiguity-aversion models provide continuous spectra between full confidence in a model and complete distrust. For example, the robust portfolio model of Maenhout [20] can be seen as embedding an ambiguity-aversion parameter. As ambiguity aversion increases, the optimal policy continuously shifts from the nominal Merton solution toward the worst-case solution.

Intermediate formulations have been proposed in the literature to capture a middle ground. Min et al. [64] construct a hybrid portfolio selection to balance the combination of the best-case and worst-case outcomes, effectively tuning the level of conservatism. Likewise, Won and Kim [65] develop a robust optimization approach that balances worst-case utility against worst-case regret, meaning the largest difference between the best utility achievable under the model and that achieved by a given portfolio. While worst-case parameters may yield an overly pessimistic portfolio, and an portfolio optimized trough worst-case regret might completely loose its robustness, the paper aims to find a trade-off between those extremes. These approaches illustrate that one can take expectations

over the uncertainty set or assign model weights to achieve a mathematically tractable mid-case criterion, rather than focusing solely on the single worst scenario. Such model-weighted or distributionally robust strategies retain some robustness to model error while avoiding the undue pessimism of pure worst-case analysis.

Empirical and numerical studies generally support the idea that moderate conservatism can improve the portfolio's risk–return profile. Fully robust portfolios often exhibit lower volatility and draw downs at the expense of substantially lower average returns. In contrast, the nominal (non-robust) strategy maximizes performance under the assumed model but can lead to disastrous outcomes if the model is wrong. Strategies that lie in between our mid case approach aim to capture a large portion of the upside available under the nominal model while still maintaining a degree of protection against model misspecification. In effect, the mid-case optimal leverage can be seen as a prudent compromise. It is lower than the naive leverage that assumes the best estimate of asset dynamics, but higher than the ultra cautious leverage dictated by the worst-case drift or volatility. In summary, incorporating a mid-case analysis provides a richer understanding of robust portfolio choice. It not only quantifies the performance loss incurred for worst-case protection, but also reinforces the link between robustness and classical risk-aversion principles. By examining the average-case alongside the worst-case, we can judge whether the robust leverage policies are unduly conservative and gauge the potential gains from taking on a bit more risk around the more likely market conditions. This perspective deepens the robustness analysis, demonstrating that the worst-case approach is part of a broader continuum of strategies indexed by one's tolerance for model uncertainty.

In this chapter, we now compare the *robust optimal leverage ratio* and the *growth rate of expected utility* derived under a worst-case parameter configuration with more optimistic parameters, which we will call *average- or mid- case parameters*. In this case we say average as if the model parameters all are equally probable and hence we take the midpoint of the assumed uncertainty intervals as the average parameter. The goal of this comparison is twofold:

1. To quantify the impact of model uncertainty on the optimal leverage choice.
2. To interpret the cost of robustness, i.e., the potential utility loss when an investor optimizes for worst-case scenarios that may not materialize.

The models introduced previously are reconsidered now also under a different parameter configuration that reflects average market conditions. The resulting leverage ratios, along with their associated long-run growth rates, highlight the *trade-off between caution and performance*. This chapter therefore connects the theoretical insights of robust control to a concrete portfolio decision: how much leverage to take in the presence or absence of uncertainty. In detail we want to compare

$$\frac{1}{T} \log \inf_{\alpha \in [\underline{\alpha}, \bar{\alpha}]} \mathbb{E}^{\mathbb{P}} [(L_T^{\alpha})^p] \quad \text{and} \quad \frac{1}{T} \log \mathbb{E}^{\mathbb{P}} \left[ \left( L_T^{\alpha^{mid}} \right)^p \right],$$

where  $\alpha^{mid}$  represents the parameters that lie in the middle of the uncertainty set. To this end we define the cost of robustness as

$$C^{rob} := \lim_{T \rightarrow \infty} \frac{1}{T} \left( \log \inf_{\alpha \in [\underline{\alpha}, \bar{\alpha}]} \mathbb{E}^{\mathbb{P}} [(L_T^{\alpha})^p] - \log \mathbb{E}^{\mathbb{P}} \left[ \left( L_T^{\alpha^{mid}} \right)^p \right] \right).$$

Next, we define the difference of optimal leverage ratios of the worst case and the average case as the robustness gap in leverage

$$G^{rob} := \Delta\beta := \beta_{worst}^* - \beta_{avg}^*,$$

which quantifies the degree to which robustness influences the optimal leverage ratio. While the absolute difference in optimal leverage ratios and utility growth provides a direct comparison between robust and average strategies, such raw values can be difficult to interpret across models or parameter regimes. To address this, we introduce relative measures that contextualize the performance of the robust strategy with respect to the average scenario.

Specifically, we define the relative leverage gap as the proportional reduction in the optimal leverage ratio due to robustness. Similarly, the relative growth loss captures the proportionality of the difference in long-term utility growth under worst and average case parameters. These relative measures offer a normalized perspective on the cost of robustness, which allows for clearer comparisons across different models and parameter settings.

$$R^C := \text{Relative Growth Loss} := \frac{C^{rob}}{\lim_{T \rightarrow \infty} \frac{1}{T} \log \mathbb{E}^{\mathbb{P}} [(L_T^{\alpha^{mid}})^p]},$$

$$R^G := \text{Relative Leverage Gap} := \frac{G^{rob}}{|\beta_{avg}^*|}.$$

## 8.1 comparison under uncertainty on the reference process models

In this first section, we consider a model that incorporates uncertainty solely in the reference process  $X$ . We consider here the case of a GBM model for  $X$ :

$$dX_t = \mu X_t dt + \sigma X_t dB_t, \quad t \geq 0,$$

where drift and diffusion uncertainty are expressed as  $(\mu, \sigma) \in [\underline{\mu}, \bar{\mu}] \times [\underline{\sigma}, \bar{\sigma}]$  and  $\underline{\mu}, \underline{\sigma} > 0$ . For any pair of  $(\mu, \sigma)$  we showed in Section 4.1

$$\mathbb{E}^{\mathbb{P}^{\mu, \sigma}} [L_T^p] = e^{p(\beta\mu - (\beta-1)r)T - \frac{1}{2}p(1-p)\beta^2\sigma^2 T}.$$

Setting now  $\alpha^{mid} := (\mu^{mid}, \sigma^{mid}) := \left(\frac{\bar{\mu}+\mu}{2}, \frac{\bar{\sigma}+\sigma}{2}\right)$  we derive

$$\begin{aligned} \frac{1}{T} \log \mathbb{E}^{\mathbb{P}} \left[ (L_T^{\alpha^{mid}})^p \right] &= \frac{1}{T} \log e^{p(\beta\mu^{mid} - (\beta-1)r)T - \frac{1}{2}p(1-p)\beta^2(\sigma^{mid})^2 T} \\ &= \frac{1}{T} \left( p(\beta\mu^{mid} - (\beta-1)r)T - \frac{1}{2}p(1-p)\beta^2(\sigma^{mid})^2 T \right) \\ &= p(\beta\mu^{mid} - (\beta-1)r) - \frac{1}{2}p(1-p)\beta^2(\sigma^{mid})^2 \\ &= pr + p(\mu^{mid} - r)\beta - \frac{1}{2}p(1-p)(\sigma^{mid})^2\beta^2. \end{aligned}$$

Before we continue with the leverage ratio, we compare this long-term expected utility to the worst-case value.

$$\begin{aligned} C^{rob} &= \frac{1}{T} \log \inf_{\alpha \in [\underline{\alpha}, \bar{\alpha}]} \mathbb{E}^{\mathbb{P}} [(L_T^{\alpha})^p] - \frac{1}{T} \log \mathbb{E}^{\mathbb{P}} \left[ \left( L_T^{\alpha^{mid}} \right)^p \right] \\ &= p(\mu^*(\beta) - r) \beta^{worst*} - \frac{1}{2} p(1-p) \bar{\sigma}^2 (\beta^{worst*})^2 \\ &\quad - p(\mu^{mid} - r) \beta^{mid*} + \frac{1}{2} p(1-p) (\sigma^{mid})^2 (\beta^{mid*})^2. \end{aligned}$$

Now we turn to finding the optimal leverage ratio and we again consider a function

$$\Lambda(\beta) := pr + p(\mu^{mid} - r) \beta - \frac{1}{2} p(1-p) (\sigma^{mid})^2 \beta^2$$

to calculate the optimal leverage ratio  $\beta^*$ . First we differentiate to get

$$\Lambda'(\beta) := p(\mu^{mid} - r) - p(1-p)(\sigma^{mid})^2 \beta.$$

We consider again different cases, considering different relationships between  $r$  and  $\mu^{mid}$ :

**Case 1**  $\mu^{mid} < r$ : We see that  $\Lambda'(\beta) = 0$  for  $\beta = \frac{\mu^{mid}-r}{(1-p)(\sigma^{mid})^2}$ . Since

$$\Lambda(0) = pr < pr + \frac{1}{2} p \frac{(\mu^{mid} - r)^2}{(1-p)(\sigma^{mid})^2} = \Lambda \left( \frac{\mu^{mid} - r}{(1-p)(\sigma^{mid})^2} \right)$$

$\beta^* = \frac{\mu^{mid}-r}{(1-p)(\sigma^{mid})^2}$  for  $\beta < 0$  and  $\beta^* = 0$  for  $\beta \geq 0$ .

**Case 2**  $r = \mu^{mid}$ : Readily one can check that  $\beta^* = 0$ .

**Case 3**  $r < \mu^{mid}$ :  $\beta^* = \frac{\mu^{mid}-r}{(1-p)(\sigma^{mid})^2}$  for  $\beta \geq 0$  and  $\beta^* = 0$  else.

If we compare this results to the previous ones we see that we are more risk-loving since we would invest not only if  $r < \underline{\mu}$  or  $\bar{\mu} < r$  but even for  $r \neq \mu^{mid}$ . Let us compare now the leverage ratios for different cases. Starting, we assume the case that  $\bar{\mu} < r$  and hence also  $\mu^{mid} < r$ :

$$\begin{aligned} G^{rob} &= \frac{\mu^{mid} - r}{(1-p)(\sigma^{mid})^2} - \frac{\bar{\mu} - r}{(1-p)\bar{\sigma}^2} = \frac{1}{1-p} \left( \frac{\bar{\sigma}^2(\mu^{mid} - r)}{(\sigma^{mid})^2 \bar{\sigma}^2} - \frac{(\sigma^{mid})^2(\bar{\mu} - r)}{\bar{\sigma}^2(\sigma^{mid})^2} \right) \\ &= \frac{1}{1-p} \frac{\bar{\sigma}^2(\mu^{mid} - r) - (\sigma^{mid})^2(\bar{\mu} - r)}{(\sigma^{mid}\bar{\sigma})^2}. \end{aligned}$$

Similarly also for the case  $\bar{\mu} > r$ .

Let us now consider these differences in a concrete setting. Several studies analyzed the behavior of standard ETFs like the S&P 500 and modeled their dynamics with a GBM model, c.f. Sinha [66], which gives reason on why we will use a GBM to model this asset. The long-run average annual return of the S&P 500 is roughly 7% so we will assume that  $[\underline{\mu}, \bar{\mu}] = [0.06, 0.1]$ . For the volatility the historical annualized volatility of the S&P 500 is about 17% so we will set  $[\underline{\sigma}, \bar{\sigma}] = [0.15, 0.25]$  and for the interest rate  $r$  we will assume

$r = 0.02$ . Finally we will assume that our risk-averseness is expressed by  $p = 0.5$ . With these assumptions we can compute:

$$\begin{aligned} C^{rob} &= \frac{1}{T} \log \inf_{\alpha \in [\underline{\alpha}, \bar{\alpha}]} \mathbb{E}^{\mathbb{P}} [(L_T^{\alpha})^p] - \frac{1}{T} \log \mathbb{E}^{\mathbb{P}} \left[ \left( L_T^{\alpha^{mid}} \right)^p \right] \\ &= 0.0324 - 0.055 \\ &= -0.0226 \end{aligned}$$

and

$$\begin{aligned} G^{rob} &= \frac{\mu^{mid} - r}{(1-p)(\sigma^{mid})^2} - \frac{\underline{\mu} - r}{(1-p)\bar{\sigma}^2} = \frac{1}{1-p} \frac{\bar{\sigma}^2(\mu^{mid} - r) - (\sigma^{mid})^2(\underline{\mu} - r)}{(\sigma^{mid}\bar{\sigma})^2} \\ &= 1.72. \end{aligned}$$

Considering now the relative change we derive

$$\begin{aligned} R^C &= \frac{C^{rob}}{\lim_{T \rightarrow \infty} \frac{1}{T} \log \mathbb{E}^{\mathbb{P}} \left[ \left( L_T^{\alpha^{mid}} \right)^p \right]} \approx \frac{0.0226}{0.055} \approx 0.411 \\ \text{and} \\ R^G &= \frac{G^{rob}}{|\beta_{avg}^*|} = \frac{1.72}{3} \approx 0.5733. \end{aligned}$$

In order to assess the impact of model uncertainty within the GBM framework, we visualize and interpret several relevant quantities across a range of plausible parameter values. Specifically, we consider multiple uncertainty ranges of  $\mu$  and  $\sigma$  and infer their impact. For visualization purposes we fix either an interval for  $\mu$  or  $\sigma$  and let the bounds of the other parameter vary and consider the impact of these changes. In detail we vary  $\mu_{low} \in [0.04, 0.08]$  and  $\mu_{high} \in [0.08, 0.12]$  while keeping volatility fixed or vary  $\sigma_{low} \in [0.10, 0.20]$  and  $\sigma_{high} \in [0.20, 0.30]$  while keeping expected returns fixed. For each of these cases, we compute:

- the *average-case optimal leverage*  $\beta_{avg}^*$ ,
- the *robust (worst-case) optimal leverage*  $\beta_{worst}^*$ ,
- the resulting *robustness gap*  $\Delta\beta = \beta_{worst}^* - \beta_{avg}^*$ ,
- the *cost of robustness*,
- and the *relative long-term growth loss* from robustness.

These quantities are illustrated in the following series of 3D surface plots. This allows for a direct comparison of how the uncertainty in either  $\mu$  or  $\sigma$  translates into growth rates and adjusted investment behavior.

## Chapter 8. Comparative analysis on optimal leverage

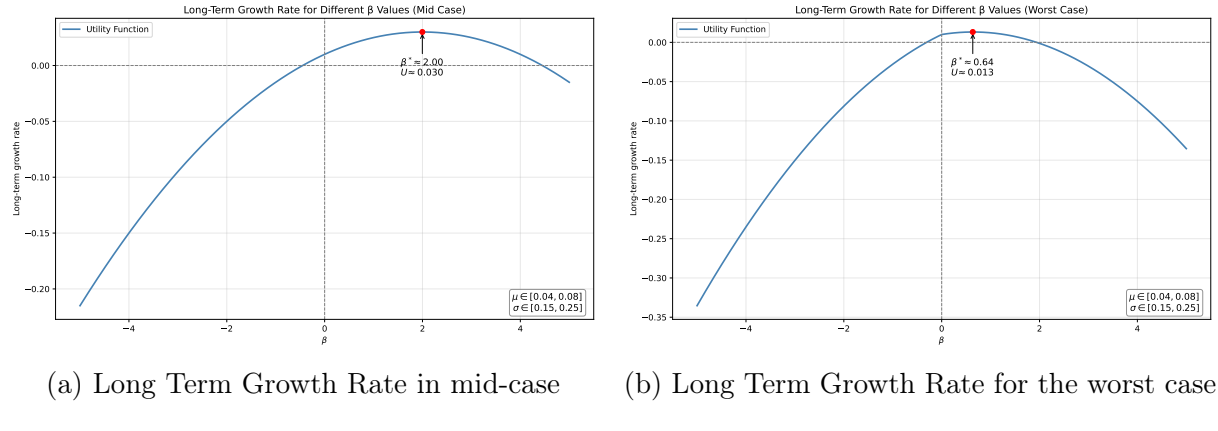


Figure 8.1: Long-term growth rate for the worst and mid case for different  $\beta$ .

Figure 8.1 shows the long-term growth rate for both mid- and worst-case scenarios as a function of the leverage ratio  $\beta$ . Whilst the graph of the long term growth rate has similar shape, the peak occurs at different  $\beta$ -values.

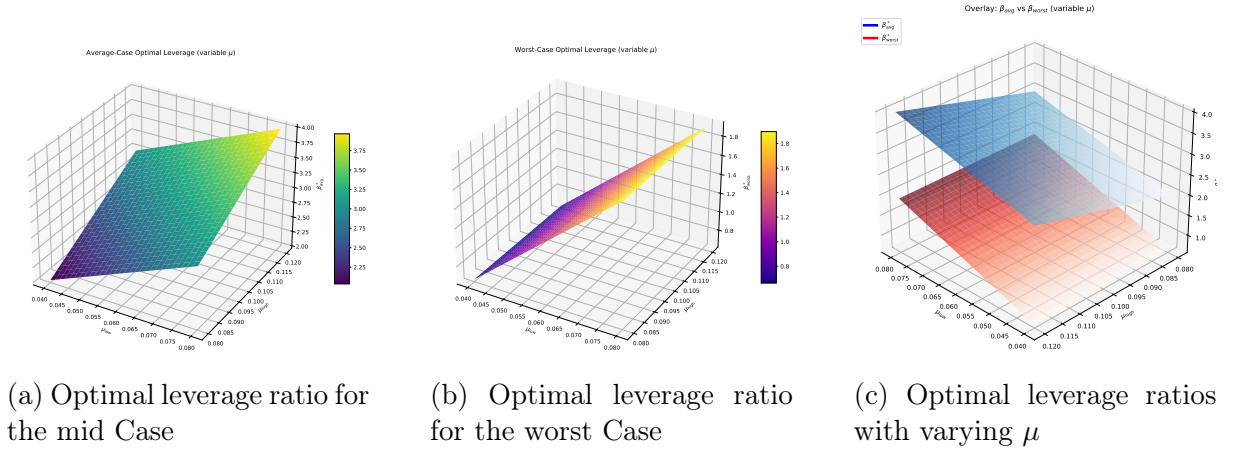


Figure 8.2: Optimal leverage ratios under varying  $\mu$ .

Figure 8.2 compares the robust and average optimal leverage ratios for different model parameters. We observe that the robust leverage ratio is systematically lower than the average one, particularly for higher levels of uncertainty. This behavior reflects the investor's conservative adjustment to adverse drift realizations.

## 8.1. Analysis of the reference process model

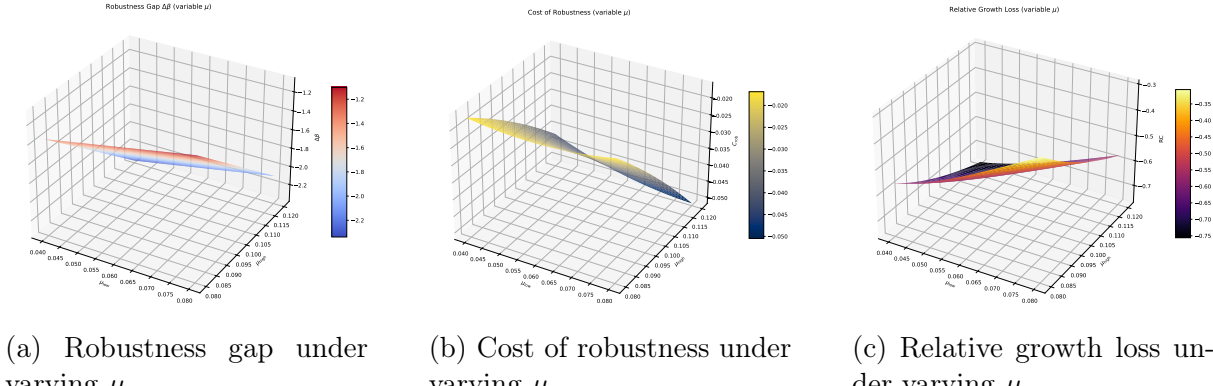


Figure 8.3: Impact of robustness.

Figure 8.3 illustrates how variations in the drift parameter  $\mu$  influence the relationship between robustness and performance. As the drift increases, the gap between the average-case and robust optimal leverage ratios widens, indicating that the robust investor adopts a more conservative position when the expected return rises. This leads to an increasing cost of robustness and a higher relative growth loss, as the robust strategy deliberately sacrifices potential gains to mitigate adverse drift realizations. The figure thus highlights the fundamental trade-off between performance and robustness as higher expected returns amplify the asymmetry between optimistic and pessimistic scenarios, making caution more costly but also more protective in the presence of model uncertainty.

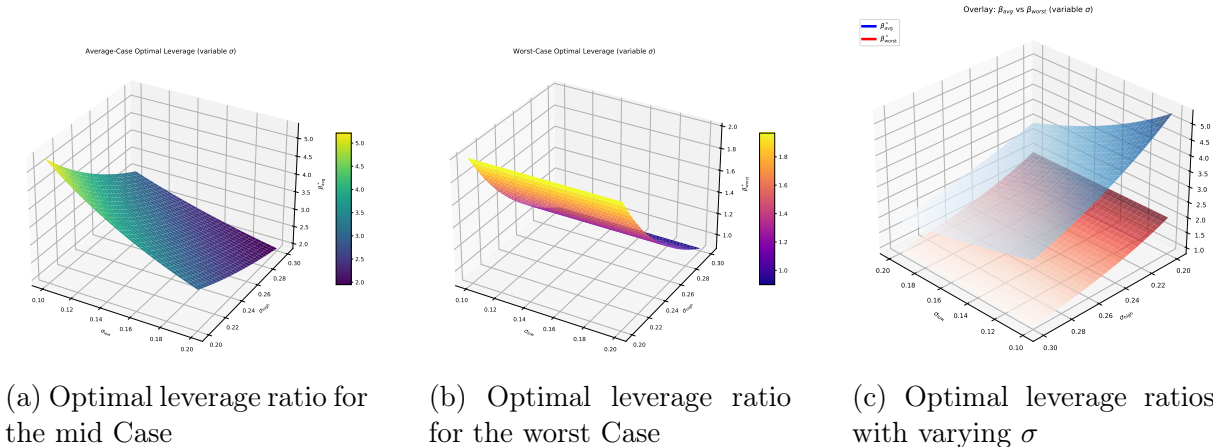


Figure 8.4: Optimal leverage ratios under varying  $\sigma$ .

Figure 8.4 presents the behavior of optimal leverage ratios under different levels of volatility  $\sigma$ . Both the average-case and robust leverage ratios decrease as volatility rises, reflecting the intuitive reduction in optimal exposure with increasing uncertainty. However, the robust leverage declines at a slower rate, resulting in a widening divergence between the two strategies for low volatility levels. This pattern underscores the heightened sensitivity of the robust solution to volatility fluctuations and confirms that volatility risk is a dominant driver of leverage adjustments in the presence of model ambiguity.

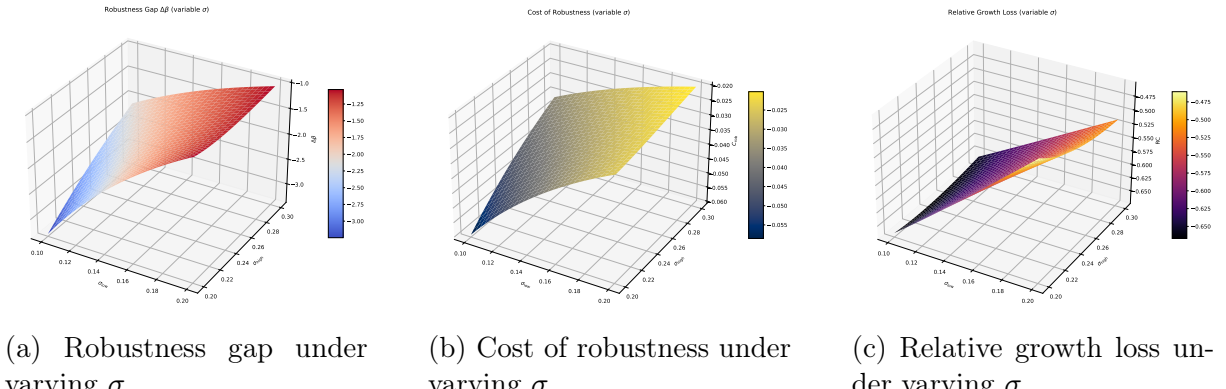


Figure 8.5: Impact of robustness.

Figure 8.5 summarizes the impact of volatility uncertainty on robustness metrics. As volatility increases, the robustness gap, the cost of robustness, and the relative growth loss all rise subsequently, demonstrating that robust strategies become increasingly conservative and performance divergent in more volatile environments. The results point out the notion that volatility uncertainty exerts a nonlinear and amplifying effect on long-run growth, emphasizing the economic significance of accounting for stochastic risk when determining leverage in uncertain markets.

## 8.2 comparison under uncertainty on stochastic volatility reference models

For this section we assume the Heston model, where uncertainty lies still on the reference process but the volatility itself is stochastic:

$$\begin{aligned} dX_t &= \mu X_t dt + \sqrt{\nu_t} X_t dW_t \\ d\nu_t &= (b - a\nu_t) dt + \sigma \sqrt{\nu_t} dB_t, \end{aligned} \tag{8.1}$$

with parameter assumptions introduced in Section 5.1. We showed that in this model we have a long term worst-case expected utility of

$$\lim_{T \rightarrow \infty} \frac{1}{T} \log v_T = p(r + \beta(\mu^* - r)) - \bar{b} \max_{\sigma \in [\underline{\sigma}, \bar{\sigma}]} \eta(\sigma).$$

We again assume as an average case the model with parameters

$$\alpha = (\mu^{mid}, \rho^{mid}, b^{mid}, a^{mid}, \sigma^{mid}),$$

where  $x^{mid} = \frac{x+\bar{x}}{2}$  for  $x \in \{\mu, \rho, b, a, \sigma\}$ .

Now we can again compare the long-term expected utility values of the worst and the average case:

$$\begin{aligned} C^{rob} &= \frac{1}{T} \log \inf_{\alpha \in [\underline{\alpha}, \bar{\alpha}]} \mathbb{E}^{\mathbb{P}} [(L_T^{\alpha})^p] - \frac{1}{T} \log \mathbb{E}^{\mathbb{P}} \left[ \left( L_T^{\alpha^{mid}} \right)^p \right] \\ &= p(r + \beta^{worst}(\mu^* - r)) - \bar{b} \max_{\sigma \in [\underline{\sigma}, \bar{\sigma}]} \eta(\sigma) - p(r + \beta^{mid}(\mu^{mid} - r)) + b^{mid} \eta^{mid}(\sigma^{mid}) \\ &= p(\beta^{worst}(\mu^* - r) - \beta^{mid}(\mu^{mid} - r)) - \bar{b} \max_{\sigma \in [\underline{\sigma}, \bar{\sigma}]} \eta(\sigma) + b^{mid} \eta^{mid}(\sigma^{mid}), \end{aligned}$$

where

$$\eta^{mid}(\sigma) = \frac{1}{\sigma^2} \left( \sqrt{(a^{mid} - p\beta\rho^{mid}\sigma)^2 + p(1-p)\beta^2\sigma^2} - (a^{mid} - p\beta\rho^{mid}\sigma) \right).$$

Now we turn to finding the optimal leverage ratio and remind us that it was stated for model parameters  $\beta \in [-5, 5]$ ,  $p = 0.5$ ,  $r = 0.015$ ,  $[\underline{\mu}, \bar{\mu}] = [0.05, 0.08]$ ,  $[\underline{\rho}, \bar{\rho}] = [-0.93, -0.75]$ ,  $[\underline{b}, \bar{b}] = [0.1, 0.2]$ ,  $[\underline{a}, \bar{a}] = [3, 10]$ ,  $[\underline{\sigma}, \bar{\sigma}] = [0.82, 0.93]$  the optimal leverage ratio is approximately 1.25 and the corresponding long-term growth rate is approximately 0.0179. So let us now compute the long-term growth rate and optimal leverage ratio for the average case.

To this end we first compute

$$\begin{aligned} & \eta^{mid} \left( \frac{0.82 + 0.93}{2} \right) \\ &= \frac{1}{0.765625} \left( \sqrt{(a^{mid} - p\beta\rho^{mid} * 0.875)^2 + p(1-p)\beta^2 * 0.765625} \right. \\ &\quad \left. - (a^{mid} - p\beta\rho^{mid} * 0.875) \right) \\ &= \frac{1}{0.765625} \left( \sqrt{(6.5 + 0.5 * \beta * 1.68 * 0.875)^2 + 0.25 * \beta^2 * 0.765625} \right. \\ &\quad \left. - (6.5 + 0.5 * \beta * 1.68 * 0.875) \right) \\ &= 1.30612 * (-6.5 - 0.735 * \beta + \sqrt{((6.5 + 0.735\beta)^2 + 0.191406\beta^2)}). \end{aligned}$$

Now:

$$\begin{aligned} & \frac{1}{T} \log \mathbb{E}^{\mathbb{P}} \left[ \left( L_T^{\alpha^{mid}} \right)^p \right] = p(r + \beta(\mu^{mid} - r)) - b^{mid}\eta^{mid}(\sigma^{mid}) \\ &= 0.5 \left( 0.015 + \beta \left( \frac{0.05 + 0.08}{2} - 0.015 \right) \right) - \frac{0.1 + 0.2}{2} \eta^{mid} \left( \frac{0.82 + 0.93}{2} \right) \\ &= 0.5 \left( 0.015 + \beta \left( \frac{0.05 + 0.08}{2} - 0.015 \right) \right) \\ &\quad - \frac{0.1 + 0.2}{2} 1.30612 * (-6.5 - 0.735 * \beta + \sqrt{((6.5 + 0.735\beta)^2 + 0.191406\beta^2)}), \end{aligned}$$

which maximizes for  $\beta^* = 5$ . Hence we continue

$$\begin{aligned} & \lim_{T \rightarrow \infty} \frac{1}{T} \log \mathbb{E}^{\mathbb{P}} \left[ \left( L_T^{\alpha^{mid}} \right)^p \right] \\ &= 0.5 \left( 0.015 + 5 * \left( \frac{0.05 + 0.08}{2} - 0.015 \right) \right) \\ &\quad - \frac{0.1 + 0.2}{2} 1.30612 * (-6.5 - 0.735 * 5 + \sqrt{((6.5 + 0.735 * 5)^2 + 0.191406 * 5^2)}) \\ &\approx 0.0869517. \end{aligned}$$

Therefore we have here that

$$C^{rob} \approx 0.0179 - 0.087 = -0.0691$$

and

$$G^{rob} \approx 1.25 - 5 = -3.75.$$

This leads now also to

$$R^C = \frac{C^{rob}}{\lim_{T \rightarrow \infty} \frac{1}{T} \log \mathbb{E}^P [(L_T^{\alpha^{mid}})^p]} \approx \frac{-0.0691}{0.087} \approx -0.7943$$

and

$$R^G = \frac{G^{rob}}{|\beta_{avg}^*|} \approx \frac{-3.75}{5} = -0.75.$$

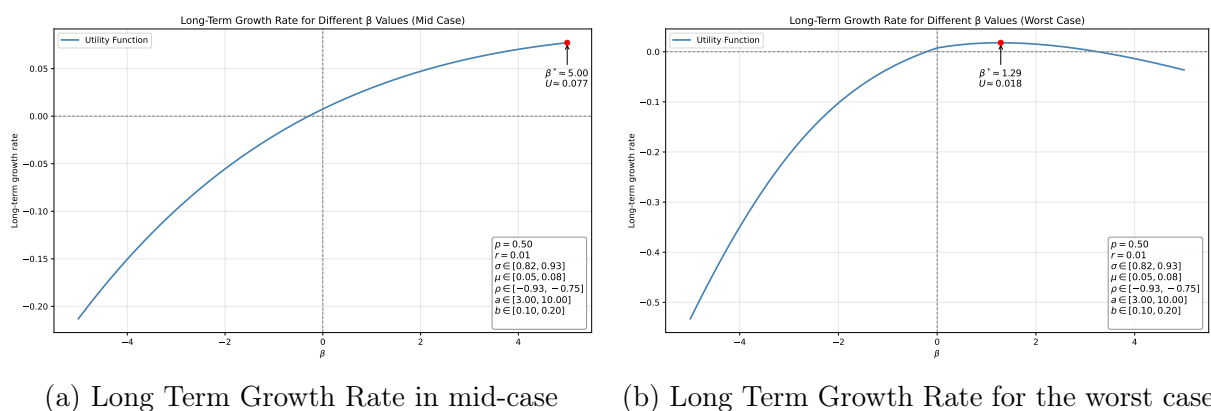


Figure 8.6: Long Term Growth Rate for the worst and mid case for different  $\beta$ .

Figure 8.6 shows the long-term growth rate for both mid- and worst-case scenarios as a function of the leverage ratio  $\beta$ . The peak of the curve occurs at different  $\beta$ -values, with the worst-case curve lying consistently below the mid-case one. We also see that for our parameter choice the long term growth rate only grows with increasing leverage ratio, whereas the curve of the worst case has a parabola shape.

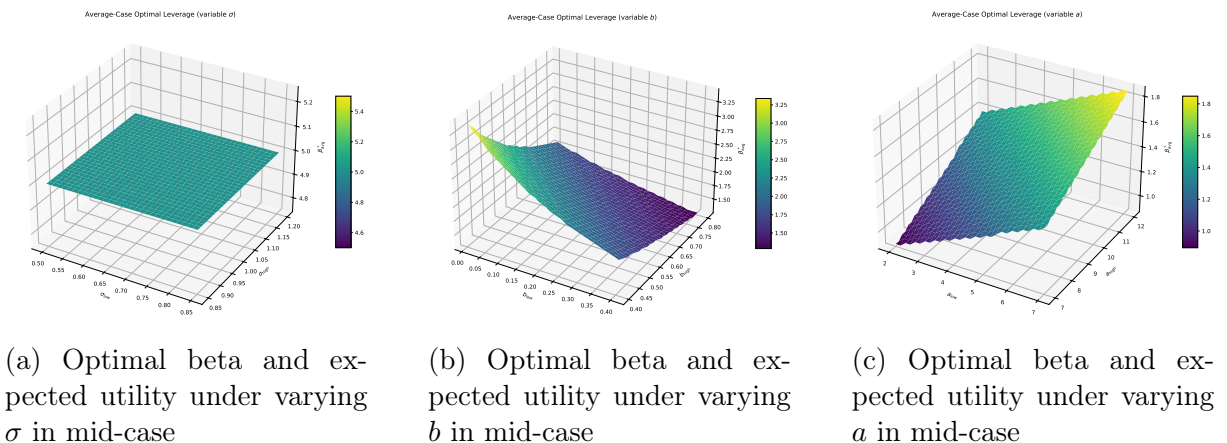


Figure 8.7: Optimal Leverage Ratios with varying parameters.

## 8.2. Analysis of the stochastic volatility reference model

---

Figure 8.7a illustrates the sensitivity of the optimal leverage ratio and the expected utility to changes in the volatility parameter  $\sigma$  within the average case scenario. The optimal  $\beta^*$  remains constant across the examined range of volatility bounds, indicating that leverage is relatively insensitive to moderate volatility fluctuations when other parameters are fixed. In contrast, the expected utility decreases as  $\sigma$  increases, reflecting the negative impact of higher volatility on long-term growth. Overall, this figure shows that in moderately uncertain environments, volatility exerts only a limited influence on the investor's optimal allocation and utility level.

Figure 8.7b examines the influence of variations in the mean reversion parameter  $b$  on the optimal leverage ratio and expected utility. As  $b$  increases, the optimal  $\beta^*$  falls sharply, suggesting that stronger mean reversion in the volatility process supports lower leverage. The expected utility surface displays the opposite behavior, gradually declining with increasing  $b$ , which reflects a trade off between higher short term exposure and the long run penalty from parameter uncertainty. These results underline the stabilizing role of mean reversion but also reveal that excessive reversion intensity can diminish long run utility.

Figure 8.7c depicts the dependence of the optimal leverage ratio and expected utility on the long term volatility level  $a$ . The optimal  $\beta^*$  rises as both the lower and upper bounds of  $a$  increase, indicating that higher baseline volatility leads to a more optimistic leverage choice. Correspondingly, the expected utility surface exhibits a rising trend for smaller values of  $a$  and flattens for larger values, confirming that lower volatility environments are associated with higher long run growth. This figure thus highlights how the structural level of volatility serves as a key determinant of leverage behavior and expected utility under model uncertainty.

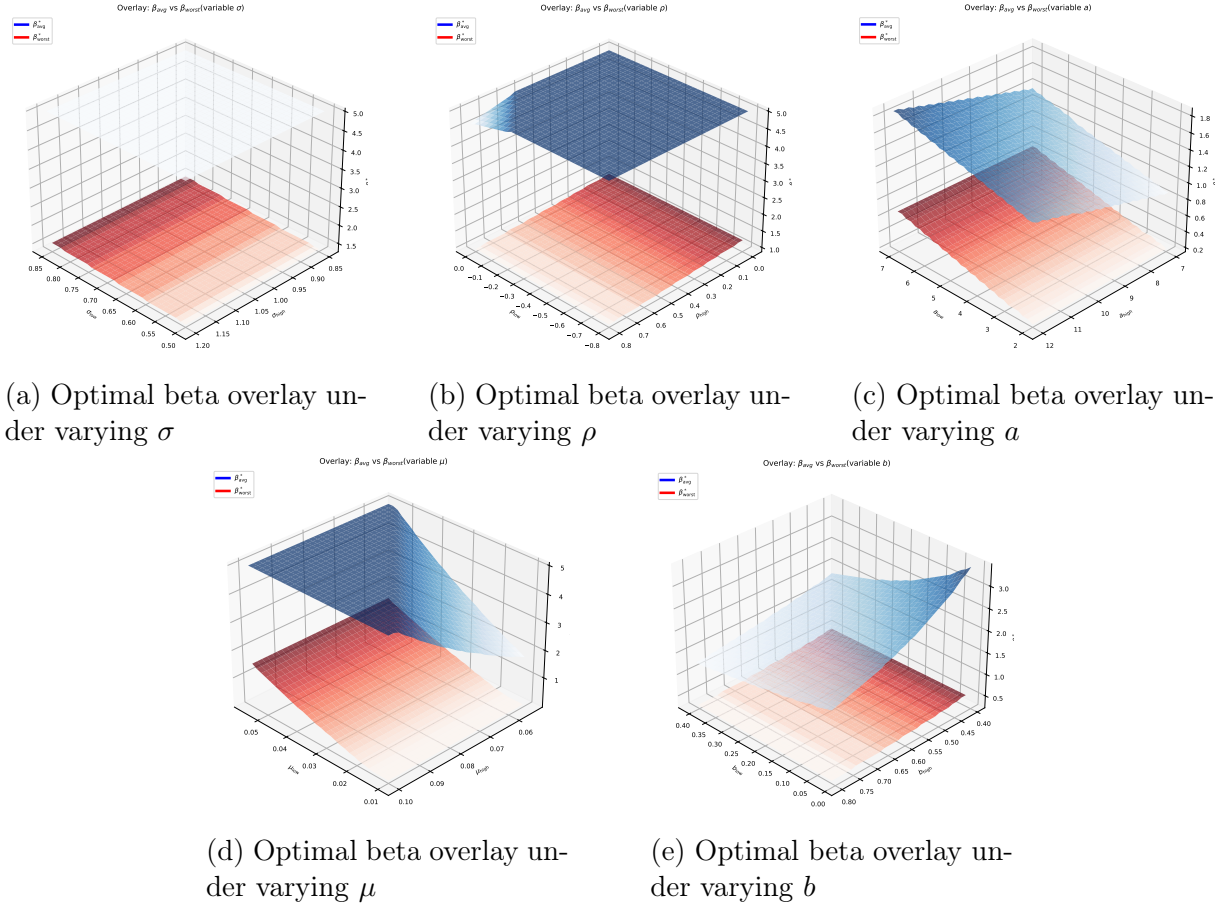


Figure 8.8: Optimal leverage ratios with varying parameters.

The analysis under the Heston model demonstrates that the optimal leverage ratio is sensitive to variations in key model parameters mean reversion parameters  $a$  and  $b$ , and less sensitive in other parameters such as drift  $\mu$  or correlation  $\rho$ . The comparison between mid-case and worst-case optimal leverage reveals the reduction in leverage under model uncertainty, highlighting the cost of robustness. Figure 8.8 presents the overlay of average and worst-case optimal leverage ratios across different parameter inputs. In each subplot, the robust leverage curve lies below the average one.

## 8.2. Analysis of the stochastic volatility reference model

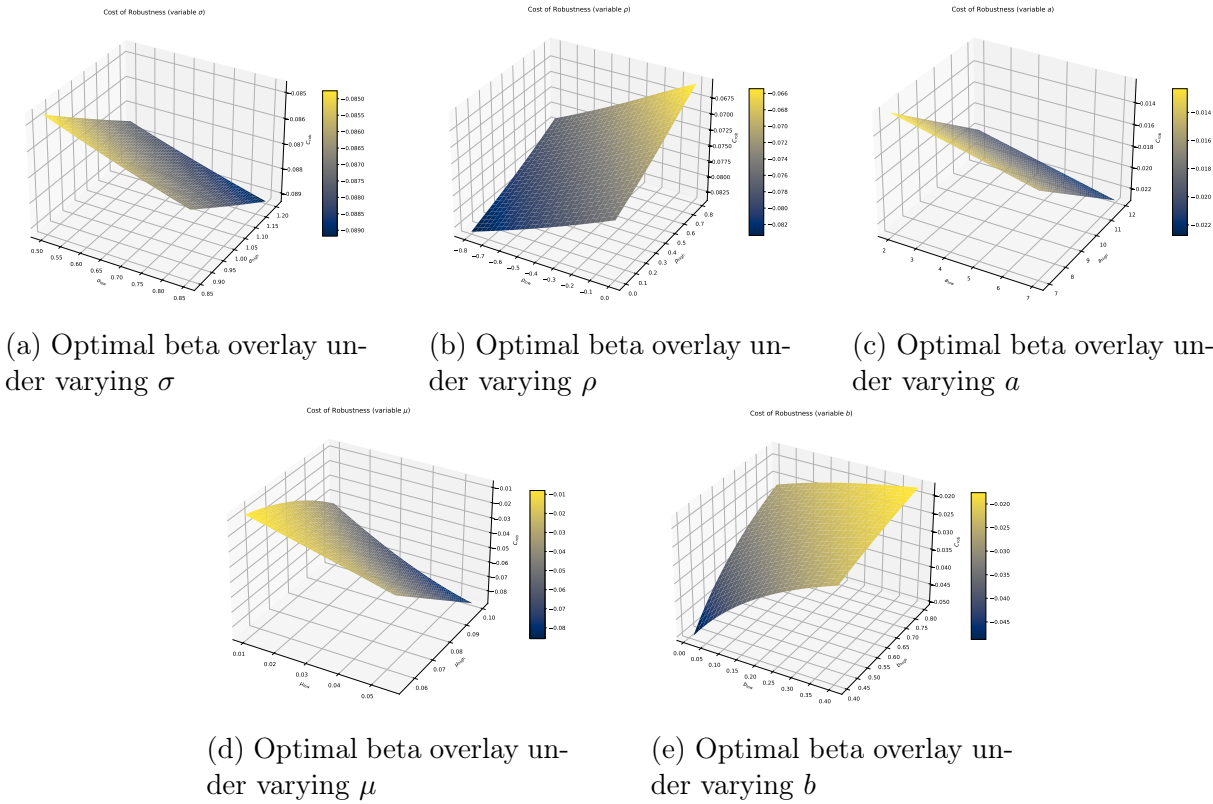


Figure 8.9: Cost of robustness for different parameters.

Figure 8.9 displays the cost of robustness for different parameters. The plotted surface rises with increasing volatility  $\sigma$ , drift  $\mu$  and mean reversion  $a$ , forming a smooth upward slope. The highest values are observed in the region, where the uncertainty range has the highest values. Interestingly for correlation factor  $\rho$  and speed of mean reversion  $b$  the highest values are found for the highest values of both the lower and upper bound, but not the interval of maximal uncertainty.

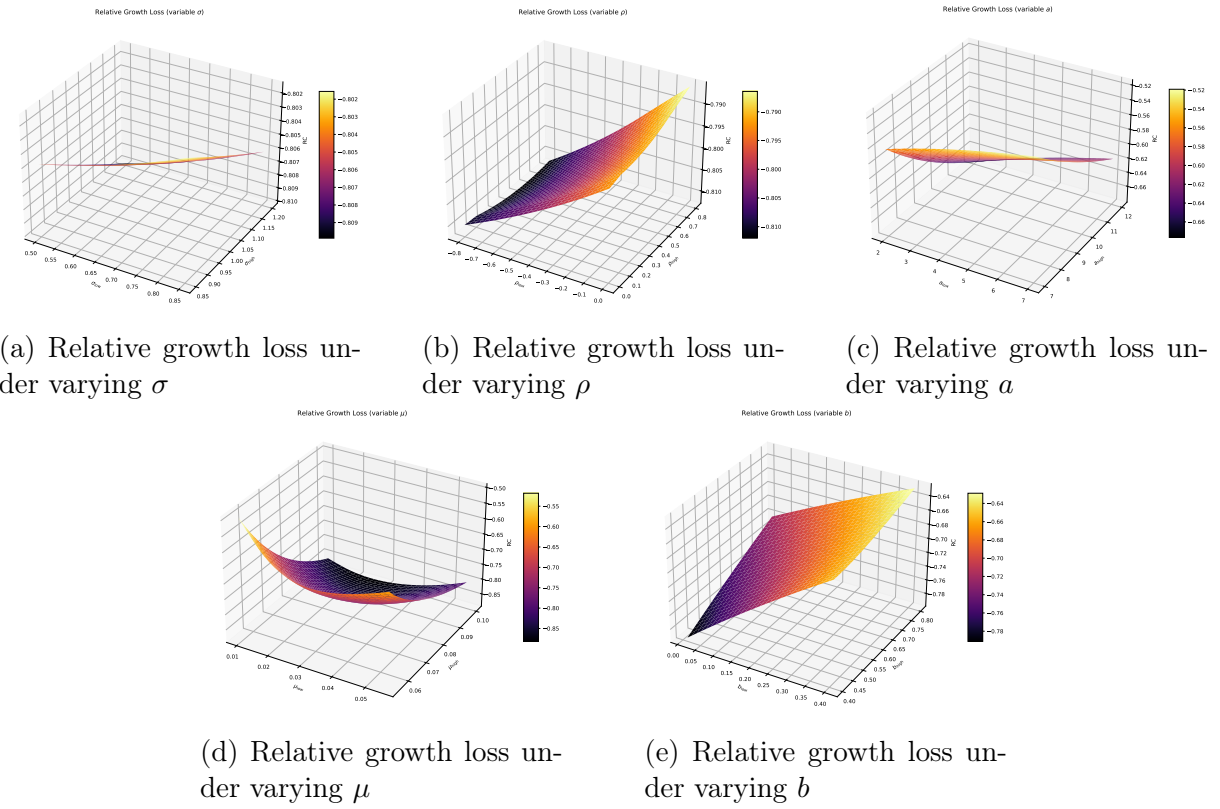


Figure 8.10: Relative growth loss for different parameters.

Figure 8.10 illustrates how the relative growth loss responds to variations in the key model parameters. The plots highlight how parameter uncertainty affects the growth rate for mid and worst case and how this translates to the relative growth rate. All parameters induce notable effects on the relative growth loss. Together, these surfaces provide a visual comparison of the sensitivity of robust optimal growth to different dimensions of model uncertainty.

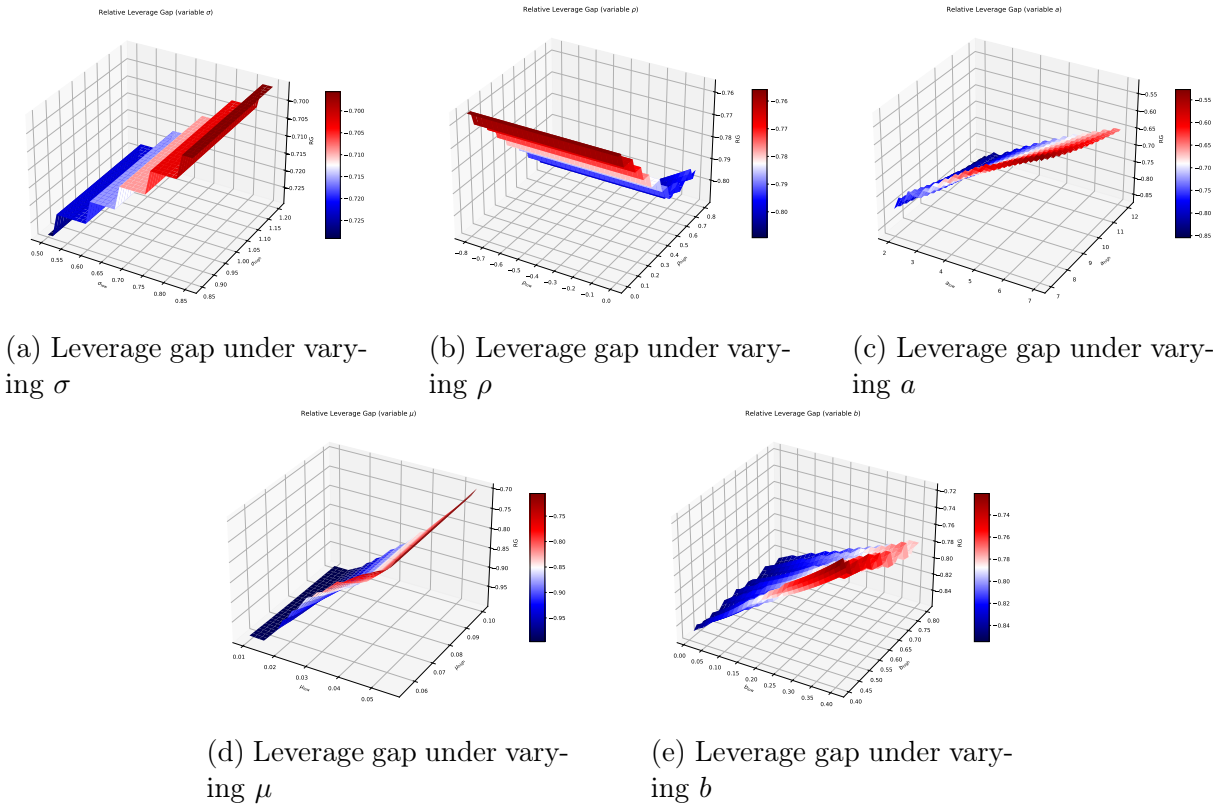


Figure 8.11: Leverage gap for different parameters.

Figure 8.11 shows the leverage gap between the worst- and average-case. The difference between both leverage ratios increases with higher lower bound for the volatility  $\sigma$ ,  $a$ ,  $b$  and drift  $\mu$ . For the correlation coefficient  $\rho$  the leverage ratio increases as the higher bound of its interval approaches 0.

### 8.3 Comparison under uncertainty on reference and interest rate models

In this section we will consider the Vasicek model, where uncertainties lie now in both the reference and the interest rate

$$\begin{aligned} dX_t &= \mu X_t dt + \varsigma X_t dW_t \\ dr_t &= (b - ar_t) dt + \sigma dB_t \end{aligned}$$

with parameter assumptions introduced in Section 6.1. We showed that in this model we have a long term worst-case expected utility of

$$\lim_{T \rightarrow \infty} \frac{1}{T} \log \inf_{\alpha \in [\underline{\alpha}, \bar{\alpha}]} \mathbb{E}^{\mathbb{P}^\alpha} [L_T^p] = p\beta\mu^*(\beta) - \frac{1}{2}p(1-p)\beta^2\varsigma^*(\beta, \underline{\rho}, \bar{\rho})^2 - \lambda(\alpha^*(\beta, \underline{\rho}, \bar{\rho})) ,$$

c.f. Proposition 6.1. In the average case scenario we have the long term expected utility

$$\lim_{T \rightarrow \infty} \frac{1}{T} \log \mathbb{E}^{\mathbb{P}^{\alpha^{mid}}} [L_T^p] = p\beta\mu^{mid} - \frac{1}{2}p(1-p)\beta^2(\varsigma^{mid})^2 - \lambda(\alpha^{mid}) ,$$

where

$$\begin{aligned}\alpha^{mid} &= (\mu^{mid}, \varsigma^{mid}, \rho^{mid}, b^{mid}, a^{mid}, \sigma^{mid}) \\ \lambda(\alpha) &= -\frac{1}{2} \left( p(\beta - 1) \frac{\sigma}{a} \right)^2 + p^2 \beta(\beta - 1) \varsigma \rho \frac{\sigma}{a} + \frac{p(\beta - 1)b}{a}.\end{aligned}$$

We set  $p = 0.5$ ,  $[\underline{\mu}, \bar{\mu}] = [0.06, 0.1]$ ,  $[\underline{\varsigma}, \bar{\varsigma}] = [0.1, 0.35]$ ,  $[\underline{\rho}, \bar{\rho}] = [-0.9, -0.5]$ ,  $[\underline{b}, \bar{b}] = [0.06, 0.1]$ ,  $[\underline{a}, \bar{a}] = [8, 14]$ ,  $[\underline{\sigma}, \bar{\sigma}] = [0.2, 0.5]$  and compare the optimal leverage ratio  $\beta^*$  under both the average and the worst case. For the worst case we numerically compute the optimal leverage ratio around 0.83 with long-term rate around 0.015. Under the mid case we compute:

$$\begin{aligned}\lim_{T \rightarrow \infty} \frac{1}{T} \log \mathbb{E}^{\mathbb{P}^{\alpha^{mid}}} [L_T^p] &= p\beta\mu^{mid} - \frac{1}{2}p(1-p)\beta^2(\varsigma^{mid})^2 - \lambda(\alpha^{mid}) \\ &= p\beta\mu^{mid} - \frac{1}{2}p(1-p)\beta^2(\varsigma^{mid})^2 \\ &\quad + \frac{1}{2} \left( p(\beta - 1) \frac{\sigma^{mid}}{a^{mid}} \right)^2 + p^2 \beta(\beta - 1) \varsigma^{mid} \rho^{mid} \frac{\sigma^{mid}}{a^{mid}} + \frac{p(\beta - 1)b^{mid}}{a^{mid}}.\end{aligned}$$

The above term is maximized for  $\beta \approx 3.54$  and therefore:

$$\lim_{T \rightarrow \infty} \frac{1}{T} \log \mathbb{E}^{\mathbb{P}^{\alpha^{mid}}} [L_T^p] \approx 0.065.$$

Numerically we compute for the worst case:

$$\beta^* \approx 0.083, \quad \lim_{T \rightarrow \infty} \frac{1}{T} \log \mathbb{E}^{\mathbb{P}^{\alpha^{mid}}} [L_T^p] \approx 0.015.$$

Hence

$$C^{rob} \approx 0.015 - 0.065 = -0.05.$$

Next, we compare the optimal leverage ratio, since this is ultimately the value we can influence and is important for investing.

$$G^{rob} \approx 0.083 - 3.54 = -3.457.$$

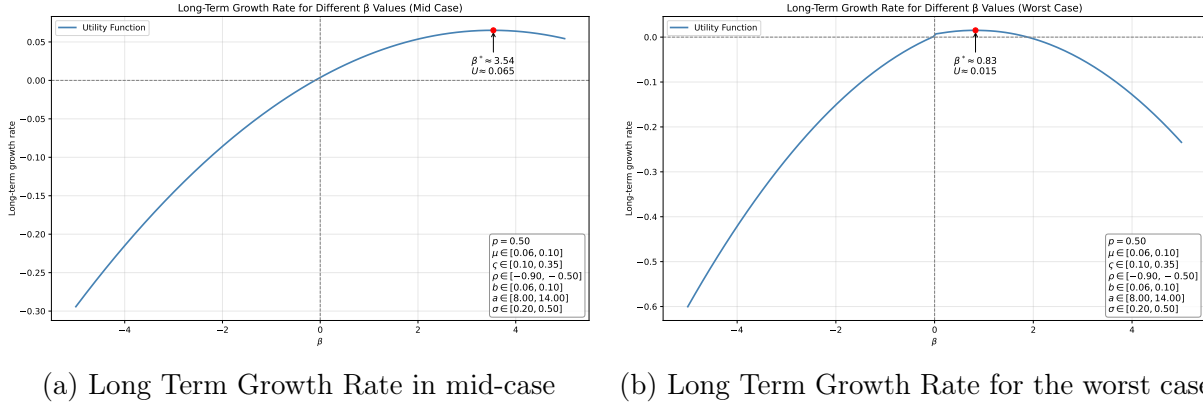
This leads now also to

$$R^C = \frac{C^{rob}}{\lim_{T \rightarrow \infty} \frac{1}{T} \log \mathbb{E}^{\mathbb{P}} [(L_T^{\alpha^{mid}})^p]} \approx \frac{-0.05}{0.065} \approx -0.7692$$

and

$$R^G = \frac{G^{rob}}{|\beta_{avg}^*|} \approx \frac{-3.457}{3.54} = -0.9766.$$

### 8.3. Analysis of the reference and interest rate model



(a) Long Term Growth Rate in mid-case      (b) Long Term Growth Rate for the worst case

Figure 8.12: Long Term Growth Rate for the worst and mid case for different  $\beta$ .

Figure 8.12 compares the long-term growth rates for different leverage ratios for the worst and mid-case. The worst-case curve lies below the average curve, showing a lower maximum growth rate across all  $\beta$ -values, with the maximum lying at a much larger leverage ratio.

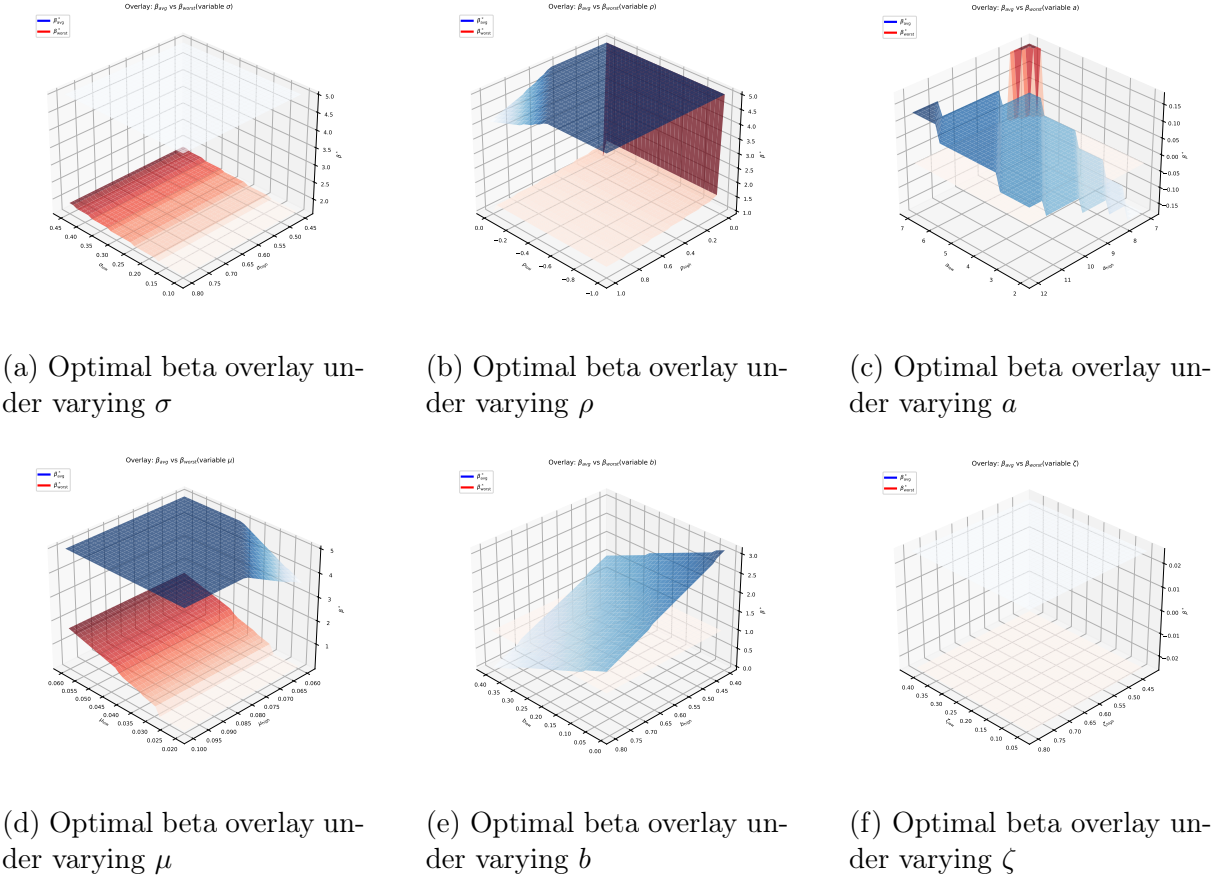


Figure 8.13: Optimal leverage ratios with varying parameters.

Figure 8.13 depicts the overlay of optimal leverage ratios for average and worst-case models across varying parameter ranges. Panels (a)–(f) illustrate the dependence on each parameter  $\sigma, \rho, a, \mu, b$  and  $\zeta$ , respectively, highlighting how each uncertainty source affects the leverage outcome. We see that for some parameters such as  $\rho$  the optimal ratio stays constant until a certain threshold is surpassed and then drastically changes. For other parameters such as  $b$  this change is slower and present across the whole range of the uncertainty set.

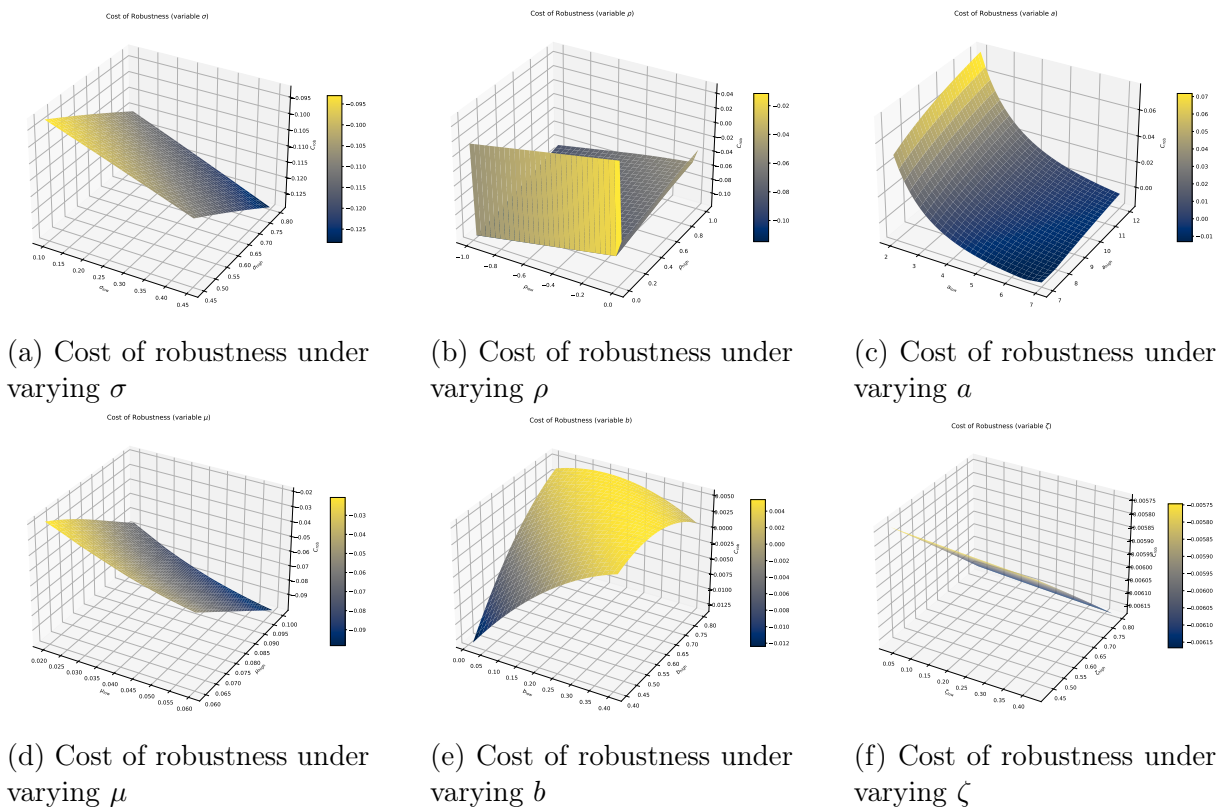


Figure 8.14: Cost of robustness for different parameters.

Figure 8.14 presents the cost of robustness as a function of the different parameters in the Vasicek model. The surfaces are mostly smooth, with the exception of the the plot under  $\rho$ .

### 8.3. Analysis of the reference and interest rate model

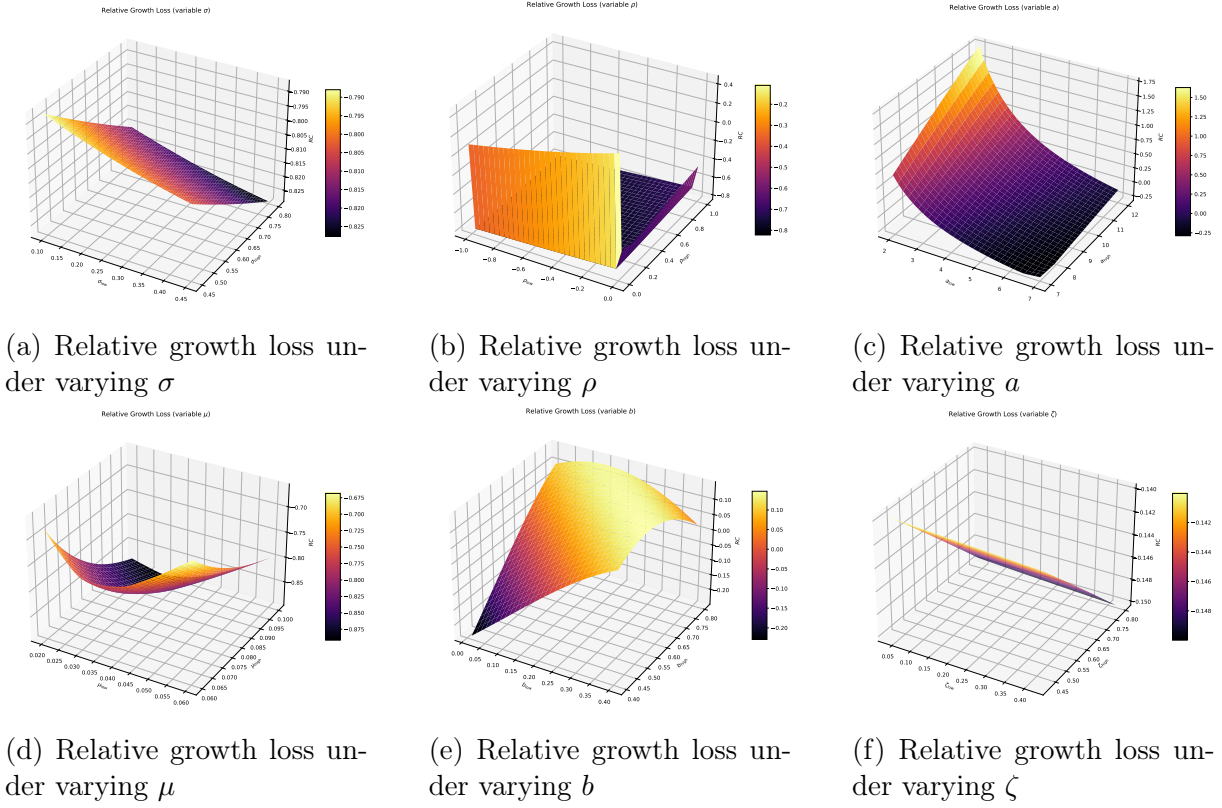


Figure 8.15: Relative growth loss for different parameters.

Figure 8.15 illustrates how the relative growth loss responds to variations in the key model parameters. The plots highlight how parameter uncertainty affects the growth rate for mid and worst case and how this translates to the relative growth rate. All parameters induce notable effects on the relative growth loss. Interestingly for  $\rho$  we notice that for a big range changing the uncertainty set does not impact the relative growth loss, which then drastically changes as the uncertainty set includes particular values. Together, these surfaces provide a visual comparison of the sensitivity of robust optimal growth to different dimensions of model uncertainty.

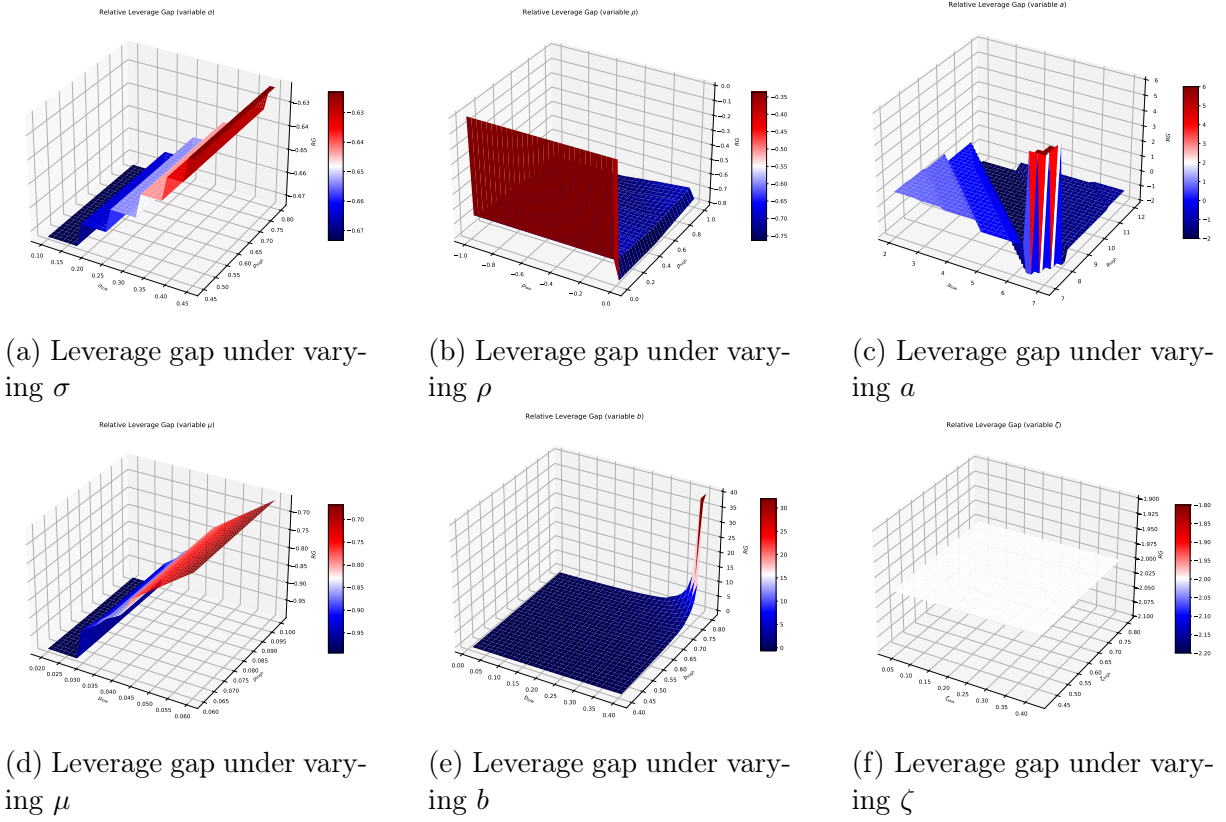


Figure 8.16: Leverage gap for different parameters.

Figure 8.16 shows the leverage gap between the worst- and average-case. The difference between both leverage ratios increases with higher lower bound for the volatility  $\sigma$  and drift  $\mu$ . For the correlation coefficient  $\rho$  we see a drastic increase as the upper bound grows beyond a certain barrier. For parameter  $a$  the gap increases dramatically as the lower and upper bound meet at the middle. Lastly for parameter  $b$  we see a big increase happening for high values whereas the gap remained 0 for a great range.

## 8.4 Comparison under uncertainty on jump diffusion process models

In this section we will consider the Bates model and compare the worst case against an average case. Recall that the Bates model assumes the following SDE

$$\begin{aligned} \frac{dX_t}{X_t} &= \mu dt + \sqrt{\nu_t} dB_t^{(1)} + (k-1)dN_t \\ d\nu_t &= (b - a\nu_t)dt + \sigma\sqrt{\nu}dB_t^{(2)}, \end{aligned}$$

where  $N_t$  is a Poisson process with intensity  $\xi$  and  $k$  is log-normally distributed with parameters  $\mu_k, \sigma_k^2$ , c.f. Haugh [61], where  $B_t^{(1)}$  and  $B_t^{(2)}$  are two Brownian motions with correlation parameter  $\rho \in [\underline{\rho}, \bar{\rho}]$  and  $\langle B_t^{(1)}, B_t^{(2)} \rangle_t = \rho t$ . Hence our parameters are

$\alpha = (\mu, \sigma, \xi, \mu_k, \sigma_k, b, a) \in [\underline{\mu}, \bar{\mu}] \times [\underline{\sigma}, \bar{\sigma}] \times [\underline{\xi}, \bar{\xi}] \times [\underline{\mu}_k, \bar{\mu}_k] \times [\underline{\sigma}_k, \bar{\sigma}_k] \times [\underline{b}, \bar{b}] \times [\underline{a}, \bar{a}]$  with  $\underline{\mu}, \underline{a}, \underline{\sigma} > 0$  and  $\underline{b} > \bar{\sigma}^2/2$ . We also assume  $\underline{a} - p|\beta|\bar{\sigma} > 0$ ,  $\underline{\mu} \geq \frac{\beta-1}{\beta}$  for  $\beta \geq 0$  and  $\bar{\mu} \leq \frac{\beta-1}{\beta}$  for  $\beta < 0$ .

We showed in section 7.2 that the expected utility of holding an LETF under this model is expressed by

$$\lim_{T \rightarrow \infty} \frac{1}{T} \log \inf_{\alpha \in [\underline{\alpha}, \bar{\alpha}]} \mathbb{E}^{\mathbb{P}} [(L_T^{\alpha})^p] = p(\beta\mu^* + (1-\beta)r) + \min_{\xi \in [\underline{\xi}, \bar{\xi}], \sigma \in [\underline{\sigma}, \bar{\sigma}]} \xi(-1 + (1 + \beta(\mu_k^* - 1))^p) - \bar{b}\eta(\sigma).$$

Under the assumption for the average case, where

$$\alpha^{mid} = (\mu^{mid}, \mu_k^{mid}, \sigma_k^{mid}, b^{mid}, a^{mid}, \rho^{mid}), \text{ with } x^{mid} = \frac{\bar{x} - \underline{x}}{2}$$

we also want to compute the long-term growth rate and optimal leverage ratio of the mid-case. We can easily see that

$$\lim_{T \rightarrow \infty} \frac{1}{T} \log \mathbb{E}^{\mathbb{P}} \left[ (L_T^{\alpha^{mid}})^p \right] = p(\beta\mu^{mid} + (1-\beta)r) + \xi^{mid}(-1 + (1 + \beta(\mu_k^{mid} - 1))^p) - b^{mid}\eta^{mid},$$

where

$$\eta^{mid} = \frac{1}{\sigma^{mid2}} \left( \sqrt{(a^{mid} - p\beta\rho^{mid}\sigma^{mid})^2 + p(1-p)\beta^2\sigma^{mid2}} - (a^{mid} - p\beta\rho^{mid}\sigma^{mid}) \right).$$

Hence

$$\begin{aligned} C^{rob} &= \frac{1}{T} \log \inf_{\alpha \in [\underline{\alpha}, \bar{\alpha}]} \mathbb{E}^{\mathbb{P}} [(L_T^{\alpha})^p] - \frac{1}{T} \log \mathbb{E}^{\mathbb{P}} \left[ (L_T^{\alpha^{mid}})^p \right] \\ &= p(\beta\mu^* + (1-\beta)r) + \min_{\xi \in [\underline{\xi}, \bar{\xi}], \sigma \in [\underline{\sigma}, \bar{\sigma}]} \xi(-1 + (1 + \beta(\mu_k^* - 1))^p) - \bar{b}\eta(\sigma) \\ &\quad - p(\beta\mu^{mid} + (1-\beta)r) - \xi^{mid}(-1 + (1 + \beta(\mu_k^{mid} - 1))^p) - b^{mid}\eta^{mid} \\ &= p\beta(\mu^* - \mu^{mid}) + \min_{\xi \in [\underline{\xi}, \bar{\xi}], \sigma \in [\underline{\sigma}, \bar{\sigma}]} \xi(-1 + (1 + \beta(\mu_k^* - 1))^p) - \bar{b}\eta(\sigma) \\ &\quad - \xi^{mid}(-1 + (1 + \beta(\mu_k^{mid} - 1))^p) - b^{mid}\eta^{mid}. \end{aligned}$$

Let us now consider a concrete case again and afterward plot the  $C^{rob}, G^{rob}, \beta^*, \beta^{mid*}$  and the long term growth rate again. Let  $p = 0.500, r = 0.015, \mu \in [0.05, 0.08], \mu_k \in [0.82, 0.98], \sigma_k \in [0.70, 1.00], \xi \in [0.05, 0.25], \rho \in [-0.93, -0.75], b \in [0.10, 0.20], a \in [3.00, 10.00], \sigma \in [0.82, 0.93]$ . Hence

$$\begin{aligned} \alpha^{mid} &= (\mu^{mid}, \mu_k^{mid}, \sigma_k^{mid}, \xi^{mid}, \rho^{mid}, b^{mid}, a^{mid}, \sigma^{mid}) \\ &= (0.065, 0.90, 0.85, 0.15, -0.84, 0.15, 6.50, 0.875). \end{aligned}$$

Now we compute numerically the optimal leverage ratios and long term growth rate for both cases and get  $\beta^* \approx 0.02$  with  $\lim_{T \rightarrow \infty} \frac{1}{T} \log \mathbb{E}^{\mathbb{P}} \left[ (L_T^{\alpha^{worst}})^p \right] = 0.007$  for the worst

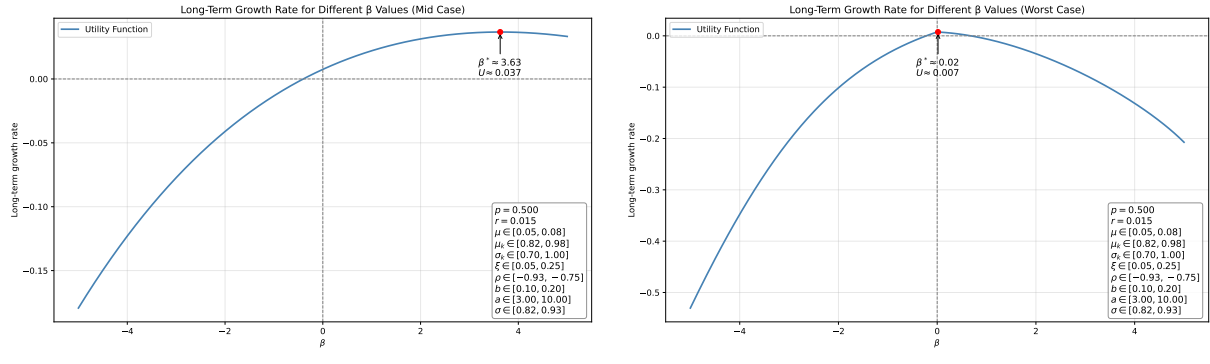
case and  $\beta^* \approx 3.63$  with  $\lim_{T \rightarrow \infty} \frac{1}{T} \log \mathbb{E}^{\mathbb{P}} \left[ \left( L_T^{\alpha^{mid}} \right)^p \right] = 0.037$  for the mid case, c.f. Figure 8.17. Hence

$$C^{rob} = 0.007 - 0.037 = -0.03$$

$$G^{rob} = 0.02 - 3.63 = -3.61,$$

$$R^C = -0.03/0.037 \approx -0.8108 \quad \text{and}$$

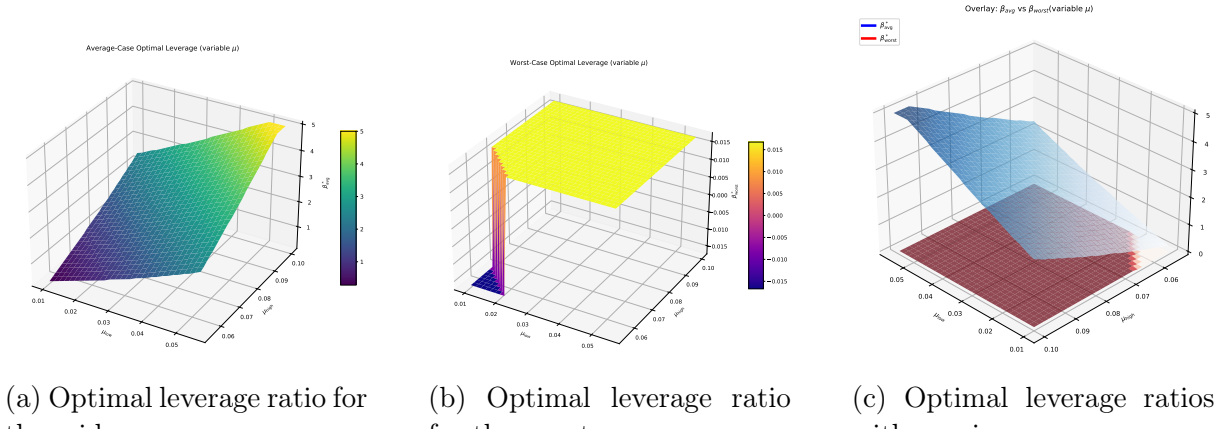
$$R^G = -3.61/3.63 \approx -0.9945.$$



(a) Long Term Growth Rate in mid-case      (b) Long Term Growth Rate for the worst case

Figure 8.17: Long Term Growth Rate for the worst and mid case for different  $\beta$ .

Figure 8.17 shows the different long term growth rate curves as function of  $\beta$  for the mid and worst case. We see that the values of the mid-case curve consistently lie above the one of the worst case. Next we see that the long term growth rate increases much longer until it reaches its maximum at  $\approx 3.63$  whereas the worst case optimal leverage ratio is  $\approx 0.02$ .



(a) Optimal leverage ratio for the mid case

(b) Optimal leverage ratio for the worst case

(c) Optimal leverage ratios with varying  $\mu$

Figure 8.18: Optimal leverage ratios under varying  $\mu$ .

Figure 8.18 illustrates how the optimal leverage ratio responds to variations in the drift parameter  $\mu$  within the jump-diffusion framework. Both the average case and worst-case leverage ratios increase with higher drift values, consistent with the intuition that a

#### 8.4. Analysis of the jump diffusion process model

---

larger expected return allows for greater exposure to the risky asset. However, the robust leverage ratio remains consistently below the average one, reflecting the conservative adjustment induced by model uncertainty and jump risk. The discrepancy between the two ratios widens with increasing  $\mu$ , highlighting that in optimistic environments the robust investor sacrifices more potential return to hedge against adverse jump outcomes. This behavior underscores the asymmetry introduced by jumps, which amplifies the trade off between risk-taking and robustness in leveraged portfolios.

## Chapter 8. Comparative analysis on optimal leverage

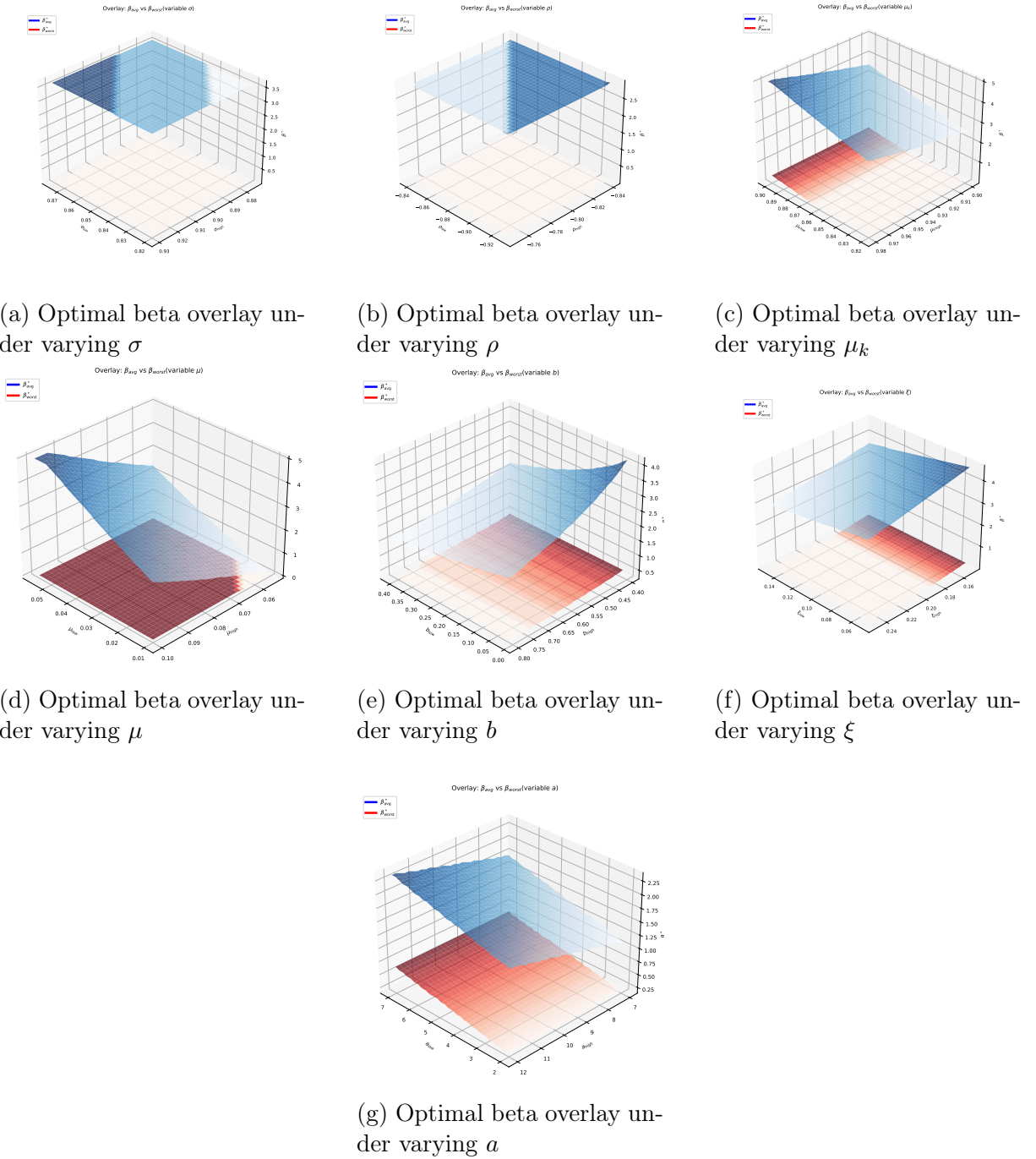


Figure 8.19: Optimal leverage ratios with varying parameters.

Figure 8.19 show the overlay of optimal leverage ratios across the mid and worst case. In this model we see that, at least in the ranges that we set, the parameters  $\sigma$  and  $\rho$  are barely influencing the optimal leverage ratio. Other parameters,  $\mu$ ,  $\zeta$  and  $b$  are influencing the mid-case greatly, while it has a smaller impact on the worst case.

## 8.4. Analysis of the jump diffusion process model

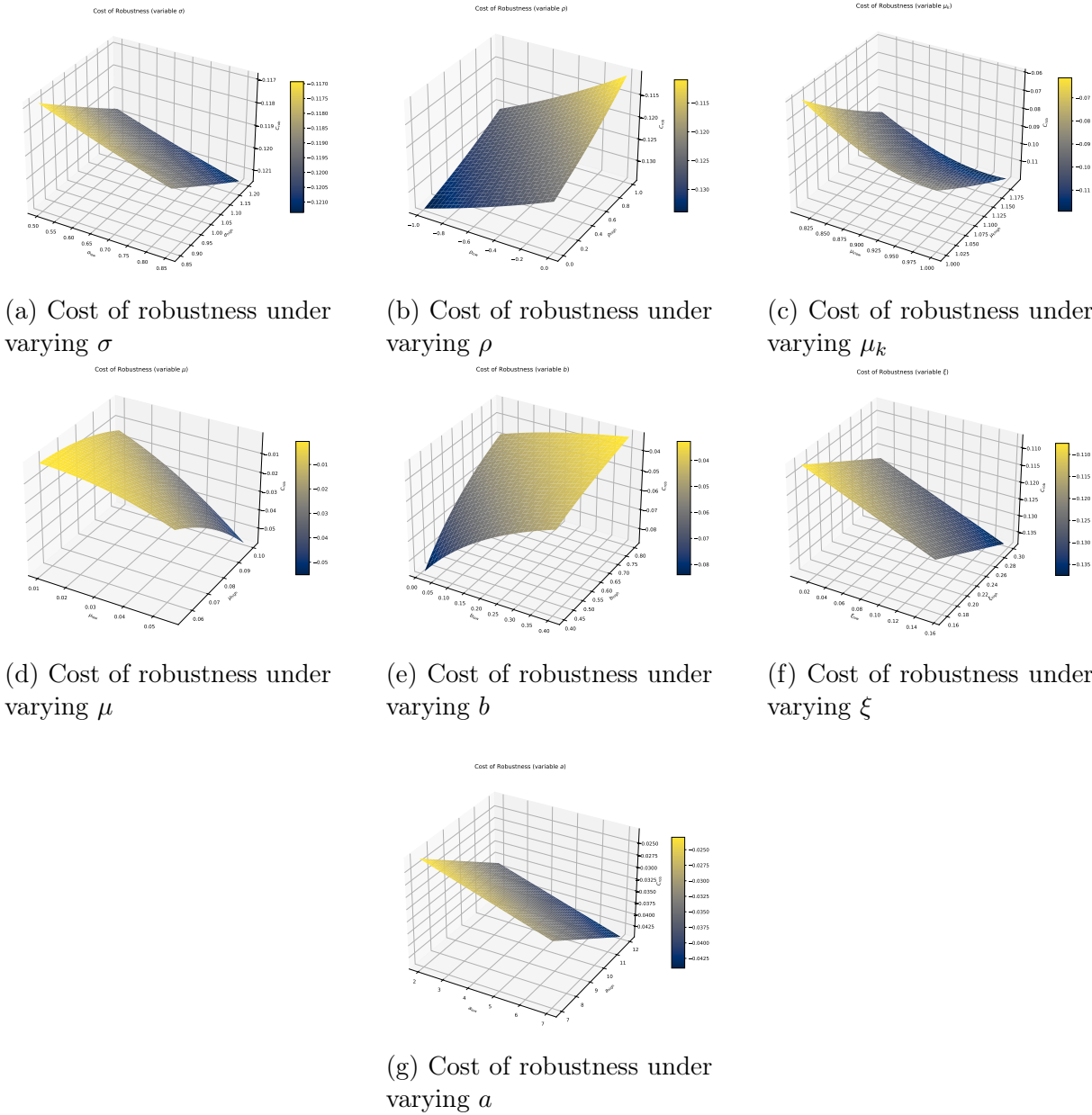


Figure 8.20: Cost of robustness for different parameters.

Figure 8.20 depicts the surfaces of the cost of robustness for the different parameter variations. Here we see that the choice of the range for all parameters impact the cost of robustness. Generally, we can say that the cost is maximized and minimized on the extremes or boundaries.

## Chapter 8. Comparative analysis on optimal leverage

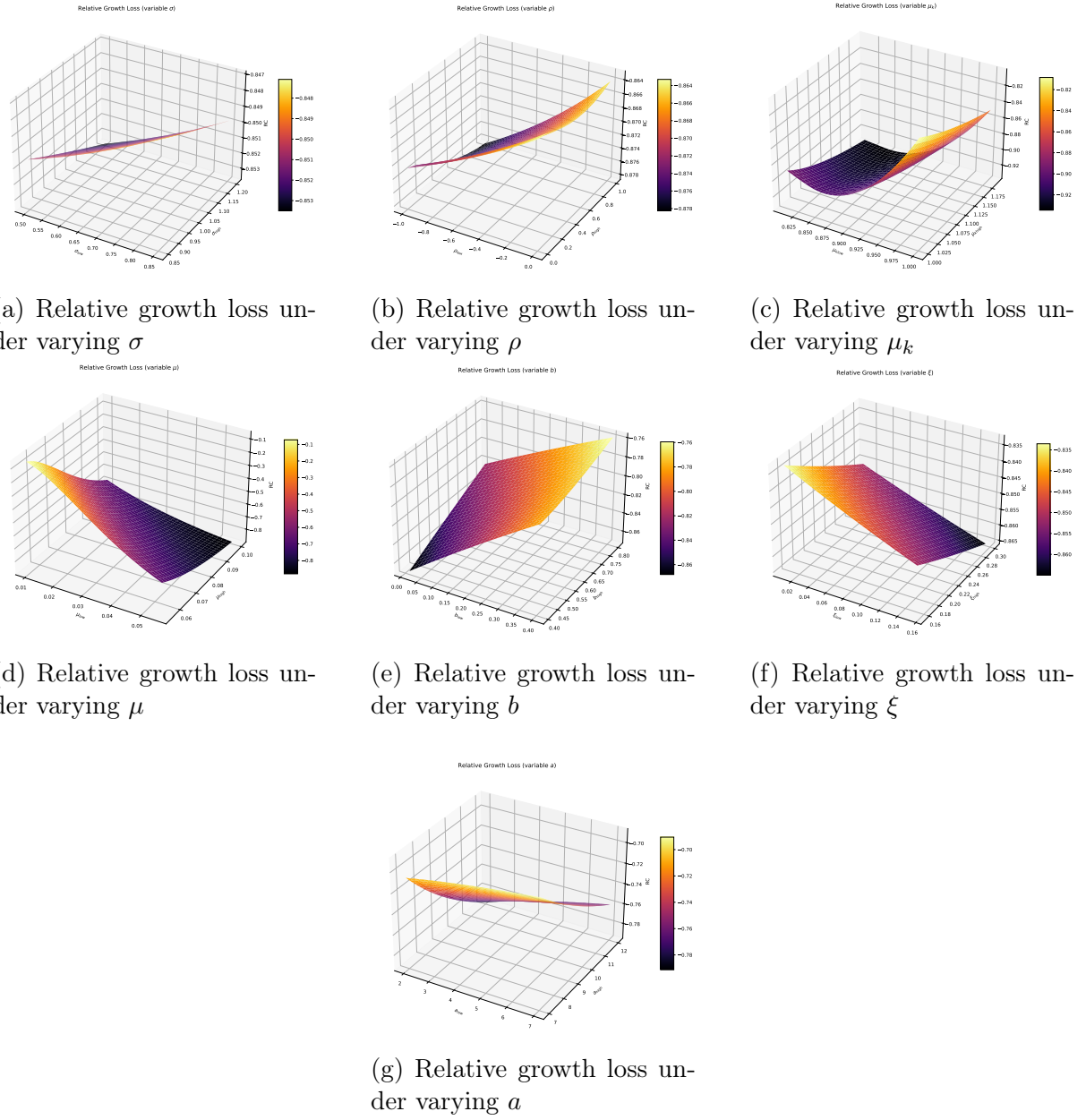


Figure 8.21: Relative growth loss for different parameters.

Figure 8.21 illustrates how the relative growth loss responds to variations in the key model parameters. The plots highlight how parameter uncertainty affects the growth rate for mid and worst case and how this translates to the relative growth rate. All parameters induce notable effects on the relative growth loss. Together, these surfaces provide a visual comparison of the sensitivity of robust optimal growth to different dimensions of model uncertainty.

## 8.4. Analysis of the jump diffusion process model

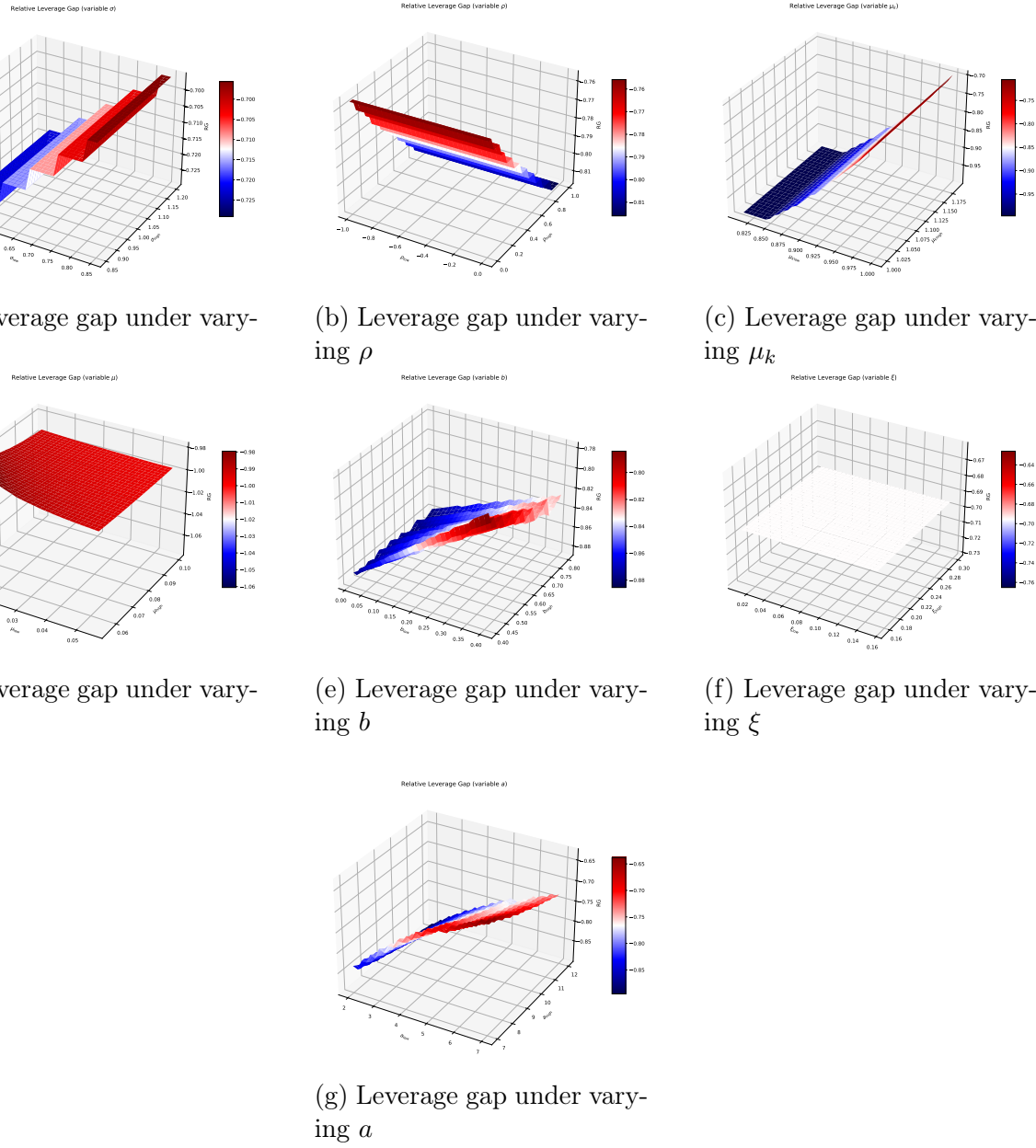


Figure 8.22: Leverage gap for different parameters.

Figure 8.22 shows the leverage gap for varying different parameters. Except for  $\zeta$  we see that the parameter range impacts the leverage gap greatly. Generally, the leverage gap is maximized and minimized on some extremes or boundaries on the parameter range. As an exception we see that for the drift parameter  $\mu$  the gap drastically increases when the lower bound gets greater than 0.01 but then stays around the same level.



# Chapter 9

## Empirical validation: Comparing optimal leverage strategies with actual ETF performance

In the preceding chapters, we developed and analyzed optimal portfolio strategies under various models of market dynamics. These strategies were derived in a model-based framework aimed at maximizing long-run expected utility for a power utility investor, subject to a given set of assumptions about the underlying index process. However, a key question remains: how do these theoretically optimal strategies perform in real markets? This chapter aims to bridge the gap between theory and practice by evaluating the empirical performance of the optimal leverage strategies derived. Specifically, we focus on a standard ETF index and examine how an investor would have performed over several time horizons had they implemented the optimal strategy derived under our framework, compared to an investment in the index itself.

To this end, we rely on established stochastic models for the ETF, such as geometric Brownian motion, using historical data to estimate key parameters like drift and volatility. Based on these parameters, we apply our theoretical framework to compute the implied optimal leverage ratio  $\beta^*$ , then simulate the wealth evolution of an investor who followed this strategy. The resulting performance is benchmarked against that of the unleveraged standard ETF investment, with comparisons in terms of several component such as return, value at risk (VaR) and maximum drawdown.

This empirical comparison provides a valuable validation of the model's practical relevance and reveals how sensitive the optimal strategy is to estimation uncertainty. In doing so, we illustrate both the benefits and limitations of model-based leverage optimization in real financial markets.

While the theoretical results developed in this thesis are asymptotic in nature, focusing on the long-run limit  $T \rightarrow \infty$ , it is of practical interest to assess how these optimal strategies perform over finite investment horizons. In this chapter, we investigate whether the leverage policies derived from long-run utility maximization remain relevant when applied over realistic time frames, such as 20 years. Although the asymptotic framework is not designed to predict short-term outcomes, prior research suggests that long-run optimal strategies can still offer valuable guidance even on moderately long horizons, see Guasoni

and Robertson [67]. By comparing the performance of these strategies to an actual standard ETF performance, we aim to evaluate the practical implications of our theoretical results and test their robustness outside of the limit case.

In order to make the analysis more transparent, we consider here an idealized environment, where the investor can maintain the desired leverage ratio perfectly at all times. In this frictionless setting, we assume that there are no tracking errors, no transaction frictions, and no fluctuations arising from the mechanics of the OTC contract used to implement leverage. The resulting dynamics therefore represent a best-case benchmark, while still abstracting from several complexities present in actual financial markets.

The assumption of perfect tracking is, of course, an abstraction. Leveraged exchange-traded products and OTC total-return swaps typically exhibit deviations from their theoretical targets due to discrete rebalancing, volatility decay, funding spreads, and other microstructural effects. However, Avellaneda and Zhang [28] demonstrate that for daily rebalancing frequencies the resulting tracking errors are extremely small over short horizons. In particular, their analysis shows that the deviation between the realised leveraged return and the continuously rebalanced theoretical benchmark remains minimal over one-day periods, thereby justifying the use of a continuous-time model as an analytically tractable approximation.

By focusing on this frictionless framework, we isolate the intrinsic behaviour of the optimal leverage rule itself, unperturbed by implementation effects. This analysis serves two purposes. First, it provides a theoretical upper bound on achievable performance, as in the absence of frictions and tracking discrepancies the optimal policy derived in earlier chapters can be executed exactly. Second, it offers a clean baseline against which the impact of market imperfections, such as rebalancing noise, can be quantitatively assessed in subsequent robustness studies.

Lastly, to ensure comparability across different market environments, we adopt a consistent set of model parameters throughout the empirical analysis. This choice allows any observed differences in outcomes to be attributed solely to the realized market dynamics rather than to changes in the underlying assumptions. In practical applications, investors would typically recalibrate parameters such as drift, volatility, and interest rates to reflect current market conditions. However, for broad equity indices like the S&P 500, these quantities can be regarded as relatively stable long-term characteristics that are not fundamentally altered by temporary market fluctuations. While crises or speculative bubbles may cause short-lived deviations, such effects tend to average out over extended horizons. Using constant parameters therefore provides a transparent and theoretically sound foundation for the subsequent comparison of leverage strategies across time.

## 9.1 S&P 500 modeled by a geometric Brownian motion

We elaborated in the previous chapter already the parameters for the S&P 500 index. We recall that it is standard in literature that one assumes a GBM model for the S&P 500 with drift parameter  $\mu = 0.8$  and diffusion parameter  $\sigma = 0.2$ . Hence, we set  $[\underline{\mu}, \bar{\mu}] = [0.06, 0.1]$ ,  $[\underline{\sigma}, \bar{\sigma}] = [0.15, 0.25]$  and  $r = 0.02$ . We showed already that the worst and mid case optimal leverage ratios are

$$\beta^{worst} = 1.28 \quad \text{and} \quad \beta^{mid} = 3.$$

### 9.1. S&P 500 modeled by a geometric Brownian motion

With those information at hand we begin our simulations. First we start by comparing the paths of different leverage strategies. We plot the paths for the leverages 1, 2, 3, 4 and 5. As a starting point we first consider the year 2005, which represents a rather usual time period with no significant events. In 2005 major equity markets generally continued their upward trend while volatility remained low, supporting the use of this year as a baseline for simulation comparisons, c.f. OECD [68].

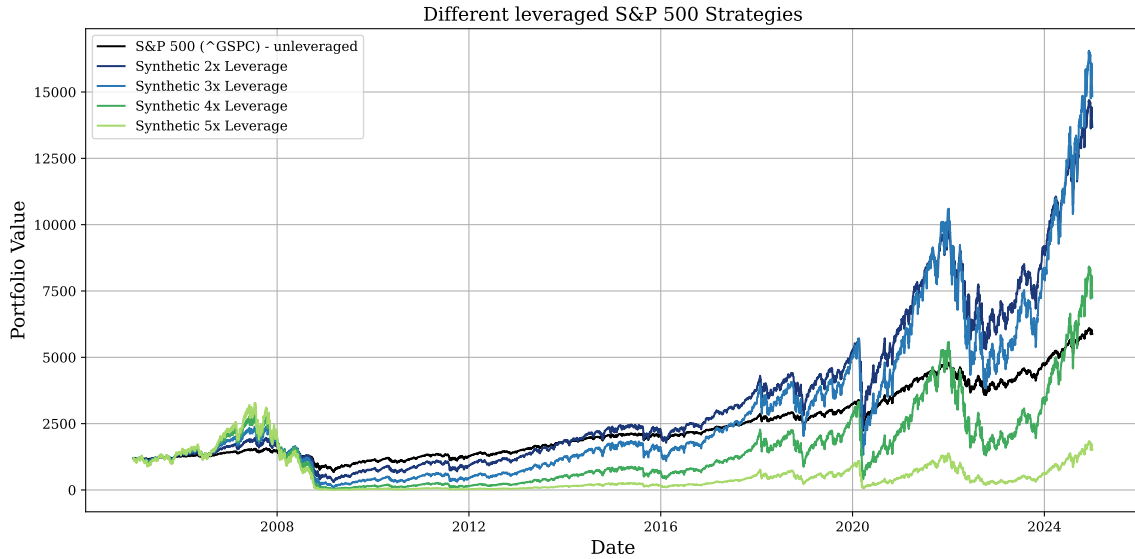


Figure 9.1: Comparison between different leverage ratios.

Next, we consider the paths for the unleveraged index as well as for the worst and mid case optimal leverage ratios.

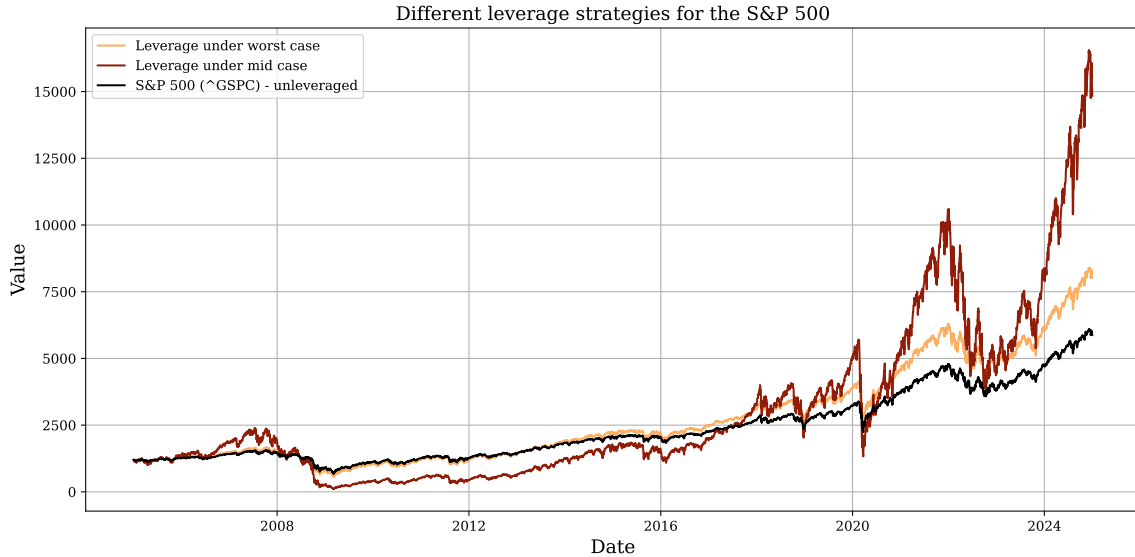
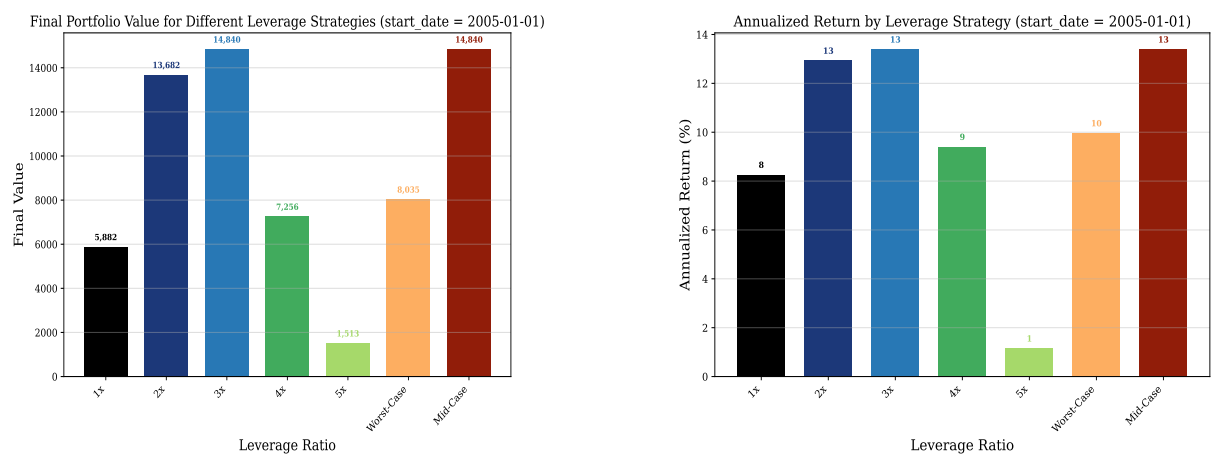


Figure 9.2: Comparison between worst-case leverage and mid-case leverage ratios.

Here, we have a first confirmation of our theory. We see that during a stressful period the

worst case assumption yields a much better curve than the mid case assumption. Also the worst-case leverage ratio is mostly above the index, which indicates a better investment than the unleveraged ETF. Next, we also see that after a longer horizon and a more stable increase of the market we see that the mid-case again outperforms both the worst and the 1x leverage ratios. This difference becomes increasingly larger the longer a direction of the market remains. Hence in the end the difference is rather big between the different leverages for the illustrated time period.

The returns, as of 01.01.2025, of different investments are illustrated in Figure 9.3, where we investigate only the final portfolio value and percentage return at terminal time for different leverage ratios under the assumption that we invested the amount of the index at the initial time in the asset.



(a) Final portfolio values for (L)ETF starting on 01.01.2005

(b) Percentage return for (L)ETF starting on 01.01.2005

Figure 9.3: Comparison of final portfolio values and percentage returns for (L)ETFs starting on 01.01.2005.

This underlines the outcomes stated before. We see that the return of the mid case is higher than of the worst case, while keeping in mind that during disadvantageous market times this could also be reversed, as we will see later again in Section 9.2. We also see here more clearly that a leverage of 5x would have had very low return, which represents the volatility drag. During the financial crisis in 2008 the value of these LETFs would have been so low that recovery is even through a much longer positive period taking a lot of time. Hence this portfolio would still be less than in the beginning 20 years later.

Next we compare different leverage ratios across different starting points, highlighting the importance of the starting point by considering the percentage return.

### 9.1. S&P 500 modeled by a geometric Brownian motion

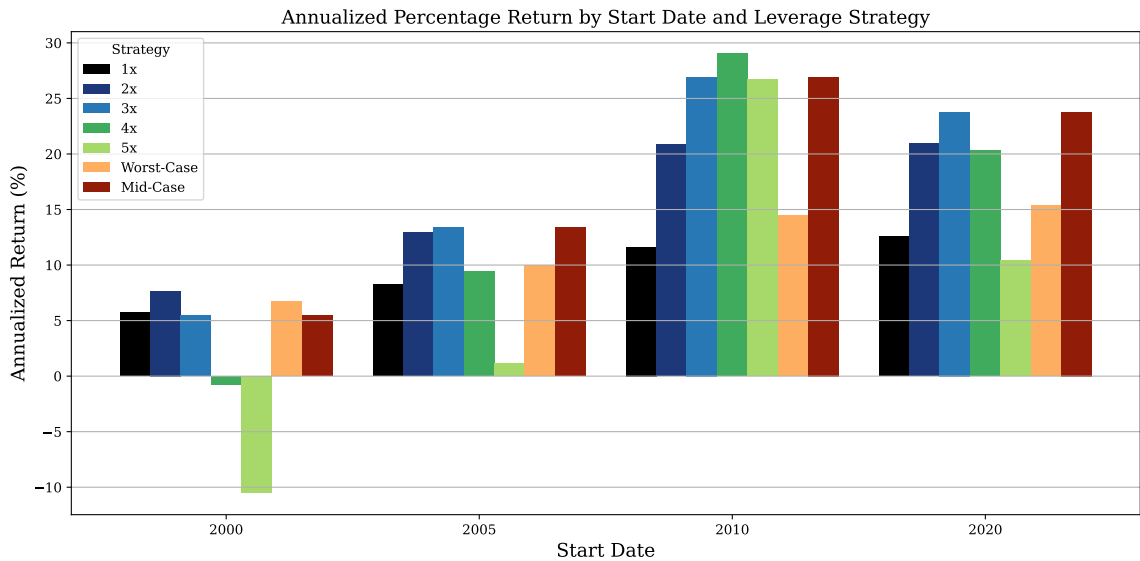


Figure 9.4: Percentage return for (L)ETF for different starting dates.

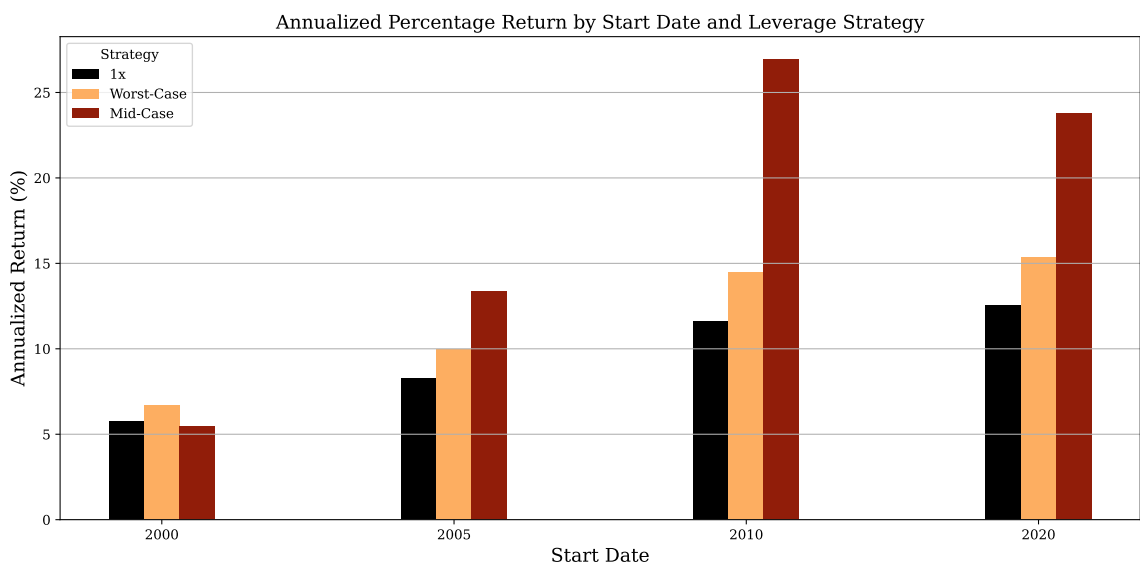


Figure 9.5: Final portfolio value for different starting dates.

Furthermore, we illustrate the paths of the LETFs. We start now first in year 2000.

## Chapter 9. Empirical validation

---

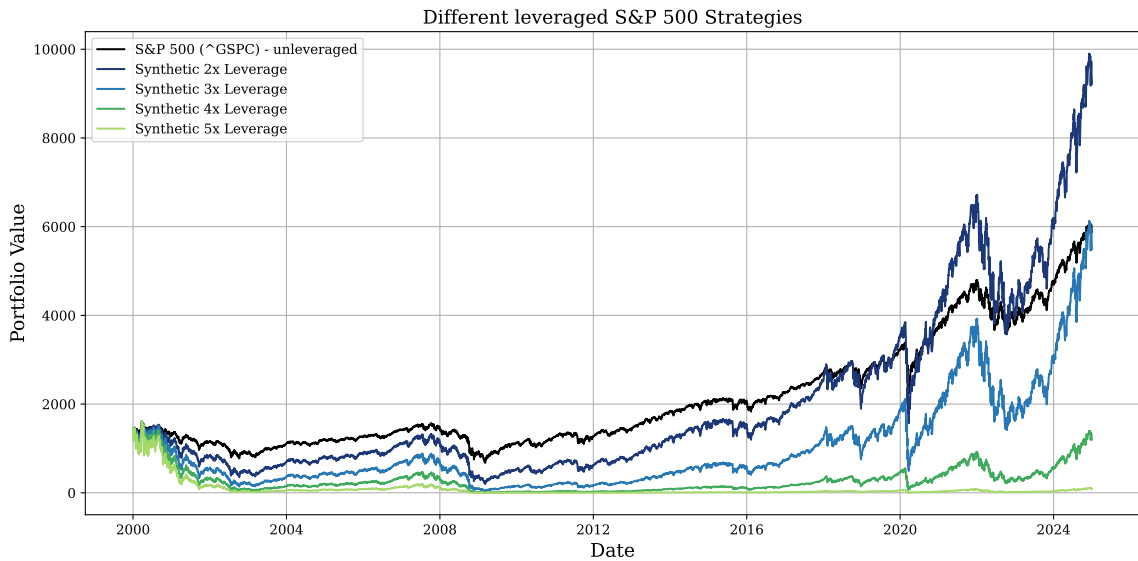


Figure 9.6: Performance of different leverage ratios starting on 01.01.2000.

Next, we consider 2010 as starting point. While the year 2005 served as a representative pre-crisis baseline characterized by relatively stable market conditions and low volatility, the year 2010 provides a contrasting environment marked by the aftermath of the global financial crisis. By starting the analysis in 2010, we capture a period of heightened market uncertainty, increased volatility, and shifting macroeconomic conditions, which together offer a valuable test of the robustness of the optimal leverage strategies. Comparing both starting points therefore allows us to evaluate how the derived policies perform across fundamentally different market regimes.

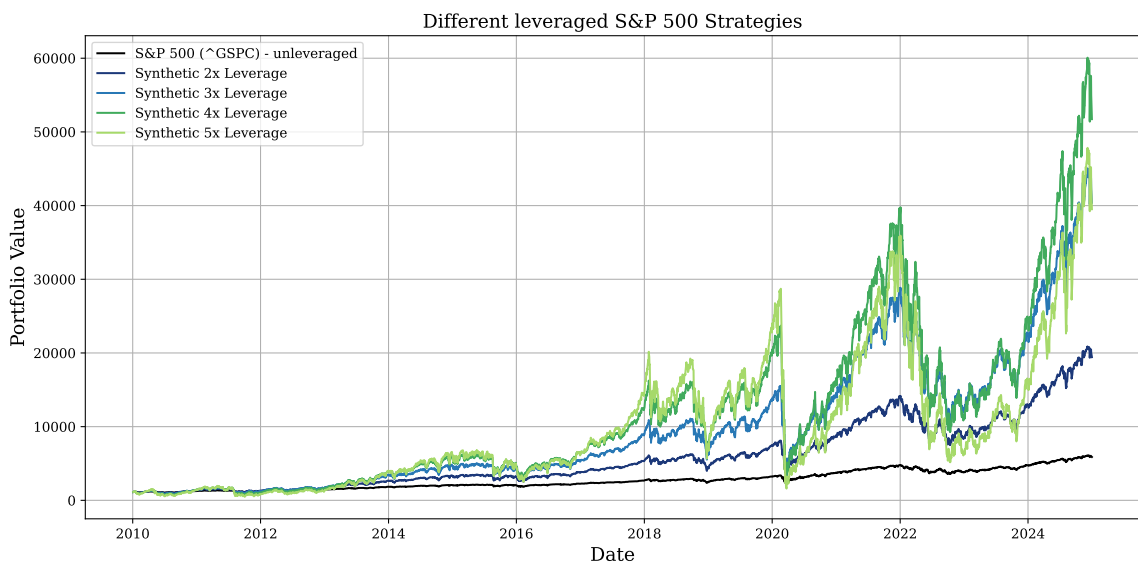


Figure 9.7: Performance of different leverage ratios starting on 01.01.2010.

Next, we consider the performance of different leverage ratios starting on 01.01.2015, comparing their realized portfolio values over time. The starting date 01.01.2015 falls

### 9.1. S&P 500 modeled by a geometric Brownian motion

into a predominantly calm equity market environment, characterized by low volatility and steadily rising equity prices.

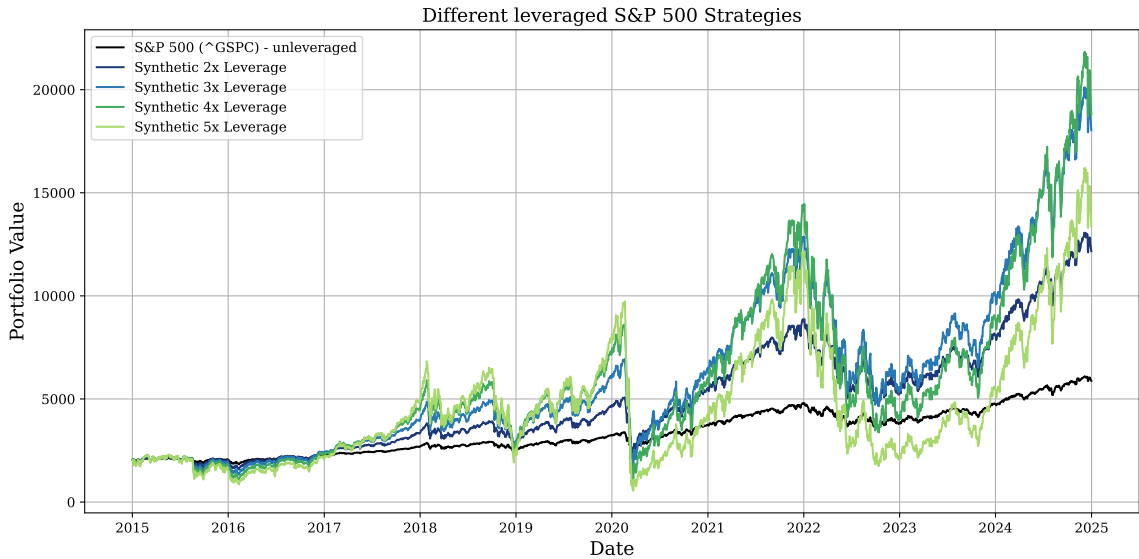


Figure 9.8: Performance of different leverage ratios starting on 01.01.2015.

Lastly, we consider a short investment horizon starting in 2020, in the midst of the COVID-19 crisis. Despite the severe initial market shock, all portfolios achieve positive returns over the considered period. This outcome can be attributed to the sharp but short-lived nature of the downturn. Equity markets experienced a rapid recovery following the monetary and fiscal interventions introduced shortly after the initial collapse. As a result, the strong rebound in the latter part of 2020 and subsequent quarters outweighed the early losses, leading to overall positive cumulative performance even for highly leveraged portfolios.

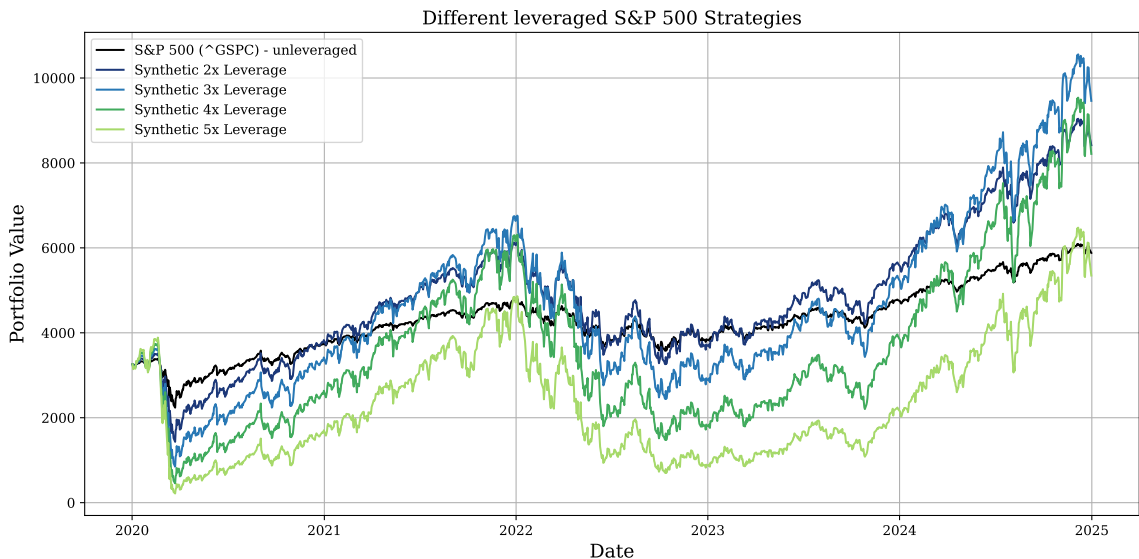


Figure 9.9: Performance of different leverage ratios starting on 01.01.2020.

In the next figure the paths of these different starting points are compared more visibly, allowing the reader to better capture each path visually.

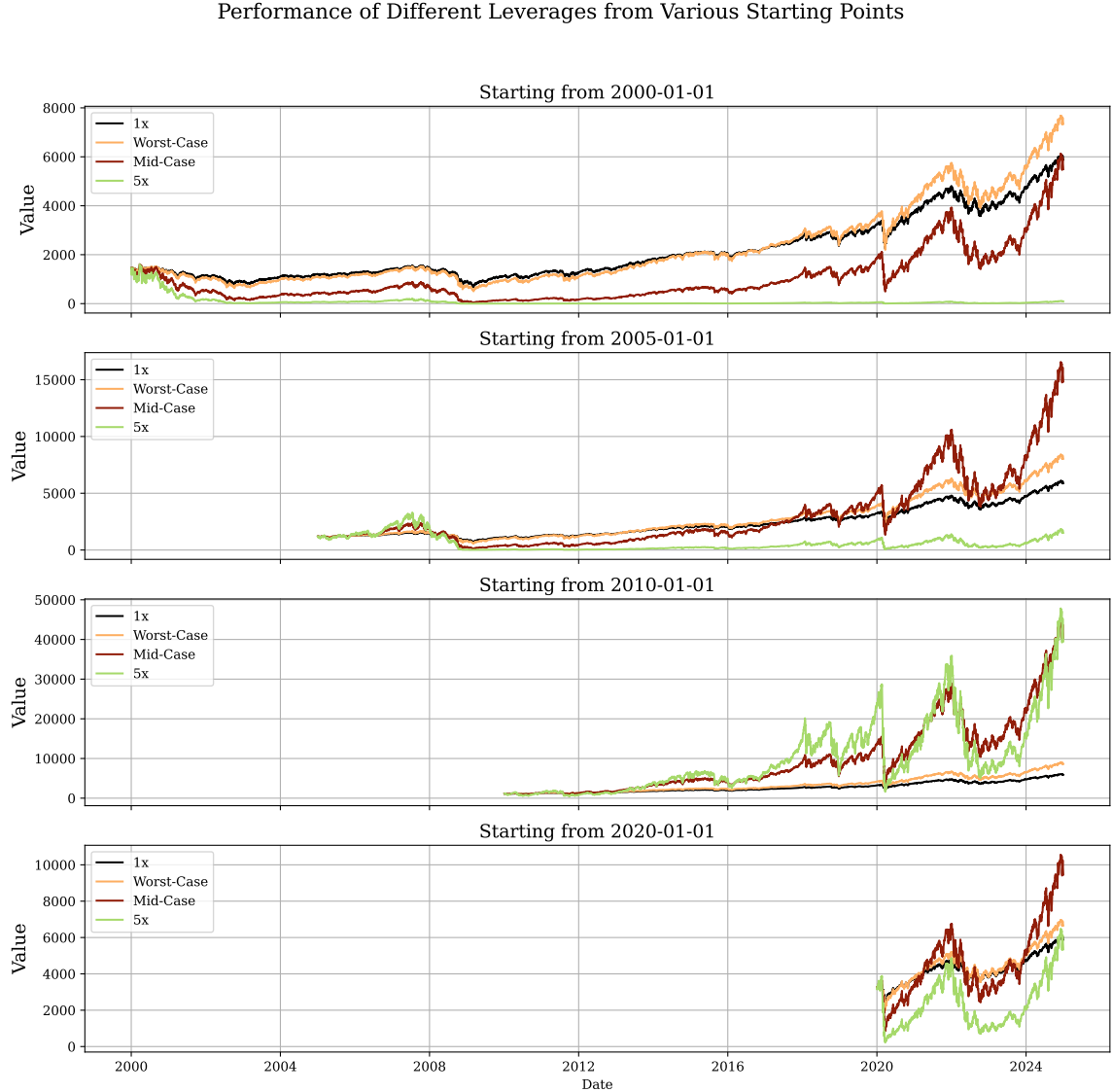


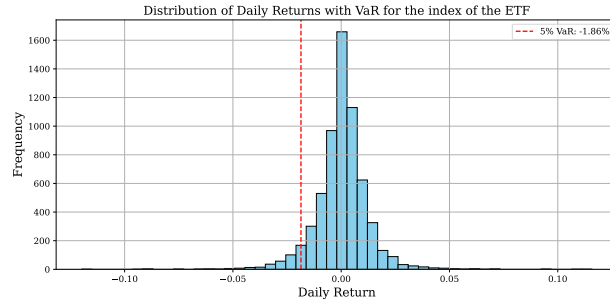
Figure 9.10: Performance of different leverage ratios for different starting dates.

In summary, our empirical analysis reveals several noteworthy patterns. First, across the majority of historical periods considered, the mid-case leverage strategy consistently outperformed the worst-case leverage strategy. However, during episodes of pronounced market stress or extreme events, the performance ranking may reverse. In such circumstances, substantial divergence between the strategies can arise, and the worst-case leverage portfolio can outperform both the mid-case strategy and even higher leveraged portfolios. This highlights the practical relevance of robustness when markets deviate sharply from typical conditions and support our idea of worst-case parameters and robustness. Moreover, we observed that, for most sample periods, both the worst-case and the mid-case leverage strategies achieved higher returns than the unleveraged benchmark

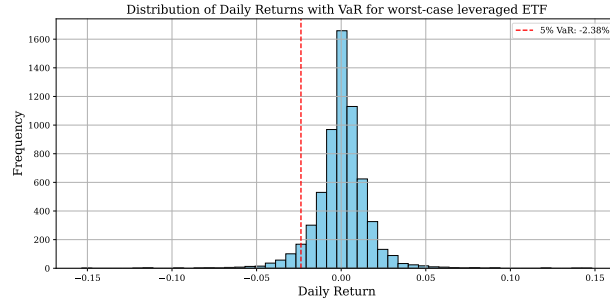
### 9.1. S&P 500 modeled by a geometric Brownian motion

index. This empirical finding lends further support to and provides validation for the theoretical framework developed throughout the thesis, demonstrating that robustly derived leverage rules can yield meaningful improvements in portfolio performance.

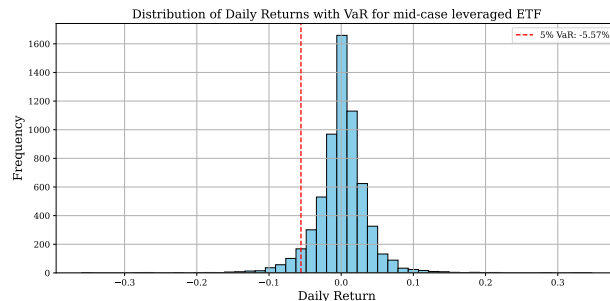
Next, we examine the risk profiles associated with the different leverage strategies. As a first step, we compute the Value-at-Risk (VaR) corresponding to each leverage ratio. In combination with the empirical distribution of daily returns, these results are presented in the following figures, providing a comparative assessment of risk across the portfolio strategies.



(a) Distribution of daily returns with VaR for the index of the ETF



(b) Distribution of daily returns with VaR for worst-case leveraged ETF



(c) Distribution of daily returns with VaR for mid-case leveraged ETF

Figure 9.11: Comparison of daily return distributions with VaR across index, mid-case leverage and worst-case leverage.

Additionally, Figure 9.12 presents an overlaid view of the daily return distributions shown

above, allowing for a direct comparison across leverage strategies.

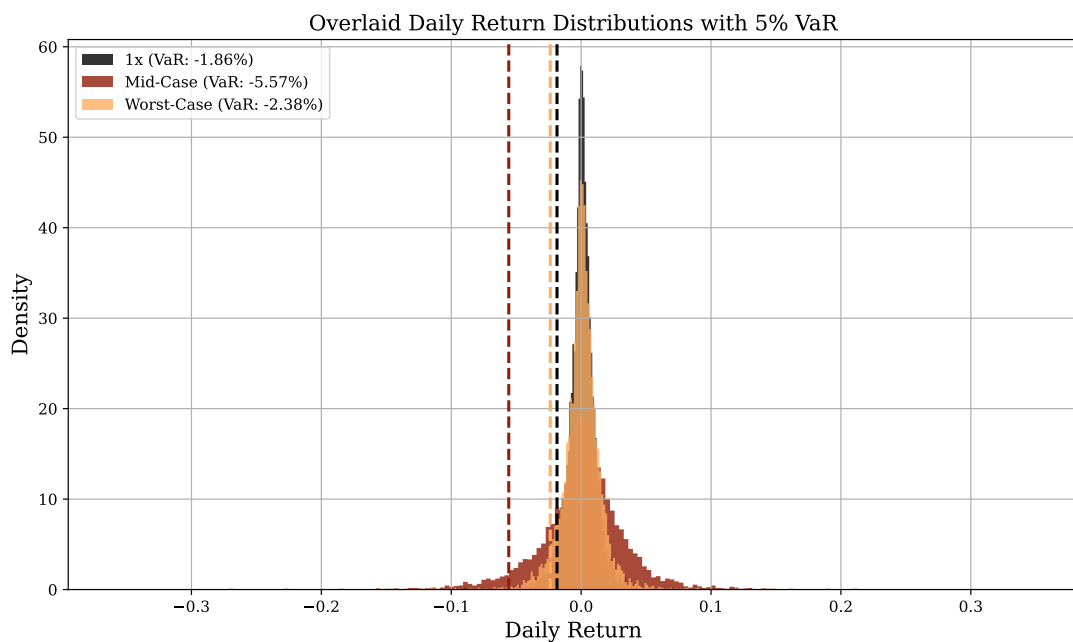
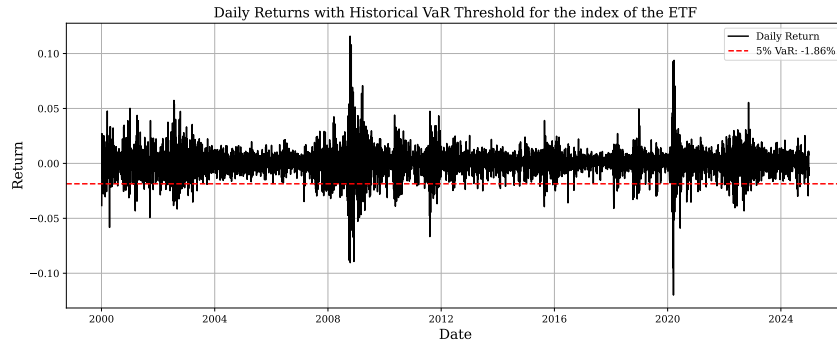


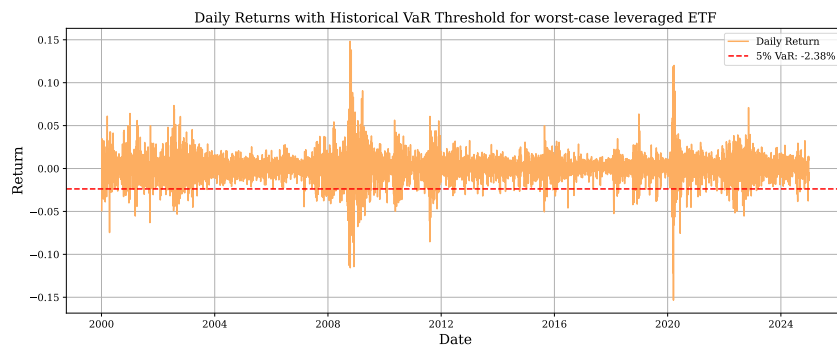
Figure 9.12: Daily return distributions.

Next, we analyze the daily returns of the different portfolios. Together with the specific VaR we plot the figures:

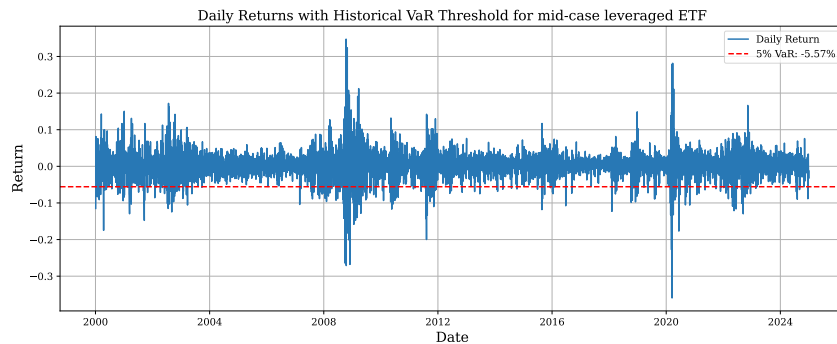
### 9.1. S&P 500 modeled by a geometric Brownian motion



(a) Daily returns with historical VaR threshold for the index of the ETF



(b) Daily returns with historical VaR threshold for worst-case leveraged ETF



(c) Daily returns with historical VaR threshold for mid-case leveraged ETF

Figure 9.13: Comparison of daily returns with historical VaR thresholds for index, mid-case leverage, and worst-case leverage

Figure 9.13 displays the daily return series for the three portfolios, the unleveraged index, the mid-case leverage, and the worst-case leverage, together with their respective historical 5% Value-at-Risk (VaR) thresholds. We see that the VaR is ordered by the value of the leverage as well as the return amplitude. Together, these subfigures provide a comparative view of how leverage affects the of tail losses when measured through the historical VaR metric.

In the subsequent figure, the frequency and clustering of VaR exceedances become even more apparent. Days on which the VaR threshold is breached tend to occur in contiguous blocks rather than in isolation. This pattern indicates that such “outlier” returns are typically associated with broader market episodes, often multi-month stress periods or crises, rather than brief, single-day events, which makes them especially relevant for higher leveraged portfolios because of the volatility decay.

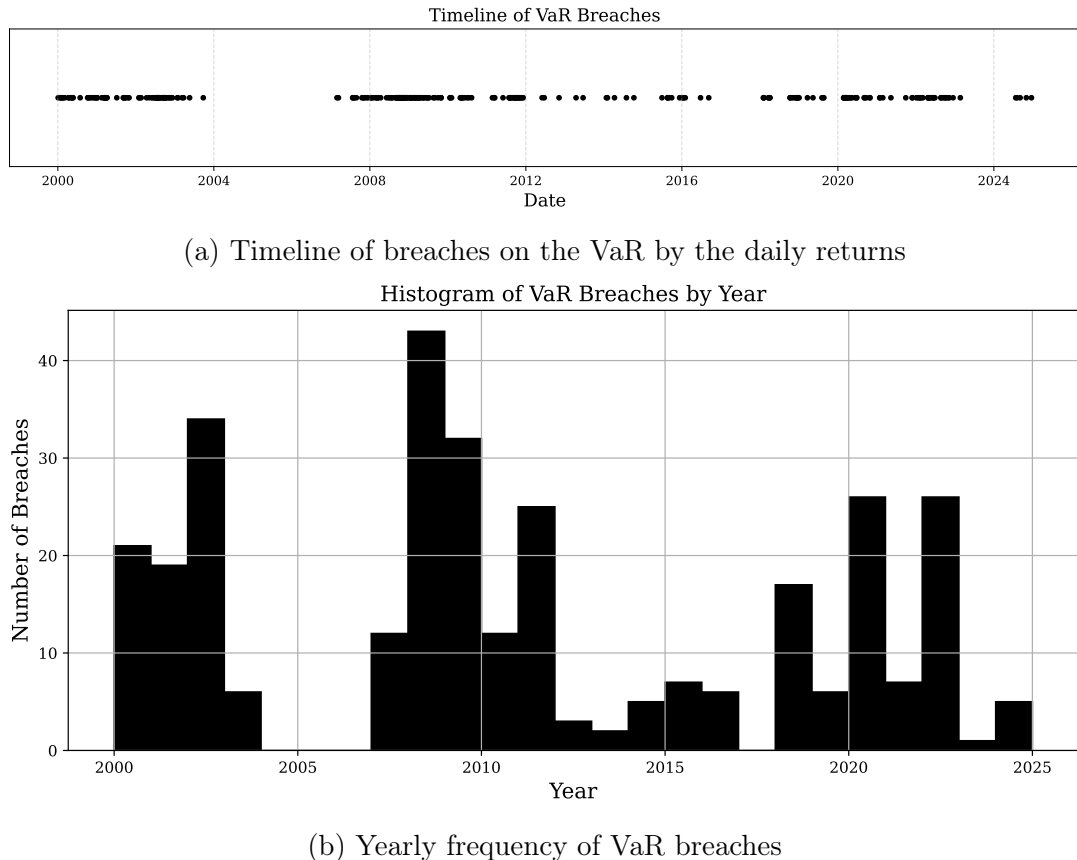


Figure 9.14: Comparison of daily returns with historical VaR thresholds for index, mid-case leverage and worst-case leverage

Further, we consolidate and report several key risk and performance metrics, including the average annual return, maximum drawdown, daily VaR, and Sharpe ratio, for the different leverage levels. In the following we defined the maximum drawdown as the largest percentage decline from the peak in the portfolio value. It captures how severe the worst loss over a given period would have been if an investor had bought at a local maximum and sold at the subsequent minimum. We compute the maximum drawdown for each calendar year and also take the average across years. Value at Risk (VaR) is calculated using historical daily returns. For a given confidence level, it represents the loss threshold that is exceeded only in a small fraction of days. It therefore summarizes the downside risk in the left tail of the return distribution. The Sharpe ratio measures risk-adjusted performance. It is computed as the average excess return relative to a constant risk-free rate divided by the volatility of returns, and then annualized using 252 trading

## 9.2. Stress testing different leverage strategies

days per year.

Leverage	Avg Annual Return 2000–2025	Max Drawdown	Daily VaR (5%)	Sharpe
1x	5.75%	-9.46%	-1.86%	0.28
Worst	6.69%	-11.76%	-2.38%	0.31
2x	7.67%	-17.03%	-3.71%	0.33
3x	5.46%	-26.03%	-5.57%	0.35
4x	-0.76%	-33.31%	-7.43%	0.36
5x	-10.50%	-37.71%	-9.29%	0.37

Table 9.1: Risk and return metrics for different leverage strategies.

This information is also integrated into following plot:

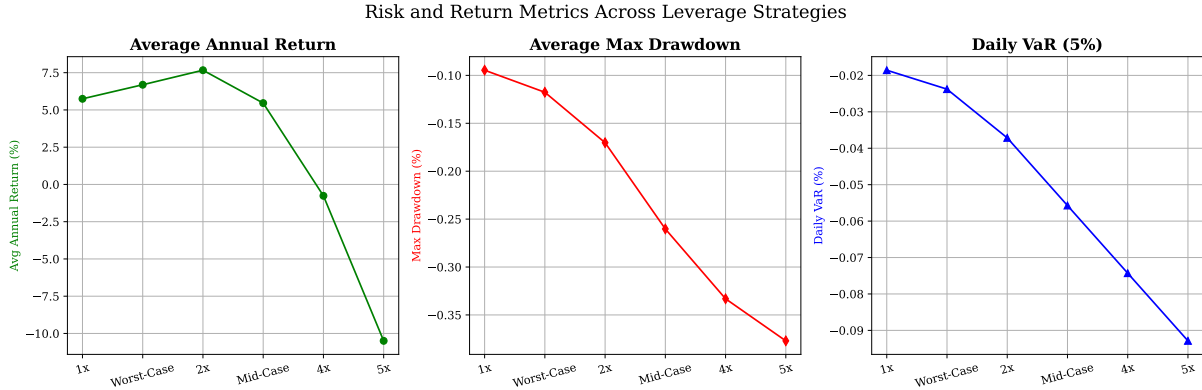


Figure 9.15: Risk and return metrics for different leverage strategies as plots.

Figure 9.15 visualizes how average annual return, average maximum drawdown and daily Value-at-Risk (VaR) evolve as leverage increases. Lower leverage levels exhibit moderate returns combined with comparatively small drawdowns and limited VaR exposure. As leverage rises, both average return decreases after a leverage of 2x but still the downside risk increase sharply, with highly leveraged portfolios experiencing substantial drawdowns and significantly more negative VaR values. The figure therefore illustrates how excessive leverage leads to rapidly deteriorating performance metrics despite an initially rising return profile.

## 9.2 Stress testing different leverage strategies

Next, we examine a concrete stress scenario from recent years: the COVID-19 pandemic. To contextualize the market environment, it is useful to recall several key dates. The first officially registered infection was reported on 01.12.2019, and by January 2020 cases had begun to appear across multiple countries, including Germany. In early February, financial markets still continued their upward trend, but on 11.03.2020 COVID-19 was declared a global pandemic, triggering a rapid and severe market collapse.

With this timeline in mind, we analyze the performance of the different portfolios and LETFs under the assumption of an investor entering the market shortly before the crash, unaware of the impending downturn. Specifically, we consider an investment made on 2020-01-15 and evaluate the portfolio evolution over a stress horizon of approximately two and a half years, ending on 2022-07-15.

We follow similar step as we did in the general case of the longer horizon without a specific event. First we look at the price paths of different leverage ratio investments and the corresponding final value and return of these investments.

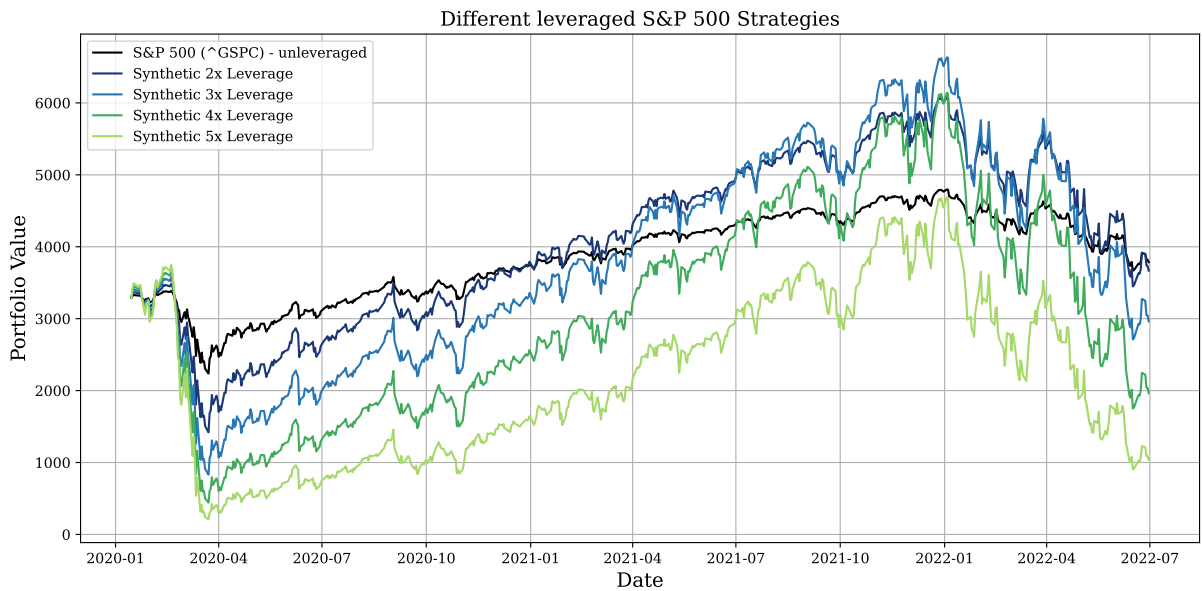
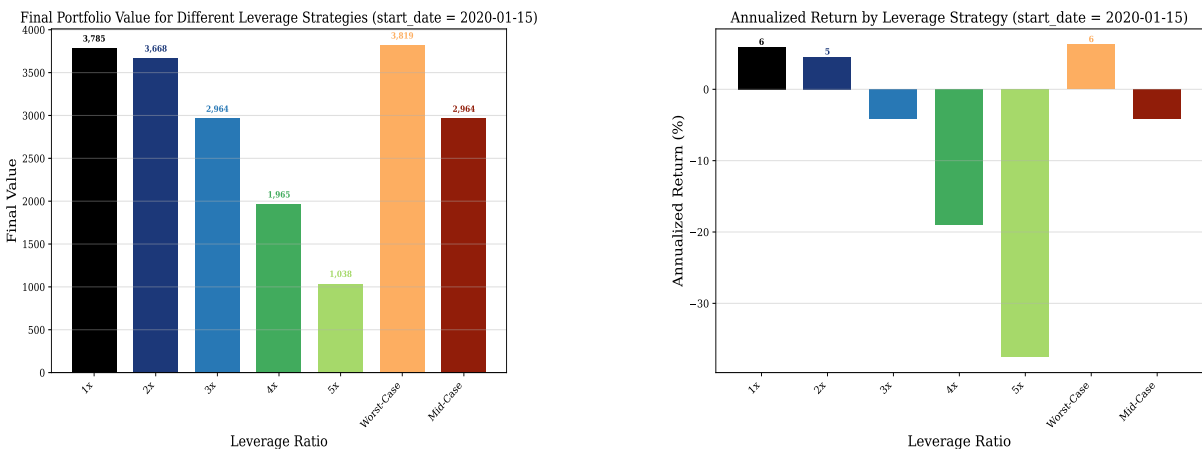


Figure 9.16: Performance of different leverage ratios starting on 15.01.2020.



(a) Final portfolio values for (L)ETF starting on 15.01.2020

(b) Percentage return for (L)ETF starting on 15.01.2020

Figure 9.17: Comparison of final portfolio values and percentage returns for (L)ETFs starting on 15.01.2020.

## 9.2. Stress testing different leverage strategies

---

Figure 9.16 compares the portfolio paths of the different leverage strategies, illustrating how varying leverage ratios affect wealth at different points in time. Figure 9.17 complements the previous figure by reporting the corresponding percentage returns for the same leverage strategies, allowing for a direct assessment of performance in return terms. Relative to the general case results presented earlier, these stress scenario figures exhibit a similar ordering across leverage strategies, with moderate leverage levels generally outperforming both unleveraged and highly leveraged positions. However, in the present setting the dispersion in outcomes is more pronounced, and higher leverage leads to substantially larger losses, reflecting the increased impact of adverse market conditions compared to the general case. Since we consider a concrete stress scenario here, note that now the worst case leveraged portfolio outperforms the mid-case leveraged portfolio.

Next we look at different investment times into the market. The first one as already discussed is the 2020-01-15 before the crash. The next one is "2020-07-15", "2021-01-15" and "2021-07-15" with an horizon until "2023-07-15".

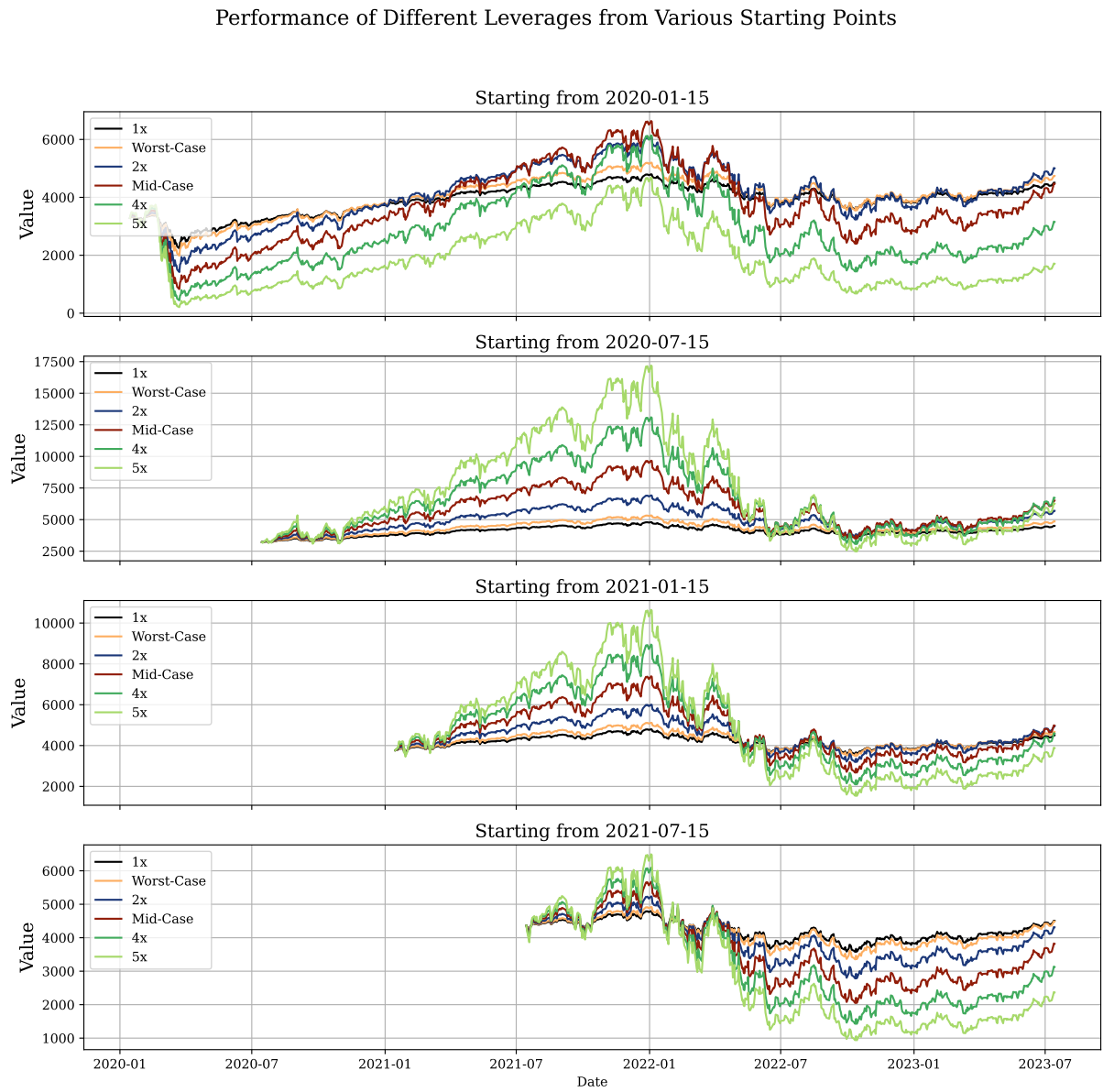


Figure 9.18: Performance of different leverage ratios starting on several times during the crisis.

## 9.2. Stress testing different leverage strategies

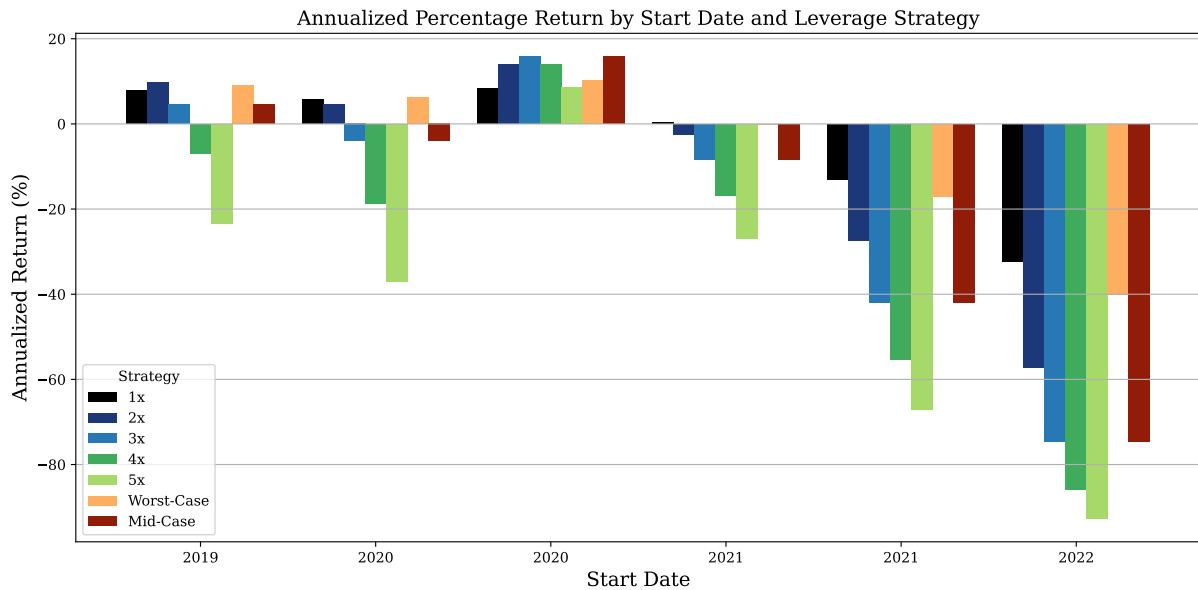


Figure 9.19: Performance of different leverage ratios starting on several times during the crisis.

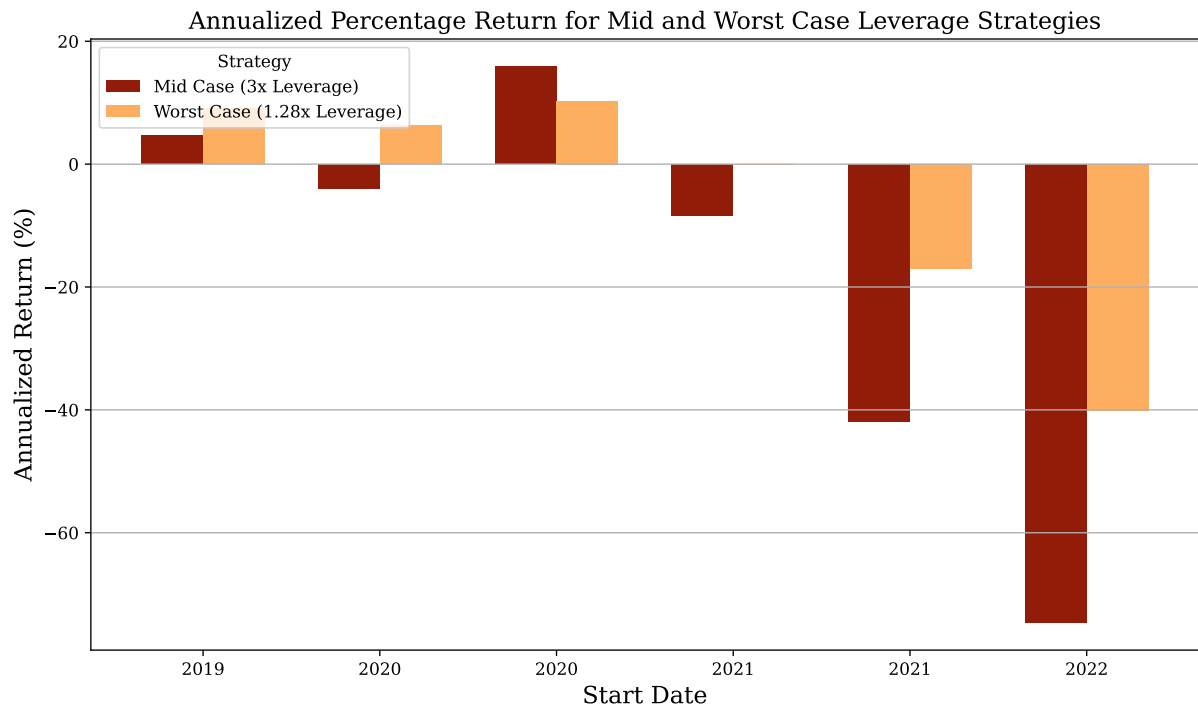


Figure 9.20: Performance of different leverage ratios starting on several times during the crisis.

Figure 9.19 and Figure 9.20 present the annualized percentage returns of different leverage strategies for different investment start dates. The figure illustrates how realized performance varies across market entry points, highlighting the sensitivity of leveraged

strategies to timing effects. Relative to the general-case results, a similar pattern emerges, with the mid-case strategy generally achieving higher returns than the worst-case strategy. However, the dispersion across start dates is more pronounced in the present scenario, and negative outcomes are more severe, particularly for later entry periods.

Additionally we also have a look at risk metrics during this period. We consider again the VaR during the period "2020-01-15" until "2022-07-15" and discuss the impact the leverage has here.

## 9.2. Stress testing different leverage strategies

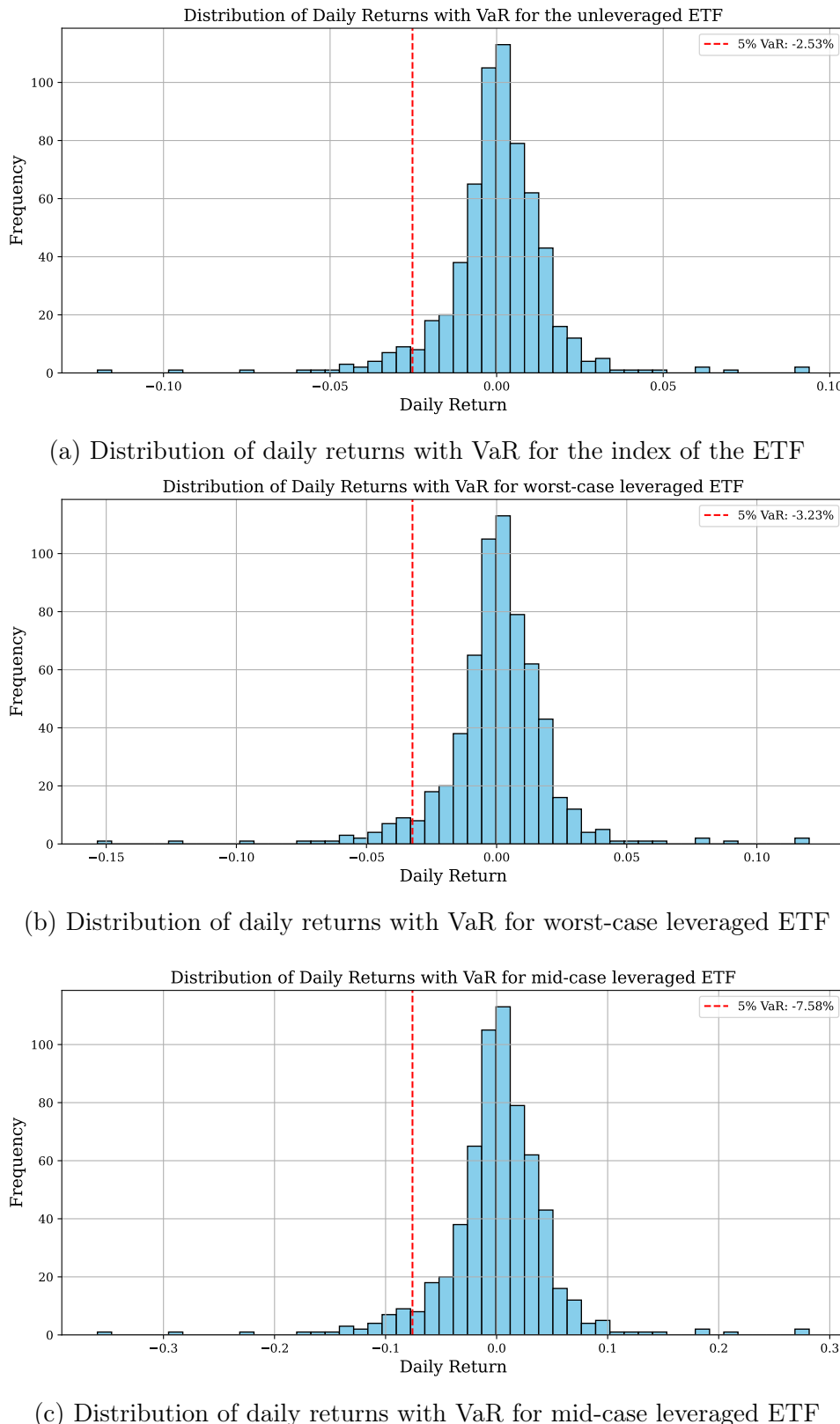


Figure 9.21: Comparison of daily return distributions with VaR across index, mid-case leverage and worst-case leverage.

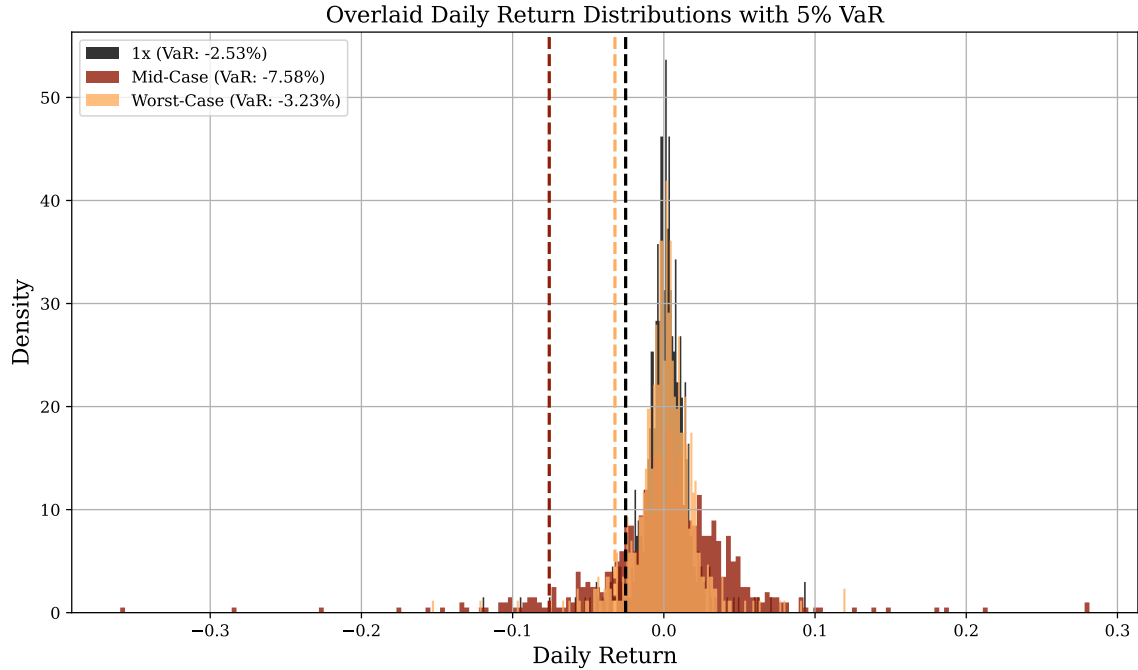


Figure 9.22: Daily return distributions.

Figure 9.22 exhibits a distributional structure that is broadly consistent with the general-case results presented earlier. In both settings, higher leverage leads to wider return distributions and heavier tails, reflecting increased downside risk. However, in the present scenario the distributions display more pronounced tail behavior and a leftward shift of the Value-at-Risk thresholds, indicating more severe adverse outcomes compared to the general case.

Next, Figure 9.23 displays the daily return series for the three portfolios under the stress period similar to the general scenario of Section 9.1. We see again that the VaR is ordered by the value of the leverage as well as the return amplitude. Together, these subfigures provide a comparative view of how leverage affects the of tail losses when measured through the historical VaR metric.

## 9.2. Stress testing different leverage strategies

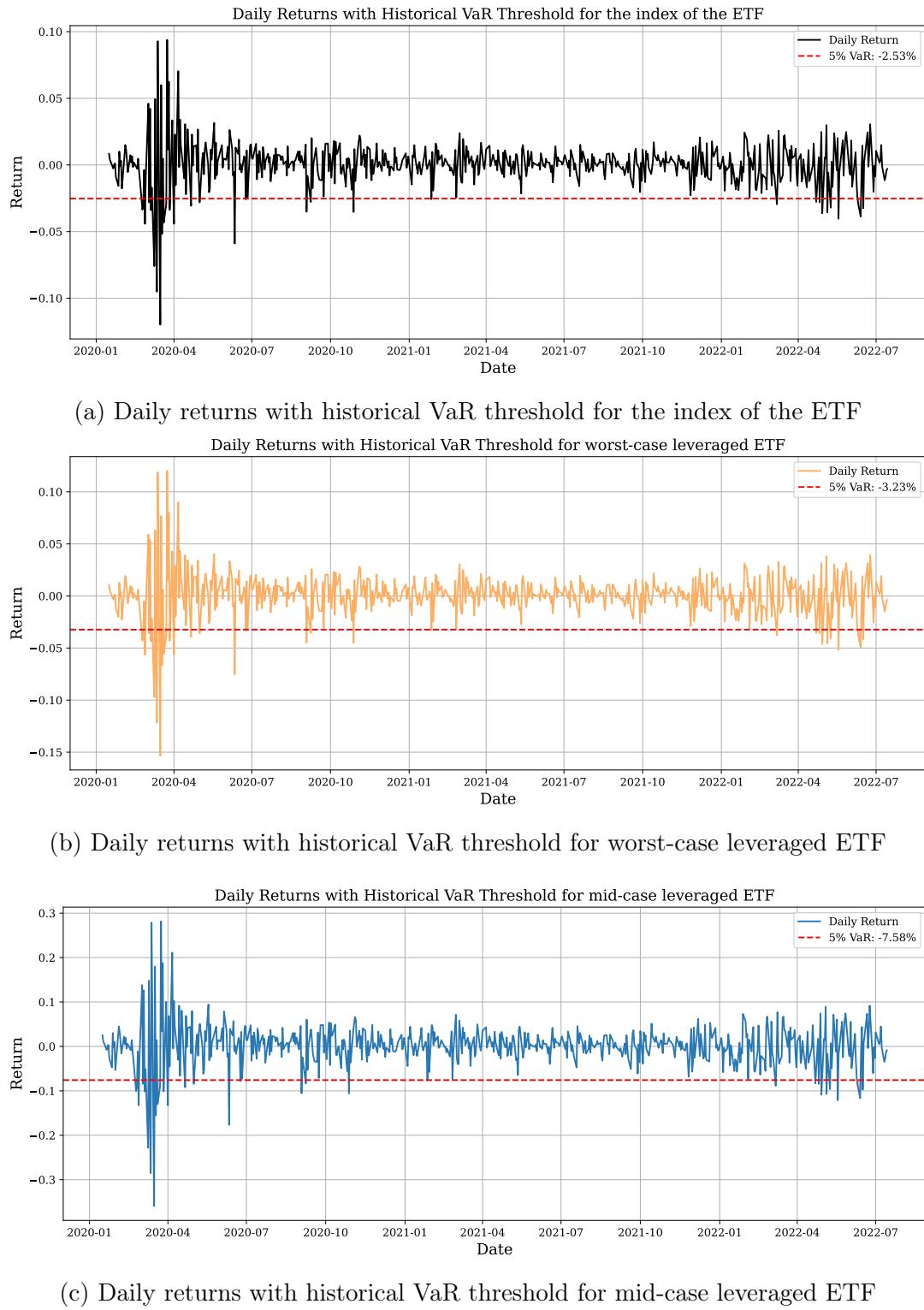


Figure 9.23: Comparison of daily returns with historical VaR thresholds for index, mid-case leverage and worst-case leverage.

In the subsequent figure, we again consider the frequency and clustering of VaR ex-

ceedances. As before we observe, that days on which the VaR threshold is breached tend to occur in contiguous blocks rather than in isolation, which makes them especially relevant for higher leveraged portfolios because of the volatility decay.

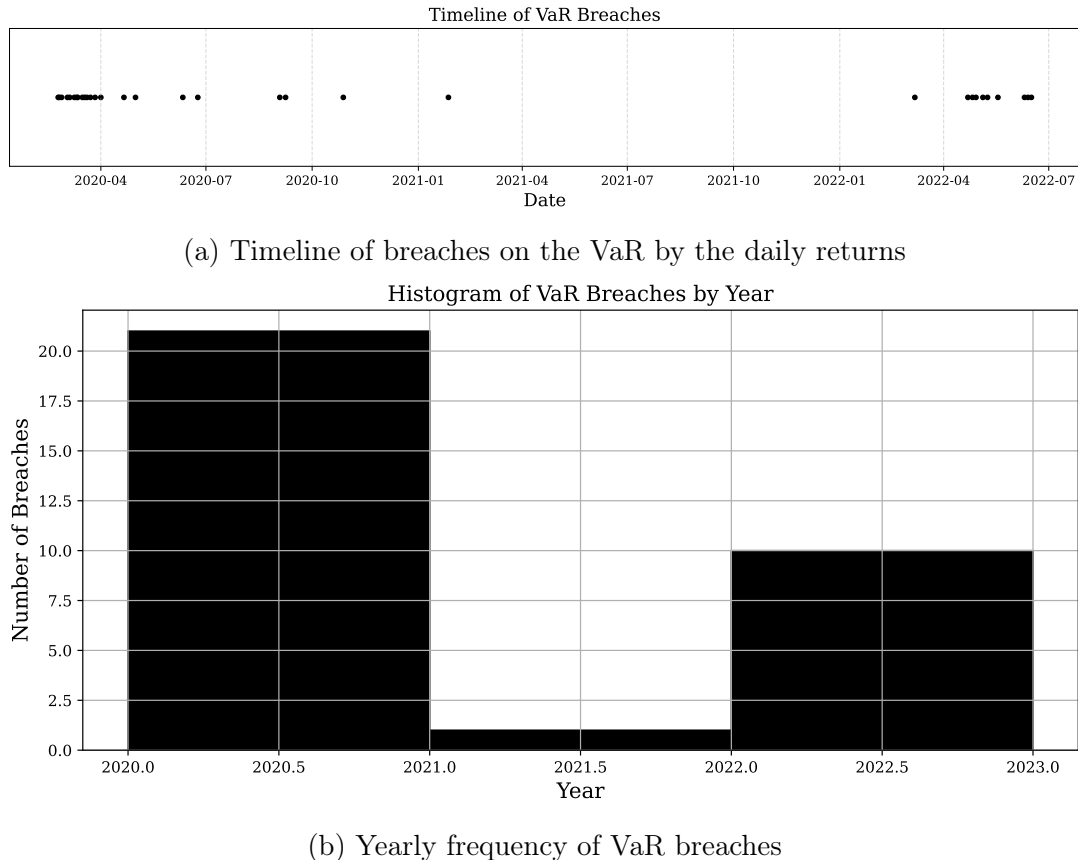


Figure 9.24: Comparison of daily returns with historical VaR thresholds for index, mid-case leverage and worst-case leverage.

Summarizing we then again consider at the following figure and table:

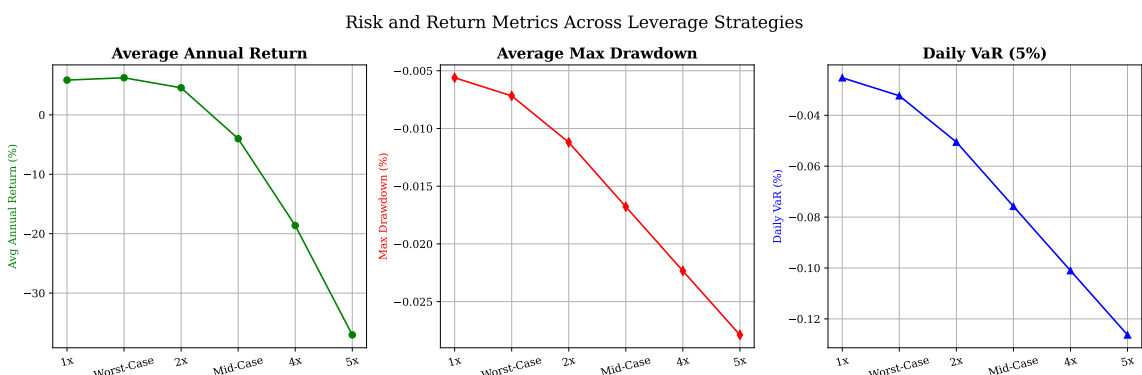


Figure 9.25: Risk and return metrics for different leverage strategies.

## 9.2. Stress testing different leverage strategies

---

Leverage	Avg Annual Return 2000–2025	Max Drawdown	Daily VaR (5%)	Sharpe
1x	5.86%	-0.56%	-2.53%	0.27
Worst	6.24%	-0.72%	-3.23%	0.29
2x	4.56%	-1.12%	-5.05%	0.31
3x	-4.01%	-1.68%	-7.58%	0.32
4x	-18.63%	-2.23%	-10.10%	0.33
5x	-37.04%	-2.79%	-12.63%	0.33

Table 9.2: Risk and return metrics for different leverage strategies.

A similar structure to the general case is observed in the preceding Figure 9.25 and Table 9.2 for the stress scenario, whilst with even more pronounced effects. This align with the intuition of a stress scenario and our theory.

Additionally we look at another metric, namely the recovery durations for the different portfolios. With recovery durations we mean the time between the peak before the crisis and the time where the portfolio the again is at the same level.

Leverage	Peak Date	Peak Price	Recovery Date	Trading Days
1x	2020-02-19	3386.15	2020-08-18	126
1.28x	2020-02-19	3412.90	2020-08-25	131
2x	2020-02-19	3480.87	2020-09-02	137
3x	2020-02-19	3573.09	2021-01-20	232
4x	2020-02-19	3662.44	2021-04-15	291
5x	2020-02-19	3748.54	2021-08-30	386

Table 9.3: Peak values and recovery durations for leveraged S&P500 strategies during the 2020 Covid-19 crash.

Table 9.3 reports the recovery durations of the different leverage strategies following drawdown events. For each strategy, the table records the time required to return to the previous peak level after a loss, thereby quantifying the persistence of drawdowns. The comparison shows how higher leverage is associated with longer recovery periods, particularly under adverse market conditions, highlighting the increased path dependency and risk of prolonged underperformance.

In this chapter, we have empirically validated the theoretical findings developed throughout the thesis. By applying the derived optimal and robust leverage ratios to historical market data, we assessed the practical relevance of our long-run optimization framework. Using the S&P 500 as a benchmark, modeled as a geometric Brownian motion, we compared the theoretical performance of leveraged portfolios with the realized performance of corresponding leveraged ETFs.

The empirical results confirm the central theoretical insight, that while leverage can amplify long-term returns under favorable conditions, parameter uncertainty and volatility effects play a decisive role in determining sustainable performance. The robust optimal leverage ratios derived in our framework consistently exhibit greater stability across

varying market environments compared to their mid-case counterparts, underscoring the value of incorporating model uncertainty in portfolio design. Additionally, across all investigated periods, the worst-case leverage strategy consistently outperforms the unleveraged index, highlighting the practical benefit.

Overall, this empirical validation demonstrates that the theoretical framework developed in this thesis not only provides analytical tractability but also yields economically meaningful and practically robust investment strategies. These findings bridge the gap between theoretical robustness analysis and real-world portfolio performance, highlighting the importance of uncertainty-aware decision-making in leveraged ETF investments.

# Chapter 10

## Conclusion

### 10.1 Summary of objectives and main findings

This thesis set out to study the robust long-term growth rate of expected utility for a leveraged exchange-traded funds (LETFs) under model uncertainty. The motivation stemmed from recognizing that real-world investors face ambiguity in key parameters and must account for misspecification or instable parameters when optimizing leverage. We assumed that the parameters of the underlying reference asset lie within an compact uncertainty set, instead of being known constants. The robust framework addresses model misspecification concerns and allows us to determine investment policies that are robust against the worst-case plausible market conditions.

Using a combination of the martingale extraction method and comparison principle, we derived explicit formulas or characterizations for the long-term growth rate of expected utility under various asset price and interest rate dynamics. By solving an eigenvalue problems we obtained closed-form expressions for this growth rate in several models, and we identified dependencies of model parameters. Crucially, we analyzed the worst-case parameters within the uncertainty set as a the combination of drift, volatility, and other model inputs that minimize the long-run growth rate. Leveraging the comparison principle, we found some the worst-case parameters at boundary values of the uncertainty set, thereby simplifying the search for the adversarial scenario. Substituting these worst-case parameters into the growth rate formulas yielded the robust long-term growth rate, which by construction is lower than or equal to the growth rate under any particular parametric assumption. We then optimized over the investor's leverage ratio  $\beta$  to find the optimal leverage that maximizes the robust growth rate.

### 10.2 Economic interpretation

The theoretical results carry clear economic implications about how ambiguity aversion influences leverage decisions. An ambiguity averse investor, who accounts for model uncertainty, behaves effectively as if they are more risk averse than an investor who fully trusts a given model. In our context, ambiguity aversion manifests as a preference for robustness over sheer performance. The investor is willing to sacrifice some expected return

in order to secure a higher worst-case outcome. This generally leads to a lower chosen leverage compared to a non-robust case.

A key insight from our findings is that ambiguity aversion increases the investor's sensitivity to volatility and model risk. Under model uncertainty, volatility is especially pernicious because it can erode long-run growth through compounding effects such as the volatility decay. The robust investor internalizes the possibility that volatility could be higher and therefore opts for a more cautious leverage. Hence, robust leverage choices are more conservative in volatile or uncertain environments, highlighting a qualitative difference. The classical outcome might predict aggressive leveraging based on historical return estimates, whereas the robust outcome emphasizes capital preservation and steady growth.

In summary, ambiguity aversion induces a more cautious stance. The investor prioritizes ensuring a baseline growth under all plausible scenarios over maximizing returns under possibly far more likely scenarios. Qualitatively, robust outcomes feature smaller leverage, lower volatility of outcomes, and more stable growth, whereas classical outcomes might promise higher returns on paper but with significantly higher vulnerability to model errors, tail events or market stress.

### 10.3 Comparison across models

An important component of this work was analyzing how robust optimal leverage and growth outcomes effects different reference asset models. We considered a broad spectrum of stochastic processes for the underlying asset driving the LETF, including the geometric Brownian motion (GBM) with constant volatility, stochastic volatility models, such as the Heston model and the 3/2 volatility model, as well as other diffusion models like the Cox–Ingersoll–Ross (CIR) type process and its 3/2 variant. We also examined cases with stochastic interest rates, the Vasicek short-rate model or an inverse-GARCH interest rate process and finally also jump diffusion models for the index to see how uncertainty in different parameters and models would affect the results. This diversity of models allowed us to identify which features of robust leverage selection are common to all settings and which are model specific nuances.

Across all models, we found a consistent qualitative pattern. The robust optimal leverage is strictly lower than the mid-case optimal leverage, reflecting a universal preference for caution. Additionally, in every model the worst-case scenario corresponds to boundary parameter selections. For example, in the GBM case with uncertain drift  $\mu$  and volatility  $\sigma$ , the worst-case for the investor is naturally  $\mu$  at its minimum allowed value and  $\sigma$  at its maximum, which yields the smallest growth rate. Consequently, the robust optimal leverage for GBM can be derived in closed-form, and it will typically be a finite leverage ratio even if the mid-case selections might suggest an unbounded optimum.

In models with stochastic volatility, such as the Heston model and the 3/2 model, the robust optimization exhibits richer behavior. We found that the correlation  $\rho$  between the asset price and its volatility and the allowed volatility range have significant impacts on the optimal leverage. Shared features still persist. For instance, a higher potential long-run volatility or slower mean-reversion in volatility pushes the worst-case growth lower, thereby reducing the robust optimal leverage compared to a scenario with favorable

volatility dynamics.

When introducing stochastic interest rates, we found that the interaction between interest rate uncertainty and leverage adds another layer of complexity. In a Vasicek-type interest rate model, for instance, the risk-free rate  $r(t)$  can fluctuate, affecting the excess return earned by the LETF over cash. The robust investor must consider worst-case interest rate paths as well. For example, a scenario where interest rates rise could narrow the excess return of the risky asset. We observed that optimal leverage in such settings can be non-monotonic in certain parameters. Nonetheless, even with stochastic interest rates, the robust strategy remains more conservative than a nominal strategy that assumes a fixed predictable  $r$ . The shared qualitative insight is that, regardless of the model, robustness induces the investor to limit leverage in proportion to the degree of uncertainty in the model's dynamics.

Each model provides a consistent message that over leveraging is suboptimal in the presence of uncertainty, but they differ in the exact calibration of the optimal leverage due to the models' specific risk factors. By comparing across models, the thesis highlighted which robust investment behaviors are robust in a broader sense and which behaviors vary with modeling assumptions. This comparative analysis also helps to validate the framework. Our robust optimization approach can flexibly accommodate various asset dynamics, from simple GBM to complex stochastic volatility and interest rate models, offering a unified perspective on long-term growth under uncertainty.

## 10.4 Practical implications

The conclusions drawn from this research carry practical significance for long-term investors, fund managers, and even LETF issuers and regulators. A key implication is the importance of conservative leverage policies in the face of model uncertainty. For a portfolio manager or an individual investor considering a leveraged ETF for long-term growth, our findings serve as a cautionary guide. The traditionally calculated optimal leverage based on historical estimates of return and volatility could be dangerously high if those estimates are uncertain. Implementing a robust optimization approach effectively yields a safer leverage level that protects the investor from severely adverse outcomes. The investor may give up some upside potential if the optimistic scenarios play out, but in exchange they gain confidence that their wealth will still grow at a reasonable rate even if conditions turn out to be worse. This trade-off is invaluable for long-term investors like retirement funds or endowments, where the priority is sustainable growth over decades rather than short-term speculation.

For LETF product issuers, understanding robust growth rates can inform the design of funds. Issuers might offer funds with moderate leverage factors that are more likely to deliver positive long-term returns under a wide range of market conditions, rather than extreme leverage products that could erode value in volatile regimes. Our framework can also aid in risk disclosures by illustrating to investors how a 3x leveraged ETF might have a much lower worst-case growth rate or even negative compared to a 2x leveraged ETF, thereby emphasizing the risk of excessive leverage. This is consistent with observations that LETFs are highly susceptible to volatility decay, and our robust approach quantifies that susceptibility in terms of long-run utility growth.

Portfolio managers and financial advisors can apply the insights by adjusting their strategic asset allocation for ambiguity. Instead of relying purely on point estimates of returns, they can incorporate uncertainty ranges for expected returns, volatilities, correlations, etc. and solve for the robust optimal exposure to leveraged assets. The result is a portfolio that may appear conservative but is actually resilient. Such a portfolio is less likely to be derailed by market regimes that deviate from historical norms. In particular, in markets with persistent high volatility or changing dynamics e.g. entering a bear market or crisis period where historical drift might no longer hold, a robust strategy will have preemptively dialed down leverage, thereby preserving capital and avoiding the compounding of losses.

There are also implications for regulators and risk managers. Leveraged ETFs pose systemic and investor protection questions, especially for retail investors who may not fully understand the risks. The robust growth rate analysis provides a formal way to stress-test leveraged investment strategies under worst-case assumptions. Regulators could require or encourage such stress-testing for products or strategies that employ high leverage, to ensure that they are not excessively dangerous in plausible scenarios. Encouraging transparency about these robust growth metrics could lead to better informed investment decisions. Overall, the value of a conservative leverage strategy under uncertainty is that it prioritizes survivability and long-run wealth accumulation over the temptation of short-run gains. This aligns well with the goals of long-horizon investors. By adopting robust optimization tools, practitioners can improve portfolio resilience and avoid strategies that maximize expected returns at the cost of exposing the investor to unacceptable long-run risks.

## 10.5 Limitations and future research

While this thesis contributes a general and flexible framework for robust leverage optimization, it is important to acknowledge its limitations and the avenues they open for future research. First, our analysis was conducted in continuous-time models under idealized assumptions such as frictionless markets, continuous rebalancing and so on. Real leveraged ETFs rebalance discretely and incur management fees and transaction costs. Although continuous-time diffusion models capture the essential phenomena such as volatility decay in the limit, discrete rebalancing and market frictions could quantitatively affect the growth rates. One limitation, therefore, is the omission of market frictions. We did not include transaction costs, bid-ask spreads, tracking errors or liquidity constraints in the model. High leverage often leads to high turnover due to rebalancing to maintain the leverage ratio, which would introduce additional costs and possibly make extremely high leverage strategies infeasible in practice. Future work could for instance integrate transaction cost models into the robust growth optimization. This would likely further penalize high leverage choices, reinforcing the qualitative conclusions but providing more realistic guidance on the optimal leverage in the presence of trading frictions.

Second, our uncertainty modeling was relatively structured. We assumed parameter uncertainty sets as compact intervals and found worst-case values within those sets. This interval based approach might be seen as a conservative but somewhat coarse way to model ambiguity. It treats the parameters as fixed unknown constants within a range,

whereas in reality, parameters could evolve or the parameters might complete change between regimes, so no compact interval would be reasonable. A natural extension would be to consider dynamic or distributional ambiguity, for instance using robust control or distributionally robust optimization techniques that allow the underlying probability law to vary within a certain divergence or confidence bound. Additionally, one could employ a data driven approach to defining the uncertainty set. For example, using historical data to construct confidence intervals or Bayesian posterior credible sets for the parameters, and then optimizing for the worst-case within those. Such an approach would ground the ambiguity in empirical evidence and possibly yield time-varying uncertainty sets that shrink or grow as new data arrives. Future research could also consider learning mechanisms, where the investor updates their ambiguity set as they observe market outcomes, blending robust control with Bayesian learning for a more adaptive strategy. Another important extension is exploring alternative asset dynamics beyond the models covered here, such as regime-switching models, where the market can switch between different volatility or drift regimes, in the robust growth framework. These models would enlarge the uncertainty in a different way, not just parameter uncertainty, but structural uncertainty in the return process. The robust optimization in such cases might show how optimal leverage adapts when facing an unknown persistent change in market volatility.

Third, our focus was on a single leveraged asset (an LETF tracking a single index). In practice, investors hold multi-asset portfolios, and there is interest in understanding robust leverage or allocation across multiple sources of risk. Extending the robust growth rate analysis to a multi-asset setting, e.g. combining multiple LETFs or mixing LETFs with unleveraged assets and bonds, would be highly relevant. This poses additional challenges, as ambiguity can exist not only in each asset's parameters but also in the correlations between assets. A multi-dimensional robust optimization would determine not just a single leverage number, but an entire portfolio composition that maximizes worst-case growth. It would be interesting to see, for instance, how a robust optimizer would allocate between a risky asset and its leveraged version.

Next, we assumed a power utility. Now, one could examine the robustness of different utility criteria, such as using exponential utility. Although log or power utility is standard for growth rate studies, due to its time-additivity and homogeneity properties, different objective formulations under ambiguity could yield different optimal policies worth comparing.

In summary, this thesis provides a foundation for robust leverage optimization, but further research is needed to relax simplifying assumptions and broaden the scope. Incorporating discrete-time effects, transaction costs, and more complex uncertainty structures would enhance the practical applicability of the results. Extending the analysis to multi-asset portfolios and more complex asset price dynamics would generalize the insights and possibly reveal new phenomena in robust long-horizon investing. The approach of this work is quite general, and we expect that with appropriate mathematical adjustments it can be applied in all these directions. The hope is that this line of research will contribute to more resilient investment strategies and better risk management for leveraged investments in practice.



# Appendix A

## Code repository

All Python scripts used to generate the figures and numerical results in this thesis are available in the following Git repository:

<https://github.com/LeonardAv/Master-thesis>.

The repository contains the full implementation and all code used to produce the figures. All plots presented in this thesis were produced using this code. Interested readers may use the code to reproduce the results, adjust parameters, and experiment with the models.

## Appendix A. Code repository

---

# Bibliography

- [1] Tim Leung, Hyungbin Park, and Heejun Yeo. Robust long-term growth rate of expected utility for leveraged ETFs. *Mathematics and Financial Economics*, 18: 671–705, 07 2024. URL <https://doi.org/10.1007/s11579-024-00371-1>.
- [2] BlackRock. *BlackRock People & Money*. Blackrock, 2024.
- [3] Daisy Maxey. *Fidelity the Latest to Caution on ETFs*, 2009.
- [4] Paul A. Samuelson. Lifetime portfolio selection by dynamic stochastic programming. *The Review of Economics and Statistics*, 1969.
- [5] Robert C. Merton. Optimum consumption and portfolio rules in a continuous-time model. *Journal of Economic Theory*, 1971.
- [6] Darrell Duffie and William R. Zame. The consumption-based capital asset pricing model. *Econometrica*, 1989.
- [7] Jakša Cvitanić and Ioannis Karatzas. Convex duality in constrained portfolio optimization. *Annals of Applied Probability*, 1992.
- [8] Michael J. Brennan. The role of learning in dynamic portfolio decisions. *European Finance Review*, 1998.
- [9] John C. Cox and Chi-fu Huang. A variational problem arising in financial economics. *Journal of Mathematical Economics*, 1991.
- [10] Marco Avellaneda, Arnon Levy, and Antonio Parás. Pricing and hedging derivative securities in markets with uncertain volatilities. *Applied Mathematical Finance*, 2: 73–88, 01 1996. doi: 10.1080/13504869500000005.
- [11] Anis Matoussi, Dylan Possamaï, and Chao Zhou. Robust utility maximization in nondominated models with 2bsde: The uncertain volatility model. *Mathematical Finance*, 25, 06 2013. doi: 10.1111/mafi.12031.
- [12] Jun Liu and Jun Pan. Dynamic derivative strategies. *Journal of Financial Economics*, 2003.
- [13] Daniel Hernández-Hernández and Alexander Schied. Robust utility maximization in a brownian market model. *Mathematics of Operations Research*, 2006.

## Bibliography

---

- [14] José Scheinkman and Lars Hansen. Long term risk : An operator approach. *Econometrica*, 79, 10 2006.
- [15] Lars Peter Hansen and Thomas J. Sargent. Robust control and model uncertainty. *Journal of Economic Dynamics and Control*, 2001.
- [16] Lars Peter Hansen and Thomas J. Sargent. *Robustness*. Princeton University Press, 2008.
- [17] Evan W. Anderson, Lars Peter Hansen, and Thomas J. Sargent. A quartet of semi-groups for model misspecification, robustness, prices of risk, and model detection. *Journal of the European Economic Association*, 2003.
- [18] Lars Peter Hansen and Thomas J. Sargent. *Robustness and ambiguity in continuous time*. Elsevier Inc., 2011. doi: doi:10.1016/j.jet.2011.01.004.
- [19] Wendell H. Fleming and Shuenn-Jyi Sheu. Risk-sensitive control and an optimal investment model. *Mathematical Finance*, 2002.
- [20] Pascal J. Maenhout. Robust portfolio rules and asset pricing. *Review of Financial Studies*, 2004.
- [21] Pascal J. Maenhout. Robust portfolio rules and the value of robustness. *Journal of Economic Theory*, 2006.
- [22] Revaz Tevzadze, Teimuraz Toronjadze, and Tamaz Uzunashvili. Robust utility maximization for diffusion market model with misspecified coefficients. *Finance and Stochastics*, 17:535–563, 2013. doi: 10.1007/s00780-012-0199-7.
- [23] Ariel Neufeld and Marcel Nutz. Robust utility maximization with lÉvy processes. *Mathematical Finance*, 28(1):82–105, 2018. doi: <https://doi.org/10.1111/mafi.12139>.
- [24] Leo Breiman. Optimal gambling systems for favorable games. *Proceedings of the Fourth Berkeley Symposium on Mathematical Statistics and Probability*, 1961.
- [25] John L. Kelly. A new interpretation of information rate. *Bell System Technical Journal*, 1956.
- [26] Linda Larsen and Nicole Branger. Robust portfolio choice with uncertainty about jump and diffusion risk. *SSRN Electronic Journal*, 01 2012. doi: 10.2139/ssrn.1982964.
- [27] Minder Cheng and Ananth Madhavan. The dynamics of leveraged and inverse exchange-traded funds. *Journal of Investment Management*, 7, 01 2010.
- [28] Marco Avellaneda and Stanley Zhang. Path-dependence of leveraged ETF returns. *SIAM J. Financial Math.*, 1:586–603, 01 2010. doi: 10.2139/ssrn.1404708.
- [29] Robert Alan Jarrow. Understanding the risk of leveraged ETFs. *Finance Research Letters*, 7:135–139, 09 2010. doi: 10.1016/j.frl.2010.04.001.

- [30] Tim Leung and Kevin Guo. Commodity leveraged ETFS: Tracking errors, volatility decay, and trading strategies. *Risk*, 11 2014.
- [31] William Trainor and E. Baryla. Leveraged ETFs: A risky double that doesn't multiply by two. *Journal of Financial Planning*, pages 48–55, 01 2008.
- [32] Tim Leung, Matthew Lorig, and Andrea Pascucci. Leveraged ETF implied volatilities from ETF dynamics 22(2). *Mathematical Finance*, 05 2016. doi: 10.1111/mafi.12128.
- [33] Roger Lee and ruming wang. How leverage shifts and scales a volatility skew: Asymptotics for continuous and jump dynamics. *SSRN Electronic Journal*, 01 2015. doi: 10.2139/ssrn.2621153.
- [34] José Figueroa-López, Ruoting Gong, and Matthew Lorig. Short-time expansions for call options on leveraged ETFs under exponential lévy models with local volatility. *SSRN Electronic Journal* 9(1), pages 347–380, 08 2016. doi: 10.48550/arXiv.1608.07863.
- [35] Tim Leung and Ronnie Sircar. Implied volatility of leveraged ETF options. *Applied Mathematical Finance*, 22, 10 2012. doi: 10.2139/ssrn.2164518.
- [36] William Trainor and Richard Gregory. Leveraged ETF option strategies. *Managerial Finance*, 42:438–448, 05 2016. doi: 10.1108/MF-12-2014-0305.
- [37] Harry Markowitz. Portfolio selection. *Journal of Finance*, 1952.
- [38] Tim Leung and Hyungbin Park. Long-term growth rate of expected utility for leveraged ETFs: martingale extraction approach. *Int. J. Theor. Appl. Finance* 20(6), 2017. doi: 10.2139/ssrn.2879976.
- [39] Hyungbin Park and Heejun Yeo. *Dynamic and static fund separations and their stability for long-term optimal investments*, 2023. URL <https://arxiv.org/abs/2212.00391>.
- [40] Alexander Cox and Sam Kinsley. Robust hedging of options on a leveraged exchange traded fund. *Annals of Applied Probability*, 29, 02 2017. doi: 10.1214/18-AAP1427.
- [41] Lars Peter Hansen and José-Alexandre Scheinkman. Long-term risk: An operator approach. *Econometrica*, 2009.
- [42] Monroe D. Donsker and S. R. S. Varadhan. Asymptotic evaluation of certain markov process expectations. *Communications on Pure and Applied Mathematics*, 1975.
- [43] Tomasz R. Bielecki and Stanley R. Pliska. Risk sensitive dynamic asset management. *Applied Mathematics and Optimization*, 1999.
- [44] Holger Kraft, Frank Seifried, and Mogens Steffensen. Consumption and investment with stochastic investment opportunities and ambiguity. *Mathematical Finance*, 2013.
- [45] Daniel Brown. Bounds on long-run performance of leveraged ETFs. *Preprint*, 2023.

## Bibliography

---

- [46] Marco Pagano, Antonio Sánchez, and Serrano Josef Zechner. Can ETFs contribute to systemic risk? Technical Report ASC Report No. 9, European Systemic Risk Board, 2019.
- [47] U.S. Securities and Exchange Commission. Sec says unclear if proposed 3x and 5x leveraged ETFs would be approved, 2025. URL <https://www.investing.com/news/stock-market-news/sec-says-unclear-if-proposed-3x-and-5x-leveraged-etfs-would-be-approved-4292746>. Published: 2025-10-16; Accessed: 2025-11-14.
- [48] Jean-Dominique Deuschel and Daniel W. Stroock. *Large Deviations. Pure and Applied Mathematics*, volume 137. Academic Press Inc., Boston, 1989.
- [49] Ross G. Pinsky. *Positive Harmonic Functions and Diffusion*, volume 45. Cambridge University Press, 1995.
- [50] Scott Robertson and Hao Xing. Large time behavior of solutions to semilinear equations with quadratic growth in the gradient. *SIAM Journal on Control and Optimization*, 53, 07 2013. doi: 10.1137/13094311X.
- [51] Ioannis Karatzas and Steven E. Shreve. *Brownian Motion and Stochastic Calculus*. Springer, New York, 1998.
- [52] John Cox, Jonathan Ingersoll, and Stephen Ross. A theory of the term structure of interest rates. *Econometrica*, 53:385–407, 02 1985. doi: 10.2307/1911242.
- [53] Peter Carr and Jian Sun. A new approach for option pricing under stochastic volatility. *Review of Derivatives Research* 10: 87–250, 10:87–150, 02 2007. doi: 10.1007/s11147-007-9014-6.
- [54] Gabriel G. Drimus. Options on realized variance by transform methods: A non-affine stochastic volatility model. *Quantitative Finance*, 12:1679–1694, 2009. doi: 10.1080/14697688.2011.565789.
- [55] Dong-Hyun Ahn and Bin Gao. A parametric nonlinear model of term structure dynamics. *The Review of Financial Studies*, 12(4):721–762, 06 2015. ISSN 0893-9454. doi: 10.1093/rfs/12.4.721. URL <https://doi.org/10.1093/rfs/12.4.721>.
- [56] Steven L. Heston. A closed-form solution for options with stochastic volatility with applications to bond and currency options. *The Review of Financial Studies*, 6(2): 327–343, 1993. ISSN 08939454, 14657368. URL <http://www.jstor.org/stable/2962057>.
- [57] Daniel W. Stroock and Srinivasa S. R. Varadhan. *Multidimensional Diffusion Processes*. Springer, Berlin, 1997.
- [58] Joanna Goard and Mathew Mazur. Stochastic volatility models and the pricing of vix options. *Mathematical Finance*, 23, 02 2012. doi: 10.1111/j.1467-9965.2011.00506.x.

- [59] Oldrich Vasicek. An equilibrium characterization of the term structure. *Journal of Financial Economics*, 5(2):177–188, 1977. ISSN 0304-405X. doi: [https://doi.org/10.1016/0304-405X\(77\)90016-2](https://doi.org/10.1016/0304-405X(77)90016-2). URL <https://www.sciencedirect.com/science/article/pii/0304405X77900162>.
- [60] Fima C. Klebaner. *Introduction to Stochastic Calculus with Applications*. Imperial College Press, 2012. ISBN 9781848168312.
- [61] Martin Haugh. *Local Volatility, Stochastic Volatility and Jump-Diffusion Models*, 2013.
- [62] Dimitris Bertsimas and Melvyn Sim. The price of robustness. *Operations Research*, 52(1):35–53, 2004. doi: 10.1287/opre.1030.0065.
- [63] Leonid Hurwicz. The generalised bayes minimax principle: A criterion for decision making under uncertainty. Technical Report 355, Cowles Commission Discussion Paper, 1951.
- [64] Liangyu Min, Jiawei Dong, Jiangwei Liu, and Xiaomin Gong. Robust mean-risk portfolio optimization using machine learning-based trade-off parameter. *Applied Soft Computing*, 113:107948, 2021. doi: 10.1016/j.asoc.2021.107948.
- [65] Joong-Ho Won and Seung-Jean Kim. Robust trade-off portfolio selection. *Optimization and Engineering*, 21(3):867–904, 2020. doi: 10.1007/s11081-020-09485-z.
- [66] Amit Sinha. The reliability of geometric brownian motion forecasts of s&p500 index values. *Journal of Forecasting*, 40:1444–1462, 04 2021. doi: 10.1002/for.2775.
- [67] Paolo Guasoni and Scott Robertson. Portfolios and risk premia for the long run. *Annals of Applied Probability*, 22(1):239–284, 2012. doi: 10.1214/11-AAP767.
- [68] OECD. Financial market trends, vol. 2005, no. 2, 2005. URL [https://www.oecd.org/content/dam/oecd/en/publications/reports/2005/03/financial-market-trends-volume-2005-issue-1\\_g1gh4983/fmt-v2005-1-en.pdf](https://www.oecd.org/content/dam/oecd/en/publications/reports/2005/03/financial-market-trends-volume-2005-issue-1_g1gh4983/fmt-v2005-1-en.pdf). Accessed: 2025-11-15.

---

## Declaration of authorship

I hereby declare that the thesis submitted is my own unaided work. All direct or indirect sources used are acknowledged as references.

I am aware that the thesis in digital form can be examined for the use of unauthorized aid and in order to determine whether the thesis as a whole or parts incorporated in it may be deemed as plagiarism. For the comparison of my work with existing sources I agree that it shall be entered in a database where it shall also remain after examination, to enable comparison with future theses submitted. Further rights of reproduction and usage, however, are not granted here.

This paper was not previously presented to another examination board and has not been published.

Location, date

Munich, 05.01.2026

Name

Leonard Averdunk

Signature

